Acute Sublethal Effects of the Neonicotinoid Imidacloprid on the Honeybee Brain Transcriptome

A THESIS SUBMITTED TO THE SCHOOL OF GRADUATE STUDIES OF BLOOMSBURG UNIVERSITY OF PENNSYLVANIA

IN PARTIAL FULFILLMENT OF THE REQUIREMENTS FOR THE DEGREE OF MASTERS OF BIOLOGY

DEPARTMENT OF BIOLOGICAL AND ALLIED HEALTH SCIENCES

BY

HEATHER J. LLEWELLYN

BLOOMSBURG, PENNSYLVANIA

SUMMER 2020

Abstract

Global declines in honeybees have been linked to widespread use of pesticides. Sublethal doses of the neonicotinoid pesticide imidacloprid have been shown to cause physiological and behavioral changes that negatively impact hive health. This study examined the effects of acute, sublethal doses of imidacloprid on the honeybee gene expression in the brain.

Experiment 1 identified an imidacloprid dosage that yielded a cellular stress response in honeybees. Honeybee foragers were harnessed, fed to satiation, and randomly assigned to control (1.5 M sucrose) or treatment groups receiving imidacloprid at doses of $1/5^{th}$, $1/10^{th}$, $1/20^{th}$, $1/50^{th}$, $1/100^{th}$, and $1/500^{th}$ of the LD_{50} (18.0 ng/bee). After four hours, impaired motor responses and elevated levels of Heat Shock Protein 70 and Superoxide Dismutase, markers of cellular and oxidative stress, respectively, were observed at sublethal imidacloprid doses. A conservative dose of 0.9 ng/bee ($1/20^{th}$ of the LD_{50}) was selected to treat bees for RNA transcriptome analysis in Experiment 2.

In Experiment 2, bees were randomly assigned to four acute-exposure groups: Control-0h, Control-4h, Treatment-0h, and Treatment-4h. Control bees were fed 1.5 M sucrose while treatment groups received 0.9 ng/bee of imidacloprid. RNA isolated from bee brain tissue was sent to the University of Illinois at Urbana-Champaign for RNA sequencing. Of the 10,597 genes recovered from the reference genome, 4,205 genes were differentially expressed. Collectively, the Differential Expression Analysis, Multidimensional Scaling Plot, and heat map agree that the Control-4h group had the greatest changes in gene expression, counter to our prediction that the greatest alteration would be in imidacloprid-treated bees. Corroborating evidence supported the *post-hoc* hypothesis that the Control-4h and the Treatment-4h samples were switched and mislabeled prior to shipping. Comparisons between Control-4h and Treatment 4-h groups remain valid. If samples were switched, only the direction of differential gene expression (i.e., up-regulation versus down-regulation) would be affected by imidacloprid. Gene set enrichment analysis indicated that the key pathways affected were: oxidative phosphorylation, longevity regulating pathway, apoptosis, peroxisome, FOXO signaling, drug metabolism- cytochrome P450, metabolism of xenobiotics by cytochrome P450, circadian rhythm, and glutathione metabolism. These gene networks relate to key

biological functions of honeybees that have the potential to affect colony viability. Future research will focus on hypothesis-driven gene expression studies that relate specific molecular changes to biological functions and organism-level performance, an integrative approach that is essential to understanding the declines of these essential pollinators.

THESIS
SUBMITTED TO THE SCHOOL OF GRADUATE STUDIES
OF
BLOOMSBURG UNIVERSITY OF PENNSYLVANIA

IN PARTIAL FULFILLMENT OF THE REQUIREMENTS FOR
THE DEGREE OF MASTERS
PROGRAM IN THE DEPARTMENT OF BIOLOGICAL AND ALLIED HEALTH SCIENCES
BY
HEATHER J. LLEWELLYN.

The undersigned thesis committee members hereby certify that they have read and recommend to the School of Graduate Studies for acceptance the thesis entitled:

Acute Sublethal Effects of the Neonicotinoid Imidacloprid on the Honeybee Brain Transcriptome

APPROVED:

Cynthia A. Surmacz — January 15, 2021

Cynthia A. Surmacz, Ph.D., Thesis Advisor — Date:

Abby Hare-Harris — 1-15-21

Abby Hare-Harris, Ph.D., Committee Member — Date:

John M. Hranitz — 15 Jan 2021

John M. Hranitz, Ph.D., Committee Member — Date:

William F. Schwindinger — 1/13/21

William F. Schwindinger, M.D., Ph.D., Committee Member — Date:

APPROVED:

Heather J. Feldhaus — 3-15-21

Heather Feldhaus, PhD., Interim Associate Vice Provost for Research and Sponsored Programs & Dean of Graduate Studies — Date:

Acknowledgments

After four years, the journey has finally come to an end. This research would not have been possible without Aucker's Apiary in Millville, Pennsylvania and Dr. John M. Hranitz for allowing the collection of honeybees from their hives. Joshua I. Petersheim spent countless hours collecting, harnessing and feeding, treating, and capturing escaped honeybees. Erin Smith worked towards the development and validation of biochemical assays for catalase and superoxide dismutase to compare oxidative stress in control and imidacloprid-treated honeybees. Both Joshua and Erin held integral roles towards the completion of this research.

The Bloomsburg University Professional Experience Grant (2019 and 2020), Bloomsburg University Graduate School, and the Charlotte P. Magnum Student Support Program allowed for travel and board to the Society for Integrative and Comparative Biology National Conference in Tampa, Florida and Austin, Texas. If it was not for this funding, priceless opportunities to present and listen to research would have been missed. The Research and Scholarship Grant from Bloomsburg University allowed for the purchase of necessary supplies to complete this thesis research. The Department of Biological and Allied Health Sciences and College of Science and Technology at Bloomsburg University of Pennsylvania which allowed me to be a part of this academic community, I am forever grateful.

My Thesis Committee: Drs. Surmacz, Hare-Harris, Hranitz, and Schwindinger for their time, patience, and willingness towards the completion of this research. My schedule was not easy to work with but yet, at any day of the week, at all hours, we met to discuss and work on all the moving parts of this project. The Keck Center for Comparative and Functional Genomics at the University of Illinois Urbana-Champaign for graciously rerunning our samples for RNA sequencing. Dr. Hare-Harris for painstakingly writing a python and R script, data cleaning, and reviewing DAVID/KEGG analysis. If it was not for you, I would still be trying to open a file and figure out where I sent my python output. Dr. Hranitz who taught me more than I ever thought I would need to know about honeybees. Dr. Klinger for calling me that fateful day in the spring of 2016 to let me know there was an advanced DNA class at 2 p.m. and that I should attend because I was accepted into the Graduate program; thank you for giving me the chance.

Dr. Surmacz, I honestly do not know what to say about this marvelous educator. She has been present for all of the highs and lows, laughs and tears, breakdowns and successes of this research. These four years have been a blessing for me. You have shown me how to persevere through any type of situation with a smile and kind words or just a simple "buck up buttercup, that's research." You have made a huge impact.

A huge thank you to my family and friends, you have allowed me to be a complete nut-case for four years. Mom, you are and will always be my biggest fan. Thank you for always believing I can do anything and everything even if I failed. My future husband, Zachary, thank you for always being there, wishing me luck, eating my feelings with me, and telling me to get it together even when I could not. Lastly, to all those who said it could not be done. It can and it was.

Table of Contents

List of Figures

List of Tables

List of Appendices

I. Introduction

Apis mellifera L., commonly known as the honeybee, is one of the world's most important pollinators both economically and ecologically. With honeybees pollinating 71 out of the 100 most common crops and accounting for 90% of the worlds food supply, it is important to determine why honeybees and other pollinators are dying off at alarming rates (Pilatic 2012, du Rand *et al.* 2015). Pesticides, malnutrition, habitat loss, parasites and pathogens have all been identified as interacting factors that contribute to the drastic loss of honeybees (du Rand *et al.* 2015).

The Biology of the Honeybee:

A bee colony contains two sexes, male and female (Figure 1). There are two classes of female bees: queen bee and worker bees. Eggs laid by the queen develop into mature honeybees. Unfertilized eggs develop into male drones (haploid), while fertilized eggs develop into either female workers or queen cells (diploid). This type of sex determination, haplodiploidism, is a characteristic of insects in the order Hymenoptera. The metamorphosis from honeybee larva to pupa takes place within sealed cells and takes 16 days after deposition of the egg for the adult queen, 21 days for worker bees, and 24 days for drones (Agriculture and Consumer Protection 1990).

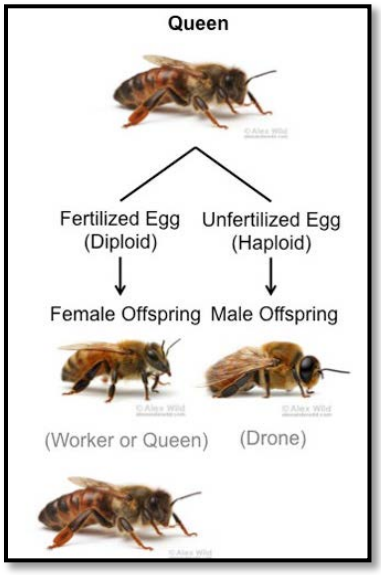

Figure 1: Differentiation of body type between classes of bees within a hive (Ellis and Mortenson 2017).

An adult queen is the reproductive female in the honeybee colony. Compared to a worker bee, the queen has a longer and plumper abdomen with a head and thorax of similar size (Ellis and Mortenson 2017). Worker honeybees possess a smaller body and are specialized for pollen and nectar collection by having longer tongues and larger crops. Worker bees have reduced ovaries, a stinger, and are not capable of mating. To assist in carrying the large amounts of pollen back to the hive, the worker bee has a unique feature called a corbicula or more commonly known as pollen basket (Ellis and Mortenson 2017). Drones, the only male caste within the hive, are easily differentiated from the females. An adult drone possesses a larger thorax, no stinger and has "fly-like" eyes that touch at the center at the top of their head. The drone's abdomen is considered bullet-shaped since it is thick with a blunt end (Ellis and Mortenson 2017). A general depiction of an adult honeybee is seen in Figure 2 below.

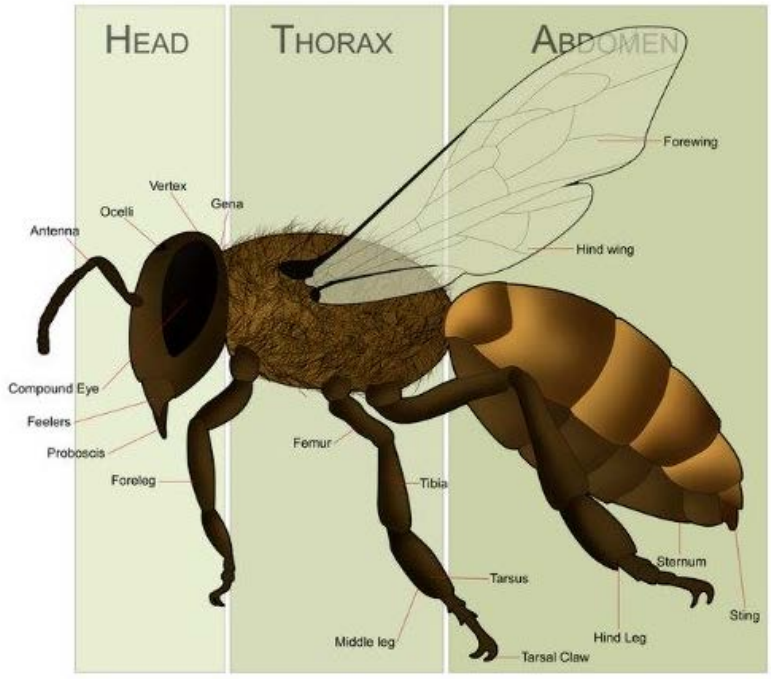

Figure 2: An adult honeybee (Photo Credit: BuzzAboutBees 2010-2020). Covered in branched hairs, an adult honeybee has three body regions: head, thorax and abdomen. The head contains compound eyes and antennae. Two pairs of wings and three pairs of legs are attached to the thorax. In females, a barbed stinger contains a poison-sac (Ellis and Mortenson 2017).

Each colony contains one fertile queen who lays eggs and 20,000-80,000 sterile worker bees that maintain the colony. In comparison to the females, there are approximately 300-800 fertile males, making the colony predominantly female (Agriculture and Consumer Protection 1990). Among the mature honeybees there are

several thousand immature bees or brood; approximately 5,000 eggs and anywhere from 25-30,000 immature bees that are in various stages of development. Approximately 10,000 of the immature bees are newly hatched larvae (Agriculture and Consumer Protection 1990).

A honeybee's role within the hive is dependent on the food source fed to them. In the first three days, all developing eggs are fed with "bee milk" or "royal jelly" produced by nurse bees, younger worker bees that are not ready to leave the hive (Agriculture and Consumer Protection 1990). After the first three days, worker and drone larvae are fed mixed food that is composed of honey and pollen. Unlike the worker and drone larvae, the queen is fed royal jelly for her entire larval life of approximately five days.

A honeybee egg measures between 1 to 1.5 mm in length and is often described as appearing like a tiny grain of rice. These eggs can be found in individual hexagonal shaped wax cells located in the brood area of the comb. The honeybee eggs hatch after three days and larvae appear (Ellis and Mortenson 2017; Figure 3). Larvae are white in color and appear as a curled "C" shape at the bottom of their wax cell. The amount of time a honeybee remains in the larval stage is dependent on caste (worker: 6 days, drone: 6.5 days, and a queen: 5.5 days). As a pupa, the honeybee body becomes extended into an upright position within the cell which is cover by the adult workers with a wax cap (Ellis and Mortenson 2017). Pupa remain under the wax cap until it is time to molt into an adult. At that time, the adult chews its way out of the cell. The length of time for pupal development is dependent on caste (worker: 12 days, drone: 14.5 days, and queen: 8 days).

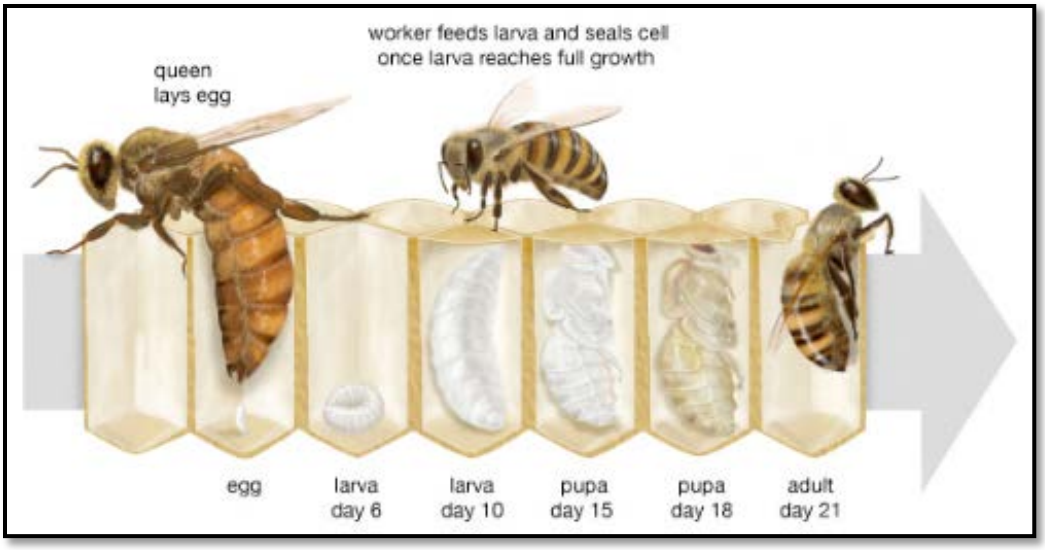

Figure 3: Life cycle of honeybees (Honeymell 2015). The life cycle of the honeybee begins with the queen laying an egg which matures into larva, pupa, and finally an adult at day 21. The worker bees fulfill their role by feeding the larva and sealing the cell.

Bee colonies display eusociality, an advanced level of organization characterized by cooperative brood care, overlapping generations within a colony, and a division of labor into reproductive and non-reproductive groups (Wilson 1971). With thousands of honeybees inhabiting one hive, each class of bee performs a different job, a division of labor described as temporal polyethism (Johnson 2008, Seeley 1985). The queen's main purpose is to mate and the drones' is to inseminate the queen. The remaining jobs fall onto the worker bees (Agriculture and Consumer Protection 1990). The nurse and forager classifications of the worker bee are age-dependent. If the worker honeybee is three weeks old or less, she is considered a nurse bee. Her roles are numerous and include: cleaning the hive/comb, feeding the brood, caring for the queen, making orientation flights, comb building and ventilating the hive, packing combs (with pollen, water, nectar and honey), executions, and finally performing guard duty which is the last stage of the nurse bee. The forager bee, a mature nurse bee, mainly concentrates on the needs of the colony such as fetching nectar, pollen, water, and propolis (a resinous cement collected by bees from buds of trees which is used as cement in repairing and maintaining the hive) (Agriculture and Consumer Protection 1990, Kuropatnicki *et al.* 2013).

Due to their roles within the hive, the distinct classes of honeybees may vary in their susceptibilities to environmental factors. A study performed by Vannette *et al.* (2015) compared the expression of antimicrobial, immune and detoxification genes in

Apis mellifera between foragers and nurse bees. Researchers observed changes in immune responses through ontogeny as the honeybee matures. In this specific example, the forager bee exhibited greater expression of genes that were associated with immune responses and detoxification activity than nurse bees. This heightened gene expression was specifically pronounced in tissues that mediate nectar processing and social interactions such as the mandibular gland and Malpighian tubules. The findings suggest that the honeybee has mechanisms to deal with the different environmental threats that could be encountered when out foraging. The ability of a specific gene's expression to shift as the honeybee makes the transition from nurse bee to forager is essential to its function.

The Honeybee Genome:

Apis mellifera is the European honeybee, one of seven species and 44 subspecies of honeybee (Engle 1999), that was used in this investigation on the effects of pesticides on the honeybee transcriptome. The genus *Apis* is an ancient lineage of bees that evolved in tropical Eurasia. The origin of *Apis mellifera* has been suggested to be Asia, the Middle East or Africa. While the native range of *Apis mellifera* spans Europe, Africa, and the Middle East, they are now found worldwide due to humans utilizing them as pollinators and for their ability to make honey (Engle 1999). The karyotype of *Apis mellifera* has been well characterized and consists of 16 chromosomes in haploid males and 32 chromosomes in the diploid females (Figure 4). *Apis mellifera* lacks sex chromosomes, a consequence of its haplodiploid sex determination.

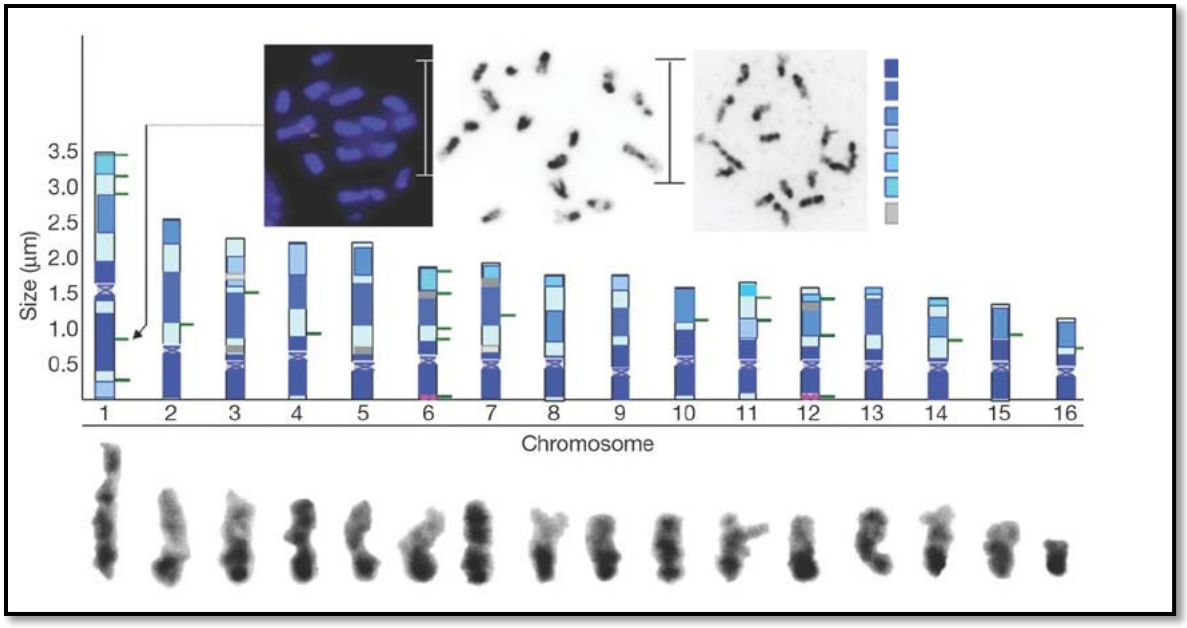

Figure 4: Ideogram and karyotype for *Apis mellifera* (Honeybee Genome Sequencing Consortium 2006). The ideogram (in blue) shows the average chromosome lengths, positions, and sizes of the heterochromatin bands. The percentage of heterochromatin mirrors the time of appearance of heterochromatic bands. The karyotype is located below the ideogram.

The genome of *Apis mellifera* was published in Nature in 2006 by the Honeybee Genome Sequencing Consortium, a partnership of over 250 scientists from 90 institutions (Honeybee Sequencing Consortium 2006). This group established that honeybees have approximately 11,000 genes, a surprisingly low number compared to other insects such as *Drosophila* (13,600 genes) and *Anopheles* (14,000 genes) (Claudianos *et al.* 2006). Possible explanations for this discrepancy are the bees' haplodiploid system of sex determination and their highly organized eusociality that limits the exposure of immature bees to the external environment, lessening the need for functions that require environmental interactions (Han *et al.* 2012).

a. *Genome Organization*

Honeybee genomes display several unique characteristics. (Honeybee Genome Sequencing Consortium 2006). A honeybee's genome can be distinguished from those of other insects by possessing a high (A+T) content, high CpG content, and lacking major transposon families. Due to the high A+T content, honeybee genes appear more frequently in (A +T) rich domains. CpG is considered an over-represented dinucleotide when compared to the mononucleotide frequencies. In genomes that have CpGs as the target of cytosine methylases display a CpG deficit. The fact that the honeybee possesses

such high CpG content is surprising given that honeybees are the first protostomes to possess DNA methylases, including CpG methyltranferase, that are similar to those found in vertebrates. Methylated cytosines are known to be frequent sites of mutation, and the expected Me-C→T mutations may contribute to the A+T richness observed in the honeybee genome (Honeybee Genome Sequencing Consortium 2006). However, the significance of cytosine methylation on the nucleotide composition of the honeybee genome remains uncertain. The honeybee genome is also unique in that it lacks most of the major families of transposons and retrotransposons. Lastly, the honeybee's telomeres appear to be relatively simple, lacking complex tandem repeats when compared to other insects (Honeybee Genome Sequencing Consortium 2006).

b. *Functional Categories of Genes*

The honeybee genome varies in both obvious and subtle ways compared to the well-annotated *Drosophila* and human genomes. The honeybee genome shows greater similarities to the vertebrate genome than the *Drosophila* and *Anopheles* genomes for genes involving circadian rhythms, RNA interference, and DNA methylation. Honeybees possess fewer genes than *Drosophila* and *Anopheles* for innate immunity, detoxification enzymes, gustatory receptors, more genes for odorant receptors, and novel genes for nectar and pollen utilization (Honeybee Genome Sequencing Consortium 2006). Key examples of gene variation in honeybees in critical functional categories are described below:

1. Immune System Pathways.

The eusocial lifestyle of the honeybee promotes favorable conditions for infectious threats such as viruses, bacteria, fungi, protists, and parasites. Honeybees protect themselves against such dangers by grooming, which is considered a social defense, by raising young in individual chambers within the hive, and by having the workers defend the hive against potential vectors of disease (Honeybee Genome Sequencing Consortium 2006). However, the honeybee genome, when compared to other insect genomes, possesses fewer genes that are implicated in insect immune pathways. While immune pathways such as Toll, Imd, and JAK/STAT are intact, their functionality is reduced by two-thirds in

comparison to honeybee paralogues (Honeybee Genome Sequencing Consortium 2006). This data suggests that honeybees utilize novel immune pathways and possess immune systems that are focused on a relatively small group of coevolved pathogens.

2. Anti-Xenobiotic Defense Mechanisms

Insecticide use is considered to be one of the factors that accounts for the major loss of honeybee populations in parts of the world. Detoxification enzymes are essential for honeybees to remove these xenobiotics that they are exposed to in the environment. When compared to *Anopheles* and *Drosophila*, the honeybee has approximately 30-50% fewer genes that encode three superfamilies of xenobiotic detoxification enzymes: carboxylesterase (CCE), cytochrome P450 (P450), and glutathione-S-transferase (GST). These xenobiotic detoxification enzymes are responsible for the metabolism of insecticides (Honeybee Genome Sequencing Consortium 2006). Up- and down-regulation of these different P450s can induce erratic behavior (Pereira *et al.* 2020). In other insects, these three superfamilies have also been shown to be the frequent source of mutations that confer insecticide resistance (Claudianos *et al.* 2006). The reduction of these anti-xenobiotic genes in bees may explain their unusual sensitivity to insecticides.

A study performed by Mao *et al.* (2013) determined that p-coumaric acid, pinocembrin and pinobanksin 5-methyl ether (all constituents found in honey) induce detoxification genes. By performing RNA-seq analysis, it was shown that p-coumaric acid up-regulates all classes of detoxification genes as well as some antimicrobial peptide genes. This is of interest since p-coumaric acid could function as a nutraceutical that regulates immune and detoxification processes. This would explain why certain bees are not affected or less affected by toxins. However, honey substitutes are often used which may compromise the bee's ability to deal with pesticides and pathogens thus contributing to colony loss (Mao *et al.* 2013).

3. Antioxidants

Enzymes that break down free radicals are conserved in bees. Unlike *Drosophil*a and *Anopheles*, there is an expansion of the sigma class of GST enzymes that protects against free radicals generated in aerobic metabolism, and fewer numbers of the theta, delta, and omega classes that protect from xenobiotics. Since free radicals are generated in bee flight muscles during long foraging trips, selective pressure may be put on these genes (Honeybee Genome Sequencing Consortium 2006).

4. Heat Shock Proteins

Heat shock proteins, or HSPs, are molecular chaperones produced in cells in response to stressful conditions. Universal in all organisms, heat shock protein genes are highly-conserved and assigned to families based upon their sequence homology and molecular weight (Feder and Hoffman 1999). Honeybees have only 6 genes in comparison to the fly (5 genes) and humans (8 genes). HSP70 proteins function in protein complexes with HSP90 which are involved in signal transduction, ligand binding as well as responding during cellular stress (Honeybee Genome Sequencing Consortium 2006). Our laboratory adapted a HSP70 ELISA to monitor cellular stress in different life stages of several species of bees (Barthell *et al.* 2002, Hranitz and Barthell 2003, Hranitz *et al.* 2009a, Hranitz *et al.* 2009b, Hranitz *et al.* 2010).

Honeybees are one of few endothermic insects and have astonishing levels of thermoregulation in colonies whose temperatures are 33-35°C. The core temperature of 33-35°C is maintained through bee activities that warm or cool the colony as needed. While the hive thermoregulates, the role of HSPs in the thermotolerance of individual honeybees appears to function as in other animals, as honeybees do not possess an increased number of genes that encode HSP70 family members (Tong *et al.* 2019).

5. Circadian Rhythm and Behavior

Circadian rhythm of the honeybee is socially regulated (Eban-Rothschild and Bloch 2011). It is common to see differences in the circadian clock among different castes. As a forager, the circadian clock is used to anticipate day-night fluctuations in their environment, time visits to flowers, dance language communication, and to determine sun-compass orientation. The worker and the queen bee however have more flexibility to their circadian rhythm. The internal clocks of the worker bees are influenced by task specialization and regulated by the direct contact with the brood. It is important to note that nurse bees, one of the youngest bees in the caste system, do not possess circadian rhythms in behavior or clock gene expression (Eban-Rothschild and Bloch 2011).

Sleep regulation is an important focus of the circadian clock. Honeybees have a distinct sleep state with a characteristic posture, reduced muscle tension, and elevated response threshold (Eban-Rothschild and Bloch 2011). The sleep state is considered a dynamic process consisting of changes between deep and light sleep. A lack of sleep often leads to an increase in the expression of sleep characteristics the next day and will interfere with learning patterns (Eban-Rothschild and Bloch 2011).

Period (per), timeless (tim), crytochrome (cry), clock (clk), cycle (cyc), vrille (vri), and Par Domain Protein 1 (pdp1) are all considered "clock genes." The honeybee genome encodes a single orthologue for each of these genes (Honeybee Genome Sequencing Consortium 2006). The honeybee genome only encodes mammalian-type paralogues but does not contain orthologues to Cry-d and Timeless1 genes that are considered essential clock genes for *Drosophila* (Honeybee Genome Sequencing Consortium 2006).

Sequencing of the honeybee genome revealed a cys-loop neurotransmitter-gated ion channel superfamily. This superfamily contains 21 subunit members, two less than *Drosophila*, and an extra nicotinic

acetylcholine receptor subunit. The members within this superfamily are known to contribute to honeybee behavior including foraging, learning, memory, olfactory signal processing, mechanosensory antennal input, and visual processing (Honeybee Genome Sequencing Consortium 2006).

Colony Collapse Disorder:

First described in France in 2006, Colony Collapse Disorder (CCD) was identified as a potential cause for the rapid decline in honeybees and other pollinators around the world. Honeybee populations in the United States have been steadily declining at a rate of 1% per year since 1947 with steeper declines seen since 1987, with a majority of these losses averaging 29-36% per year over the last four winters (Pilatic 2012). Figure 5 shows the United States managed honeybee colony loss within the past decade.

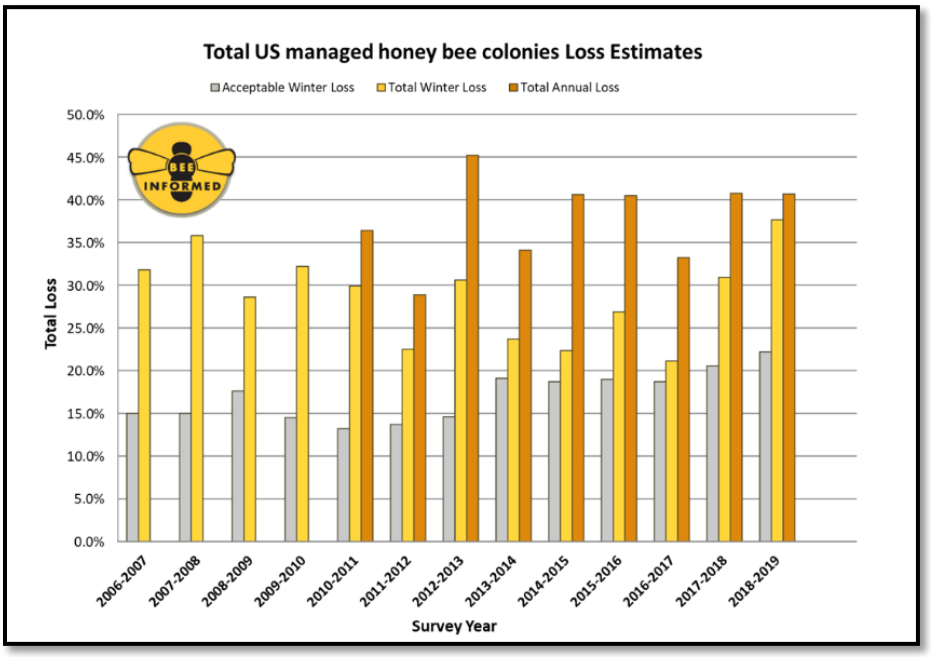

Figure 5: U.S. managed honeybee colony loss estimates (Bee Culture 2019). Acceptable levels of winter loss are compared to total winter loss and total annual loss of honeybee colonies between 2006-2007 and 2018-2019. The total annual loss has surpassed the total winter loss and nearly doubled, almost tripled, the acceptable levels for 2010-2011 through 2018-2019 years.

Symptoms of CCD are distinct from other loss epidemics and include (Pilatic 2012):

1. Colonies found suddenly empty of adult bees leaving their brood unattended.
2. No sign of dead bees.
3. No hive pests or food robbers despite there being plenty of honey and pollen

stores.

4. Common hive parasites are not present at levels that are thought to cause population decline.

Most scientists agree that there is no one single cause of CCD, but rather a combination of factors, such as nutritional stress, pathogens, and pesticides, that weaken bee colonies by impairing the honeybee's immunity (vanEngelsdorp *et al.* 2009).

Nutritional stress can affect colony health in several ways such as immune system suppression and reducing reproductive viability of the honeybees (Pilatic 2012). A key factor in nutritional stress is habitat loss. Due to the loss of habitat, the honeybee has a less varied and nutritious diet (Pilatic 2012). Contributing factors may include a decreased ratio of open to developed land and the use of broad-spectrum herbicides on herbicide-resistant, genetically engineered crops (Benbrook 2009).

Pathogens have also been implicated as a cause of CCD. In many cases, this is complicated by multiple pathogens present at the same time between separate bee colonies (each colony expresses different diseases in various combinations) (du Rand *et al.* 2015). The most common pathogens are parasitic mites, viruses and gut fungus. *Varroa* mites, the most important pests to honeybees, rapidly increase in population size after invading the hive and attach to developing larvae thereby devastating a colony. The *Varroa* mite sucks hemolymph from both the brood and the adult bees, affecting bee development within the brood and weakening the adult bees (Le Conte *et al.* 2010). *Varroa* mites also act as vectors to transmit a number of viruses that can weaken the colony (Zemene *et al.* 2015). Viruses that may contribute to CCD are deformed wing virus and other related paralysis viruses that threatened bee survival by causing adult bees to lose their ability to fly (Coulon *et al.* 2018). Also implicated in CCD is the fungus *Nosema*, a pathogen that affects the digestive system of the workers (van Dooremalen *et al*. 2018). Other potential reasons for CCD are new and emerging diseases, immune-suppressing stress due to any of the reasons previously mentioned, and a lack of genetic diversity (United States Environmental Protection Agency 2016).

Pesticides as Environmental Stressors:

Pollinating insects are at risk for continuous exposure to a multitude of agrochemicals (Pereira *et al.* 2020). In the U.S., over 1 billion pounds of pesticides are

used annually, amounting to $14 billion in sales (Atwood and Paisley-Jones 2017, Alavania 2009). Over 1,200 active ingredients are approved, contributing to 18,000 different commercial formulations (Pilatic 2012). There are five major classes of pesticides: organophosphates, carbamates, pyrethyroid, neonicotinyls and chlorinated hydrocarbons (Agronomy 2017). A study performed by Frazier and colleagues (2008) analyzed 108 pollen samples and identified a total of 46 different types of agrochemicals. A total of 17 different types of agrochemicals were identified from a single pollen sample in an *Apis mellifera* colony.

The neonicotinyls are a synthetic insecticide related to nicotine. Neonicotinoids bind irreversibility to nicotinic acetylcholine receptors (nAchR), ligand-gated ion channels on postsynaptic membranes. Acetylcholine is the major excitatory neurotransmitter in the honeybee brain and controls a wide-range of behaviors essential for survival. Due to the distinct features of their nAchR subtypes, insects are much more sensitive to neonicotinoid pesticides than birds or mammals (Tomizawa *et al.* 2000). Compared to other classes of insecticides, neonicotinoids are less toxic to birds and mammals than insects leading to their widespread usage as insecticides (Agronomy 2017). Neonicotinoids have been an integral part of the global insecticide market since the 1990s. At least 143 million of the 442 million acres of United States croplands are planted with crops treated with 1 of 3 neonicotinoid pesticides that are known to be highly toxic to bees (Pilatic 2012). These pesticides are clothianidin, imidacloprid and thiamethoxam.

The mechanism of action of neonicotinoids on honeybee neurons has been recently reviewed (Cabirol and Haase 2019). Neonicotinoids are acetylcholine agonists. After binding to the nAchR, neonicotinoids produce a biphasic response. Initially, there is an increase in the frequency of depolarization of the postsynaptic neuron followed by a complete block to nerve signal propagation (Schroeder and Flattum 1984). Bees treated with neonicotinoids initially show hyperactivity followed by convulsions and eventual paralysis (Cabirol and Haase 2019). As shown in Figure 6, under normal conditions, acetylcholinesterase in the synaptic cleft breaks down acetylcholine which prevents overstimulation of the nAchRs. Neonicotinoids cannot be broken down by acetylcholinesterase leading to overstimulation of the postsynaptic neuron. The specific

effects of neonicotinoids on the bee brain are complicated by the diversity of nAchRs and their differential expression in various brain regions and developmental stages (Cabirol and Haase 2019).

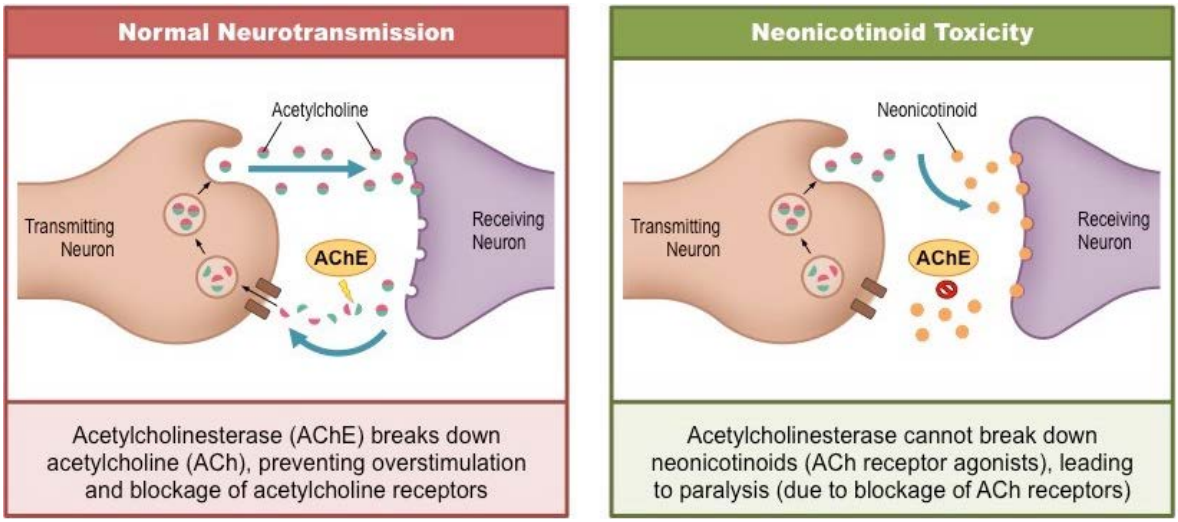

Figure 6: Neurotransmission with acetylcholine and neonicotinoids (Photo Credit: BioNinja NA). Nicotinic acetylcholine receptors, also known as nAchRs, are cholinergic receptors. These receptors form ligand-gated ion channels within the plasma membranes of postsynaptic neurons in the central nervous system of the honeybee.

There are two classes of broad-spectrum neonicotinoids: nitroguanidines and cyanoamines (Wu-Smart et al. 2016). Nitroguanidines are highly toxic to honeybees and consist of imidacloprid, clothianidin, thiamethoxam and dinotefuran. Cyanoamines are not as acutely toxic to the honeybee and include thiacloprid and acetamiprid (Wu-Smart et al. 2016). Levels of these neonicotinoids in bee food sources are typically minute, ranging from <1 to 8.6 ppb in nectar and <1 to 51 ppb in pollen (Goulson 2013) (Appendix B-D). However, one type of exposure, corn seedling guttation, has been shown to expose bees to neonicotinoid doses that exceed the LD_{50} (Girolami *et al.* 2009). Even though neonicotinoid concentrations in nectar and pollen may be well below their toxic lethal doses, they may produce sublethal effects in the bees that can have dramatic effects on the colonies.

Environmental risks caused by neonicotinoids are still in question. Predominately used as seed dressings, this process provides better targeting of the crop than spray applications and with no action from the farmer, the crops are protected for several months following sowing (Goulson 2013). Although there is evidence that neonicotinoid application provides effective control of a range of insect pests, it is not clear as to the

extent this has on increased farm production or if there are increased economic benefits when compared to alternatives (Goulson 2013). Other contributing factors to increase production or profits are improved crop varieties, widespread use of artificial fertilizers, new agronomic techniques and the development of successive generations of pesticides. There is also a scant amount of studies to compare the effectiveness of neonicotinoids with alternative means of pest control (Goulson 2013).

The persistence of neonicotinoids in soil is of great concern. Studies have shown that between 1.6 and 20% of the active ingredient of seed dressings is absorbed by crops, whereas the uptake by traditional spray applications exceed 50% (Goulson 2013). Up to 2% of the active ingredient is lost as dust during sowing, causing mortality to honeybees flying nearby, and can be deposited on field vegetation at concentrations from 1-9 ppb (Goulson 2013). More than 90% of the neonicotinoid active ingredient enters the soil and can persist for 200, to > 1,000 days. Due to the high translocation rate of neonicotinoids in plants, insecticides like imidacloprid, reach the flowers, leaving residue in the nectar and pollen (Pereira *et al.* 2020). Foragers will continue to visit imidacloprid-treated crops despite nectar and pollen contamination. These trips remain regular but at a slower rate (Kessler *et al.* 2015, Pereira *et al.* 2020). Although the foragers' cognitive process is not significantly affected, the nectar odor that is brought back to the hive with them recruits additional bees to visit the "contaminated" flowers, ultimately increasing the amount of insecticide in the hive (Pereira *et al.* 2020).

The neonicotinoid imidacloprid became the world's largest selling insecticide, and second largest selling pesticide in 2008 with registered uses for over 140 crops in 120 countries (Jeschke *et al.* 2011). In 2010, it was estimated that 20,000 tons of imidacloprid was produced globally, with 14,000 tons produced by China, which then exported 8,000 tons (Simon-*Delso et al.* 2015). With over 400 products for sale in the United States, imidacloprid can be found as liquids, granules, dust, and packages that dissolve in water. It is used for crops, inside and outside the home, as well as flea medications for animals (Gervais *et al.* 2010). The two largest manufacturers of imidacloprid in the United States are Crop Science and Albaugh LLC AgriStar (Figure 7; Bayer Crop Science 2017, Albaugh LLC 2017).

$C_9H_{10}ClN_5O_2$

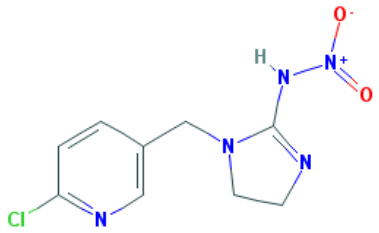

Figure 7: Chemical structure and molecular formula of imidacloprid (National Center for Biotechnology Information 2020). IUPAC name of *N*-{1-[(6-Chloro-3-pyridyl)methyl]-4,5-dihydroimidazol-2-yl}nitramide.

The number of deleterious effects that imidacloprid has on honeybees continues to grow as more research is performed. Since neonicotinoids act on the central nervous system, there are many physiological and behavioral impairments that have been observed in worker bees. For example, bees exposed to sublethal doses of imidacloprid have impaired foraging and homing abilities, suppressed immunity, delayed larval development and reduced longevity, and diminished olfactory learning and memory capacity (Henry *et al.* 2012**,** DiPrisco *et al.* 2013, Wu *et al.* 2012, Pereira *et al.* 2020, Decourtye *et al.* 2004a, Decourtye *et al.* 2004b, Decourtye *et al.* 2003).

Pesticide Dynamics in Honeybees:

First defined by entomologist William Morton Wheeler in 1918, trophallaxis is defined as the transfer of food or other fluids among members of a community (Wainselboim *et al.* 2000). While worker bees acquire neonicotinoids directly from consuming contaminated nectar or pollen, the queen bee may be exposed indirectly through trophallaxis or food-sharing. A study by Wu-Smart and Spivak (2016) demonstrated that environmentally relevant doses of imidacloprid had harmful effects on queens (egg-laying and locomotor activity) and colony development (brood production and pollen stores). These effects were less evident in larger colonies. Larger colony populations may act as a buffer to pesticide exposure. Trophallaxis may help to lessen the toxicity of pesticides by evenly distributing them among nest mates. This dilutes the pesticides with uncontaminated food or bodily fluids already in the gut, rendering them less harmful.

In addition to neonicotinoid pesticides, honeybees are exposed to other non-neonicotinoid pesticides such as fungicides and pyrethroids. A key mechanism used by insects to counteract the effects of these toxins is metabolic resistance (du Rand *et al.*

2015). The major enzyme superfamilies that detoxify toxins are cytochrome P450 monooxygenases, glutathione transferases, and carboxylesterases. As previously noted, there is a 30-50% or more reduction in the number of genes that encoded these enzyme families compared to other insect genomes (Honeybee Genome Sequencing Consortium 2006). It is possible that because honeybees have fewer detoxification genes, their ability to metabolize multiple toxins simultaneously are hindered (du Rand *et al.* 2015). For example, fungicides inhibit cytochrome P450s that are important in insecticide detoxification pathways (Johnson 2006). As previously mentioned, CCD has no single cause which raises the possibility of synergy. For example, a pesticide in combination with a fungicide can enhance toxicity. Studies have also shown synergistic effects between pathogens and pesticides which led Poquet *et al.* (2015) to pose the question: Does a pesticide promote pathogenicity of the pathogen or does the pathogen increase toxicity of the pesticide?

The mechanisms used by healthy honeybees to detoxify neonicotinoid insecticides are not well characterized. The goal of the du Rand study (2015) was to shed light on the molecular mechanisms that honeybees use to detoxify nicotine, a toxic natural alkaloid found in plants in the *Solananceae* family, such as tobacco. Nicotine and synthetic neonicotinoid pesticides have similar modes of action; both mimic acetylcholine by binding to nAchRs. This study used mass spectroscopy-based metabolic and proteomic analysis to determine metabolic pathways and protein networks involved in nicotine detoxification in newly emerged worker bees. The results indicated that honeybees actively detoxify nicotine to its less-toxic metabolites, cotinine and cotinine N-oxide (Phase I detoxification). This was followed by Phase II detoxification, conjugation with glutathione catalyzed by glutathione-S-transferases. A total of 1470 proteins were identified with nearly 100 proteins that were up-regulated and 60 that were down-regulated. The largest groups of up-regulated proteins include those whose functions related to energy metabolism (ATP synthesis, glycolysis, TCA cycle enzymes, etc.) suggesting increased energy production to support detoxification processes. Also, up-regulated were proteins involved in detoxification, heat shock, and anti-oxidant responses. The authors proposed that the increased energy production led to increases in reactive oxygen species, which induced the expression of antioxidants and stress response

proteins. Based on their results, du Rand *et al.* (2015) proposed a model in which nicotine exposure activates detoxification, oxidative, and stress response pathways in concert with an increase in energy metabolism (Figure 8). These complex responses of honeybees to nicotine provide a basis for us to predict the outcomes of our studies investigating the effects of imidacloprid on the honeybee transcriptome.

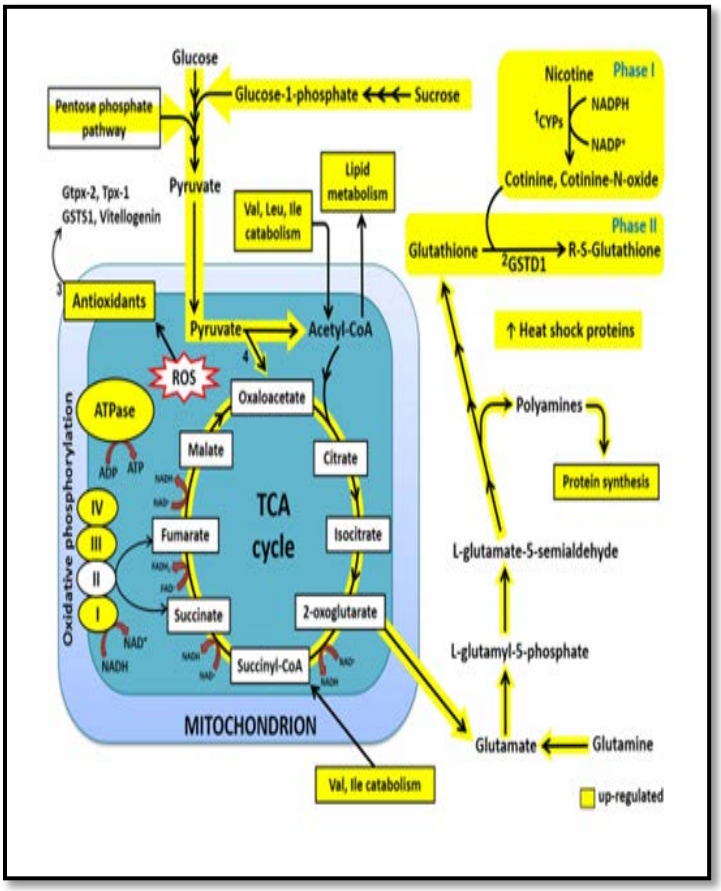

Figure 8: Proposed mechanisms underlying the honeybee response to nicotine exposure (du Rand *et al.* 2015).

Effects of Neonicotinoid Pesticides on the Honeybee Transcriptome:

While previous studies have found that sublethal doses of neonicotinoids impair learning, memory capacity, foraging, and immunocompetence in honeybees, not much is known about their molecular effects. Since undertaking this thesis work, several laboratories have conducted studies to determine the effects of neonicotinoid pesticides on the honeybee transcriptome. A study performed by Shi and colleagues (2017) examined the transcriptome profile of honeybees after sub-chronic exposure to

thiamethoxam, a second-generation neonicotinoid, at 10 ppb over 10 days. Overall, there were 609 differentially-expressed genes. Of these 609 genes, 225 genes were up-regulated while 384 were down-regulated. The differentially-expressed genes were mainly found to be associated with metabolism, biosynthesis, and translation (Shi *et al.* 2017). Zhiguo *et al.* (2019) reported down-regulation of brain genes related to immune, detoxification, and chemosensory responses in honeybees after chronic oral exposure to sublethal doses of imidacloprid. They proposed that this may contribute to decreased olfactory learning abilities in imidacloprid-treated bees. Work by Wu *et. al* (2017) has shown that genes encoding the major royal jelly proteins, essential for the health of sustainable colonies, were strongly down-regulated in honeybee larvae exposed to sublethal doses of imidacloprid.

Effects of neonicotinoids on the honeybee brain appear to be dose dependent. Christen *et al.* (2018) reported that honeybees treated for 48 hours with 0.3 ng/bee of imidacloprid had 7 coding regions up-regulated and 19 regions down-regulated. When this study was repeated with 3 ng/bee of imidacloprid, a total of 36 regions were up-regulated and 77 regions were down-regulated providing evidence that different genes are transcribed when bees are exposed to different amounts of imidacloprid. In particular, genes related to metabolism and detoxification were differentially expressed, generally in a concentration-dependent manner. Collectively, these studies highlight the utility of transcriptome profiling in providing insights into the mechanisms mediating the toxicity of pesticides. Clearly, future studies are needed to tease out such details as dose dependency, chronic versus acute exposures, laboratory versus field exposures, synergistic effects, and differences among caste members and developmental stages. Importantly, for a better understanding of the effects of neonicotinoids on honeybees, future studies are needed that link their molecular effects to physiology and behavior.

Sublethal Stress in Honeybees:

Regulatory agencies assess the impact a pesticide or chemical agent has by determining the acceptable risk. Acute toxicity is quantified by determining the dose at which half of the insects die within a specific time frame, denoted as LD_{50} as seen in Figure 9 (Pilatic 2012).

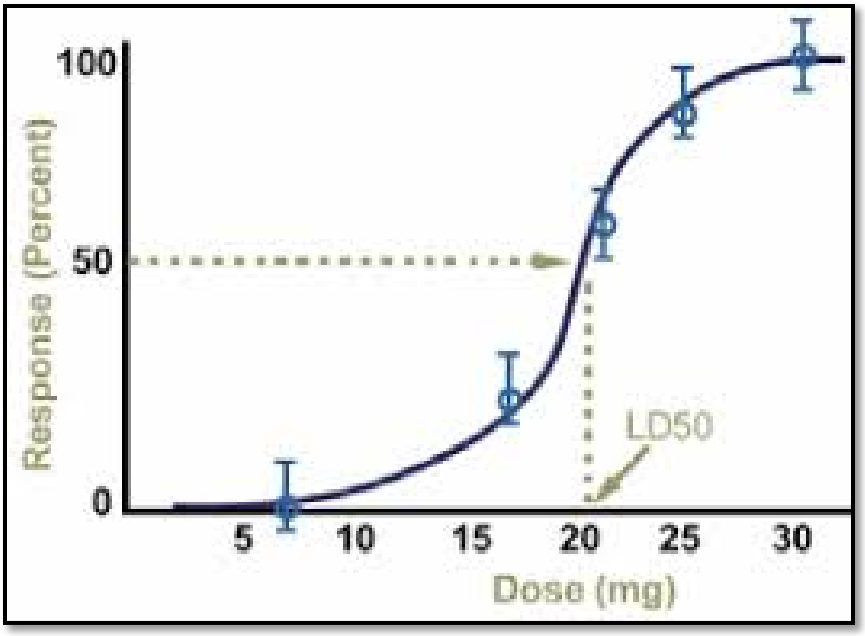

Figure 9: Dose-response relationship for acute toxicity (Möller NA). Also known as lethal toxicity, the LD_{50} (denoted by the grey arrow) is determined by the dose at which half of the insects die within a specific time frame.

The symptoms of acute toxicity include agitation, vomiting, wing paralysis, arching of the abdomen, and uncoordinated movement. More common in field exposure, sublethal toxicity has symptoms of disorientation, reduced mobility and foraging, impaired memory and learning, and shifts in communication behavior (Blacquière *et al.* 2012). While these sublethal effects do not kill individual bees, they may have a profound impact on the dynamics and function of the whole colony. For example, these sublethal impacts may interfere with the food collection process for the colony impairing foraging, the proboscis extension reflex, olfactory learning and memory (Blacquière *et al.* 2012). Sublethal effects may also negatively impact reproductive rate, survival of larvae, and recruitment into nurse castes which ultimately weakens the hive, leading to colony losses that may not become apparent for weeks (Blacquière *et al.* 2012). Furthermore, the reduced viability and quantity of the stored sperm in the mated queen may compromise the queen's breeding success (Wu-Smart and Spivak 2016).

A leading hypothesis for CCD is sublethal stress due to environmental stressors such as pesticides, disease and parasites, habitat change and loss (Bryden *et al.* 2013). Redundancy in social bee colonies allows for a significant loss of their workers without any significant impact on colony function and productivity. However, if bees become

impaired rather than die, this may impose undue stress on the colony which can lead to a cumulative effect on normal colony function through indirect mortality and production losses not attributed to pesticides (Bryden *et al.* 2013). The Sublethal Stress (SLS) Model introduced by Bryden *et al.* (2013) incorporates the effects of sublethal stress on colony function to explain these colony dynamics. The SLS Model (Figure 10) predicts that colonies can either persist or become extinct, dependent on the initial conditions that determine whether or not the colony exceeds critical reproductive and mortality rates (Bryden *et al.* 2013).

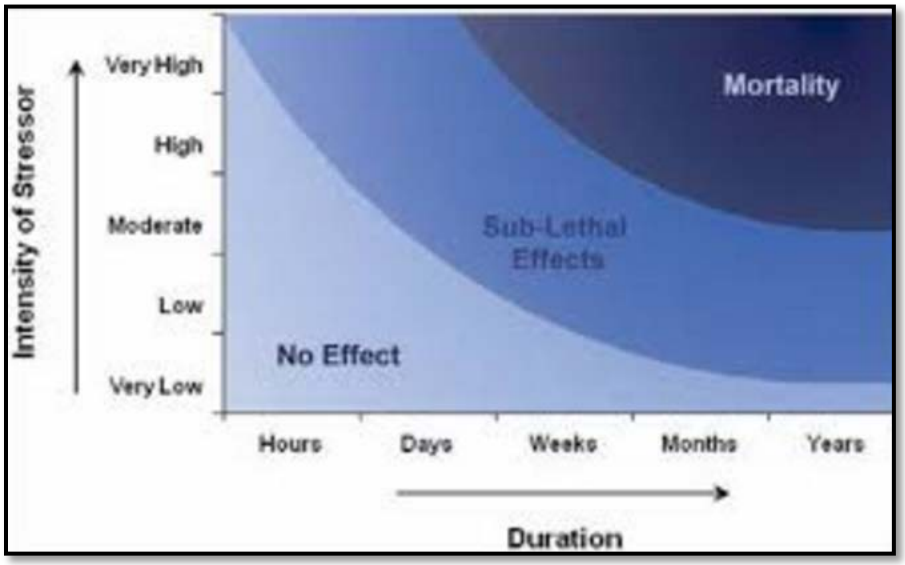

Figure 10: Sublethal Stress (SLS) Model (based on the Bryden model 2013). The model shows the relationship between the intensity of a stressor and its duration and how this could lead to no effect, sublethal effects or mortality.

To test this mathematical model, Bryden's laboratory compared colony dynamics in bumble bees treated with field-relevant doses of imidacloprid. The patterns of colony sizes, birth rates, and death rates fit the SLS Model. Bumble bee colonies failed when they were exposed to sublethal levels of imidacloprid for an extended period of time resulting in a decrease in colony function (Bryden *et al.* 2013). By testing models against data collected from failing colonies, it was concluded that social bee colonies have positive density dependence, are subject to an Allee effect (that population size or density is correlated with the mean individual fitness of a population), and that there is a critical stress level for the success of a colony (Bryden *et al.* 2013, Drake and Kramer 2011).

They concluded that small increases in the level of stress can swing the pendulum towards success or failure of the hive.

The SLS Model was compared to two alternative models: the Khoury Model and the LA Model. The Khoury Model included lethal stress but not the impairment and feedback caused by sublethal stress whereas the LA Model includes the toxic effects from pesticides at the larval stage (Bryden *et al.* 2013). These three models were fitted using the NISS algorithm that calculates a likelihood value for a model based on all possible paths. From this modeling, it was determined that the SLS Model best matched the pattern of birth rates decreasing and death rates increasing in the treated colonies. It was concluded that colony function is important, in explaining the dynamics of the treated colonies and therefore suggests a mechanism by which sublethal effects on individual bees can lead to colony failure (Bryden *et al.* 2013). This study demonstrates that sublethal stressors must have a chronic impact before effects are observed and that stressors that impair colony function cause an Allee effect, making colonies susceptible to stress at earlier points in their life cycle. The authors point out the irony that the elaborate social organization that leads to the success of social bees may also be a key factor contributing to colony failure and their population declines.

Cellular Responses to Stressors by Honeybees:

A general indicator of cellular stress is Heat Shock Protein 70 (HSP70). Although normally present in cells, HSP70 levels become elevated at times of stress to help maintain stress resistance (e.g., Hranitz *et al.* 2009). HSP70, a molecular chaperone, works by binding peptides to prevent misfolding during exposure to foreign toxic substances or other stressful conditions. Once the stressor is removed, the peptides are released and are able to return to their normal cell functions. If stress levels become too elevated, it is possible for HSP70 to activate apoptotic mechanisms and cause cell death to avoid an inflammatory response. When cells are exposed long-term to stress, irreversible consequences such as loss of nervous system control, delayed growth, and inability to process sensory input for foraging may occur (Feder *et al.* 1997, Jones *et al.* 2007). HSP70 is an excellent marker for measuring cellular stress in honeybees and has proven useful in a variety of applications, such as evaluating management practices, assessing seasonal changes, and in toxicological studies (Hranitz *et al.* 2009).

Although there are linear and threshold models of stress, the hormesis toxicology model can explain the entire range of physiological stress responses. Hormesis is defined as a dose-response relationship that is stimulatory at low doses and inhibitory at higher doses (Deng *et al.* 2001). The hormetic model illustrates variable stimuli proportions as parabolic curves. This allows for inferences on positive, negative, and peak response levels across a range of treatments (Calabrese 2008). Figure 11 illustrates hormesis as it relates to stress and effect or dose and response.

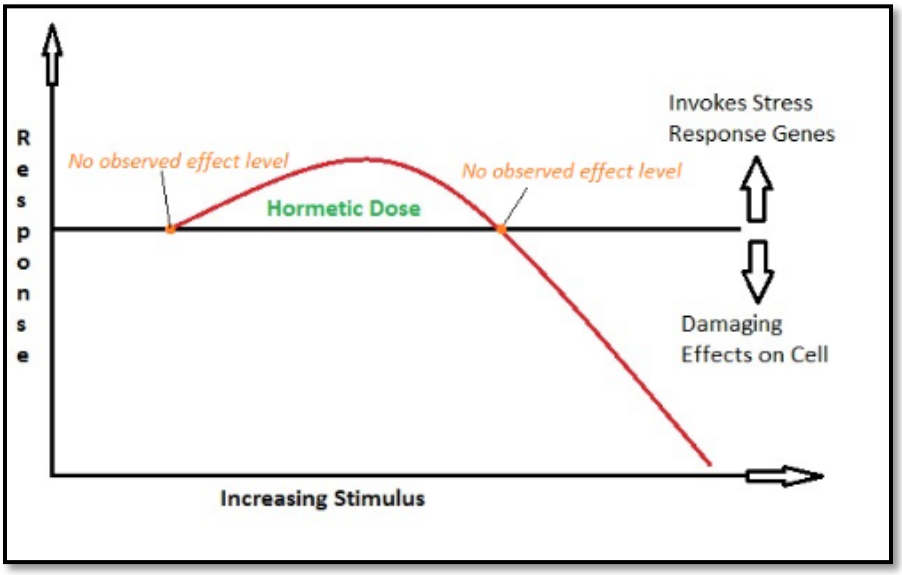

Figure 11: Hormesis dose-response curve (Merritt 2011-2020). Hormesis is a U- or J-shaped dose-response curve characterized by a low-dose stimulatory and high-dose inhibitory responses. A stimulus that produces a harmful biological effect at a moderate to high doses may produce beneficial effects at lower doses (Calabrese 2008).

The hormesis model was useful in describing the response of honeybees to ethanol in a study performed by Hranitz and colleagues (2010). This study, based on work by the Abramson Laboratory at Oklahoma State University, previously demonstrated that ethanol intoxication has dramatic effects on learning and behavior in the bee. Intoxicated honeybees were less active, had poor motor coordination, demonstrated preference for sugar in ethanol solutions, showed increased levels of aggression, displayed impaired foraging decisions and poor communication, and had a similar time course of elevated blood alcohol elevation as humans (Abramson *et al.* 2000, 2002, 2003, 2004a, 2004b, 2005; Bozic *et al.* 2006, 2007). Levels of HSP70 were measured at 4-hours post-ingestion in control bees fed 1.5 M sucrose or bees fed with 2.5%, 5%, or 10% ethanol (Figure 12; Hranitz *et al.* 2010). A hormetic response was

observed with peak levels of HSP70 noted at 5% ethanol. HSP levels were lower at higher (10%) and lower (2.5%) ethanol concentrations.

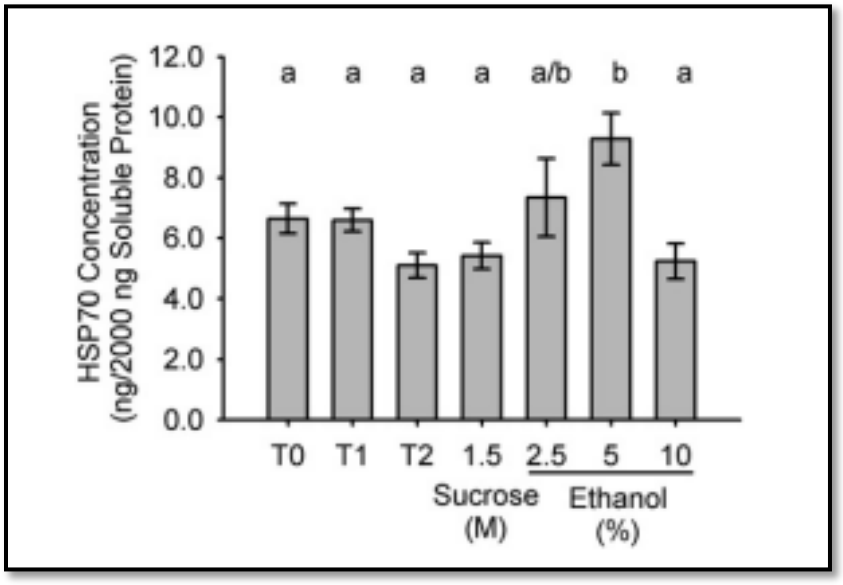

Figure 12: HSP70 concentrations among pretreatment groups of honeybees and those treated with ethanol (Hranitz et al. 2010). The above graph shows high stress levels, as indicated by HSP70, appeared when cellular stress was induced with ethanol intoxication. A hormesis curve is noted among the treatment group. **A** is significantly different than **B** at $p < 0.05$.

RNA microarray studies of gene expression in the honeybee brain following the four-hour exposure to ethanol showed significant changes in 609 genes. Gene ontology analysis revealed changes in brain metabolism, cellular stress, and signaling pathways, protein synthesis, and carbohydrate and lipid metabolism (Hranitz et al. unpublished). A similar approach will be applied to this investigation to determine the effects of sublethal doses of imidacloprid on the honeybee brain transcriptome.

Oxidative Stress:

Pesticides have been found to produce oxidative stress in honeybees (Henry *et al.* 2005). Oxidative stress occurs when reactive oxygen species accumulate in an organism and cause damage (Berlett and Stadtman 1997). Reactive oxygen species (ROS) are unstable chemical species containing oxygen that are formed during aerobic metabolism. Examples of ROS include peroxide, hydroxyl radicals, and superoxide. Under normal circumstances, ROS are in low concentrations. When an organism is under high stress, ROS begins to accumulate in cells causing damage to DNA, lipids, and proteins. ROS have been linked to diseases such as cancer, diabetes, and heart disease in humans. ROS

are degraded by antioxidant enzymes such as superoxide dismutase, catalase, and glutathione transferase. Superoxide dismutase (SOD) converts superoxide, a powerful ROS, to the less dangerous hydrogen peroxide. Catalase and glutathione transferase (GST) work to convert hydrogen peroxide to water. High levels of these antioxidant enzymes in organisms is an indicator of oxidative stress (Finkel and Holbrook 2000).

The link between pesticides and levels of antioxidants enzymes in honeybees has been demonstrated in recent field studies. A study performed by Dussaubat *et al.* (2016) reported increased catalase and GST activity in the head of queen bees following exposure to environmentally relevant concentrations of imidacloprid. Chakrabarti *et al.* (2014) compared the effects of the pesticide paraquot on the levels of antioxidant enzymes in laboratory and field populations of two native Indian bees. The results showed elevated levels of antioxidant enzymes in bees exposed to sublethal doses of pesticides in the field and in the laboratory compared to controls. The authors postulated that these higher levels of antioxidants help to protect bees during exposure to environmental stressors. Oxidative stress has been shown to decrease the survival and homing abilities of honeybees (Simone-Finstrom *et al.* 2016). This is important since most crops are pollinated by honeybees that are transported from state to state, a procedure called migratory management. It has been found that migratory management induces oxidative stress in bees and produces effects that are similar to that of CDD. The study concluded that there was a significant decrease in lifespan and foraging capabilities of the affected bees (Simone-Finstrom *et al.* 2016). Together these studies underscore the need to understand the mechanisms underlying the toxicity of neonicotinoid pesticides and their contribution to pollinator decline.

II. Objectives and Research Questions

Goal: The overall goal of our research is to describe the integrated responses by the honeybee to sublethal doses of the common neonicotinoid, imidacloprid. This research expands on previous studies in our laboratory, and on independent studies, by investigating the physical, cellular, and molecular responses to imidacloprid by the honeybee brain.

Specific Objectives: This research was conducted in two phases- Experiment 1 and Experiment 2. The specific objectives of each are:

- Experiment 1: The Effects of Sublethal Doses of the Neonicotinoid Pesticide Imidacloprid on Motor Function and Cellular Responses in Honeybees.
    - To determine the effects of sublethal doses of imidacloprid on motor function and overall cellular stress as determined by the levels of Heat Shock Protein 70 and the oxidative stress enzyme Superoxide Dismutase.
    - To identify a sublethal dosage of imidacloprid that yields a significant cellular stress response that will be used in Experiment 2.
- Experiment 2: The Effects of Sublethal Doses of Imidacloprid on Gene Expression in the Honeybee Brain
    - To compare overall gene expression in brain tissue of the control and imidacloprid treatment groups.
    - To determine which functional classes of genes are up-regulated or down-regulated following imidacloprid treatment.
    - To examine differences in gene expression that occur following imidacloprid treatment in pathways regulating detoxification, heat shock proteins, oxidative enzymes, energy metabolism, circadian rhythms, cell signaling, apoptosis, and longevity.

Hypotheses:

- Bees exposed to sublethal doses of the neonicotinoid imidacloprid will display impaired motor functions and a significant cellular stress response reflected by increased levels of Heat Shock Protein 70 and the oxidative enzyme Superoxide Dismutase.
- A dose of imidacloprid can be determined that yields a significant cellular stress response in honeybee brains.
- Gene expression patterns will be altered in the brain tissue in imidacloprid treated bees compared to controls.

- Bees treated with imidacloprid will express different functional classes of genes compared to control bees.
- Pathways regulating detoxification, heat shock proteins, oxidative enzymes, energy metabolism, and apoptosis will be up-regulated, while pathways regulating circadian rhythms, cell signaling, and longevity will be down-regulated in imidacloprid-treated bees.

Significance of the Study: This study investigates how acute sublethal exposure to imidacloprid, the most widely used neonicotinoid pesticide, affects gene expression in an economically crucial pollinator. An understanding of the specific gene networks and cellular pathways affected by sublethal imidacloprid intoxication may help the scientific community to better understand the mechanisms of neonicotinoid toxicity underlying the sublethal pesticide effects contributing to pollinator declines. This work can serve as a springboard for future hypothesis-driven gene expression studies that relate specific molecular changes to biological functions and organism-level performance. This integrated approach, connecting the responses of organisms in the field to their underlying cellular and molecular mechanisms, is essential to understanding and preventing CCD.

III. Methods

Experiment 1: The Effects of Sublethal Doses of the Neonicotinoid Pesticide Imidacloprid on Motor Function and Cellular Responses in Honeybees

a. *Experimental Design*

Figure 13 outlines the overall design of Experiment 1. First, honeybees were collected, harnessed, and fed with 1.5 M sucrose to satiation. Surviving, healthy honeybees were randomly assigned to control or treatment groups after 22-24 hours after harnessing and feeding. The total number of honeybees is n=149 (Negative Control= 20, Positive Control= 18, $1/5^{th}$= 19, $1/10^{th}$= 18, $1/20^{th}$= 17, $1/50^{th}$= 20, $1/100^{th}$= 20, and $1/500^{th}$= 17). Control groups were fed 1.5 M sucrose while treatment groups received sublethal doses of imidacloprid in 1.5 M sucrose (Appendix E and F). After 4 hours, bees were tested for motor responses and bee heads were removed and frozen for subsequent

measurement of HSP70, a marker of cellular stress, and SOD, a marker for oxidative stress. After evaluating these results, an optimal sublethal dose of imidacloprid was selected to dose bees in Experiment 2 for determining its effects on the bee brain transcriptome.

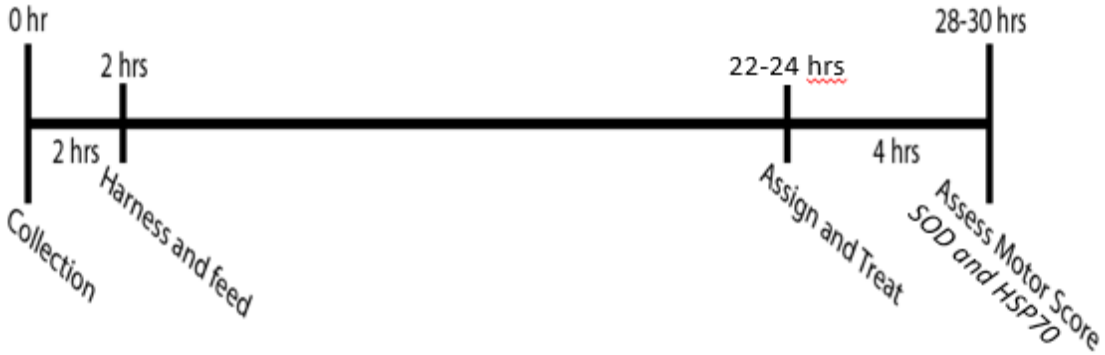

Figure 13: Experiment 1 design. Upon collection, the honeybees were harnessed in modified 1.5 mL microcentrifuge tubes and fed to satiation. After 22-24 hours at room temperature (22°C), bees were randomly assigned to a control or treatment group. At 4 hours after treatment, motor scores were assessed, or bee heads were removed for analysis of HSP70 and SOD.

b. Honeybee Collection:

Honeybees were collected locally at hives maintained by Dr. John M. Hranitz, Bloomsburg, PA. Bees were recruited to a feeder located 10 meters from the hive. The feeder consisted of an inverted mason jar containing a 50% sucrose solution with a few drops of orange extract (Figure 14a). Bees were then captured in groups of 2-3 in clear plastic collection jars with holes in the lid and transported to the laboratory on campus in a cooler (Figure 14b). Bees were anesthetized at -20°C for about 3-5 minutes until immobile and then were restrained in harnesses modified from 1.5 mL microcentrifuge tubes with thin strips of duct tape placed between the head and thorax (Figure 14c). Bees were fed 1.5 M sucrose to satiation and held for 22-24 hours at room temperature (22°C).

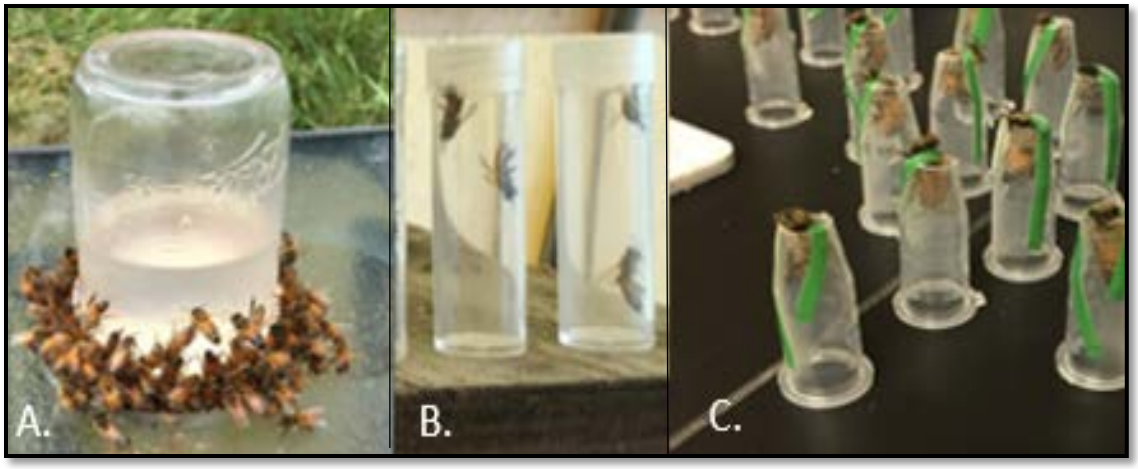

Figure 14: Honeybee feeder, collection, and harnessing. A) A glass mason jar inverted on the lid of a petri dish was used as a feeder. The feeder contained a 50% sucrose solution and orange extract as an attractant. B) Once a significant number of bees were attracted to the feeder, carefully, two or three bees were captured into a clear collection jar with a lid that contained holes so that they could be transported. C) Honeybees were harnessed in modified 1.5 mL microcentrifuge tubes and secured with a thin piece of duct tape.

Negative and positive control bees were fed 1.5 M sucrose. The bees in the negative control group remained at room temperature (22-25°C) while bees in the positive control groups were placed in an incubator set to (42°C). A temperature of 42°C was chosen because it falls slightly below the critical thermal maximum for *Apis mellifera*, 42.8 ± 2.8°C (Atmowidjojo *et al.* 1997). Cellular stress responses have been shown to reach their peak slightly below the critical thermal maximum (Atmowidjojo *et al*. 1997). Honeybees in the treatment groups were fed with imidacloprid (Macho®4.0, AgriStar, 40.07 g imidacloprid/100 g solution) in 1.5 M sucrose at doses of 3.6 ng/µL ($1/5^{th}$), 1.8 ng/µL ($1/10^{th}$), 0.9 ng/µL ($1/20^{th}$), 0.36 ng/µL ($1/50^{th}$), 0.18 ng/µL ($1/100^{th}$) and 0.036 ng/µL ($1/500^{th}$) of the LD_{50} (18 ng/bee) (Figure 15; Karahan *et al.* 2015). Both control and treatment groups were monitored for four hours. At the completion of the treatment, motor coordination was evaluated, and bee head capsules were removed and frozen at -80°C to be used in HSP70 or SOD assays.

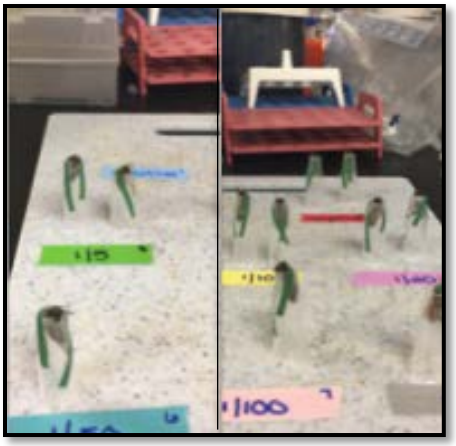

Figure 15: Honeybee treatment. Honeybees were randomly assigned following the satiation period. The treatment groups were color coordinated, labeled with the treatment doses, and numbered. The honeybees were separated and faced away from each other to avoid trophallaxis.

c. *Motor Testing*:

Four hours after treatment, all groups of honeybees (n=149) were scored in four categories of motor function: leg movement, abdomen movement, antennae responsiveness, and proboscis extension reflex. Leg and abdomen movement were simply observed while the bee was in the harness. The antennae and proboscis extension reflex were tested by bringing a Q-tip dipped in 1.5 M sucrose close to the antennae and proboscis and observing the response. Each test was scored either 0 for no function, 1 for impaired function, or 2 for normal function. The maximum score that each bee could obtain was 8 and a minimum score was 0.

d. Homogenization of Bee Head Capsules

After treatment, frozen head capsules were homogenized in microcentrifuge tubes with a pestle in phosphate buffered saline (PBS) containing 0.2% sodium azide, 2 mM p-tosyl-L-arginine methyl ester (TAME), and a protease inhibitor cocktail (Roche), pH 7.6. The homogenates were then centrifuged at 16,000 g for 20 minutes at 4°C. The supernatant was removed and stored at -80°C.

e. Superoxide Dismutase (SOD) Assay

Superoxide Dismutase Colorimetric Activity Kit by Arbor Assays (Kit K028-H1) was used to test for SOD in thawed bee head supernatants. SOD neutralizes superoxide radicals (O_2^-). In this assay, xanthine oxidase produces superoxide in the presence of oxygen. The superoxide produced converts a colorless substrate into a yellow-colored product. The reactions involved in the assay are shown below (Figure 16). When more

SOD is present in the samples, the superoxide concentration will decrease, resulting in less yellow-colored product.

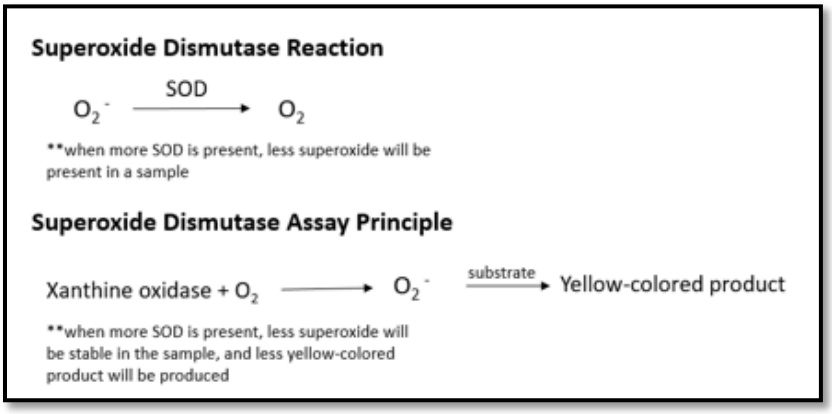

Figure 16: Superoxide dismutase reaction and assay principle (Arbor Assays).

Standards were prepared by making serial dilutions of the bovine erythrocyte SOD standard provided in the kit at concentrations of 4.0 U/mL, 2.0 U/mL, 1.0 U/mL, 0.5 U/mL, 0.25 U/mL, 0.125 U/mL, and 0.0625 U/mL. Ten µL of the appropriate standards and samples were pipetted in duplicate into a 96-well Corning Costar 3695 plate. Ten µL of assay buffer was pipetted into the top row of wells to serve as a blank. This was followed by additions of 50 µL of substrate solution and 25 µL of xanthine oxidase solution to each well. The plate was incubated at room temperature for 20 minutes and the absorbance was then read at 450 nm using a Tecan Genios Plus Microplate Reader and Magellan software (Figure 17).

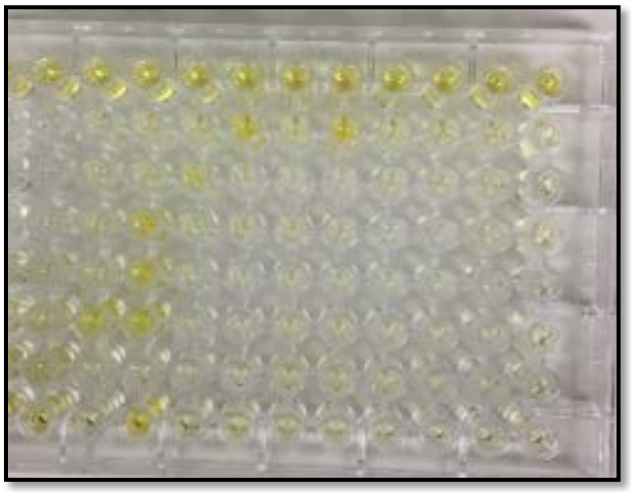

Figure 17: SOD assay microplate. Xanthine oxidase produces superoxide in the presence of oxygen. The superoxide produced converted the colorless substrate into a yellow-colored product. Greater levels of SOD in the sample result in less of a yellow-colored product.

SOD activity was calculated for each sample in U/mL using MyAssay software. Samples were corrected for protein content by dividing the SOD activity by the protein concentration in the sample which had previously been determined.

f. *Protein Assay*

The protein concentration of each sample was determined using a colorimetric dye-binding assay (Bio-Rad RC DC Protein Assay Kit). The homogenization buffer served as blanks and standards were prepared by making serial dilutions of Bovine Serum Albumin (BSA stock- 7.1 µg/µL) in homogenization buffer (Appendix G).

Using the Bio-Rad Protein Assay Kit, Reagent A^1 was prepared by adding 50 µL of Reagent S to 2.5 mL of Reagent A. Five µL aliquots of the protein standards, blanks, and samples were pipetted in triplicate into a 96-well Corning Costar 3695 plate. Next, 25 µL of A^1 was added to each well, followed by 200 µL of Reagent B. Plates were then gently agitated using a rotator. After 15 minutes, absorbance was measured at 750 nm using the Tecan Genios Plus Microplate Reader (Figure 18).

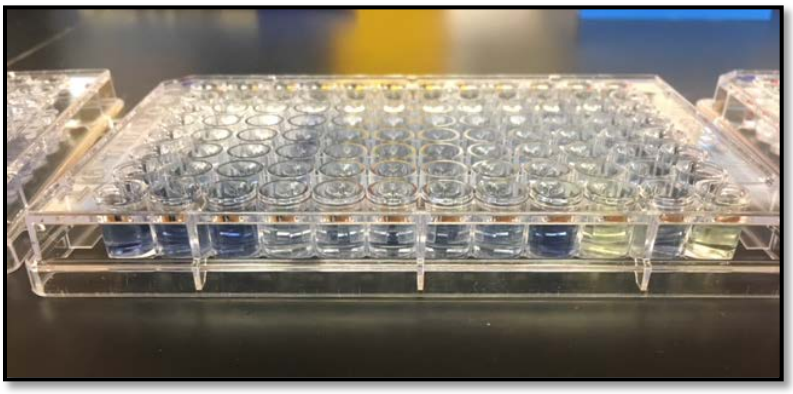

Figure 18: Bio-Rad DC Protein Assay. The variations in the intensity of the blue color represent different amounts of protein in the samples. Wells remained a greenish-yellow color if there was no protein or very little protein in the sample.

g. HSP70 ELISA

HSP70 levels were quantified using monoclonal ELISA with primary antibody Mouse anti-Bovine HSP70 (Sigma H5147) and secondary antibody Goat anti-Mouse IgG Horseradish Peroxidase (Sigma A0168) (Barthell *et al.* 2002, Hranitz and Barthell 2003). It has been shown by immunoblotting that the primary antibody binds both the constitutive or cognate and the inducible forms of HSP70 (Sigma).

Using the results obtained from the BioRad Protein Assay, thawed homogenate supernatants were diluted to a protein concentration of 400 ng/µL in homogenization buffer and stored at -80°C. A standard curve was prepared using stock bovine HSP70 (1µg/µL) (Sigma H9776) to yield final amounts ranging from 10 to 500 ng per well. Homogenate buffer served as blanks. Five µL of homogenization buffer, HSP standards (Appendix H), or samples were loaded to designated cells in triplicate. Each sample well contained equal amounts of soluble protein, 2000 ng. 195µL of binding buffer (10 mM Na_2CO_3/$NaHCO_3$, pH 9.6) was added to each well using a multichannel pipettor, covered in plastic wrap, and incubated at 4°C overnight.

After 24 hours, the binding buffer was removed from the microplate by inversion. Each well was washed once with 200 µL of Phosphate Buffered Saline containing 0.05% Tween 20, pH 7.6 (PBST). The PBST was removed by inversion. Known as the blocking step, 200 µL of PBST with 1% BSA was added per well, wrapped in plastic wrap, and incubated at 37°C for 1 hour. The wells were then washed once with 200 µL of PBST. Mouse anti-bovine HSP70 (primary antibody) was added (200 µL per well) and incubated at 37°C for one hour. Plates were subsequently washed four times with 200 µL of PBST. The secondary antibody (Goat Anti-mouse Horseradish Peroxidase) was added (200 µL per well) and incubated at 37°C for one hour. Each microplate was then washed six times with 200 µL of PBST. Following the series of washes, 150 µL of TMB Substrate (BioRad) was added per well, the plate covered with plastic wrap, and incubated at room temperature on a shaker for up to 30 minutes. During this time, the samples turn various shades of blue. To stop the reaction, 100 µL of 1M sulfuric acid was added resulting in different shades of yellow (Figure 19).

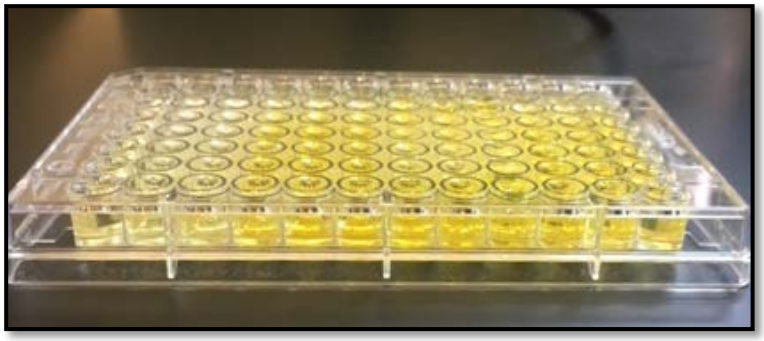

Figure 19: Monoclonal antibody ELISA test for HSP70. The amount of HSP70 in each well is determined by the intensity of the yellow color produced when sulfuric acid was added to halt the reaction.

The absorbance was then read at 450 nm using the Tecan Genios Plus microplate reader. The slope of the HSP Standard Curve was used to calculate the HSP concentration of each sample.

h. *Statistics:*

Motor function tests were analyzed with a nonlinear regression fitted using the sigmoidal dose response curve in GraphPad Prism v. 6.0 was performed. Chi square analysis was performed on the frequencies (counts) of bees in each category for each treatment (SPSS Statistics). Values of $p<0.05$ were considered significant. For SOD and HSP70 Assays, one-way ANOVA and Post-Hoc Tukey tests were conducted using JMP Pro v.12 software to test for difference among the treatments. To construct the TD_{50} curve, the percentage of impaired bees (motor score <8) was graphed versus the dose of imidacloprid received. Values of $p<0.05$ were considered significant. There was no correction for multiple testing for motor function, SOD, and HSP70 performed.

Experiment 2: The Effect of Sublethal Doses of Imidacloprid on Gene Expression in the Brain

a. Experimental Design

The overall design of Experiment 2 is shown in Figure 20. Honeybees were collected, as described in Experiment 1, and were randomly assigned to four groups: Control-0h (C0), Control-4h (C4), Treatment-0h (T0), and Treatment-4h (T4). Control groups were fed 10 μL of 1.5 M sucrose. Treatment groups received $1/20^{th}$ of the LD_{50} (0.9 ng/bee) of imidacloprid in 10 μL of 1.5 M sucrose. This sublethal dose was selected based on the results of Experiment 1 as one of the peak values in the hormetic HSP70 response to the pesticide but one dose lower than the dose that produced impaired locomotor function. Honeybee heads were excised at time 0 or 4 hours and the brains dissected. Total RNA was isolated from the brain tissue and transported overnight on dry ice to the Keck Center at University of Illinois Urbana-Champaign. Genome-wide RNA sequencing was conducted by the Keck Center. Following post-sequencing analysis, pathway analysis was used to identify pathways altered by imidacloprid treatment.

Figure 20: Experiment 2 design. Roughly 10-14 honeybees were assigned to each group and treated (Control-0h, Control-4h, Treatment-0h, and Treatment-4h). Bee heads were removed, and total RNA was isolated in dissected brains. The isolated RNA was sent to the University of Illinois for RNA sequencing. Lastly, pathway analysis was performed to identify key pathways of interest.

b. Honeybee Collection and Treatments:

Honeybees were collected using the same method as described in Experiment 1. Bees were harnessed and fed 1.5 M sucrose to satiation. After 22-24 hours, the bees were randomly assigned to Control-0h (C0), Control-4h (C4), Treatment-0h (T0), and Treatment-4h (T4). Treatment groups received $1/20^{th}$ of the LD_{50} (0.9 ng/bee) of imidacloprid that was determined based on the results of Experiment 1. A $1/20^{th}$ LD_{50} dose of imidacloprid was a sublethal dose that was enough to elicit a stress response without being debilitating. Upon completion of treatment (0 Hour or 4 Hour), the bee head capsules were removed using sterile scissors and stored at -80^{o}C in a sterile tube until brain dissection was performed. The total number of honeybees collected was n= 43 (C0= 12, C4= 11, T0= 9, T4= 11).

c. Head Capsule Dissection:

Head capsules were removed from the -80^{o}C freezer and placed on dry ice. The dissecting microscope, microscalpel, forceps, petri dish, and surrounding lab bench was cleaned with RNase Away (Molecular BioProducts). The honeybee head was placed in a petri dish containing dry ice and 200 proof ethanol (Figure 21a). The anterior exoskeleton was removed with a microscalpel exposing the brain (Figure 21b). Further dissection removed retinal tissue and the compound eye lens (Figure 21c). Finally, the bee brain was removed from the rest of the remaining head capsule (Figure 21d).

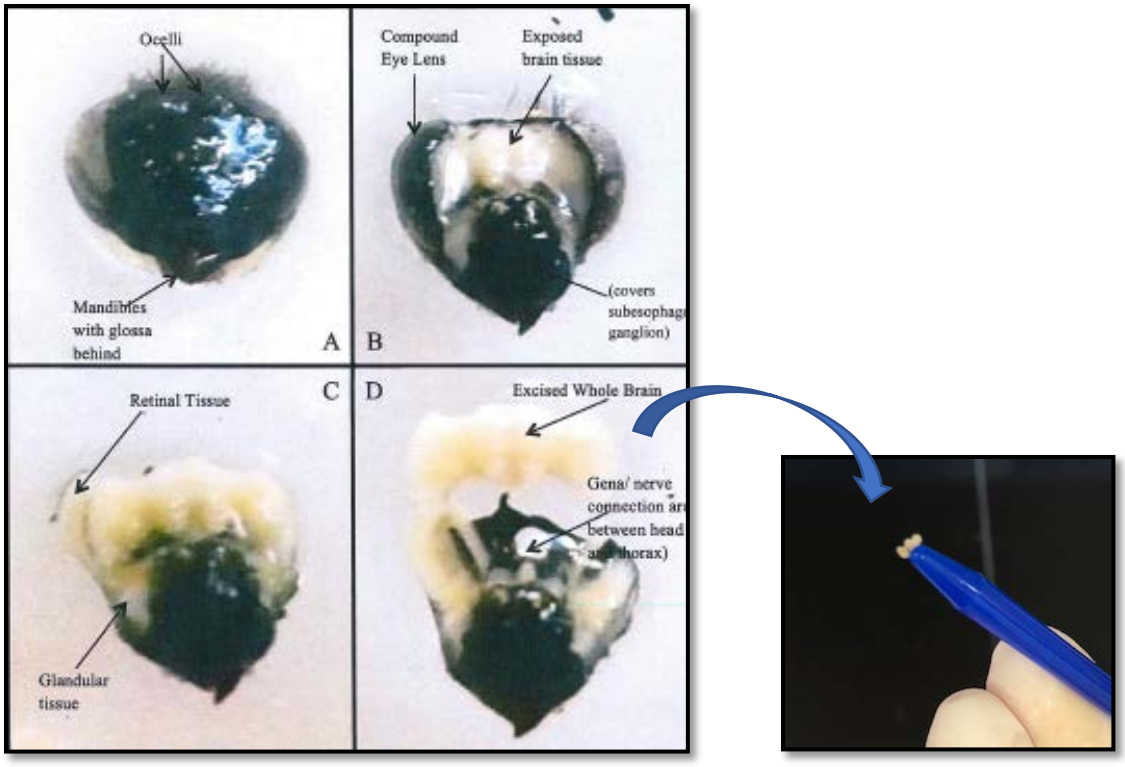

Figure 21: Procedure for isolating the honeybee brain (Photo Credit: Megan Duell 2014). A) Bee head capsules were placed on a slurry of dry ice and ethanol. B) The exoskeleton is chipped away during dissection, exposing the brain. C) Eye tissue and the lens are removed to see the boundary between retinal and brain tissue. D)The ivory-colored brain resembles the shape of a bat and is removed. The blue arrow indicates the actual size of the excised brain shown on the tip of a small pestle in comparison with fingers in the background.

d. RNA Isolation

RNA was isolated from honeybee brains using a modified Trizol-RNeasy method based on the procedure outlined in the Qiagen RNeasy kit as described by Sen Sarma *et al.* (2009). The Qiagen RNeasy technology for purifying RNA, outlined in Figure 22, combines the selective binding of RNA to a silica-based membrane with a fast microspin technology.

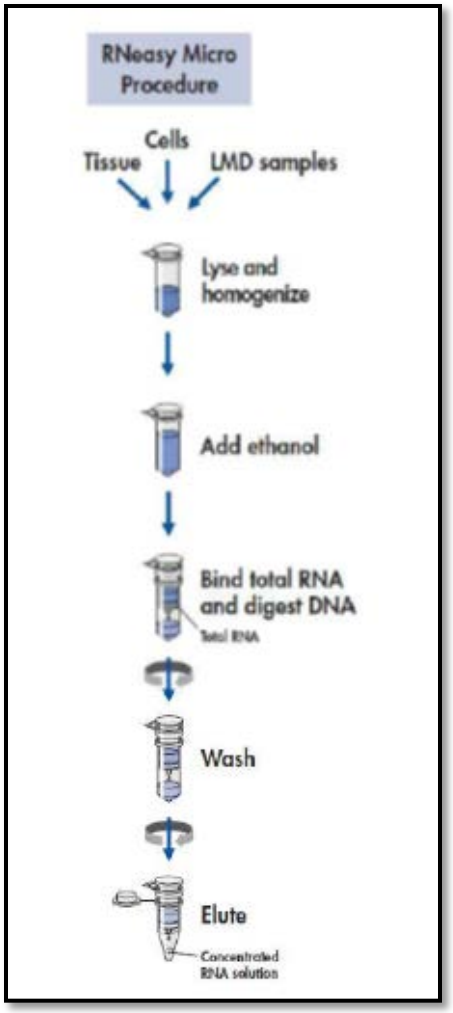

Figure 22: Schematic of RNA isolation procedure (Qiagen 2020). RNeasy Protect Mini Procedure for animal tissue is illustrated above. The procedure was modified to perform this research.

Standard procedures for handling RNA were employed during the RNA isolation steps. All surfaces and instruments were cleaned with RNase-Away (Molecular BioProducts) to remove RNases that are abundant in the environment. Gloves were worn at all times. After homogenization with TRIzol (Invitrogen), the specimens were incubated on the benchtop for five minutes. Equal parts of RNase free water and chloroform were added, vortexed for 15 seconds, and incubated for an additional three minutes. The specimens were then centrifuged at 14,500 RPM for 15 minutes at 4°C.

Following centrifugation, the aqueous phase was carefully removed without disturbing the interface and placed into a sterile RNase Free 1.5 mL collection tube. An equal amount of 70% ethanol was added to each sample and vortexed for 10 seconds. Approximately 700 µL of the aqueous-ethanol solution was transferred into a RNeasy

mini spin column sitting in a 2 mL collection tube and centrifuged for 30 seconds at 12,000g at room temperature. The flow-through was poured back into the column which was placed into a new 1.5 mL collection tube and centrifuged again for 30 seconds at 12,000g at room temperature discarding the flow-through after centrifugation was complete.

Forty μL of a DNase/RDD buffer stock mixture was added to the column and incubated at room temperature for 15 minutes. After this, 350 μL of RW1 buffer was added to the RNeasy column and centrifuged at 12,000g for 15 seconds at room temperature. Once the column was transferred to a new 2 mL collection tube, 500 μL RPE buffer was added onto the column and centrifuged for 15 seconds at 12,000g at room temperature. The liquid was decanted from the tube and the column was replaced. An additional 500 μL RPE buffer was added to the column and centrifuged for 2 minutes at 12,000g at room temperature. The liquid was decanted, and the column replaced. The samples were then centrifuged at 12,000g for one minute to remove any residual ethanol. The RNeasy column was transferred to a new 1.5 mL tube. Thirty μL of RNase free water was pipetted onto the column and centrifuged at 12,000g for one minute. An additional 30 μL of RNase free water was added onto the column and centrifuged for one minute. The purified RNA in the eluate was stored in 1.5 mL microcentrifuge tubes at -80°C.

The quality and quantity of the purified RNA was assessed by determining the ratio of absorption at 260 nm and 280 nm using the Nanodrop (Spectrophotometer ND-1000) to confirm the amount and quality of the RNA present. For high-quality RNA, the desired A260/A280 ratio is in the range of 1.9-2.1 (Mater Methods 2012). Table 1 compiles the average absorption ratio and the average RNA concentration along with the calculated standard deviation for each testing group.

Table 1: Average absorption ratio and average protein present. The average A260/280 ratio and the average RNA concentrations were determined for each treatment group (n=6).

Treatment Group	Average Concentration A260/A280 Ratio (ng/µL)	Concentration A260/A280 Ratio (ng/µL) Standard Deviation	Total RNA (ng) Average	Total RNA (ng) Standard Deviation
Control-0h	1.88	0.069	38.0	3.92
Control-4h	1.69	0.061	42.3	11.9
Treatment-0h	1.90	0.099	48.2	9.05
Treatment-4h	1.86	0.043	32.8	10.9

The six highest quality RNA samples for each treatment group were selected based on the A260/A280 ratio for RNA sequencing. To confirm RNA presence, a formaldehyde-agarose gel electrophoresis was performed on four specimens chosen at random. Formaldehyde was included in the gel to denature RNA and inhibit RNAses (Figure 23).

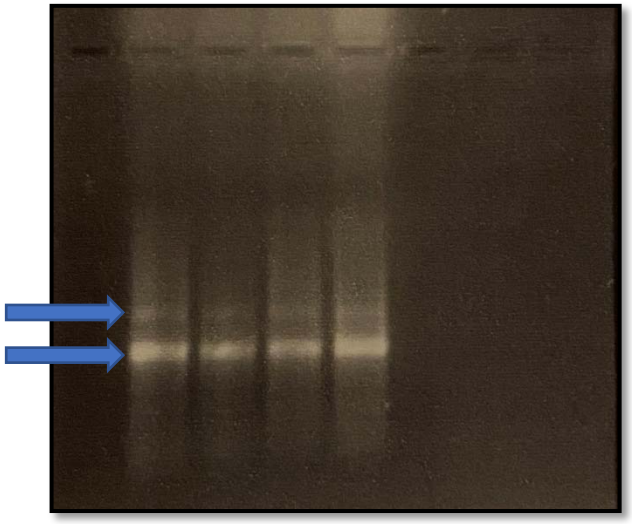

Figure 23: Formaldehyde gel for RNA. Formaldehyde-agarose gel electrophoresis was run to confirm the presence of RNA. Ribosomal RNA bands are denoted by the blue arrows and mRNA is a range of sizes indicated as a smear. The formaldehyde gel contained: 1% agarose gel, MOPS (20 mM MOPS(3-(N-morpholino) propanesulfonic acid), 2 mM sodium acetate, 1 mM EDTA, pH 7.0), and 2.2 M formaldehyde. Loading dye contained 2 microliters of ethidium bromide. The gel was run for approximately 45 minutes at 95 volts.

The purified RNA samples were shipped to the Keck Center for Comparative and Functional Genomics at the University of Illinois Urbana-Champaign for RNA sequencing. Samples were placed individually in a cryocentrifuge tube, labeled with a roman numeral and sample number (Appendix I), packed in dry ice, and shipped via FedEx.

e. RNA Sequencing:

RNA was sequenced using the Illumina Next Generation Sequencing platform, sequencing by synthesis. This four-step process involves 1) preparation of an mRNA library; 2) cluster amplification; 3) sequencing; and 4) alignment to a reference genome. In step 1, a TruSeq Stranded mRNA library was prepared as outlined in the workflow diagram in Figure 24. In overview, the total RNA for each sample was mRNA enriched and then fragmented. A first strand of cDNA was synthesized followed by the synthesis of the second strand of cDNA using dUTPs. The 3' ends were adenylated and the adaptors ligated. After ligation, the dUTPs were enzymatically removed to prepare for PCR amplification. At the completion of the PCR amplification, the created library was validated by the use of qPCR and Bioanalyzer. Lastly, the library was pooled and normalized, resulting in the final library.

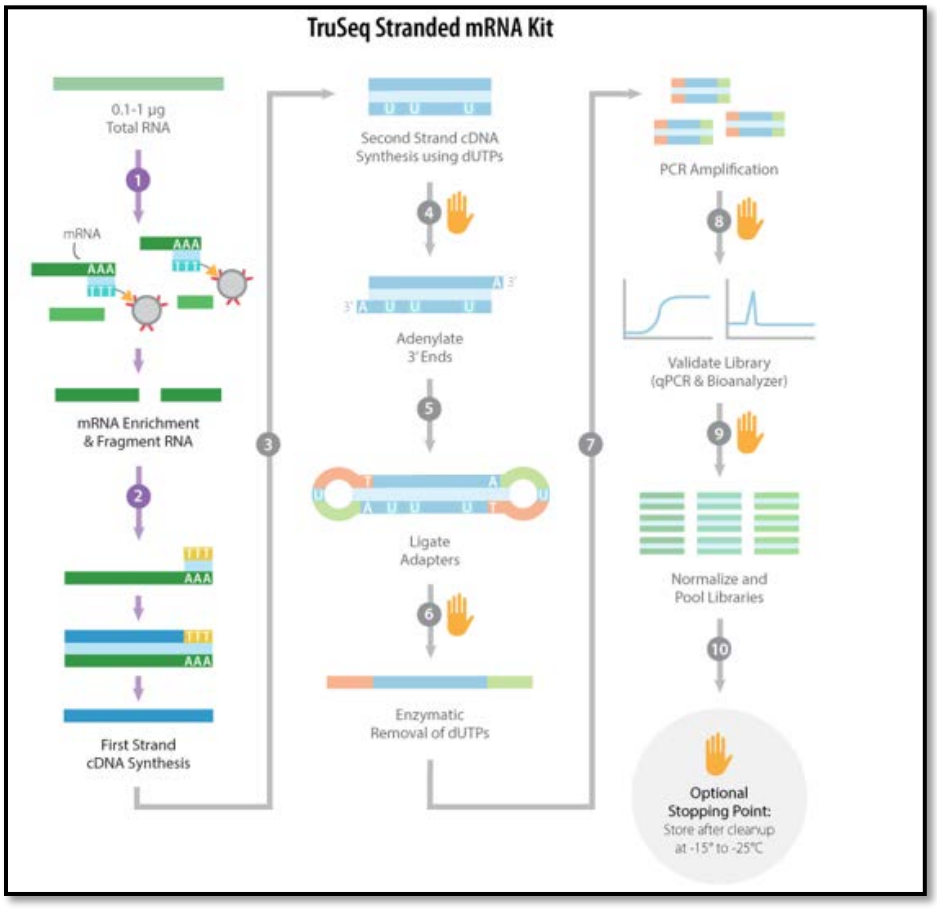

Figure 24: TruSeq Stranded mRNA library preparation workflow (Photo Credit: TruSeq mRNA library Preparation Kit protocol). TruSeq stranded mRNA kit sequences RNA by synthesis via Illumina Sequencing.

In step 2, the mRNA library was loaded into a flow cell and the fragments were hybridized to the surface of the flow cell. The mRNA fragments were amplified into clone clusters by bridge DE amplification. In step 3, sequencing by synthesis utilized fluorescently-labeled nucleotides to sequence the RNA on the flow cell surface. For each sequencing cycle, a single labeled dNTP was added to the nucleic acid chain thus serving as a terminator for polymerization. Upon addition of each dNTP, the fluorescent dye is imaged to allow for identification of the base and then is cleaved so the same process can be performed on the next nucleotide. Since the base identity is determined one at a time from signal intensity measurements during each cycle, the raw error rates are reduced, resulting is highly accurate base-by-base sequencing (Illumina 2010). Finally, in step 4, the data are aligned and compared to the reference genome as described below.

Upon completion of RNA sequencing, the number of reads per gene were normalized due to potential differences in the number of reads as well as potential differences in RNA composition. The *Apis mellifera* reference genome Amel_HAv.3.1 has a total of 12,090 genes. Due to low detectable expression, a total of 1,493 genes were filtered out resulting in 10,597 genes that were eligible for differential expression analysis (Valizadegan and Drnevich 2019).

f. Post-Sequencing Analysis and Statistics:

Results of RNA sequencing were reported by Negin Valizadegan and Jenny Drnevich of the Keck Center for Comparative and Functional Genomics at University of Illinois Urbana Champaign. The *Apis mellifera* transcriptome derived from genome Amel_HAv3.1 and Annotation Release 104 from the National Center for Biotechnology Information was used for quasi-mapping and gene counts (Valizadegan and Drnevich 2019). The Sequencing Center's report was summarized using Multi-QC version 1.6 (Appendix J and K). A quality check on the raw data indicated that the reads were of high quality and no adaptor sequences were found. Salmon version 0.13.1 was used to quasi-map reads to the transcriptome and to determine the abundance of each transcript (Patro *et al.* 2017). Approximately 70.1% to 82.3% of the reads were mapped to the transcriptome. The unmapped reads were discarded (Valizadegan and Drnevich 2019). In order to compare expression levels among the control and treatment groups, the number of reads per gene were normalized using the EDE-R package, an essential step given that

there could be differences in the total number of reads and variations in RNA composition.

To identify treatment effects, a multi-dimensional scaling plot was constructed with the top 5,000 most variable genes using limma (Valizadegan and Drnevich 2019). Differential gene expression analysis was conducted using the limma-trend method (Valizadegan and Drnevich 2019) by comparing the following pairs: Treatment-0h versus Treatment-4h, Control-0h versus Control-4h, Treatment-0h versus Control-0h, and Treatment-4h versus Control-4h. A test for any interaction between treatment and time was also performed. To adjust for multiple testing, a "global" False Discovery Rate (FDR) correction was done across p-values for all comparisons. The number of up-regulated and down-regulated genes for each pairwise comparison was made using an FDR p-value of <0.1. A heatmap was made to visualize the overall gene expression patterns with a significant one-way ANOVA, FDR <0.05.

A total of 10,597 genes were returned post-sequencing. Of the 10,597 genes, a total of 7,806 genes were considered characterized (ie., functional and/or pathway information available and/or has a mammalian homolog). The gene expression differences among the control and treatment groups were determined using R programming with the use of one-way ANOVA corrected with Bayesian probabilities. In our laboratory, an automated algorithm was developed to identify genes where the expression data was inconsistent for more than two out of the six bee samples within a specific pairwise comparison. Any genes where >33% of the data was inconsistent (over-/under-expression among the samples) were removed from that treatment group. Table 2 breaks down the treatment comparison and the number of genes removed from each comparison. The specific outlier genes removed from each comparison can be found in Appendix L. The automated algorithm was written in the Python 2.7 programming language (Van Rossum and Drake 1995, Appendix M).

Table 2: Number of genes removed for each comparison. A total of 10,597 genes were identified after RNA sequencing. A bee sample was deemed an outlier if it differed greatly from the other bees in the assigned treatment group. A gene was removed from analysis if more than two bees out of the six bee samples for a specific gene were identified as going in the opposite direction.

Treatment Group	Number of Genes Removed
Treatment-4h versus Treatment-0h	15
Control-4h versus Control-0h	80
Treatment-0h versus Control-0h	25
Treatment-4h versus Control-4h	137

g. Gene Enrichment and Pathway Analysis:

Changes in gene expression among control bees and bees exposed to 0.9 ng/bee ($1/20^{th}$ of LD_{50}) of imidacloprid were examined by making four pairwise comparisons (Figure 25).

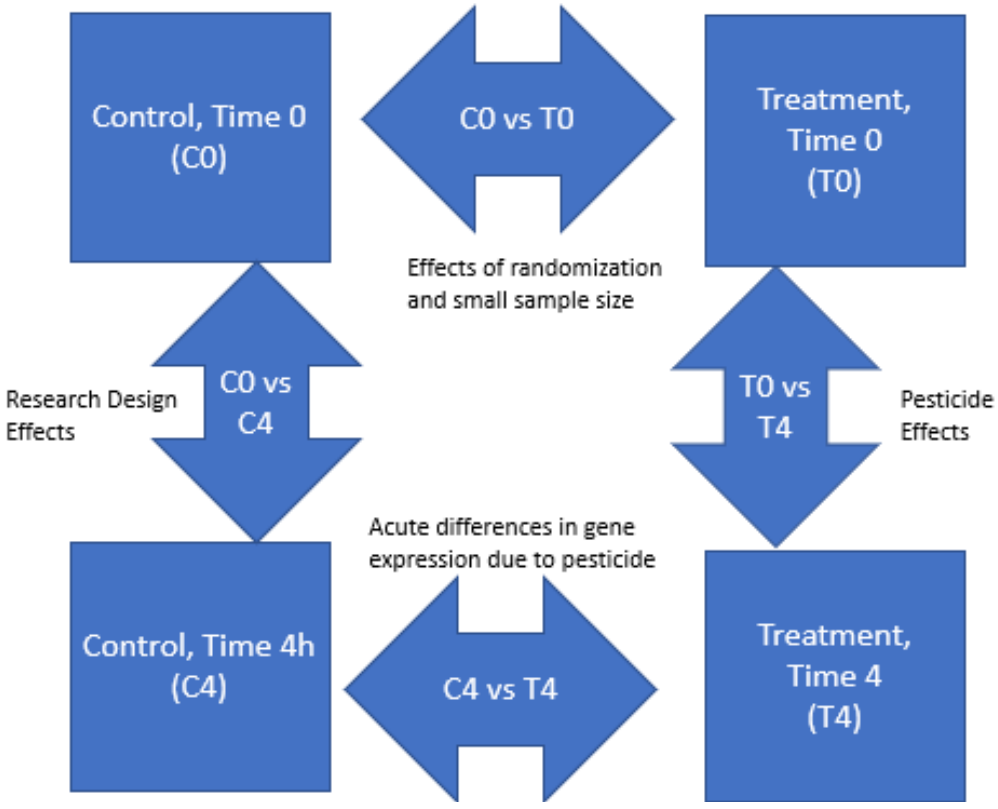

Figure 25: Pairwise comparisons of control and imidacloprid-treated bees. The schematic illustrates the statistical comparisons made among four treatment groups.

The groups Control-0h and Control-4h were compared to assess research design effects while Control-0h and Treatment-0h were compared to asses randomization and the small sample size. Therefore, if a gene is shown to be up-regulated or down-regulated in one of these comparisons, it is not due to the treatment and is an artifact of the experimental design. Our main focus is on the effects of pesticide treatment, that is, in the differential gene expression of Treatment-4h compared to Treatment-0h and Control-4h compared to Treatment-4h.

DAVID, standing for Database for Annotation, Visualization, and Integrated Discovery, was utilized for Functional Analysis (Nature Protocols 2009). DAVID Bioinformatics Resource 6.8 uses gene set enrichment to provide functional annotation, gene functional classification, gene ID conversion, and gene name batch viewer for individuals to use in order to understand biological meaning behind a large list of genes. The identification numbers for were entered into the Gene List, identified as Entrez ID numbers, determined to be a gene list, and submitted. This process was performed for all significant ($p<0.1$) down-regulated and up-regulated genes separately. A function or functional cluster that had an FDR $p<0.05$ was identified as significant. The function of the cluster, group enrichment score, and FDR were documented. The overall group enrichment score is based on the modified Fisher's Exact p-value for each term member. The higher the enrichment score, the more enriched, and the smaller the p-value (Nature Protocols 2009). This process was performed for Treatment-4h versus Treatment-0h and Control-4h versus Control-0h.

Standing for Kyoto Encyclopedia of Genes and Genomes, KEGG Mapper (KEGG Mapper 2020) was used for Pathway Analysis. This database is a resource that helps to visualize the interactions among genes in various pathways and shows how a change in the function of gene can alter the function of genes further downstream. To retrieve a list of pathways, a gene list was inputted into KEGG. For this research, all 10,597 genes were entered. If a gene was considered significant ($p<0.1$), the gene was designated purple (down-regulated) or pink (up-regulated). If the gene was not significant ($p>0.1$) then it was designated orange (up-regulated) or red (down-regulated). After the genes were entered, the analysis searched the knowledge base and identified pathways that contained a gene from the list that was inputted. The genes, both significant and not significant,

appeared in the pathway with the appropriate color designation. A pathway was deemed interesting based on previous studies and literature about the effects of neonicotinoids on the honey bee. This process was performed for Treatment-4h versus Treatment-0h and Control-4h versus Control-0h.

IV. Results

Experiment 1: The Effects of Sublethal Doses of the Neonicotinoid Pesticide Imidacloprid on Motor Function and Cellular Responses in Honeybees

Motor Function Responses of Honeybees:

Figure 26 shows the motor responses of honeybees exposed to sublethal doses of imidacloprid ranging from $1/5^{th}$ to $1/500^{th}$ of the LD_{50}. A motor score of 8, represented normal leg and abdomen movement, antennae responsiveness, and a proboscis extension reflex. No differences were observed in the motor scores of the bees in the positive (heat shock) and negative (room temperature) control groups ($p<0.05$). Motor scores in both positive and negative controls were normal, near 8. Lower motor scores, less than 8, were observed in honeybees that were treated with sublethal doses of imidacloprid. All of the scored motor functions were impaired relatively to the same degree. Honeybees in the treatment groups 1.8 ng/bee ($1/10^{th}$ LD_{50}) and 3.6 ng/bee ($1/5^{th}$ LD_{50}) had lower motor scores than negative and positive controls ($p <0.05$). Motor responses of the bees exposed to imidacloprid doses ranging from 0.9 ng/bee ($1/20^{th}$ of the LD_{50}) to 0.036 ng/bee ($1/500^{th}$ of the LD_{50}) did not differ compared to controls.

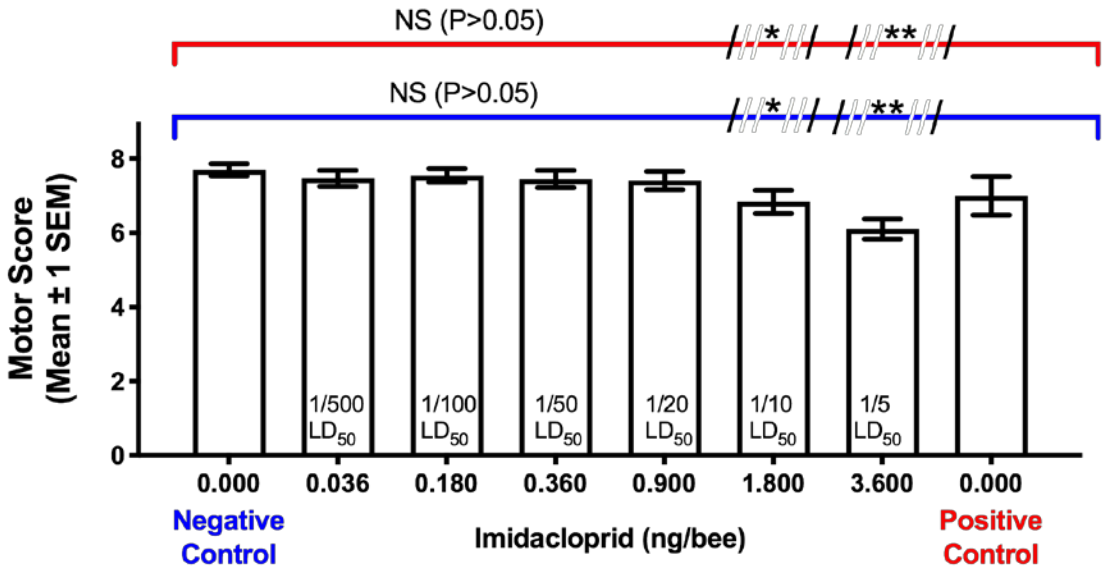

Figure 26: Average motor scores of honeybees exposed to sublethal doses of imidacloprid. Honeybees were exposed to serial dilutions of the oral LD_{50} of imidacloprid (18.0 ng/bee) or 1.5 M sucrose (controls). Bars representing means ± standard error (n=261). Chi-square analysis was performed (SPSS Statistics). Means connected by the blue line did not differ from the negative control. Means connected by red line did not differ from the positive control. Means connected to the black line did not differ from the 1/100th LD50 treatment (SOD only). Broken lines with asterisk(s) indicate where means differed from a comparison: *=P<0.05, **=P<0.01. NS represents no significant differences.

Dose-response analysis of the percentage of bees that were impaired (motor scores < 8) per treatment showed a strong sigmoidal curve fit with an estimated toxic dose at which 50% of bees were impaired (TD_{50}) of 1.78-2.25 ng/bee (Figure 27). A supplemental table of the average motor scores is provided in Appendix N.

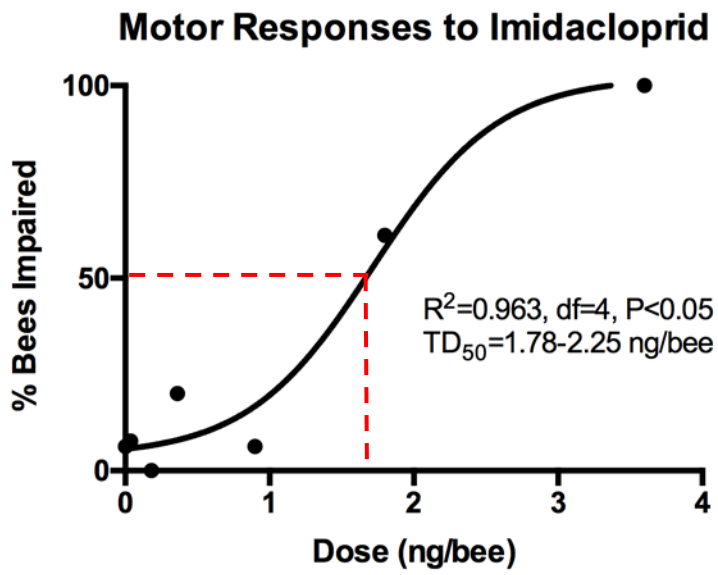

Figure 27: Imidacloprid motor response curve. Percentage of bees that were impaired were plotted at each sublethal dose of imidacloprid to determine the toxic dose 50 (TD_{50}). A nonlinear regression fitted a sigmoidal dose-response curve in GraphPad v6 by Prism.

Superoxide Dismutase (SOD) Activity in Honeybees:

Figure 28 shows the SOD activity in homogenized honeybee head capsules exposed to sublethal doses of imidacloprid ranging from $1/5^{th}$ to $1/500^{th}$ of the LD_{50}. No differences were observed in the SOD activity in the bees in the positive (heat shock) and negative controls (room temperature). The results of the Tukey-Kramer post-hoc test indicated elevated SOD activity in both the $1/5^{th}$ (3.6 ng/bee) and the $1/10^{th}$ (1.8 ng/bee) doses when compared to the $1/100^{th}$ (0.18 ng/bee) dose (ANOVA: F=3.2897, p=0.0037).

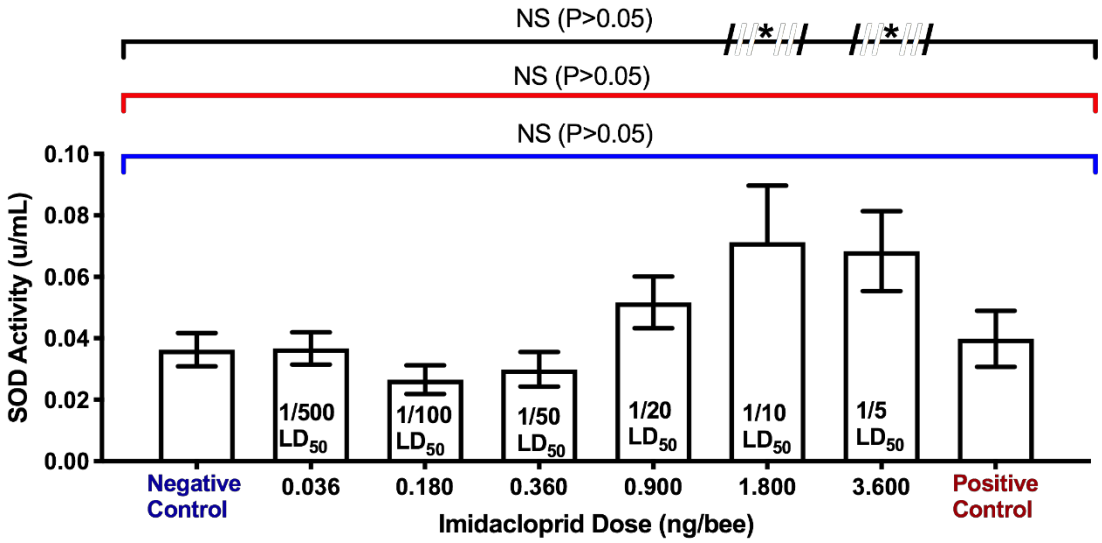

Figure 28: SOD activity in honeybees treated with imidacloprid. There is a significant difference in the SOD activity between the 1/5th dose (3.6 ng/bee) and the 1/100th dose (0.18 ng/bee) and between the 1/10th dose and the 1/100th dose of imidacloprid (ANOVA: F=3.2897, p=0.0037). Means connected by the blue line did not differ from the negative control. Means connected by red line did not differ from the positive control. Means connected to the black line did not differ from the 1/100th LD50 treatment (SOD only). Broken lines with asterisk(s) indicate where means differed from a comparison: *=P<0.05.

HSP70 Concentrations in Honeybees:

The levels of the cellular stress marker HSP70 in bees exposed to sublethal doses of imidacloprid are shown in Figure 29. The positive controls, bees that were heat shocked at 42°C, had increased levels of HSP70 compared to the negative controls (samples that were fed 1.5 M sucrose and left at room temperature). The Tukey-Kramer post-hoc test indicated that HSP70 levels in the 0.18 ng/bee (1/100th dose of LD_{50}) and 3.6 ng/bee (1/5th dose of LD_{50}) treatments were lower ($p<0.05$) than the positive control. The 3.6 ng/bee (1/5th dose of LD_{50}) treatment disrupts the cellular stress response of the honeybees. Doses of 1.8 ng/bee (1/10th of LD_{50}) to 0.36 ng/bee (1/50th of LD_{50}) showed intermediate levels of stress that overlapped both positive and negative controls.

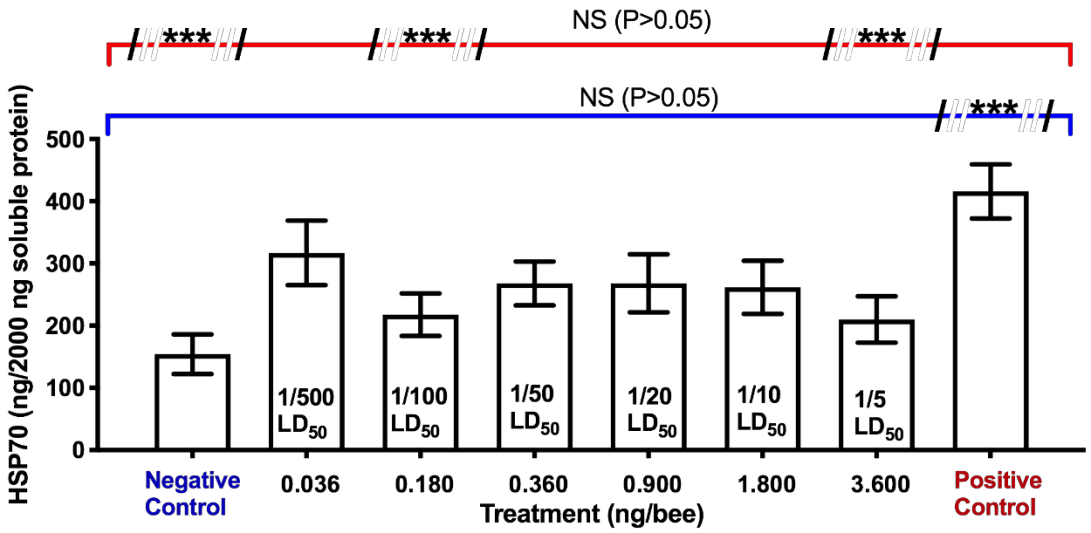

Figure 29: The effects of sublethal doses of imidacloprid on HSP70 levels in honeybees. One-way ANOVA (JMP Pro 12.2.0) indicated significant differences among groups. Means connected by the blue line did not differ from the negative control. Means connected by red line did not differ from the positive control. Means connected to the black line did not differ from the 1/100th LD50 treatment (SOD only). Broken lines with asterisk(s) indicate where means differed from a comparison: ***=P<0.001.

Overall Results for Experiment 1:

Data from all of these tests, motor response scores (Figure 26 and 27), SOD activity (Figure 28), and HSP70 concentrations (Figure 29) indicate that a dose of 0.9 ng/bee was intermediate among doses with an elevated stress response that was not associated with impaired motor coordination. Therefore, a conservative sublethal imidacloprid dose of 0.9 ng/bee ($1/20^{th}$ of LD_{50}) was selected to treat bees for RNA transcriptome analysis for Experiment 2. We hypothesized that an intermediate dose of 0.9 ng imidacloprid/bee would induce a sublethal stress response but not likely elicit a massive apoptotic response, typical of an imidacloprid exposure from which bees might recover from in nature.

Experiment 2: The Effect of Sublethal Doses of Imidacloprid on Gene Expression in the Brain

Gene Expression Analysis: RNA-Sequencing:

The RNA sequencing analysis report, shown in Appendix J, contains the output from the raw read files. FastQC (Appendix K) was used to generate quality check reports for the sequencing reads of all 24 honeybees (n=6 per treatment group). The average per-

base read quality scores for all samples had a Phred score, a measure of the quality of the identification of the nucleobases generated by automated DNA sequencing, over 30. This value indicates that all of the samples after sequencing were of high quality, with a less than 1 in 1,000 probability of an incorrect base call and a 99.9% base call accuracy (Technical Note 2011; Appendix K).

Gene expression patterns in the four groups were analyzed by determining differential gene expression (DGE) in pairwise comparisons. We predicted that the group treated with imidacloprid, the Treatment-4h group, would have the greatest number of differentially expressed genes compared to the other three groups, Control-0h, Control-4h, and Treatment-0h. The DGE results however, do not match our prediction. Very few genes were differentially expressed in the Treatment-4h group compared to the Treatment-0h group (121 genes, sum of down-regulated and up-regulated genes). Surprisingly, there were many more differentially expressed genes in pairwise comparisons involving the Control-4h group than comparisons between the other treatment groups. For example, the number of differentially expressed genes were greater in Control-4h group compared to the Control-0h (4,285 genes, sum of down-regulated and up-regulated genes) groups and the Treatment-4h and Control-4h (3,872 genes, sum of down-regulated and up-regulated genes). Few genes were differentially expressed in a comparison of Treatment-0h and Control-0h (232 genes, sum of down-regulated and up-regulated genes). This result was anticipated because these groups, the Control-0h and Treatment-0h, were included in the experimental design to assess randomization and the small sample size. Therefore, the 232 genes that are up-regulated or down-regulated in this comparison, are not due to the treatment but rather are artifacts of the experimental design.

Differential gene expression (DGE) was performed for all four pairwise comparisons including a test for interaction between treatment and time (Table 3) (Valizadegan and Drnevich 2019).

Table 3: Differential Gene Expression (DE) for all four pairwise comparisons (Valizadegan and Drnevich 2019). The number of down-regulated, up-regulated, and non-significant genes were identified among all four pairwise comparison. The total number of significant differentially expressed genes is the sum of the significant down-regulated and up-regulated genes in each comparison ($p<0.1$).

	T4vsT0	C4vsC0	T0vsC0	T4vsC4	Interaction
Down-Regulated	46	2,369	35	1,663	1,091
Not Significant	10,476	6,312	10,365	6,725	7,805
Up-Regulated	75	1,916	197	2,209	1,701
Total Number of Significant Differentially Expressed Genes	121	4,285	232	3,872	2,792

There are many more differentially expressed genes in pairwise comparisons involving the Control-4h group than comparisons between the other treatment groups. Like the DGE data, the multi-dimensional scaling plot clearly shows that gene expression patterns in the Control-4h group differs from the other three groups. The Control-4h group is sharply separated on the X axis from the other three groups. To illustrate overall expression patterns, a one-way ANOVA was calculated across all four groups to select genes to visualize in a heat map. Using an FDR <0.05, a total of 3,819 genes were identified as different across the four treatment groups (Figure 31). The comparisons that are most important to examine are Control-4h versus Control-0h and Treatment-4h versus Control-4h. Control-4h versus Control-0h comparison reveals the effects of experimental manipulation on control animals; therefore, there should not be a large change in differential expression in comparison to the treatment group (Treatment-4h versus Control-4h). The heat map reveals that the Control-4h shows a greater change in gene expression when compared to Control-0h, Treatment-0h, and Treatment-4h.

To adjust for multiple testing that occurred due to the increased number of differentially expressed genes in the Control-4h, a “global” False Discovery Rate (FDR) correction was performed across the p-values for all five comparisons. This ensured that a gene with the same raw p-value in two different comparisons would not end up with extremely different FDR p-values.

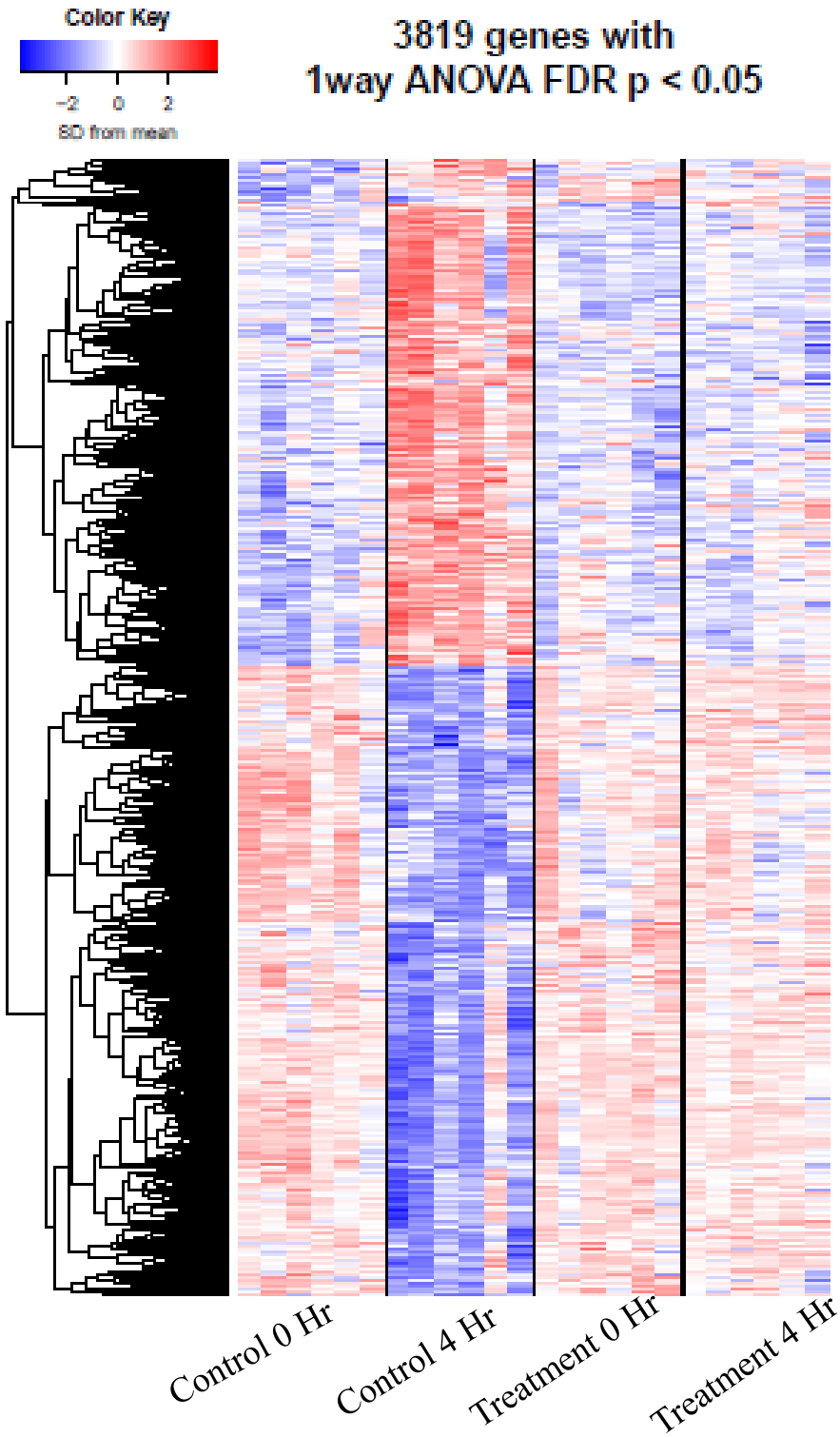

Figure 30: One-way ANOVA heat map of Control-0h, Control-4h, Treatment-0h, and Treatment-4h (Valizadegan and Drnevich 2019). Each lane within a group represents an individual bee (1-6). Genes that have been down-regulated are colored blue, up-regulated genes are colored red, and white denotes no change in gene expression. The color intensity represents the degree of gene expression change.

Multi-dimensional scaling, a method used to visualize the level of similarity of individual cases of a dataset at a higher level, was used to identify possible treatment effects. The multi-dimensional scaling plot in Figure 31 is based on 5,000 of the most variable genes. Dimension 1 (X-axis) illustrates approximately 25% of the total variability and explains the separation of the Control at Time 4h samples from the other groups. Dimension 2 (Y-axis) encompasses approximately 17% of the variability. This does not explain groupings of the effect of treatment, control, and/or the time, however (Valizadegan and Drnevich 2019). It would be expected for the multi-dimensional scaling plot to show Control-0h, Control-4h, and Treatment-0h to be clustered relatively close while Treatment-4h showed greater separation. The overall findings of this plot; however, show that Control-4h specimens (depicted by the red circle) had the greatest variability in comparison to Control-0h, Treatment-0h, and Treatment-4h.

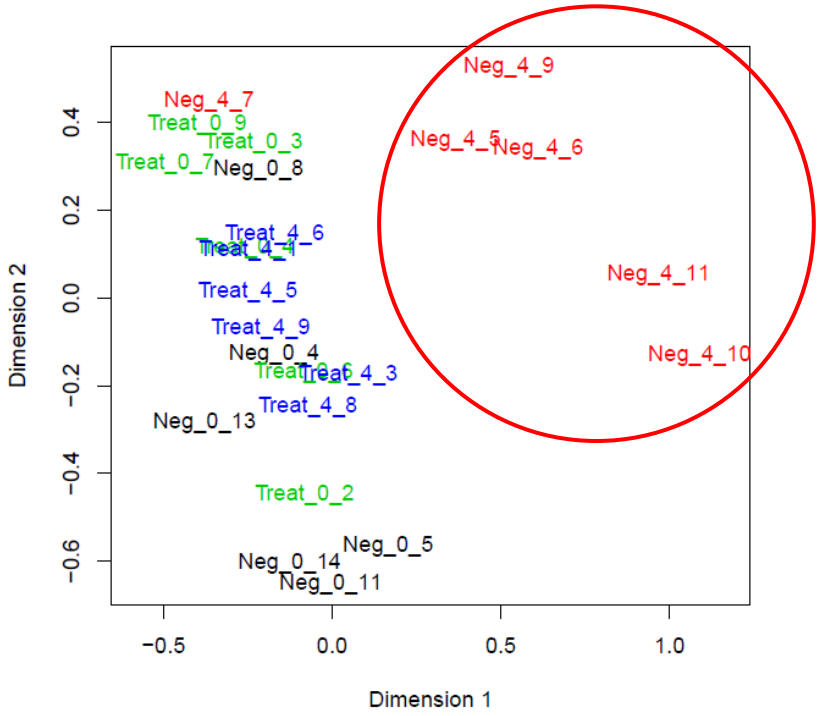

Figure 31: Multi-dimensional scaling plot performed on 5,000 of the most variable genes (Valizadegan and Drnevich 2019). Each individual bee in the four groups is represented on the plot (n=6 for each group). Each of the four groups is represented by a different color. Control-0h bees are labeled Neg_0 followed by the sample bee number and appear in black. Control-4h bees are labeled Neg_4 followed by the sample bee number and appear in red. Treatment-0h hour bees are indicated by Treat_0 followed by the sample bee number and are in green. Treatment-4h bees are indicated by Treat_4 followed by the sample bee number in blue.

A list of the top 100 most significant differentially expressed genes for Treatment-4h and Control-0h can be found in Appendix O. All 10,597 honeybee genes were analyzed in KEGG. The Control-4h versus Control-0h is of interest since this comparison contained the greatest differential gene expression. The schematic from Figure 25 illustrates that this should show effects from research design; however, further investigation into the large differential gene expression difference is needed. Table 4 lists key genes and pathways that were significantly changed in the Control-4h versus Control-0h group comparison.

Table 4: Key Pathways and genes at Control-4h and Control-0h. Pathway analysis was performed using KEGG. Significant genes had a p-value <0.1.

Key KEGG Pathways	KEGG Genes	Up-regulated	Down-Regulated	KO #
Circadian Rhythm-Fly	Period circadian protein (Per)		√	K02633
Metabolism of Xenobiotics by Cytochrome P450	Glutathione s-transferase D1 (GstD1) Glutathione s-transferase (GstS1)	√ √		K00799 K04097
Drug Metabolism-Cytochrome P450	Glutathione s-transferase D1 (GstD1) Glutathione s-transferase (GstS1)	√ √		K00799 K04097
Glutathione Metabolism	Glutathione s-transferase D1 (GstD1) Glutathione s-transferase (GstS1)	√ √		K00799 K04097
FOXO Signaling Pathway	Catalase (Cat) Insulin-like receptor-like (InR-2) Phosphatase and tensin-like (Pten) Superoxide dismutase 2, mitochondrial (Sod2)	 √	√ √ √	K03781 K04527 K01110 K04564
Peroxisome	Catalase (Cat) Dehydrogenase/reductase SDR family member 4 (DHRS4) Fatty acyl-CoA reductase 1 (FAR1) Superoxide dismutase 1 (Sod1) Superoxide dismutase 2, mitochondrial (Sod2)	 √ √	√ √ √	K03781 K11147 K13356 K04565 K04564
Longevity Regulating Pathway-Multiple Pathways	Adenylate cyclase 3 (Ac3) Catalase (Cat) Heat shock protein cognate 4 (Hsc70-4) Insulin-like receptor-like (InR-2) Superoxide dismutase 1 (Sod1) Superoxide dismutase 2, mitochondrial (Sod2)	√ √ √	 √ √ √	K08043 K03781 K03283 K04527 K04565 K04564
Apoptosis-Fly	Broad-complex (Br-c) Cytochrome c (CytC) Ecdysteroid-regulated gene E74 (E74) Ecdysone receptor isoform A (Ecr)	√ √	 √ √	K02174 K08738 K09428 K14034

	Mushroom body large-type Kenyon cell-specific protein 1 (Mblk-1)	√		K20015
	Ultraspiracle (Usp)	√		K14030
Oxidative Phosphorylation	ATP synthase lipid-binding protein, mitochondrial (ATP5G2)	√		K02128
	Cytochrome c oxidase subunit VIb polypeptide 1 (Cox6b1)	√		K02267
	Cytochrome c oxidase subunit 6c (Cox6bc)	√		K02268
	NADH dehydrogenase (ubiquinone) 1 beta subcomplex, 2, 8kDa (Ndufb2)		√	K03958
	NADH-ubiquinone oxidoreductase 75 Dka subunit, mitochondrial (Ndufs1)	√		K03934
	NADH dehydrogenase [ubiquinone] iron-sulfur protein 5 (Ndufs5)	√		K03938
	Cytochrome b-c1 complex subunit 10 (Uqcr11)		√	K00420
	Vacuolar H^+ ATP synthase 16 Dka proteolipid subunit (Vha16)		√	K02155

Significant genes with a $p<0.1$ in the comparison Control-4h versus Control-0h and Treatment-4h versus Treatment-0h were analyzed with DAVID. Just as the KEGG analysis showed, the Control-4h versus Control-0h comparison contained the greatest amount of gene enrichment. Although both DAVID and KEGG analysis yielded similar findings, these findings are inconsistent with the expectation that Treatment-4h versus Treatment-0h would reflect the greatest change due to pesticide treatment. The results of the DAVID analysis showed that Zinc Finger, Transmembrane, GTP-binding, Ubiquitin Protein Transferase Activity, ATP-binding, and Intracellular Signal Transduction had significant down-regulated enrichment changes in genes in the Control-4h versus Control-0h comparison. DAVID analysis also found that Ribosome, Small Nucleolar Ribonucleoprotein, Large Ribosomal Translation, Nucleotide Binding, Immunoglobulin, RNA Polymerase, DNA-templated Transcription, and Pheromone/General Odorant Binding had significant up-regulated enrichment changes in genes in the Control-4h versus Control-0h comparison.

V. Discussion

Motor Function Responses:

Bees exposed to sublethal doses of imidacloprid showed impaired motor responses compared to positive and negative control bees at doses of 1.8 ng/bee ($1/10^{th}$ LD_{50}) and 3.6 ng/bee ($1/5^{th}$ LD_{50}). Motor responses did not differ between the positive and negative control groups. This was expected since the positive control group, while

subjected to heat stress, was incubated at a temperature about 1°C below the critical thermal maximum for honeybees (Atmowidjojo *et al.* 1997). Motor responses were still intact at this temperature. Sigmoidal dose-response model predicted that 50% of the forager population had impaired motor responses between 1.78-2.25 ng/bee of imidacloprid (Figure 27). This range of values includes the $1/10^{th}$ LD_{50} of imidacloprid (1.80 ng/bee) in our experiment.

Because of their widespread use, water solubility, persistence in the soil, and uptake by plants, neonicotinoid pesticides are broadly present in the environment. Neonicotinoids have been found in trace levels in plants, pollen and nectar and have been detected in bees wax, honey, and honeybees themselves (reviewed in Blacquière *et al.* 2012). While the levels of neonicotinoids employed in agriculture are not lethal to bees, chronic sublethal exposures may occur. For example, honeybees can reach our observed TD_{50} value of 1.78 to 2.25 ng in a few trips to common field plants treated with imidacloprid. Stoner *et al.* (2012) found that squash nectar contains 10 μg/L, or 10 pg/μL of imidacloprid. Sylvester *et al.* (1983) reported that bees can carry up to 62 μL of nectar. This would mean bees can carry 0.620 ng of imidacloprid from a full trip to a squash plant. Based on this, in less than three trips worker honeybees could experience the TD_{50} value of 1.78 to 2.25 ng/bee. Girolami *et al.* (2009) found that corn guttation holds up to 200 mg/L, or 200 ng/μL of imidacloprid. One exposure to corn guttation would be lethal and partial consumption of only 0.1 μL would lead to dosages greater than the TD_{50} value of 1.78-2.25 ng/bee. These sublethal exposures combined with other stressors fit the criteria of the Sublethal Stress Model (Bryden 2013) and can impair the health of the hive.

The declines in motor responses of honeybees exposed to sublethal doses of imidacloprid may have significant consequences. Flight patterns, behavior, and foraging ability have all been shown to be reduced in honeybees exposed to imidacloprid (Tan *et al.* 2014, Karahan *et al.* 2015, Decourtye *et al.* 2004a, Decourtye *et al.* 2004b). This could be attributed to the impaired motor function of honeybees. Worker bees who do not forage efficiently will take longer to return to the hive and worker bees that cannot fly properly may not return to the hive at all. Impairments in the proboscis extension reflex and in antennae movement could lead to problems locating and foraging nectar. The

reduction in antennae function could diminish the ability of the bees to detect location, resulting in altered flight patterns.

The overall impairment of worker bees can negatively affect the health of the hive by lowering its nectar and pollen supplies. Contaminated food in the hive can also lead to weakened larvae that will grow into the next generation of worker bees. This may also lower the worker bees' ability to defend the hive. Guard bees specialize in olfaction-based nestmate recognition and alarm-pheromone-mediated recruitment of nestmates to sting. Stinging is determined by visual, tactile, and olfactory stimuli (Hunt 2007). Overall, the impaired motor functions of worker bees are detrimental to a honeybee colony. A decline in motor responses due to imidacloprid intoxication could result in delayed decision-making and other cognitive skills (Tan *et al.* 2014). When these factors are compounded with other sublethal stressors such as mites, nutritional stress, or environmental stress, it is evident that the effects on the hive may be devastating.

Superoxide Dismutase (SOD) Activity:

SOD is a potent antioxidant enzyme that is a marker of oxidative stress. SOD combats oxidative stress by scavenging the superoxide anion, a reactive oxygen species, and converting it to hydrogen peroxide, a substrate of catalase. Elevated levels of SOD have been proposed to serve as an organism's first line of defense to prevent the damaging effects of superoxide on cellular biomolecules (Ighodaro and Akinloye 2018). In our study, SOD activity was higher in bees treated with the $1/5^{th}$ (3.6 ng/bee) and the $1/10^{th}$ (1.80 ng/bee) doses of imidacloprid compared to those that received the $1/100^{th}$ (0.180 ng/bee) dose (Figure 28). As seen in the case of motor responses, no significant difference was observed in SOD activity between the positive (incubated at 4 hours at 42°C) and negative control (room temperature). This response is to be expected since SOD is not affected by temperature.

Several studies reported an increase in the activities of oxidative enzymes such as catalase, glutathione-S-transferases, superoxide dismutase, and xanthine oxidase in bees after sublethal exposure to pesticides such as pyrethroids and organophosphates (Chakrabarti *et al.* 2015). Chakrabarti *et al.* (2015) observed in field studies of native bees that SOD levels were greater in bees from agricultural areas with high pesticide use compared to those from pesticide-free zones. Oxidative stress is known to influence the

survival and homing ability of honeybees; increases in oxidative stress resulted in decreased survival and foraging abilities of the affected honeybees (Simone-Finstrom *et al.* 2016). Our findings, elevated SOD levels following exposure to sublethal doses of imidacloprid, are indicative of oxidative stress and suggest that honeybee foragers and the overall health of the colony could be negatively impacted.

Heat Shock Proteins (HSP70):

Heat shock proteins function as molecular chaperones to prevent misfolding of cellular proteins during conditions of heat stress or other types of cellular stress, including exposure to toxins (Feder *et al.* 1997). The positive controls, bees that were heat shocked at 42°C for four hours, had increased levels of HSP70 compared to the negative controls (samples that were fed 1.5 M sucrose and remained at room temperature). HSP70 levels in the 0.18 ng/bee ($1/100^{th}$ dose of LD_{50}) and 3.6 ng/bee ($1/5^{th}$ dose of LD_{50}) treatments were lower than the positive control (ANOVA values, $p < 0.05$). The 3.6 ng/bee ($1/5^{th}$ dose of LD_{50}) treatment had a decreased cellular stress response as reflected by HSP70 levels while doses of 1.8 ng/bee ($1/10^{th}$ of LD_{50}) and 0.3 ng/bee ($1/50^{th}$ of LD_{50}) showed intermediate levels of stress that overlapped both positive and negative controls. These findings support the hormesis model with a dose-relationship that is stimulatory at low doses and inhibitory at higher doses (see Figures 11 and 29). The $1/500^{th}$ dose appears to be an exception. We cannot account for the discrepancy but this could be due to errors when making up the solution or other unknown regulatory mechanisms.

Previous studies have shown that HSP70 is a useful predictor of cellular stress in honeybees. Chacon-Almeida *et al.* (2000) observed an induction of heat shock proteins in the larval fat body of honeybees incubated at 42°C for 2 hours. Work performed by Hranitz and colleagues (2010) demonstrated that ethanol doses that affect honeybee learning and behavior cause significant increases in HSP70 concentrations, a cellular stress response. The dose-response relationship between ethanol concentration and HSP70 levels also followed the pattern of the hormesis model. In a study by Sahebzadeh and Lau (2017), worker bees infested with *Varroa* mites or exposed to sublethal acaracides such as thymol or eucolyptol showed a dose dependent up-regulation of all HSPs, pointing to their utility as biomarkers when bees are exposed to toxic or

pathogenic stress. These studies lend support to our findings that the elevated levels of HSP70 that we observed in honeybees exposed to sublethal doses of imidacloprid are indicative of cellular stress.

Determination of Imidacloprid Dose to Use for Experiment 2:

Sublethal doses of imidacloprid impaired motor responses and produced elevated levels of HSP70 (marker of cellular stress) and SOD (marker of oxidative stress) in honeybees (Figures 26-29). As mentioned in the Introduction, the hormesis model illustrates parabolic curves with positive, negative, and peak response levels across a spectrum of doses. Lower doses of imidacloprid elicited a beneficial, protective effect within the hormetic zone while a 3.6 ng/bee ($1/5^{th}$ dose of LD_{50}), a high dose, resulted in inhibition. A conservative sublethal imidacloprid dose of 0.9 ng/bee ($1/20^{th}$ of LD_{50}) was selected to treat bees for RNA transcriptome analysis for Experiment 2. This dose of 0.9 ng/bee was intermediate among doses with an elevated stress response. We estimated that 0.9 ng imidacloprid/bee would induce a sublethal stress response but not likely produce a massive apoptotic response, typical of an imidacloprid exposure from which bees might recover from in nature.

Mortality:

The experiment-wide mortality rate of the restrained bees after 22-24 hours for Experiment 1 was 38%. Despite the mortality rates, negative and positive controls were significantly different in stress response. There was 0% mortality of bees in Experiment 2 treatments.

RNA-Seq Results:

Collectively, the DE analysis, Multi-dimensional Scaling Plot, and the one-way ANOVA heat map agree that the Control-4h group had the greatest changes in gene expression compared to the other groups. This is counter to our prediction that the greatest changes would be in the bees treated with imidacloprid. Our Control-4h samples showed elevations in SOD gene expression (Table 3). This finding contradicts our independent results from Experiment 1. Specifically, Experiment 1 showed that SOD activity was elevated in bees treated with imidacloprid compared to controls.

The increased gene expression in the Control-4h group that was observed is also inconsistent with previous studies. For example, a study of similar design by the Hranitz laboratory showed that RNA expression was affected by ethanol. A total of 609 microarray ESTs in the honeybee brain displayed different expression to acute (4 hour) ethanol treatment (personal communication). Furthermore, a review of the imidacloprid literature shows varied and significant impacts of this pesticide on the physiology and behavior of honeybees that would likely be reflected in genome-wide responses (Henry *et al.* 2012, DiPrisco *et al.* 2013, Wu-Smart *et al.* 2012, Pereira *et al.* 2020, and Decourtye *et al.* 2004). Recent studies investigating the effects of neonicotinoids on the honeybee transcriptome have also shown significant changes in gene expression in bees following neonicotinoid treatment. For example, Shi *et al.* (2017) reported a total of 609 differentially expressed genes when bees were treated with the second-generation neonicotinoid thiamethoxam.

Post-Hoc Hypothesis and Supporting Evidence:

There is a wealth of corroborating evidence that suggests that the Control-4h and the Treatment-4h samples were mislabeled and switched. These discrepancies have led us to propose a *post-hoc* hypothesis that the Control-4h and Treatment-4h samples were mislabeled prior to shipping to University of Illinois Urbana-Champaign. RNA isolation of Control-4h and Treatment-4h bees were performed on the same day so this mishap may have occurred at that time.

Several steps were taken to investigate the possibility of a switch between the Control-4h and Treatment-4h groups. First, the laboratory notebook was checked to confirm that the sample numbers and RNA concentration values matched the document that was sent with the specimens to University of Illinois Urbana-Champaign. Second, the Control-4h and Treatment-4h specimens that were not sent for RNA sequencing were re-analyzed for RNA content. The repeated RNA yields were not consistent with the original measurements; however, the RNA concentrations were consistent between the two measurements of the same samples about one month apart. Third, University of Illinois Urbana-Champaign repeated RNA sequencing on the remainder of each original bee sample. As a final attempt to understand the results from RNA sequencing, further data analysis was performed on the output provided by University of Illinois Urbana-

Champaign. A Python code was used to identify outliers within the same treatment group for a given expression level. A gene or honeybee was deemed an outlier if it met one of the following criteria: if more than two bee samples out of the six samples for a specific gene were identified to be going in the opposite direction (positive and negative) or if the read value returned was greater than 2 standard deviations (SD) different from the other honeybee samples with that treatment group. The results of this data cleaning with outliers removed can be found in Table 5.

Table 5: Removal of genes and outliers using Python. The number of genes removed from each treatment comparison and the number of outliers or honeybees removed per treatment comparison from the gene list is reflected below. Significance was $p<0.1$.

	T4vsT0	**T0vsC0**	**C4vsC0**	**T4vsC4**
Number of Genes Removed	15	25	80	137
Number of Outliers	2,669	2,804	2,804	2,669

The results in Table 6 show that the removal of outliers from the dataset did not change the interpretation of the differential gene expression. The Control-4h group still displayed most of the changes in gene expression. Based on the supporting evidence, we feel confident that the Control-4h and Treatment-4h samples were switched and mislabeled. The pair-wise comparisons of the Control-4h and Treatment-4h bees have been renamed to reflect this mislabel (Table 6). This label change will remain for the rest of the discussion. The gene expression data in Table 6 has been cleaned by the removal of outliers in Table 5.

Table 6: Results of further data cleaning using Python. The total number of genes that are up-regulated and down-regulated are based on the genes that are considered significant. The number of genes for each comparison takes into account the outliers that were removed from the gene list. Significance was based on p-value <0.1.

	C4vsT0	T0vsC0	T4vsC0	T4vsC4
Down-Regulated	37	32	2,353	1,569
Not Significant	10,476	10,365	6,312	6,725
Up-Regulated	69	175	1,852	2,166
Genes Removed	15	25	80	137

Pathway and Gene Set Enrichment Functional Analysis:

The molecular responses by the honeybee brain transcriptome to acute sublethal doses of imidacloprid can be interpreted by examining statistical comparisons among the four groups. Our focus is on comparing the differential expression between Treatment-4h and Control-0h, post label change, which directly looks at the effects of pesticide treatment. Of the 10,597 total genes, 4,205 genes were considered significant (2,353 down-regulated genes and 1,852 up-regulated genes). Key cellular pathways that were affected by imidacloprid treatment were the peroxisome pathway, metabolism of xenobiotics by cytochrome P450, circadian rhythm, drug metabolism, FOXO signaling, longevity regulating pathways, apoptosis, and oxidative phosphorylation (Table 4).

The peroxisome pathway provides a clear example of the cellular stress produced by the exposure of bees to sublethal doses of imidacloprid (Figure 32). In the Control-4h-Treatment-0h comparison (Appendix P), both catalase and SOD were down-regulated, indicative of little to no cellular stress. However, in the Treatment-4h-Control-0h comparison, catalase is down-regulated while SOD is up-regulated. This is confirmed by the SOD assay performed in Experiment 1. This provides additional supporting evidence that a switch occurred between Treatment- 4h and Control-4h. If a switch did not occur, then SOD would have been elevated in the controls which is opposite of what was shown in the SOD assay.

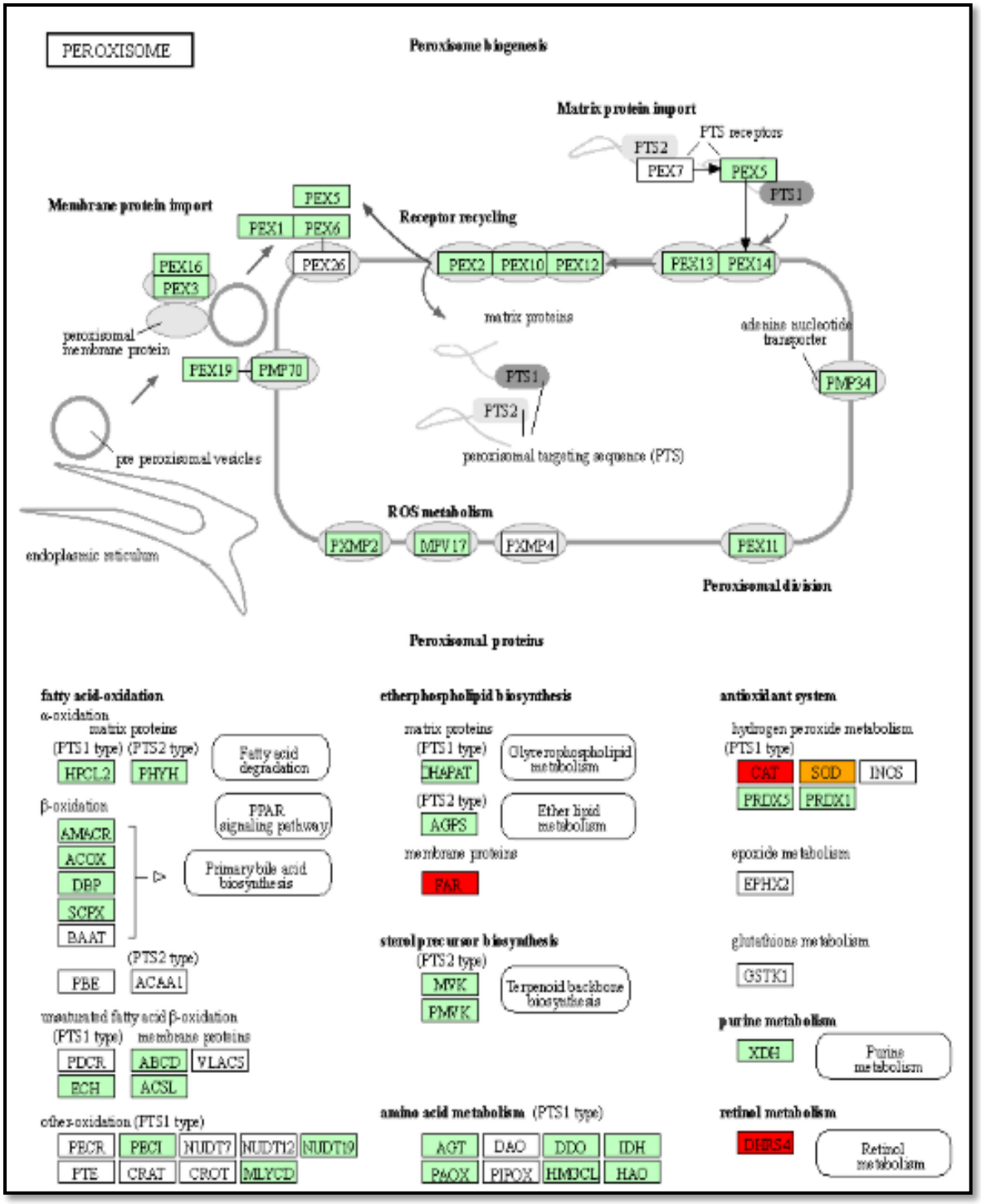

Figure 32: Peroxisome Pathway of Treatment-4h-Control-0h. KEGG was used as the enrichment analysis database. Genes colored red are considered down-regulated (not significant) and genes colored orange are considered up-regulated (not significant) (significance $p<0.1$). Enzymes are indicated by the green color.

Seven genes involved in circadian rhythm are found in the honeybee genome. One of the major ones, the Period (per) gene was dramatically affected when exposed to

imidacloprid. A comparison between Treatment-4h-Control-0h revealed significant down-regulation of the Per gene (Figure 33). The Control-4h-Treatment-0h comparison (Appendix P) showed a non-significant down-regulation of Per. Changes in circadian locomotor rhythms, mating behavior, and development time from egg to adult are affected by mutations in Per (Toma *et al.* 2000). While mRNA levels of Per were found to shift in bees of all ages, the most significant changes could be found in foragers (Toma *et al.* 2000). Karahen *et al.* (2015) found that imidacloprid reduced foraging activity by honeybees, where bees spent more time between trips in the hive. Tasman *et al.* (2020) investigated the effects of imidacloprid on bumble bees and discovered that concentrations as low as 1µg/L caused reductions in locomotion and foraging activities and mistiming that resulted in increased foraging at night and increased daytime sleeping. These changes in honeybee behavior could have dramatic effects on the survival of the colony.

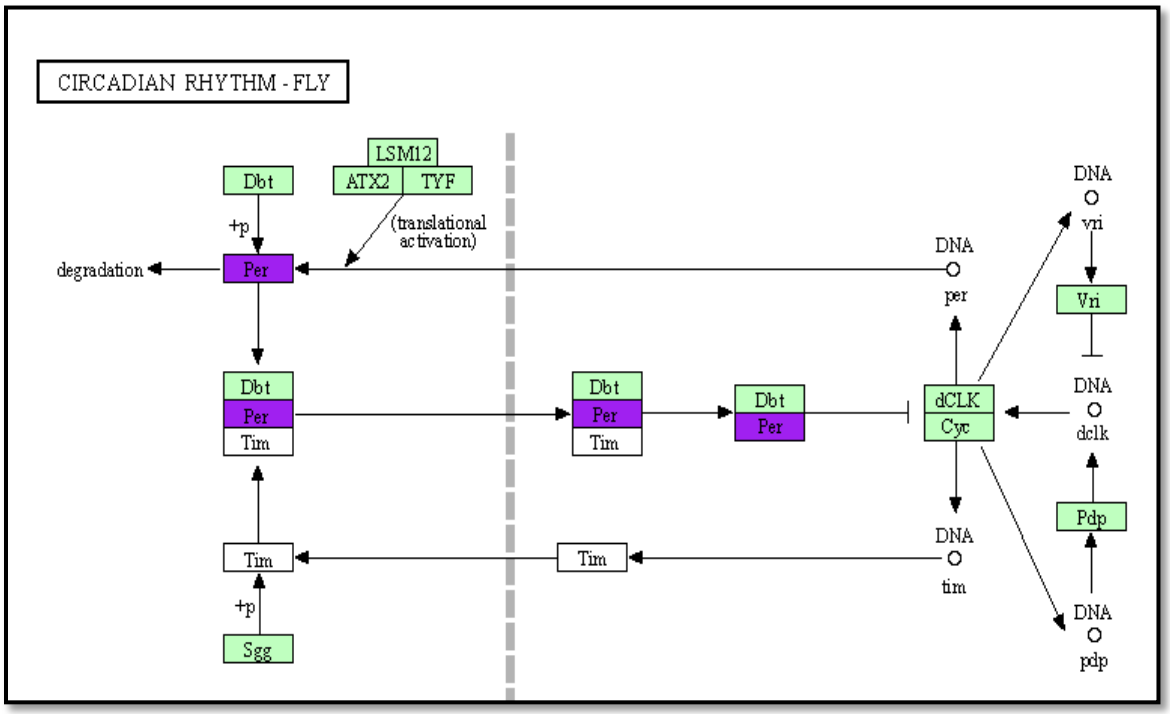

Figure 33: Circadian Rhythm Pathway-Fly Treatment-4h-Control-0h. KEGG was used as the enrichment analysis database. Genes that are colored purple are considered significantly down-regulated (significance $p<0.1$). Enzymes are indicated by the green color.

Forkhead box transcription factors (FOXO) are proteins involved in a wide range of cellular functions such as cellular differentiation, apoptosis, cell cycle regulation, autophagy, DNA damage and repair, and as mediators of oxidative stress (Farhan *et al.*

2017). The Treatment-4h and Control-0h comparison revealed a significant reduction in expression of the PTEN gene (Figure 34). An inhibition of PTEN enzyme activity (acts as a tumor suppressor by regulating cell division) leads to a decrease in FOXO. During oxidative stress, FOXO induces autophagy, a process which clears accumulated toxins and promotes cell survival (Maiese 2015, U.S. Library of Medicine 2015). In the case of imidacloprid-treated bees where FOXO is reduced, there may be less autophagy, resulting in a greater accumulation of toxins and lowered cell survival. Oxidative stress has also been reported to modify the interactions of FOXO with other proteins that ultimately can affect the survival of neurons (Maiese 2015). The interpretation of the FOXO pathways is further complicated by its acetylation and numerous different forms.

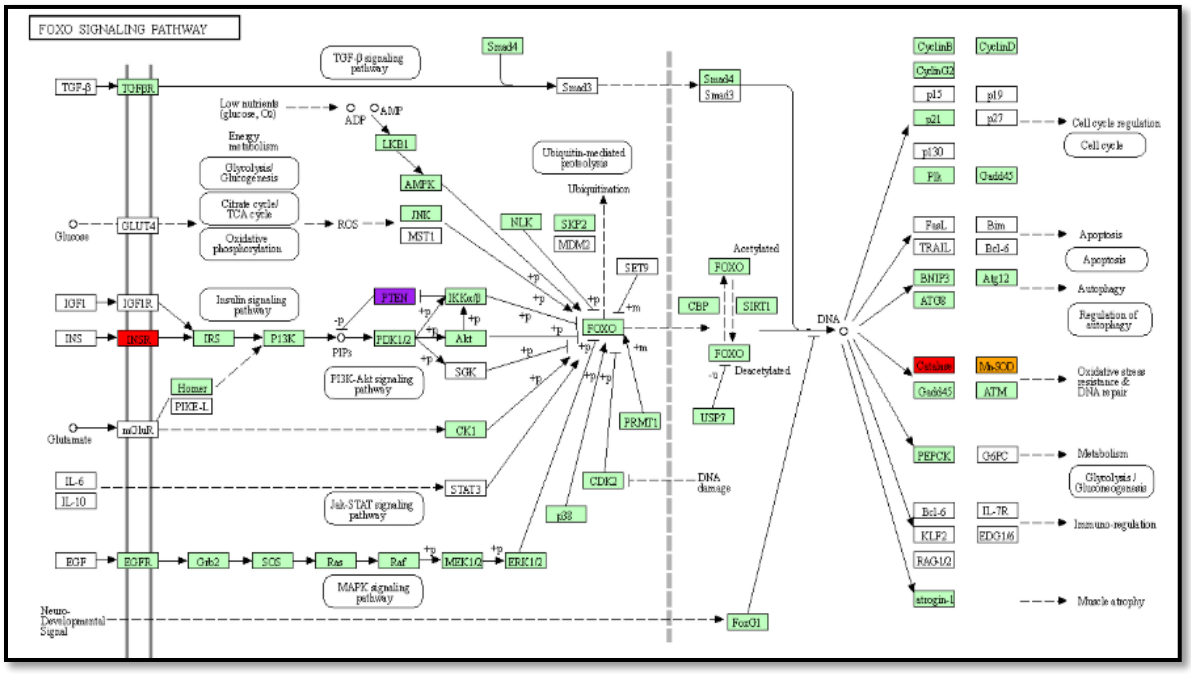

Figure 34: FOXO Signaling Pathway Treatment-4h-Control-0h. KEGG was used as the enrichment analysis database. Genes that are colored red are considered down-regulated (not significant), genes that are colored purple are significantly down-regulated, and genes that are colored orange are considered up-regulated (not significant) (significance $p<0.1$). Enzymes are indicated by the green color.

Detoxification enzymes are essential for honeybees to remove xenobiotics, such as neonicotinoids, that they are exposed to in their environment. Possessing roughly 30-50% fewer detoxification genes than *Anopheles* and *Drosophila*, bees are particularly vulnerable to the effects of xenobiotics. Xenobiotics are detoxified by three superfamilies of enzymes carboxylesterase (CCE), cytochrome P450 (P450), and glutathione S-transferase (GST) (Honeybee Genome Sequencing Consortium 2006, du Rand *et al.*

2015). As seen in Table 4, pathways for drug metabolism-cytochrome P450, metabolism of xenobiotics by cytochrome P450, and glutathione metabolism are significantly up-regulated in the imidacloprid treated group (0.9 ng/bee of imidacloprid) compared to the control group. This was due to the up-regulation of glutathione-S-transferases, a family of Phase II detoxification enzymes that catalyze the conjugation of glutathione to a variety of toxic compounds for the purpose of detoxification. In addition to its role in detoxification, glutathione-S-transferases have been shown to protect bees against oxidative damage caused by ROS (Yan *et al.* 2013). Glutathione-S-transferase has previously been shown to be up-regulated in honeybees following exposure to nicotine (du Rand *et al.* 2015). The up-regulation of the xenobiotic, drug metabolism and glutathione pathways suggest that the honeybee is actively attempting to eliminate the imidacloprid by converting it to a less toxic form. This is crucial, given the reduced amounts of detoxification genes in honeybees and their unique sensitivity to insecticides (Appendix Q).

The Longevity Regulating Pathway compares multiple species. For the purpose of this discussion, the pathway in flies will be considered since they are the most comparable to the honeybee. In this pathway, Control-4h-Treatment-0h (Appendix P) comparison shows that various forms of SOD and adenylate cyclase are up-regulated and heat shock protein cognate (the constitutive form) and insulin-like receptor-like are down-regulated in imidacloprid-treated bees. The change in regulation of SOD again supports that a switch occurred between the Treatment-4h and Control-4h; however, there is no real change in longevity when comparing the treatment group to the control group Appendix Q). It is interesting to note that HSP70 remained down-regulated (not statistically significant) while the results of the HSP 70 assay showed a significant change between concentrations. This could be explained by post-translational regulation, which is faster than that of post-transcriptional regulation.

The Oxidative Phosphorylation Pathway, located on the cristae of the mitochondria, consists of a collection of complexes and enzymes responsible for the aerobic production of ATP. In the imidacloprid treatment group, Complexes I through IV are up-regulated resulting in an increase in electron transport down the chain and subsequent increase in the flux of protons across the cristae to the intermembrane space.

The last step in the pathway is the ATPase that uses the energy produced by the proton gradient to synthesize ATP. ATPases are classified into three groups; F, V, and P types. F-type ATPases are the more common proton-translocating ATP synthases found in the cristae of mitochondria and also in the membranes of bacteria and chloroplasts that catalyze the hydrolysis or synthesis of ATP (Ozawa *et al.* 2000). V-type ATPase use the energy of hydrolysis to pump protons across membranes to establish electrochemical gradients that can be used to drive transport processes (Beyenbach and Wieczorek 2006). The important genes to note are subunit c in both the F-type and V-type ATPase. In the control group (Appendix P), both these genes are down-regulated (not statistically significant) while in the imidacloprid-treated group the F-type ATPase is up-regulated (not statistically significant) while the V-type ATPase is significantly down-regulated (Appendix Q). Our findings suggest that aerobic metabolism in the honeybee is significantly impacted at multiple steps in the oxidative phosphorylation pathway; however, from our findings, whether or not the changes we report increase or decrease aerobic metabolism cannot be predicted. Other studies suggest that the effects of neonicotinoid pesticides decrease aerobic metabolism which decreases energy stores (triglycerides and glycogen) and metabolic fuel (i.e., glucose) (Cook 2019, Tong *et al.* 2019). Therefore, we can hypothesize that the acute gene changes in oxidative and glucose metabolism disrupt normal aerobic metabolism and contribute to energetic stress in honeybees.

A closer look at the function or functional clusters from DAVID revealed noteworthy categories of enriched clusters of genes that were up-regulated were those involved in transcription, translation, and pheromone/general odorant binding (Table 7). Enriched clusters of genes that were down-regulated include transmembrane proteins and those engaged in intracellular signaling, ATP and GTP binding, ubiquitin-protein transferase activity, and zinc fingers (Table 7). To determine if a function or functional cluster was considered to be significant, the FDR had to have a p-value of <0.05. Further analysis showed an inverse relationship between the enrichment score and FDR p-value; the higher the enrichment score, the smaller the p-value making that function of the cluster more enriched. A complete list of unique genes within each annotation cluster can be found in Appendix R.

Table 7: Enriched genes at Treatment-4h and Control-0h. DAVID was used for enrichment analysis. Genes that had an FDR<0.05 were considered significantly enriched.

Annotation Cluster	Cluster Function	Up-regulated	Down-Regulated	Enrichment Score
1	Zinc ion binding Zinc finger, RING/FYVE/PHD-type Zinc finger, RING-type RING		√	5.46
2	Membrane Transmembrane helix Transmembrane Integral component of membrane		√	4.8
3	Small GTPase mediated signal transduction Small GTP-binding protein domain GTP binding		√	2.94
4	Ubiquitin-protein transferase activity Ubl conjugation pathway Ligase helix HECT HECTc		√	2.8
5	Serine/threonine-protein kinase, active site Protein kinase, ATP binding site Kinase Serine/threonine-protein kinase Protein serine/threonine kinase activity Protein kinase, catalytic domain S TKc Protein kinase-like domain Nucleotide-binding ATP-binding		√	2.79
6	Intracellular signal transduction Protein kinase C-like, phorbol ester/diacylglycerol binding C1		√	2.78
1	Ribosome Structural constituent of ribosome Translation Ribosome	√		22.67
2	Sm Ribonucleoprotein LSM domain Like-Sm (LSM) domain Small nucleolar ribonucleoprotein complex	√		2.54
3	Large ribosomal subunit Translation protein SH3-like domain	√		1.93
4	RNA recognition motif domain Nucleotide-binding, alpha-beta plait Nucleotide binding RRM	√		1.82
6	IG Immunoglobulin subtype Immunoglobulin domain Immunoglobulin-like domain IGc2 Immunoglobulin subtype 2	√		1.38

7	RNA polymerase DNA-directed RNA polymerase activity	√		1.27
11	Transcription, DNA-templated	√		0.96
12	Pheromone/general odorant binding protein PhBP	√		0.95

A comparison of Treatment-4h versus Control-0h and Control-4h versus Treatment-0h provided a clearer picture of what is happening to pesticide-treated honeybees at the gene function level. The first noticeable difference is the total amount of annotation clusters found when the significant genes were inputted into DAVID for analysis. Control-4h versus Treatment-0h (Appendix S) found only two annotation clusters in comparison to the Treatment-4h versus Control-0h found multiple annotation clusters, six of which are relevant to this study (Appendix R); Transmembrane (up- and down-regulated) and Immunoglobulin (up-regulated).

Another difference between the two groups was that reactive oxygen species, heat shock protein, and apoptosis were all found to be down-regulated in Treatment-4h versus Control-0h but the dual oxidase gene (although not considered significant $p>0.05$) was down-regulated in the Control-4h versus Treatment-0h. Part of this study looked at SOD as an indicator of oxidative stress and HSP as an indicator of cellular stress. The dual oxidase family has the sole function to produce reactive oxidative species (Ameziane-El-Hassani *et al.* 2016). This function correlates with the reduction of the gene in Control-4h versus Treatment-0h; if the honeybees are not in contact or producing harmful oxygen molecules then an increase in this gene is unnecessary. As a whole, ROS in the Treatment-4h versus Control-0h were significantly reduced. In turn resulting to a build-up of toxic oxygen molecules. Although the KEGG analysis showed an elevation in the pesticide-treated honeybees (Figure 32 and 34) in comparison to the sucrose-treated honeybees (Appendix P), it was not considered a significant elevation to compensate for the amount of toxicity within the cells. This finding further provides evidence that both oxidative and cellular stress are occurring when honeybees do come in contact with pesticides.

It is apparent that Annotation Cluster 1 in down-regulated genes (Table 7) had the highest enrichment score. Zinc fingers are proteins that interact with DNA, RNA and other proteins, and are essential for maintaining homeostasis. Zinc fingers regulate

cellular processes such as transcription, ubiquitin-dependent protein degradation, signal transduction, DNA repair, cell proliferation, differentiation, and apoptosis (Cassandri *et al.* 2017). These specific proteins have been implicated in the development of neurodegenerative disorders. Zinc fingers provide the "checks and balances" within the honeybee. If these necessary genes are altered for any reason, the "checks and balances" no longer exist causing a slow downward spiral of control. This study is an excellent example of that.

VI. Limitations

Several limitations have been identified in this research. A relatively small sample of six honeybees per treatment group was sent for transcriptome analysis due to the high cost of RNA sequencing. However, this number is typical of transcriptome analysis (Christen *et al.* 2018) and is in the acceptable sample size recommended by the Keck Center at the University of Illinois Urbana-Champaign. Due to a switch of the Control-4h and Treatment-4h samples when labeling, the effects of sublethal dose of imidacloprid on the individual genes and pathways has to be confirmed by qRT-PCR before publishing the results of Experiment 2. Despite corroborating evidence for the *post-hoc* switch hypothesis, particularly the elevated SOD activity in imidacloprid-treated bees in Experiment 1, further testing would be required to confirm the results of our transcriptome analyses.

Another limitation of this research is the type of the post-RNA sequencing analysis employed. DAVID's ability to use gene set enrichment to help understand the meaning behind large lists of genes is valuable; however, there are limitations to what the database can and cannot do. Of the 10,597 genes, only those genes considered significantly ($p<0.1$) up-regulated and down-regulated were uploaded into DAVID separately. This is because DAVID cannot distinguish the representation by just the Entrez ID given; the user must tell DAVID what is being uploaded. The pathway analysis that was used was KEGG, an over-representation analysis (ORA). This method identifies the pathway membership from the inputted gene list. Some limitations of ORA include: 1) the analysis only considers the number of genes in a pathway and does not account for over-expression or under; 2) a gene list must be specified and often uses significant hits

from the expression analysis, thereby missing more subtle effects; 3) the analysis assumes each gene is independent of other genes, and assumes each pathway is independent; and 4) has no statistical output (Farhad *et al.* 2020). A more inclusive analysis to use would be Pathway Topology (PT) which uses a functional class scoring methodology (FCS). FCS calculates gene-level expression statistics from expression data, uses these statistics to calculate pathway-level statistics, and identifies pathways that are significantly affected (Bayerlová *et al.* 2015). Pathway topology incorporates information about the pathway members such as cellular location and similarity of protein structure similarity. PT also calculates Perturbation Factor (PF) which is the total effect on a specific gene and Impact Factor (IF) which is the sum of all PF's for each gene in a pathway (García-Campos *et al.* 2015). A Pathway Topology program such as iPathwayGuide could not be utilized due to lack of reference for *Apis mellifera*.

A final limitation relates to the inherent challenges of conducting toxicology research on honeybees. By design, this laboratory study evaluated the effects of a single pesticide on adult bees under controlled conditions. It could be argued that this may not reflect the exposure to pesticides under field conditions, where bees are subjected to multiple chemicals, pathogens, varying weather conditions and foraging environments, and genetic predisposition. There is debate in the literature regarding the imidacloprid doses used in laboratory studies (Carreck and Rarnieks 2014). Entine (2018) contends that honeybees in the field have greater opportunities to forage on food sources that are not contaminated with neonicotinoids, making a case that bee's dilute pesticides with "clean forage." This is in contrast to laboratory bees which are solely fed neonicotinoid-spiked "food."

However, there are several counterarguments to be made. First, clean forage is difficult to find in agricultural landscapes. For example, neonicotinoid pesticide residues have been found to contaminate soils and persist in crops and wildflowers in agricultural landscapes in Europe, where a ban has been in place (Wintermantel *et al.* 2020). Second, due to memory and learning, foraging bees display flower constancy and show limited recruitment to alternate floral resources (Wagner *et al.* 2013, Van Nest *et al.* 2018). Authors have argued that the excellent olfactory sense of bees allows them to detect and avoid pesticides, but preliminary evidence indicates that this is not true (Plascencia *et al.*

2015). Third, agricultural monocultures provide the largest volume of forage to bees, providing noticeable hive growth. Such monocultures provide a much higher contaminated nectar flow than alternate sources can provide of uncontaminated nectar. Field borders and hedgerows play a role in maintaining persistence of hives when crops are not in bloom (Sardinas and Kremen 2015, Dolezal *et al.* 2019). The sublethal doses of imidacloprid used in this study do represent environmentally relevant exposure rates for bees foraging in both rural and urban settings. In the wild, even a small loss of motor coordination, activity level, etc. results in less foraging, increased mortality, less effective foraging and sublethal stress that can be harmful to the hive (Bryden *et al.* 2013).

Responses to pesticides may also differ following the oral exposures used in our study compared to field exposures that may include direct physical contact of bees with contaminated dust or pollen. Bees in our laboratory study received acute 4h exposures to imidacloprid. The response of imidacloprid on the transcriptome may differ from chronic exposures.

VII. Future Directions

Our research identified 4,205 genes that had experienced significant up- and down-regulation after acute sublethal exposure to the neonicotinoid pesticide imidacloprid. To help confirm the imidacloprid-induced changes in the gene expression that was detected from the RNA-Seq study, future hypothesis-driven research will be conducted to validate the RNA-seq results. The future study will:

i. Identify and confirm genes that do not show changes in gene expression, then utilize the genes as reference genes for gene expression studies in the honeybee brain tissue.

ii. Directly test the hypothesis that Treatment-4h and Control-4h samples were switched and mislabeled prior to shipping to University of Illinois Urbana-Champaign by confirming gene expression changes that were detected in our RNA-seq study that parallel the results from the SOD and HSP70 Assay. The specific genes that will be tested are the Heat Shock Cognate (HSC70) in

the stress apoptotic pathway and Superoxide Dismutase (SOD) in the oxidative stress pathway.

iii. Confirm the gene expression changes for other high priority genes that connect organism-level responses with underlying molecular mechanisms and biological functions. The key focus will be on:

1. Circadian rhythm gene pathways that correspond with altered foraging behavior (Karahan et al. 2015, Cakmak et al. 2018)
2. Cell communication, signal transduction, and drug binding gene sets that may correspond with motor coordination (Llewellyn 2020)
3. Response to stimulus and cellular response to stimulus gene sets that may correspond with performance on sucrose sensitivity tests (Salazar, In prep.)
4. Macromolecule modification and protein modification gene sets that may correspond with recovery from or survival of acute intoxication stress.

VIII. Conclusion

The overall goal of our research is to describe the integrated responses by the honeybee to sublethal doses of the common neonicotinoid, imidacloprid. The two objectives of Experiment 1 were: 1) to determine the effects of sublethal doses of imidacloprid on motor function and overall cellular stress as determine by the levels of HSP70 and the oxidative stress enzyme SOD, and 2) to identify a sublethal dosage of imidacloprid that yields a significant cellular stress response to use in transcriptome studies in Experiment 2. We hypothesized that bees exposed to sublethal doses of the neonicotinoid imidacloprid will display impaired motor functions and a significant cellular stress response reflected by increased levels of HSP70 and the oxidative enzyme SOD. Furthermore, we hypothesized that a dose of imidacloprid could be determined that yields a significant cellular stress response in honeybee brains. The results of these experiments confirm numerous literature reports that field-relevant, sublethal doses of

imidacloprid impact honeybee physiology and behavior (Pereira *et al.* 2020, Eban-Rothschild and Bloch 2011, Honeybee Genome Sequencing Consortium 2006, Wu-Smart and Spivak 2016, Christen *et al.* 2018, Dussaubat *et al.* 2006, Chakrabarti *et al.* 2014, Simone-Finstrom *et al.* 2016). We observed that motor responses of honeybees were impaired and levels of HSP70 and SOD were elevated when honeybees were acutely exposed to sublethal doses of imidacloprid. Experiment 1 achieved these goals by identifying a sublethal dose (0.9 ng/bee, < TD_{50} for motor impairment, 1.78-2.25 ng/bee) that coincides with pesticide-induced cellular and oxidative stress, but does not cause motor impairment. This was important because it is a sublethal dose likely to be encountered in nature, a dose which bees would appear to be unaffected in an apiary or in direct-mortality toxicological assays. At the same dose, bees display elevated pesticide-induced, sublethal stress that may contribute to CCD.

Experiment 2 examined the effects of this sublethal dose (0.9 ng/bee) on gene expression in the honeybee brain. The specific objectives were: 1) to compare overall gene expression in brain tissue of the control and imidacloprid treatment groups; 2) to determine which functional classes of genes are up-regulated or down-regulated following imidacloprid treatment; and 3) to examine difference in gene expression that occur following imidacloprid treatment in pathways regulating detoxification, heat shock proteins, oxidative enzymes, energy metabolism, circadian rhythms, cell signaling, autophagy, apoptosis, and longevity. We hypothesized that gene expression patterns will be altered in the brain tissue in imidacloprid treated bees compared to controls and will express different functional classes of genes compared to control bees. We proposed that pathways regulating detoxification, heat shock proteins, oxidative enzymes, energy metabolism, and apoptosis would be up-regulated, while pathways regulating circadian rhythms, cell signaling, and longevity would be down-regulated in imidacloprid-treated bees.

A total of 4,205 genes were identified as differentially expressed. However, differential expression analysis, a multi-dimensional scaling plot, and the one-way ANOVA heat map revealed that the greatest changes in gene expression occurred in the Control-4h group, contrary to our hypothesis and previous transcriptome studies in the literature. Our independent results in Experiment 1 and 2 provide corroborating evidence

supporting the *post-hoc* hypothesis that the Control-4h and the Treatment-4h samples were switched when the samples were mislabeled prior to shipping to the University of Illinois Urbana-Champaign. Future studies are planned to directly test the *post-hoc* hypothesis by confirming gene expression changes by RT-qPCR that were detected in our RNA-sequencing study that parallel the results from the SOD and HSP70 Assay. The specific genes that will be tested are the Heat Shock Cognate 70 (HSC70) in the stress apoptotic pathway and Superoxide Dismutase (SOD) in the oxidative stress pathway.

Although a switch of the samples likely occurred, the comparison between the Control-4h and the Treatment-4h groups remain valid, since only the direction of differential gene expression (up-regulated versus down-regulated) would be affected. Pathway analysis indicated that multiple pathways were affected including oxidative phosphorylation, longevity regulating pathway, apoptosis, peroxisome, FOXO signaling, drug metabolism-cytochrome P450, metabolism of xenobiotics by cytochrome P450, circadian rhythm, and glutathione metabolism. Similar pathways have been altered in bees exposed to nicotine (du Rand *et al.* 2015), ethanol (Hranitz *et al.* unpublished), and thiamethoxam (Shi *et al.* 2017). The specific alterations we observed support our prediction that pathways that regulate detoxification, heat shock proteins, oxidative enzymes, energy metabolism, and apoptosis will be up-regulated while pathways that regulate circadian rhythms, cell signaling, and longevity will be down-regulated in imidacloprid-treated bees. These alterations in gene networks relate to key biological functions of honeybees that have the potential to affect the viability of the colony.

Long term, our aim is to understand the specific gene networks and cellular pathways affected by sublethal imidacloprid intoxication in order to understand the molecular mechanisms of neonicotinoid toxicity and its contribution to pollinator declines. This research serves as a foundation for future hypothesis-driven gene expression studies that relate specific molecular changes that occur with neonicotinoid toxicity to biological functions. Future studies can target gene expression changes for other high priority genes that connect organism-level responses in the field with underlying molecular mechanisms. This will not only allow us to understand neonicotinoid toxicity but may also prevent pollinator declines and CCD.

IX. Literature Cited

Abramson CI, Kandolf A, Sheridan A, Donohue D. Bozic J, Meyers JE, Benbassat D. (2004a). **Development of ethanol model using social insects: III.** Preferences for ethanol solutions. *Physiological reports* 94(1):227.

Abramson CI, Place AJ, Aquino IS, Fernandez A. (2004b). **Development of ethanol model using social insects: IV.** Influence of ethanol on the aggression of Africanized Honeybees (*Apis mellifera* L.) *Physiological Reports* 94(3): 1107.

Abramson CI, Stone SM, Ortez RA, Luccardi A, Vann KL, Hanig KD, Rice J. (2000). **Development of an ethanol model using social insects 1: Behavior studies of the Honeybee (*Apis mellifera* L.).** *Alcoholism-Clinical and Experimental Research* 24(8):1153.

Abramson CI, Fellows FW, Browne BL, Lawson A, Ortiz RA. (2003). **Development of an ethanol model using social insects: II.** Effects of Antabuse ® on consumatory responses and learned behavior of the Honeybee (*Apis mellifera* L.*). Physiological Reports* 92(2): 365.

Abramson CI, Sanderson C, Painter J, Barnett S, Wells H. (2005). **Development of an ethanol model using social insects: V.** Honeybee foraging decisions under the influence of alcohol. *Alcohol* 36(3):187.

Agriculture and Consumer Protection. (1990). **Chapter 2 Colony life and social organization.** www.fao.org.

Albaugh LLC. (2017). Company. Retrieved from albaughllc.com/company/.

Ameziane-El-Hassani R, Schlumberger M, Dupuy C. (2016). **NADPH oxidases: new actors in thyroid cancer?** *Nat Rev Endocrinol*. 12(8):485-94. doi: 10.1038/nrendo.2016.64.

Atmowidjojo, A. H., Wheeler, D. E., Erickson, E. H., & Cohen, A. C. (1997). **Temperature tolerance and water balance in feral and domestic Honeybees, Apis mellifera L.** *Comparative Biochemistry and Physiology Part A: Physiology*, *118*(4), 1399-1403.

Atwood, D and Paisley-Jones, C. (2017). Pesticide Industry Sales and Usage 2008-2012, Market Estimate. epa.gov

Alavanja M. C. (2009). **Introduction: pesticides use and exposure extensive worldwide.** *Reviews on environmental health*, *24*(4), 303–309. https://doi.org/10.1515/reveh.2009.24.4.303

Barthell JF, Hranitz JM, Thorp RW, and Shue MK. (2002). **High temperature responses in two exotic leafcutting bee species: Megachile apicalis and M. rotundata (Hymenoptera: Megachilidae).** *The Pan-Pacific Entomologist.* 78(4): 235-246.

Bayer Crop Science. (2017). Insecticides. Retrieved from https://www.cropscience.bayer.us/products/insecticides/.

Bayerlová, M., Jung, K., Kramer, F. *et al.* (2015). **Comparative study on gene set and pathway topology-based enrichment methods.** *BMC Bioinformatics* 16: 334. https://doi.org/10.1186/s12859-015-0751-5

Bee Culture. (2019). **Catch the Buzz- during the 2018-2019 winter an estimated 37.7% of managed Honeybee colonies in the United States were lost.** https://www.beeculture.com/catch-the-buzz-during-the-2018-2019-winter-an-estimated-37-7-of-managed-honey-bee-colonies-in-the-united-states-were-lost/

Benbrook, C. (2009). **Impacts of genetically engineered crops on pesticide use: the first thirteen years.** Boulder, CO. The Organic Center.

Berlett BS and Stadtman ER. (1997). **Protein oxidation in aging, disease, and oxidative stress.** *J Biol Chem* 272(33):20313-6.

Beyenbach, Klaus and Wieczorek, Helmut. (2006). **The V-type H^+ ATPase: molecular structure and function, physiological roles and regulation.** *Journal of Experimental Biology* 209:577-589.

Blacquière T, Smagghe G, van Gestel C, Mommaerts V. (2012). **Neonicotinoids in bees: a review on concentrations, side-effects and risk assessment.** *Ectotoxicology* 21:973-992. DOI 10.1007

Bozic J, Abramson CI, Bedencic M. (2006). **Reduced ability of ethanol drinkers for social communication in Honeybees.** (*Apis mellifera c*arnica Poll.). *Alcohol* 38(3):179.

Bozic J, DiCesare J, Wells H, Abramson CI. (2007). **Ethanol levels in Honeybee hemolyph resulting from alcohol ingestion.** *Alcohol* 41(4):281.

Bryden J., Gill RJ, Mitton RAA, Raine NE, Jansen VAA. (2013). **Chronic sublethal stress causes bee colony failure.** *Ecology Letters* 16(12):1463-1469.

Cabirol, A., & Haase, A. (2019). **The Neurophysiological Bases of the Impact of Neonicotinoid Pesticides on the Behaviour of Honeybees.** *Insects*, *10*(10), 344. https://doi.org/10.3390/insects10100344

Cakmak I, Hranitz J, Blatzheim L, Bower C, Polk T, Levinson B, Wells H. (2018). **Effects of thiamethoxam on the behavior of foraging Honeybees with artificial flower choices.** *Uludag Bee Journal* 18(1):2-13.

Calabrese EJ, Stanek EJ, III, Nascarella MA, Hoffman GR. (2008). **Hormesis Predicts Low-Dose Responses Better Than Threshold Models.** *International Journal of Toxicology* 27(5):369.

Carreck, Norman and Ratnieks, Francis. (2014). **The dose makes the poison: have "field realistic" rates of exposure of bees to neonicotinoid insecticides been overestimated in laboratory studies?.** *Journal of Apicultural Research.* 53(5):607-614. DOI: 10.3896/IBRA1.53.5.08

Cassandri M, Smirnov A, Novelli F, Pitolli C, Agostini M, Malewicz M, Melino G, and Rashellà G. (2017). **Zinc-finger proteins in health and disease.** *Cell Death Discovery.* 3.

Chacon-Almeida L, Simões Z, and Bitondi M. (2000). **Induction of heat shock proteins in the larval fat body of Apis mellifera L. bees.** *Apidologie,* Springer Verlag. 31(4): 487-501

Chakrabarti P, Rana S, Sarkar S, Smith B, Basu P. (2015). **Pesticide-induced oxidative stress in laboratory and field populations of native Honeybees along intensive agricultural landscapes in two eastern indian states.** *Apidologie* 46(1):107-29.

Christen V, Schirrmann M, Frey J, and Fent K. (2018). **Global Transcriptomic Effects of Environmentally Relevant Concentrations of the Neonicotinoids Clothianidin, Imidacloprid, and Thiamethoxam in the Brain of Honeybees (***Apis mellifera*). *Environmental Science and Technology.* 2(13): 7534-7544.

Claudianos, C., Ranson, H., Johnson, R. M., Biswas, S., Schuler, M. A., Berenbaum, M. R., Feyereisen, R., & Oakeshott, J. G. (2006). **A deficit of detoxification enzymes: pesticide sensitivity and environmental response in the honeybee.** *Insect molecular biology*, *15*(5), 615-636. https://doi.org/10.1111/j.1365-2583.2006.00672.x

Cook SC. (2019). **Compound and Dose-Dependent Effects of Two Neonicotinoid Pesticides on Honey Bee (*Apis mellifera*) Metabolic Physiology.** *Insects*, *10*(1), 18. https://doi.org/10.3390/insects10010018

Coulon, M., Schurr, F, Martel, AC, Cougoule, N, Begaud, A., Mangoni, P, Dalmon, A, Alaux, C. LeConte, Y, Thiery, R, Ribiere-chabert, M, Dubois, E. **Metabolization of thiamethoxam (a neonicotinoid pesticide and interaction with the chronic bee paralysis virus in honeybees.** *Pesticide Biochemistry and Physiology*, Vol. 144, p10-18, 2018.

Decourtye A, Lacassie E, Pham-Delegue MH. (2003). **Learning performances of honeybees (*Apis mellifera* L.) are differentially affected by imidacloprid according to the season.** *Pest Manag Sci* 59:269-278.

Decourtye A, Devillers J, Cluzeau S, Charreton M, Pham-Delegue MH. (2004a). **Effects of imidacloprid and deltamethrin on associative learning in honeybees under semi-field and laboratory conditions.** *Ecotoxicol Environ Saf* 57:410-419.

Decourtye A, Armengaud C, Renou M, Devillers J, Cluzeau S, Gautheir M, Pham-Delegue MH. (2004b). **Imidacloprid impairs memory and brain metabolism in the honeybee (*Apis mellifera* L.)**. *Pest Biochem Physiol* 78:83-92.

Deng C, Graham R, and Shukla R. (2001). **Detecting and Estimating Hormesis Using a Model-Based Approach.** Human and Ecological Risk Assessment: An International Journal. 7: 849-866.

DiPrisco G, Cavaliere V, Annoscia D., Varricchio P, Caprio E, Nazzi,F, Gargiuli G,Pennacchio F. (2013). **Neonicotinoid clothianidin adversely affects insect immunity and promotes replication of a viral pathogen in Honeybees.** *Proc of the Natl Acad Sci.* 110(46):18466-18471.

Dolezal AG, St Clair AL, Zhang G, Toth AL, and O'Neal ME. (2019). **Native habitat mitigates feast-famine conditions faced by Honeybees in an agricultural landscape.** Proceedings of the National Academy of Sciences of the United States of America. 116(50): 25147-25155.

Drake, J. M. & Kramer, A. M. (2011). Allee Effects. *Nature Education Knowledge* 3(10):2.

du Rand EE, Smit S, Beukes M, Apostolides Z, Pirk C, Nicolson S. (2015). **Detoxification mechanisms of Honeybees *(Apis mellifera)* resulting in tolerance of dietary nicotine.** *Scientific Reports* 5:11779 DOI: 10.1038.

Dussaubat C, Maisonnasse A, Crauser D, Tchamitchian S, Bonnet M, Cousin M, Kretzschmar A, Brunet J, Le Conte Y. (2016). **Combined neonicotinoid pesticide and parasite stress alter honeybee queens' physiology and survival.** *Scientific Reports* 6:31430.

Eban-Rothschild A., Bloch G. (2012). **Circadian Rhythms and Sleep in Honeybees.** In: Galizia C., Eisenhardt D., Giurfa M. (eds) *Honeybee Neurobiology and Behavior.* Springer, Dordrecht

Ellis JD and Mortenson AN. (2011). **Featured Creatures.** University of Florida: Entomology and Nematology.
http://entnemdept.ufl.edu/creatures/misc/bees/cape_honey_bee.htm

Engel, MS. (1999). **The taxonomy of recent and fossil Honeybees (Hymenoptera: Apidae: *Apis*).** *Journal of Hymenoptera Research*. 8:165-195.

Entine, Jon. (2018). **"Gold standard" assessing neonicotinoids: Field bee hive studies find pesticides not major source of health issues.** Genetic Literacy Project.

Farhad M, Ovens K, Hogan DJ, and Kusalik AJ. (2020). **Gene Set Analysis: Challenges, Opportunities, and Future Research.** *Frontiers in Genetics.* 11

Farhan, M., Wang, H., Gaur, U., Little, P. J., Xu, J., & Zheng, W. (2017). **FOXO Signaling Pathways as Therapeutic Targets in Cancer.** *International journal of biological sciences*, *13*(7), 815–827.

Feder ME, Blair N, Figeuras H. (1997). **Natural thermal stress and heat-shock protein expression in *Drosophila* larvae and pupae.** *Functional Ecology* 11:90-100.

Feder ME and Hoffman G. (1999). **Heat-shock proteins, molecular chaperones, and the stress response: evolutionary and ecological physiology.** *Annual Review of Physiology.* 61(1): 24-282.

Finkel T and Holbrook NJ. (2000). **Oxidants, oxidative stress and the biology of ageing.** *Nature* 408(6809):239.

Frazier M, Mullin, C., Frazier, J. Ashcraft, S. (2008) **What have pesticides got to do with it?** *American Bee Journal.* Vol 148, p521-523.

García-Campos M, Espinal-Enríquez J, and Hernández-Lemus E. (2015). **Pathway Analysis: State of the Art.** *Front. Physiol*. DOI:10.3389.

Gervais, J. A., Luukinen, B., Buhl, K., & Stone, D. (2010). **Imidacloprid general fact sheet.** Oregon State University Extension Services: National Pesticide Information Center.

Girolami, V., Mazzon, L., Squartini, A., Mori, N., Marzaro, M., Di Bernardo, A., et al. (2009). **Translocation of neonicotinoid insecticides from coated seeds to seedling guttation drops: A novel way of intoxication for bees.** *Journal of Economic Entomology, 102*(5), 1808-1815.

Goulson, David. (2013). **An overview of the environmental risks posed by neonicotinoid insecticides.** *Journal of Applied Ecology* 50, 977-987.

Henry M, Reguin M, Requier F, Rollin O,Odoux J-F, Aupinel P, Qiao D, Seidler F, Slotkin T. (2005). **Oxidative mechanisms contributing to the developmental neurotoxicity of nicotine and chlorpyrifos.** *Toxicol and Applied Pharmacol*. 206(1):17-26.

Honeybee Genome Sequencing Consortium. (2006). **Insights into social insects from the genome of the honeybee *Apis mellifera.*** *Nature* 443(26): 931-949.

Honeymell. (2015). **Reproduction of Honeybees.** https://www.honeymell.com/en/bees/25-reproduction-of-honey-bees

Hrantitz et al. (2010). **An ethanol-induced hermetic stress response in Honeybees (*Apis mellifera)* brain tissue.** *Integrative and Comparative Biology* 50:E245-E245.

Hranitz JM and Barthell JF. (2003). **Heat shock protein 70 during development of the leafcutting bee, Megachile rotundata (Hymenoptera: Megachilidae).** *Southwestern Entomologist.* 28(2): 97-104.

Hranitz JM, Barthell JF, Abramson CI, Brubaker KD, Wells H. (2009a). **Stress protein responses in Honeybees: Is it useful to measure stress responses of individual bees in the hive?** *Uladag Bee Journal* 9(2): 60-71.

Hranitz JM, Abramson CI, Carter RP. (2009). **Ethanol increases HSP70 concentrations in honeybee (*Apis mellifera* L.) brain tissue.** *Alcohol* 44:275-282.

Hunt, GJ. (2007). **Flight and fight: A comparative view of the neurophysiology and genetics of Honeybee defensive behavior.** *Journal of Insect Physiology* 53(5):399-410.

Ighodaro OM and Akinloye OA. (2018). **First line defense antioxidants-superoxide dismutase (SOD), catalase (CAT) and glutathione peroxidase (GPX): Their fundamental role in the entire antioxidant defense grid.** *Alexandria Journal of Medicine* 54(4):287-293.

Illumina. (2010). **Illumina Sequencing Technology.** https://www.illumina.com/documents/products/techspotlights/techspotlight_sequencing.pdf

Johnson, B.R. (2008). **Within-nest temporal polyethism in the Honeybee.** *Behav Ecol Sociobiol* 62:777.

Johnson RM, Wen Z, Schuyker MA, Berenbaum MR. (2006). **Mediation of pyrethroid insecticide toxicity to hyoney bees (Hymenoperia:Apidae) by Cytochrome P450 monooxygenases.** *Econ Entomol,* Aug 99 (4) 1046-50

Jones JC, Helliwell P, Beekman M, Maleszka R, and Oldroyd BP. (2005). **The effects of rearing temperature on developmental stability and learning and memory in the Honeybee, *Apis mellifera.*** Journal of Comparative Physiology a-Neuroethology Sensory *Neural and Behavioral Physiology* 191(12):1121-1129.

Karahan A, Cakmak I, Hranitz JM, Karaca I, Wells H. (2015). **Sublethal imidacloprid effects on Honeybee flower choices when foraging.** *Ecotoxicology* 24:2017-2025.

KEGG Mapper. (2020). https://www.genome.jp/kegg/mapper.html

Kessler, S., Tiedeken, E., Simcock, K. *et al.* (2015). **Bees prefer foods containing neonicotinoid pesticides.** *Nature* 521, 74–76.

Kuropatnicki Andrzej, Szliszka Ewelina, and Krol Wojciech. (2013). **Historical Aspects of Propolis Research in Modern Times.** *Evid Based Complement Alternat Med*. DOI: 10.1155/2013/964149.

Le Conte Y, Ellis M, and Ritter W. (2010). ***Varroa* mites and Honeybee health: can *Varroa* explain part of the colony losses?** *Apidologie* 41(3):353-363. DOI: https://doi.org/10.1051/apido/2010017.

Maiese, Kenneth. (2015). **FOXO Proteins in the Nervous System Analytical Cellular Pathology.** 2015. DOI:10.1155/2015/569392

Mao W, Schuler M, and Berendaum M. (2013). **Honey constituents up-regulate detoxification and immunity genes in the western Honeybee *Apis mellifera***. *PNAS* 110(22): 8842-8846.

Mater Methods. (2012). 2:201.

Merritt, Chris. (2011-2020). **Hormesis: Why you may not be reaching your goals?** https://www.bspnova.com/hormesis-why-you-might-not-be-reaching-your-goals/

Möller, Gregory. (NA). **Dose-Response Relationships.** University of Idaho. https://www.webpages.uidaho.edu/foodtox/lectures/lecture05/L5-Dose%20-%20Response%20Relationships.pdf

National Center for Biotechnology Information. (accessed on July 22,2020). **PubChem Database.** CID=86287518, **https://pubchem.ncbi.nlm.nih.gov/compound/Imidacloprid**

Nature Protocols. (2009). 4(1):44. https://david.ncifcrf.gov/

Ozawa, K., Meikari, T., Motohashi, K., Yoshida, M., & Akutsu, H. (2000). **Evidence for the presence of an F-type ATP synthase involved in sulfate respiration in Desulfovibrio vulgaris.** *Journal of bacteriology*, *182*(8), 2200–2206. https://doi.org/10.1128/jb.182.8.2200-2206.2000

Pereira NC, Diniz TO, and Ruvolo-Takasusuki MCC. (2020). **Sublethal effects of neonicotinoids in bees: a review.** *Sci. Elec. Arch 13*(7). DOI: http://dx.doi.org/10.36560/13720201120.

Pilatic, Heather. (2012). **Pesticides and Honeybees: State of Science.** www.panna.org

Plascencia M, Carson R, Hranitz JM, Barthell JF, Cakmak I, Gonzalez VH. (2015). **Testing the pesticide avoidance hypothesis by bees and flies in a Mediterranean arthropod community.** *Integrative and Comparative Biology.* 55:E315-E315.

Poquet Y, Vidau C, Alaux C. (2015). **Modulation of pesticide response in Honeybees.** Apidologie 47:412-416.

Qiagen. (2020). RNeasy Micro Handbook. HB 1920-002.

Sahebzadeh, Najmeh & Lau, Wei. (2017). **Expression of heat-shock protein genes in Apis mellifera meda (Hymenoptera: Apidae) after exposure to monoterpenoids and infestation by Varroa destructor mites (Acari: Varroidae).** *European Journal of Entomology.* 114. 195-202. 10.14411/eje.2017.024.

Salazar T, Young C, Naranjo S, Pastor M, Gunes N, Cakmak I, Barthell J, Hranitz J. (In Prep.) **Effects of sublethal doses of insecticides on Honeybees (Hymenoptera: Apidae).** *Ecotoxicology.*

Sardinas HS and Kremen C. (2015). **Pollination services from field-scale agricultural diversification may be context-dependent.** *Agriculture Ecosystems and Environment.* 207:17-25.

Schroeder ME and Flattum, RF. (1984). **The mode of action and neurotoxic properties of the nitromethylene heterocycle insecticides.** *Pesticide Biochemistry and Physiology (22)2*:148-160

Seeley, TD. (1985). **Honeybee Ecology.** Princeton University Press, Princeton, NJ.

Sen Sarma M, Rodriguez-Zas SL, Hong F, Zhong S, Robinson GE. (2009). **Transcriptomic profiling of central nervous system regions in three species of Honeybee during dance communication behavior.** *PLoS ONE* 4(7):e6408.

Simon-Delso, N., Amaral-Rogers, V., Belzunces, L. P., Bonmatin, J., Chagnon, M., Downs, C., et al. (2015). **Systemic insecticides (neonicotinoids and fipronil): Trends, uses, mode of action and metabolites.** *Environmental Science and Pollution Research, 22*(1), 5-34.

Simone-Finstrom M, Li-Byarlay H, Huang MH, Strand MK, Rueppell O, Tarpy DR. (2016). **Migratory management and environmental conditions affect lifespan and oxidative stress in Honeybees.** *Scientific Reports* 6:32023.

Shi, TF, Wang YF, Liu F, Qi, L, Yu, LS. (2017). **Influence of the neonicotinoid insecticide thiamethoxam on miRNA Expression in the Honeybee (Hymenoptera: Apidae).** *Journal of Economic Entomology.* Col xx, p 1-7

Stoner KA and Eitzer EB. (2012). **Movement of soil-applied imidacloprid and thiamethoxam into nectar and pollen of squash (*Cucurbita pepo*).** *PLoS One* 7(6)

Sylvester, H., Rinderer, T., & Bolten, A. (1983). **Honey sac contents: A technique for collection and measurement in foraging Honeybees (hymenoptera: Apidae).** *Journal of Economic Entomology*, *76*(1), 204-206.

Tan, K., Chen, W., Dong, S., Liu, X., Wang, Y., & Nieh, J. C. (2014). **Imidacloprid alters foraging and decreases bee avoidance of predators.** *PLoS One, 9*(7), e102725.

Tasman K, Rands S, and Hodge J. (2020). **The neonicotinoid insecticide imidacloprid disrupts bumblebee foraging rhythms and sleep.** bioRxiv. https://www.biorxiv.org/content/10.1101/2020.04.07.030023v1.full

Technical Note: Sequencing: Quality Scores for Next-Generation Sequencing. Assessing sequencing using Phred quality scoring. (2011). Illumina Inc. https://www.illumina.com/documents/products/technotes/technote_Q-Scores.pdf

Toma, D. P., Bloch, G., Moore, D., & Robinson, G. E. (2000). **Changes in period mRNA levels in the brain and division of labor in Honeybee colonies.** *Proceedings of the National Academy of Sciences of the United States of America*, *97*(12), 6914–6919. https://doi.org/10.1073/pnas.97.12.6914

Tomizawa M, Lee DL, and Caasida J. (2000). **Neonicotinoid Insecticides: Molecular Features Conferring Selectivity for Insect versus Mammalian Nicotinic Receptors**. *Journal of Agricultural and Food Chemistry* 48(12):6016-24. DOI: 10.1021/jf000873c.51.48

Tong L, Nieh JC, and Tosi S. (2019). **Combined nutritional stress and a new systemic pesticide (flupyradifurone, Sivanto®) reduce bee survival, food consumption, flight success, and thermoregulation**. *Chemosphere*, *237*, 124408. https://doi.org/10.1016/j.chemosphere.2019.124408

United States Environmental Protection Agency. (2016). **Colony Collapse Disorder.** www.epa.gov.

U.S. National Library of Medicine. (2015). **PTEN Gene.** https://ghr.nlm.nih.gov/gene/PTEN#:~:text=Normal%20Function,or%20in%20an%20uncontrolled%20way.

Valizadegan N and Drnevich J. (2019). **John M Hranitz RNA-Seq Report.** University of Illinois.

van Dooremalen, C, Cornelissen, B, Poleij-hok-ahin, C, Blacquiere, T. (2018). **Single and interactive effects of Varroa destructor, Nosema spp., and imidacloprid on Honeybee colonies (Apis mellifera).** *Exosphere.* Vol 9. pe02378.

vanEngelsdorp D, Evans JD, Saegerman C, Mullin C, Haubruge E, Nguyen BK et al. (2009). **Colony collapse disorder: A descriptive study.** *PLoS ONE* 4(8): e6481.

Van Nest BN, Otto MW, and Moore D. (2018). **High experience levels delay recruitment but promote simultaneous time-memories in Honeybee foragers.** *Journal of Experimental Biology.* 221(23).

Van Rossum, G and Drake Jr, FL. (1995). *Python reference manual*. Centrum voor Wiskunde en Informatica Amsterdam.

Vannette R, Mohamed A, Johnson B. (2015). **Forager bees (*Apis mellifera*) highly express immune and detoxification genes in tissues associated with nectar processing.** *Scientific Reports* 5:16224 DOI 10.1038

Wagner AE, Van Nest BN, Hobbs CN, Moore D. (2013). **Persistence, reticence and the management of multiple time memories by forager Honeybees.** *Journal of Experimental Biology.* 216(7): 1131-1141

Wainselboim AJ et al. (2000). **Trophallaxis in the honeybee Apis mellifera (L.): the interaction between flow of solution and sucrose concentration of the exploited food sources.** *Anim Behav* 59(6):1177-1185.

Wilson, EO. (1971). **The Insect Societies.** Cambridge, MA: Belknap Press of Harvard University Press.

Wintermantel D, Odoux JF, Decourtye A, Henry M, Allier F, and Bretagnolle V. (2020). **Neonicotinoid-induced mortality risk for bees foraging on oilseed rape nectar persists despite EU moratorium.** *Science of the Total Environment.* 704.

Wu MC, Chang YW, Lu KH, and Yang EC. (2012). **Gene expression changes in Honeybees induced by sublethal imidacloprid exposure during the larval stage.** *Insect biochemistry and molecular biology* 88.

Wu-Smart, J and Spivak, M. (2016). **Sub-lethal effects of dietary neonicotinoid insecticide exposure on Honeybee queen fecundity and colony development** *Scientific Reports* 6:32108 DOI:10.1038.

Yan H, Jia H, Gao H, Guo X, and Xu B. (2013). **Identification, genomic organization, and oxidative stress response of a sigma class glutathione S-transferase gene (AccGSTS1) in the Honeybee, *Apis cerana cerana.*** *Cell Stress Chaperones.* 2013 Jul; 18(4): 415–426. DOI: 10.1007/s12192-012-0394-7

Zemene M, Bogale B, and Derso S. (2015). **A Review on Varroa Mites of Honeybees.**

Zhiguo L, Tiantian Y, Chen Y, Matthew H, Jingfang H, Jingnan HU, Hongyi N, Songkun S. (2019). **Brain transcriptome of Honeybees (*Apis mellifera*) exhibiting impaired olfactory learning induced by a sublethal dose of imidacloprid.** *Pesticide Biochemistry and Physiology*. 156: 36-43.

Appendix A: Animal Research (IACUC) Approval.

Thesis or Departmental Paper Proposal Assurance of Compliance with University Research Requirements

Date August 3, 2020

Heather J. Llewellyn ID# 384784

Student's Name (please print)

Program of Study Masters of Biology

I have reviewed the thesis or departmental paper proposal submitted by the above named student and have concluded that:

- ☐ There is no human subject involvement and no human subject research is required
- ☐ Human subject research review is required.
- ☐ There is no animal use involved and no animal use review is required.
- ☑ Animal use review is required.
  IACUC review is not required for invertebrate animals such as the insects used in this study.

Project Advisor

Department Chairperson

A completed copy of this form should be included with the thesis/departmental paper proposal submitted to the Office of Graduate Studies & Research, CEH 212.

Appendix B: Literature data on neonicotinoid residues in bee-collected pollen, honey, and bees (Blacquière et al. 2012).

Substrate	Country	Dominant Crop	Design and Analysis	Chemical	Sample Size	% Positive	Concentration (ug kg^{-1} fresh weight) Mean | + Range	Notes	References
Pollen	USA(Florida, California,Pennsylvania or 13 states) + samples from outside USA and Canada	No data	2007/2008 survey included 13 apiaries in Florida+California, 47 colonies in Pennsylvania orchards and from "other" samples; no further data analysis	Imida. Thiam. Aceta. Thiac.	350	2.9 0.29 3.1 5.4	3.1 | <2.0-912 53.3 1.9 | <5.0-124 5.4 | <1.0-115	Many pesticides detected	Mullin et al. (2010)
Honey Bees	USA(Florida, California,Pennsylvania or 13 states) + samples from outside USA and Canada	No data	2007/2008 survey included 13 apiaries in Florida+California, 47 colonies in Pennsylvania orchards and from "other" samples; no further data analysis	Imida. Thiam. Aceta. Thiac.	140	0 0 0 0	<2.0 <1.0 <2.0 <1.0	Many pesticides detected	Mullin et al. (2010)
Bee Wax	USA (Florida, California, Pennsylvania or 13 states) + samples from outside USA and Canada	No data	2007/2008 survey included 13 apiaries in Florida+California, 47 colonies in Pennsylvania orchards and from "other" samples; no further data analysis	Imida. Thiam. Aceta. Thiac.	208	0.96 0 0 1.9	- |2.4-13.6 <1.0 <5.0 0.1|<1.0-8.0	Many pesticides detected	Mullen et al. (2010)

Appendix C: Lethal and sub-lethal effects by imidacloprid to individual (organism level) honey bees as determined in different studies by oral exposure under laboratory conditions (Blacquière et al. 2012).

Species	Exposure	Side-effects	References
Apis mellifera	Lab+Oral: acute exposure to 0.12 and 12 ng/ bees	Reduction of associative learning at 12 ng/bee^{-1}	Decourtye et al. (2004a, b)
Apis mellifera	Lab+Oral: acute exposure to 0.2-3.2 mg/L	LD_{50} -48h: 30 ng/bee$^{-=1}$	Decourtye et al. (2003)
Apis mellifera	Lab+Oral: chronic exposure (no information on concentration)	Lowest observed effect concentration on survival of winter bees: 24 ug/kg^{-1} Lowest observed effect concentration on associative learning via proboscis extension reflex assay on winter bees (12 ng/bee^{-1}) and summer bees (12 ng/bee^{-1})	Decourtye et al. (2003)
Apis mellifera	Lab+Oral: acute exposure to 0.1-81 ng/bee	LD_{50}-48h: between 41 and >81 ng/bee^{-1} No-observed effect dose :</= 1.25 ng/bee; reduced sucrose uptake by 33% at 81 ng/bee^{-1}	Nauen et al. (2001)
Apis mellifera	Lab+Oral: acute exposure to 0.7 mg/seed	LD_{50}-48h: 4-41 ng/bee^{-1}	Schmuck et al. (2001)
Apis mellifera	Lab+Oral: chronic exposure (39 days) to sunflower nectar contaminated with 0.002-0.02 ug/kg^{-1}	No-observed effect concentration for mortality, feeding activity, wax comb production, breeding performance and colony vitality: 0.02 ug/kg^{-1}	Schmuck et al. (2001)

Appendix D: Concentrations of imidacloprid causing lethal and sublethal effects on (micro)-colony level in honey bees as determined in different studies by oral exposure under laboratory conditions (Blacquière et al. 2012).

Species	Exposure	Toxicity	References
Apis mellifera	Lab+Oral: 100-1,000 ug/L^{-1}	500-1,000 ug/L^{-1}: bees disappeared at the hive/feeding site up to 24 hours	Bortolottie et al. (2003)
Apis mellifera	Lab+Oral: 0.12-12 ng/bee^{-1} in syrup (acute) Lab+Oral: 24 ug/kg^{-1} in syrup (24h)	Increase of the cytochrome oxidase labeling, negative effect on the proboscis extension reflex assay with 12 ng/bee^{-1} but not with 0.12 ng/bee^{-1} Negative effect on the proboscis extension reflex assay	Decourtye et al. (2004a, b)
Apis mellifera	Lab+Oral: >100ug/kg^{-1} (chronic)	No-observed effect concentration survival: 2-20 ug/kg^{-1} in sunflower nectar 20 ug/L^{-1}: decrease in foraging activity; >100 ug/L^{-1}: reduce in foraging behavior for 30-60 minutes >50 ug/L^{-1}: increase in interval between successive visits at a feeder	Schmuck (1999); Schmuck et al. (2001)

Appendix E: Macho® Stock solution preparation.

Stock Solution Preparation

Sucrose Solution:

Molar Mass: 342.3 g/mol

$C_{12}H_{22}O_{11}$

$$1.5\ M\ Sucrose\ Solution\ \times 342.3\frac{g}{mol}Sucrose = 513.45\ g\ Sucrose\ \times 0.1 = 51.345\ g\ Sucrose\ in\ 100\ mL\ Ultra\ Pure\ Water$$

This solution was used as part of the stock solutions for imidacloprid treatment and was refrigerated at 4°C.

Macho Solution:

$$\frac{4lbs}{1gal} = \frac{18{,}14.37g}{3785.41mL} = \frac{0.4793g}{mL}\left(\frac{10^9 ng}{g}\right)\left(\frac{mL}{10^3\mu L}\right) = 479{,}306\frac{ng}{\mu L}\ jug$$

$$C1V1 = C2V2$$

$$\left(479{,}306\frac{ng}{\mu L}\right)V1 = \left(3.6\frac{ng}{10\mu L}\right)(10\ mL)$$

$$V1 = 0.0075\ mL\ for\ 25\ mL = 0.0187\ mL$$

Stock 1/5 LD_{50}:

100 µL from Macho jug added to 1,000 mL Ultra Pure Water = 187 µL of stock added to 25 mL stock Sucrose Solution

*Macho is kept at room temperature per pesticide directions.

Appendix F: Treatment group preparation.

Treatment (ng/bee)	[ng/µL] for 10 µL Feeding	1/5 Stock Solution (mL)	1.5 M Sucrose Solution
1/5 LD_{50}	3.6	10	0
1/10 LD_{50}	1.8	5	5
1/20 LD_{50}	0.9	2.5	7.5
1/50 LD_{50}	0.36	1	9
1/100 LD_{50}	0.18	0.5	9.5
1/500 LD_{50}	0.036	0.005	9.995
Total		19.005 mL	40.995 mL

All treatment solutions should be stored in the refrigerator at 4℃.

Appendix G: Bovine stock albumin standard preparation.

The BSA standards, determined using $C_1V_1=C_2V_2$ with a stock solution of 7.1 µg/µL of Bovine Stock Albumin, used are seen in the table below:

Standards	[Protein]	BSA (µL)	Homogenization Buffer (µL)
1	0.22187	6.25	193.75
2	0.44375	12.5	187.5
3	0.8875	25	175
4	1.775	50	150
5	3.55	100	100
6	5.0	140.8	59.2
7	7.1	200	0

Appendix H: Stock bovine HSP70 standard preparation.

Standard	1:10 Standard Diluted	[Final] ng	Volume HSc70 (µL)	Volume Buffer (µL)
1	√	10	4	196
2	√	30	12	180
3		50	2	198
4		80	3.2	196.8
5		100	4	196
6		300	12	188
7		500	20	180

Enough of each standard was prepared to load 5µL in triplicate per microplate.

Appendix I: Information needed to submit RNA for library construction and sequencing to University of Illinois Keck Center.

* a word or excel file with: sample ID, label on tube, concentration (Qubit) and volume. Also, information on how the samples will be pooled and sequenced (i.e. how many lanes, which samples should be pooled in each lane, single-read or paired-end, etc). This form can be filled out completely to satisfy this request.

* Submit at least 1ug of total RNA in a minimum volume of 20ul and a maximum volume of 50ul of RNAse-free water

* total RNA should be free of genomic DNA (either DNAsed or otherwise free of contamination with gDNA).

* run an aliquot (~50 to 100ng) of the total RNA on a 1% agarose gel next to a DNA ladder and send us a picture before you submit the sample. This picture will be used to evaluate integrity of the total RNA as well as presence/absence of gDNA. See representative gels and bioanalyzer traces here: http://biotech.illinois.edu/htdna/services-equipment/illumina

* alternatively, run the total RNA on an RNA bioanalyzer chip or AATI Fragment Analyzer and send us the .pdf file.

* **on-campus only:** account number to be used for the project. Charges will not be applied until after the data is delivered but the account is needed to set up the project.
* **off-campus only**: Off-campus user form or TTA must be in place. Charges will be applied at contract execution or after work is completed, depending upon negotiated terms.

*Shipping Address:
University of Illinois Keck Center
Attn: Chris Wright
1201 W. Gregory Dr.
334 ERML
Urbana, IL 61801
(217) 333-4372

1) PI Name: John M. Hranitz
2) Customer Name: Bloomsburg University of Pennsylvania
3) Date: April 8, 2019
4) FOAPAL (on-campus customers only):

Sample ID (this name will be used to name you fastq files). Use only letters, numbers and underscores.	Label on Tube (we strongly suggest #1-xx)	Concentration (Qubit or Nanodrop?), ng/ul	Volume, ul	Total RNA (ng)	Final Pool #
Neg. 0-13	I-A	2	30	35.8	0
Neg. 0-14	I-B	1.92	30	36.2	0
Neg. 0-8	I-C	1.86	30	45.4	0
Neg. 0-11	I-D	1.86	30	34.8	0
Neg. 0-4	I-E	1.85	30	36.5	0
Neg. 0-5	I-F	1.8	30	39.2	0
Neg. 4-6	II-A	1.73	30	47	0
Neg. 4-7	II-B	1.8	30	56.1	0
Neg. 4-9	II-C	1.66	30	48.6	0
Neg. 4-10	II-D	1.66	30	46.5	0
Neg. 4-11	II-E	1.66	30	31.2	0
Neg. 4-5	II-F	1.64	30	24.5	0
Treat. 0-2	III-A	1.78	30	50.7	0
Treat. 0-3	III-B	2.05	30	47.9	0
Treat. 0-4	III-C	1.94	30	56.8	0
Treat. 0-7	III-D	1.93	30	57.9	0
Treat. 0-9	III-E	1.89	30	40.9	0
Treat. 0-6	III-F	1.8	30	34.7	0
Treat. 4-6	IV-A	1.9	30	24.9	0
Treat. 4-8	IV-B	1.91	30	25.2	0
Treat. 4-1	IV-C	1.87	30	50.3	0
Treat. 4-5	IV-D	1.84	30	39.9	0
Treat. 4-9	IV-E	1.83	30	22	0
Treat. 4-3	IV-F	1.8	30	34.7	0

5) Quality check of RNA: run an aliquot (~50 to 100ng) of the total RNA on a 1% agarose gel next to a DNA ladder and attach or embed the image here. This picture will be used to evaluate integrity of the total RNA as well as presence/absence of gDNA. Alternatively, run the total RNA on an RNA bioanalyzer chip and attach the .pdf file.

6) How many lanes for sequencing, type of run (single-read or paired-end) and length of run (100nt, 2x150nt, etc):

*Number of lanes: 2
*Single or Paired-reads: Single

*Run type and read length: HiSeq 4000 100nt single-end read

MiSeq (1 lane per run):
Nano 2x250nt (500k – 1M paired reads)
Bulk 2x250nt (10-20M paired reads)
Bulk 2x300nt (25-50M paired reads)

NovaSeq options:

Flowcell	Read Type and Length	Price per Lane	# of Single-Reads	# of Paired-Reads	Gb/lane
SP	Single-reads, 100bp	$1,720	380 million		40
	Paired-reads, 2x150bp	$2,720		750 million	120
	Paired-reads, 2x250bp	$3,770		750 million	200
S1	Single-reads, 100bp	$3,400	750 million		80
	Paired-reads, 2x100bp	$4,890		1.5 billion	160
	Paired-reads, 2x150bp	$5,270		1.5 billion	240
S2	Single-reads, 100bp	$6,450	1.5 billion		165
S4	Paired-reads, 2x150bp	$8,990		5-6 billion	750-850

7) Any additional comments, special instructions, etc:

Appendix J: RNA-Seq Report prepared by the University of Illinois.

John M Hranitz RNA-Seq Report

Negin Valizadegan and Jenny Drnevich, HPCBio, University of Illinois

Jun 7, 2019

Contents

Location of results and codes for reproducibility

All deliverables for the basic analysis results are in a zipped file that can be downloaded from box.com. Please unzip the file after transferring to your computer (on most PCs: right click and select "Extract all"). The individual gene results are in the files "jmhranitz_results_24Samples_2019-05-30.xlsx", the raw gene-level counts (summed from all transcripts) are in the file "2019-05-17_Gene_level_counts.xlsx" and the normalized logCPM values for all samples are in the file "jmhranitz_gene_logCPMvalues_2019-05-30.xlsx". Note that the .html files in the "interactive_results" folder need to be kept with the "css" and "js" subfolders. The "final_report" folder contains the file "Reports_jmhranitz_Honeybee_2019Apr.Rmd" that generated this report and includes the R codes for the entire analysis. All necessary files to run the analysis, including the raw transcript-level counts in .RData format are also in the "final_report" folder. The .Rmd file was rendered in .html and pdf formats and the figures generated in each are also available in the "Reports_jmhranitz_Honeybee_2019Apr_files" folder.

Quality Check, alignment and count generation

Reference sequences

The *Apis mellifera* transcriptome and Annotation Release 104 from NCBI are used for quasi-mapping and count generation. This transcriptome is derived from genome Amel_HAv3.1. Since the quasi-mapping step only uses transcript sequences, the annotation file was solely used to generate transcript-gene mapping table which was kept in RData file "txID2GeneID.RData" for obtaining gene-level counts.

Quality check on the raw data

We reviewed the QC report, "Project_rmhranitz_24_RNAseq_multiqc_report.html" sent by the sequencing center that performed FASTQC[1] (version 0.11.8) on individual samples then was summarized into a single html report by using MultiQC[2] version 1.6. Average per-base read quality scores are over 30 in all samples and no adapter sequences were found indicating those reads are high in quality. Thus, we skipped the trimming step and directly proceed to transcripts mapping and quantification.

[1]Andrews, S. (2010). FastQC: a quality control tool for high throughput sequence data. Available at: https://www. bioinformatics.babraham.ac.uk/projects/fastqc/

[2]Ewels, P., Magnusson, M., Lundin, S., & K?ller, M. (2016). MultiQC: summarize analysis results for multiple tools and samples in a single report. Bioinformatics, 32(19), 3047-3048.

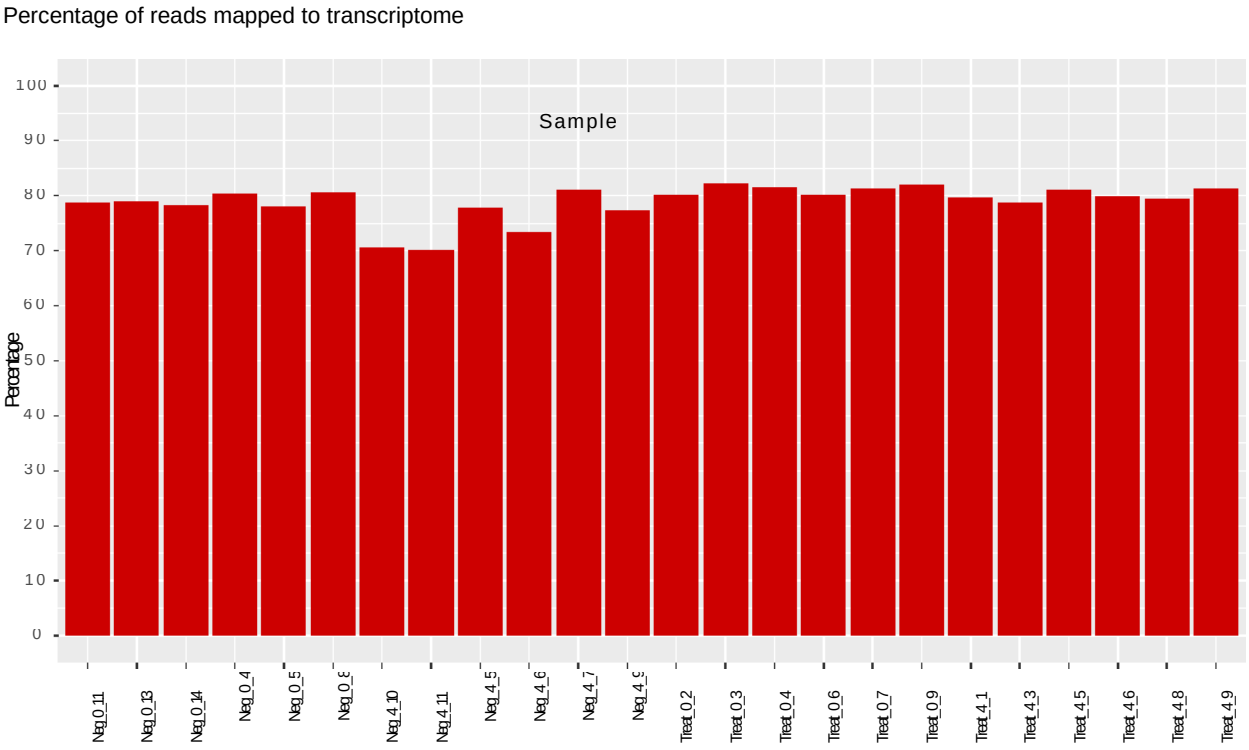

Figure 1: Figure 1. ReadFate plot

Alignment and gene-level quantification

Salmon[3] version 0.13.1 was used to quasi-map reads to the transcriptome and quantify the abundance of each transcript. The transcriptome was first indexed, then quasi-mapping was performed to map reads to transcriptome with additional arguments **`--seqBias`** and **`--gcBias`** to correct sequence-specific and GC content biases and **`--numBootstraps=30`** to compute bootstrap transcript abundance estimates. Gene-level counts were then estimated based on transcript-level counts using the "bias corrected counts without an offset" method from the tximport package. This method provides more accurate gene-level counts estimates and keeps multi-mapped reads in the analysis compared to traditional alignment-based method[4].

Percentage of reads mapped to the transcriptome ranged from 70.1 to 82.3% (Figure 1). The unmapped reads were discarded while the number of remaining reads (range: 28.7 - 50.8 million per sample) were kept for statistical analysis.

Basic statistical analysis

Normalization and filtering

When comparing expression levels, the numbers of reads per gene need to be normalized not only because of the differences in total number of reads, but because there could be differences in RNA

composition such that the total number of reads would not be expected to be the same. The TMM (trimmed mean of M

[3]Patro, R., Duggal, G., Love, M. I., Irizarry, R. A., & Kingsford, C. (2017). Salmon provides fast and bias-aware quantification of transcript expression. Nature methods, 14(4), 417.

[4]Soneson C, Love MI, Robinson MD (2015). "Differential analyses for RNA-seq: transcript-level estimates improve gene-level inferences." F1000Research, 4. doi: 10.12688/f1000research.7563.1.

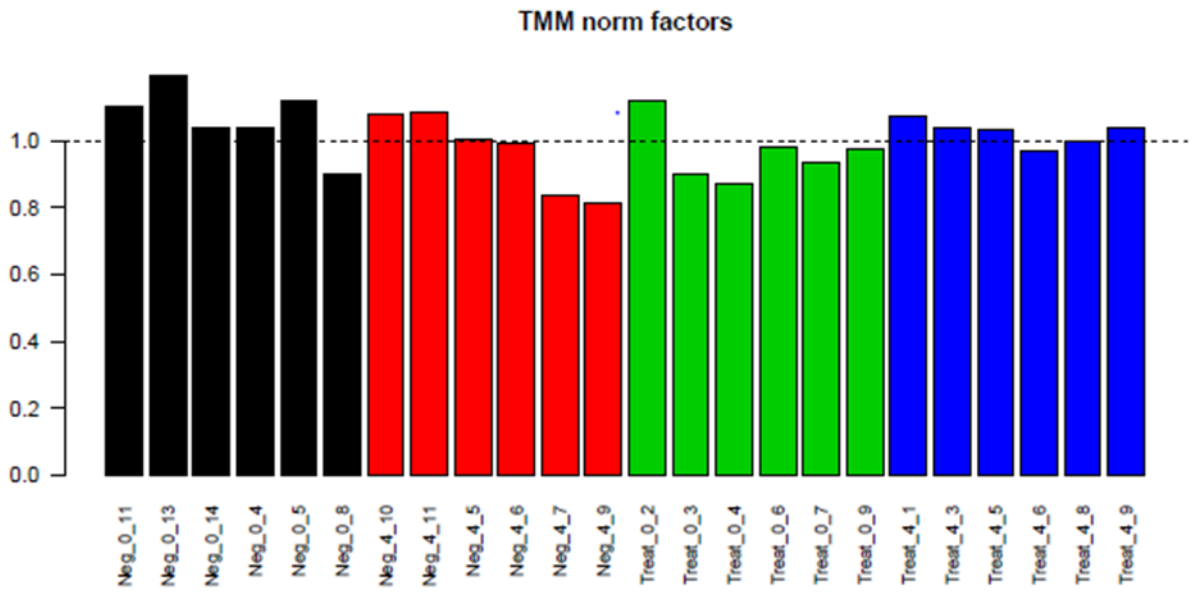

Figure 2: Figure 2. TMM nomalization factors to correct for RNA composition

values) normalization[5] in the edgeR package[6] uses the assumption of *most genes do not change* to calculate a normalization factor for each sample to adjust for such biases in RNA composition. In this dataset, TMM normalization factors fluctuates between 0.81 and 1.2 but the variation is between individuals, not groups, which suggests no group-level overall differences in RNA composition. While the NCBI Amel_HAv3.1 Annotation Release 104 gene models have a total of 12,090 genes, some of these might not have detectable expression. Therefore, we set the detection threshold at 0.5 cpm (counts per million) in at least 3 samples, which resulted in 1,493 genes being filtered out, leaving 10,597 genes to be analyzed for differential expression that contain 99.99% of the reads. After filtering, TMM normalization was performed again and normalized log2-based count per million values (logCPM) were calculated using edgeR's cpm() function with prior.count = 3 to help stabilize fold-changes of extremely low expression genes.

Clustering

Multidimensional scaling in the limma[7] package was used to identify potential treatment effects at higher level. The normalized logCPM values of the top 5,000 variable genes were chosen to construct the multidimensional scaling plot (Figure 3). Dimension 1 which explains around —25% of the total variability, explains the separation of negative control at time 4 from the rest of the groups. Dimension 2 which contains —17% of the variability does not explain groupings of the effect of treatment, negative control and/or time. An interactive version of this plot can be found at "interactive_results/MDSclustering_postFiltering.html".

[5]Robinson MD, Oshlack A (2010). A scaling normalization method for differential expression analysis of RNA-seq data. Genome Biology 11, R25.

[6]Robinson MD, McCarthy DJ, Smyth GK (2010). "edgeR: a Bioconductor package for differential expression analysis of digital gene expression data." Bioinformatics, 26(1), 139-140.

[7]Ritchie, M.E., Phipson, B., Wu, D., Hu, Y., Law, C.W., Shi, W., and Smyth, G.K. (2015). limma powers differential expression analyses for RNA-sequencing and microarray studies. Nucleic Acids Research 43(7), e47

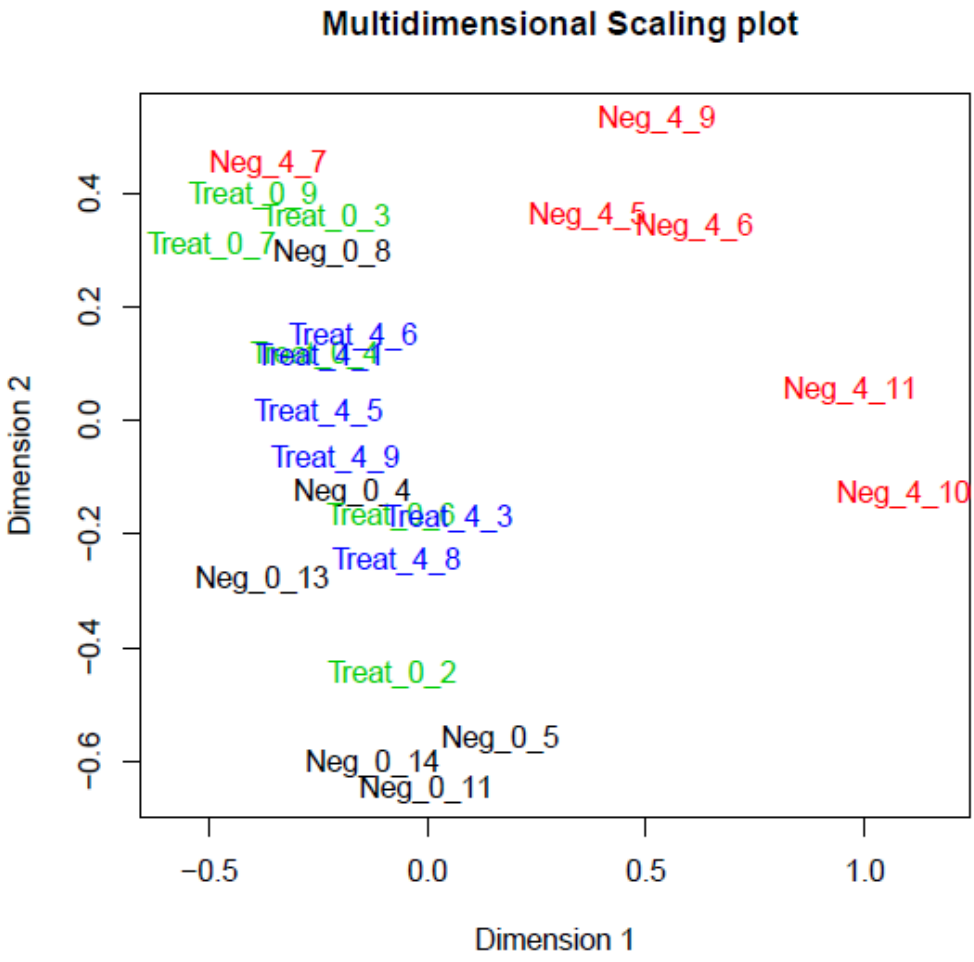

Figure 3: Figure 3. Multidimensional Scaling on the top 5,000 most variable genes.

Table 1: Table 1. Number of differenially expressed genes (global FDR p < 0.1)

	T4vsT0	N4vsN0	T0vsN0	T4vsN4	Interact
Down	**46**	**2369**	**35**	**1663**	**1091**
NotSig	10476	6312	10365	6725	7805
Up	**75**	**1916**	**197**	**2209**	**1701**

Differential expression testing

Differential gene expression (DE) analysis was performed using the limma-trend method[8,9] and all four logical pairwise comparisons were computed, along with a test for any interaction between treatment and time. Because pairwise comparisons involving the Neg_4 group had so many more DE genes than comparisons between other groups, we adjust for multiple testing correction by doing a "global" False Discovery Rate correction[10] across p-values for all 5 comparisons together. This ensures that a gene with the same raw p-value in two different comparisons would not end up with vastly different FDR p-values. The number of up and down regulated genes using FDR p-value < 0.1 for the four logical pairwise comparisons and the interaction test are in Table 1. Interactive versions of the results for each comparison are in ".html" files in the "interactive_results" folder. We also calculated the equivalent of a oneway ANOVA test across all four groups to select genes to visualize their overall expression patterns in a heatmap. False discovery rate correction was done separately for the oneway ANOVA, and at FDR < 0.05, 3819 genes showed differences across the groups, mainly the Neg_4 group was different from the others (Figure 4).

Functional annotation

Gene name, Gene Ontology ID and GO terms for each gene was obtained by using the org.Apis_mellifera.eg.sqlite database from AnnotationHub package from Bioconductor[11] release 3.9. KEGG pathways for each gene were retrieved directly from http://www.genome.jp/kegg using the KEGGREST package on May 30, 2019 .

Hardware and software descriptions

The read quality check and count generation was done using CNRG's *Biocluster* high-performance computing resource. All analyses from summation of counts to the gene level (including the codes in .Rmd file) were done on a laptop in R version 3.6.0 (2019-04-26)[12] using packages as indicated below.

R and package versions

```
## R version 3.6.0 (2019-04-26)
## Platform: x86_64-apple-darwin15.6.0 (64-bit)
```

[8]Chen Y, Lun ATL and Smyth GK. From reads to genes to pathways: differential expression analysis of RNA-Seq experiments using Rsubread and the edgeR quasi-likelihood pipeline [version 2; referees: 5 approved]. F1000Research 2016, 5:1438 (doi: 10.12688/f1000research.8987.2)

[9]Law, C. W., Chen, Y., Shi, W., & Smyth, G. K. (2014). voom: Precision weights unlock linear model analysis tools for RNA-seq read counts. Genome biology, 15(2), R29.

[10]Benjamini, Y., & Hochberg, Y. (1995). Controlling the false discovery rate: a practical and powerful approach to multiple testing. Journal of the Royal statistical society: series B (Methodological), 57(1), 289-300.

[11]Gentleman, R. C., Carey, V. J., Bates, D. M., Bolstad, B., Dettling, M., Dudoit, S., ... & Hornik, K. (2004). Bioconductor: open software development for computational biology and bioinformatics. Genome biology, 5(10), R80.

12R Core Team (2017). R: A language and environment for statistical computing. R Foundation for Statistical Computing, Vienna, Austria. URL https://www.R-project.org/.

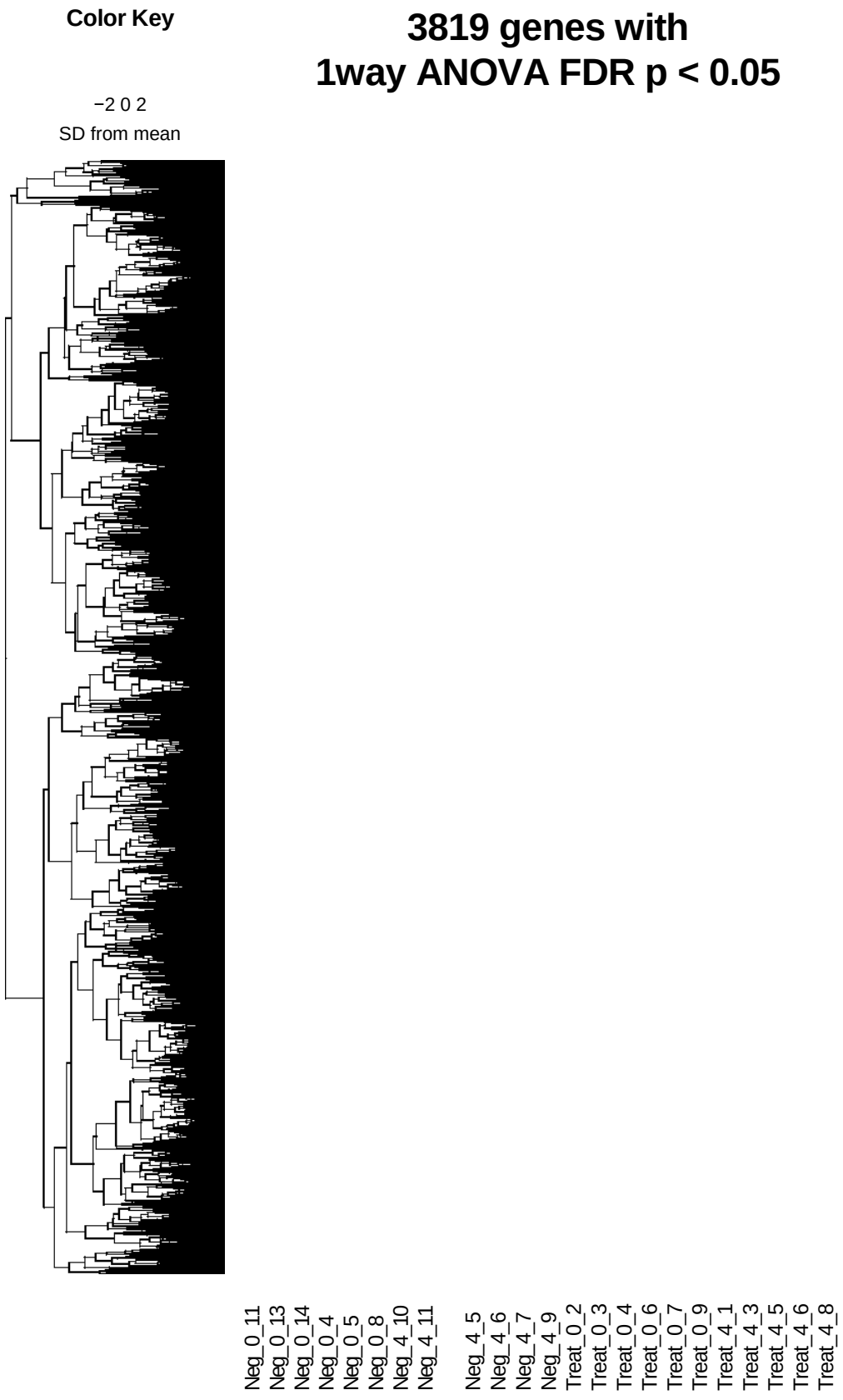

Figure 4: Figure 4. Heatmap of expression patterns of genes with a significant one-way ANOVA

Appendix K: Sequence quality from Multi-QC report.

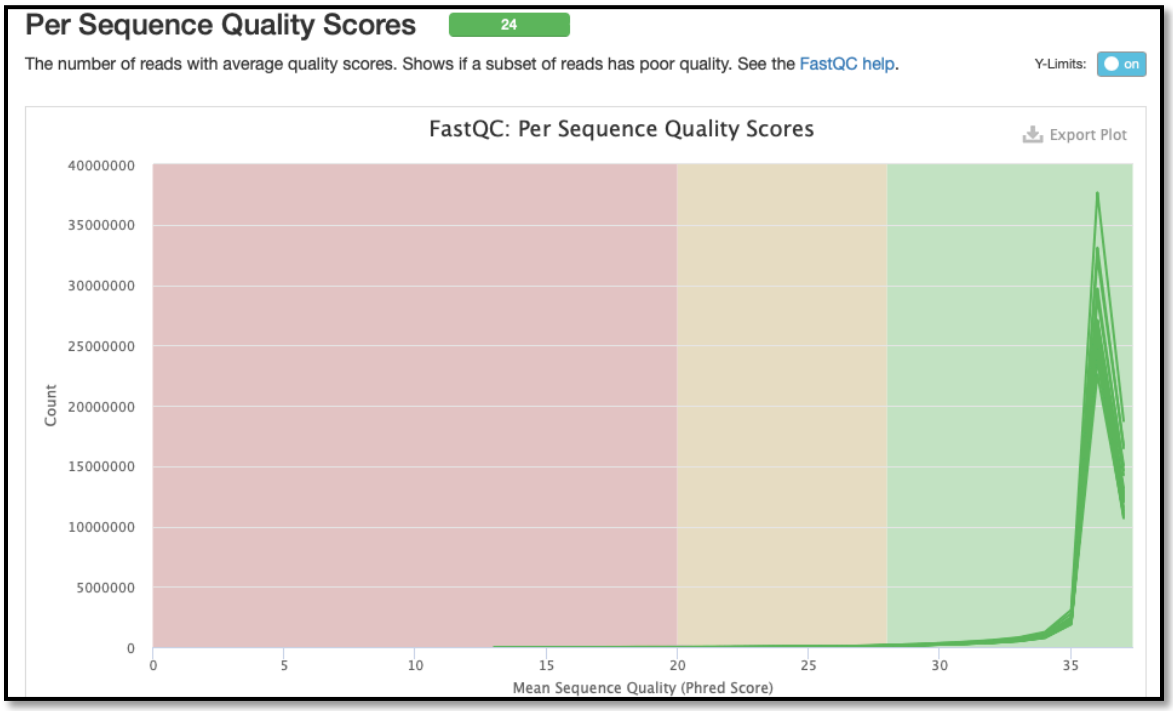

Appendix L: Outlier genes removed from each comparison group.

Control 4 Hour-Treatment 0 Hour	Treatment 4 Hour-Control 0 Hour	Treatment 0 Hour-Control 0 Hour	Treatment 4 Hour-Control 4 Hour
LOC102654530	LOC100577041	LOC102654769	LOC113218730
LOC102655462	LOC107964312	LOC102656780	LOC727126
LOC408310	LOC113219186	LOC107965596	LOC107964028
LOC726513	LOC113218895	LOC107965494	LOC113218895
LOC100578618	Mir6058	LOC100577266	LOC102654676
LOC102656697	LOC107965500	LOC102654837	LOC725965
Or63	LOC102654676	LOC100577278	LOC100577041
LOC102654769	LOC100578137	LOC113218598	LOC107966041
LOC725762	LOC102655174	LOC100576599	LOC107965500
LOC100576417	LOC102655148	LOC113219192	LOC725469
LOC100577069	LOC113218910	LOC100577149	LOC410107
LOC102656780	LOC100578882	LOC102654300	LOC413166
LOC102656729	LOC100576914	LOC107965117	LOC102655148
LOC102655825	LOC413532	Or63	LOC107964312
LOC100577908	LOC113219427	LOC102656697	LOC725762
	LOC102654659	LOC102654810	LOC413574
	LOC413574	LOC102656919	Mir6042
	LOC727035	LOC107964750	LOC113219059
	LOC100577278	LOC102656729	LOC107964934
	LOC102653680	LOC102654804	LOC727035
	LOC102656189	LOC107964633	LOC102655107
	Mir3726	Mir9883	LOC102655174
	LOC102655107	LOC102654490	LOC107964975
	LOC102653600	Apd-2	LOC724312
	LOC102654231	LOC410603	Mir6058
	LOC107965601		LOC100576914
	LOC102656705		LOC113218527
	LOC102653975		LOC727335
	LOC107965171		LOC102654660
	LOC100577817		LOC724895
	LOC100578397		LOC100578446
	Mir9865		LOC113218978
	LOC725965		LOC727642
	LOC102654917		LOC102654659
	LOC100577474		LOC100577521
	LOC100577042		LOC100578137
	LOC113219125		LOC113218765
	LOC725469		LOC113219186
	Or25		LOC551263
	LOC102655232		LOC726072
	Mir6049		LOC726863
	LOC726468		LOC113219196
	LOC726850		Or105
	LOC107964633		LOC102656294
	LOC100576944		LOC107964152
	Mir125		LOC724860
	LOC107965228		LOC409751
	LOC113219070		LOC410231
	LOC102654757		LOC724386
	LOC113219128		LOC100577752
	LOC102656145		LOC100576082
	LOC113219009		LOC102655724
	LOC725606		LOC102656479
	Eyg		LOC102656705
	LOC102654300		LOC102653680

	Mir3759 LOC102654929 LOC102655235 LOC100577149 LOC102654924 LOC724895 LOC113219151 LOC727642 LOC113218881 LOC113219388 LOC107964043 LOC113218774 LOC410687 LOC102653852 LOC107965367 LOC100578057 LOC100577559 LOC107964737 LOC107965375 LOC113218672 LOC107965480 LOC107964483 LOC100577266 LOC724429 LOC100578177		LOC107964737 LOC113219200 LOC107965534 LOC113219050 LOC102653963 LOC113218668 LOC113218910 LOC725945 LOC100576688 LOC107965073 LOC100576172 LOC410254 LOC100578882 Mir6049 LOC102656719 LOC100578177 LOC724645 Mir3726 LOC107964006 LOC102653852 LOC100578193 LOC413532 LOC107965228 LOC113219340 LOC724934 Mir9865 LOC113218946 LOC113219185 LOC725831 LOC113218795 LOC724921 LOC113218522 LOC113219051 LOC113219388 LOC113219370 LOC725935 LOC100576901 LOC100576609 LOC724624 LOC113218653 LOC102654144 LOC725589 LOC102655670 LOC102656570 LOC100576944 LOC102655155 LOC107965158 LOC102656509 LOC100576439 LOC107965805 LOC102653600 LOC107965171 LOC410334 LOC100578130 LOC100577069 LOC113219009 LOC113219128 Eyg Mir125 LOC413693 LOC107965375 LOC113218881

			LOC410736 LOC727237 LOC100577817 LOC724429 LOC102654622 LOC102654948 LOC725302 LOC102656864 LOC411387 LOC100577373 LOC100578474 LOC410687 LOC113218672 LOC113219125 LOC113219070 LOC100577559 LOC102656387 LOC100576387 LOC551632 LOC100578729

Appendix M: Python script.

```
infile = open('log_fc_heather.txt','rU')    #reads the existing gene file
out1 = open('outliers_c0.txt','w')  #writes new file
out2 = open('badgenes_c0.txt','w')
out3 = open('avg_FC_c0.txt','w')
out4 = open('outliers_c4.txt','w')
out5 = open('badgenes_c4.txt','w')
out6 = open('avg_FC_c4.txt','w')
out7 = open('outliers_t0.txt','w')
out8 = open('badgenes_t0.txt','w')
out9 = open('avg_FC_t0.txt','w')
out10 = open('outliers_t4.txt','w')
out11 = open('badgenes_t4.txt','w')
out12 = open('avg_FC_t4.txt','w')


def Average(lst):   #defines a function
    return sum(lst)/len(lst)    #returns sum of list and the amount in the list

def detect_outlier(data_1): #defines a function
    outliers = []
    mean_1 = np.mean(data_1)
    std_1 = np.std(data_1)

    for y in data_1:
        z_score = float((y - mean_1)/std_1)
        if np.abs(z_score) > threshold:
            outliers.append(y)  #adds item to a list
    return outliers
#read through every line and return outliers

def runallthings(beelist, outfile1, outfile2, outfile3):
    badgenes = 0
    pos, neg = 0,0
    for bee in beelist:

        if bee < 0.0: #if bee is less than 0 then it identifies as negative
            neg +=1
        else:   #if greater than 0.0 then it identifies as positive
            pos+=1
    dif = abs(pos-neg)  #removes bee from list if there is a greater than 2 read dif
    if dif > 2:

##        bee_outliers = detect_outlier(beelist)
##        if len(bee_outliers) > 0:
##
##            for elt in bee_outliers:
##                beelist.remove(elt)
##
##                c0bee_average = Average(beelist)
##        else:
##
##            c0bee_average = Average(beelist)
        # double # means script was commented out and does not get run

        bee_average = Average(beelist)
        outfile3.write('%s\t%s\t%s' % (gene_symbol, entrezid, bee_average))
        for elt in beelist:
            outfile3.write('\t%s' % (elt))
        outfile3.write('\n')
        #writes a string file with tabs inbetween and on a new line based on gene sym

##        outfile1.write('%s\t%s' % (gene_symbol, entrezid))
##        for elt in beelist:
##            outfile1.write('\t'+str(elt))
##        outfile1.write('\toutliers:')
##        for elt in bee_outliers:
##            outfile1.write('\t'+str(elt))
##        outfile1.write('\n')
    else:
        outfile2.write(gene_symbol+'\n')
        badgenes +=1

headerline = infile.readline()
out3.write('gene\tsymbol\taverage_FC_c0\tc0_1\tc0_2\tc0_3\tc0_4\tc0_5\tc0_6\n')
out6.write('gene\tsymbol\taverage_FC_c4\tc4_1\tc4_2\tc4_3\tc4_4\tc4_5\tc4_6\n')
out9.write('gene\tsymbol\taverage_FC_t0\tt0_1\tt0_2\tt0_3\tt0_4\tt0_5\tt0_6\n')
out12.write('gene\tsymbol\taverage_FC_t4\tt4_1\tt4_2\tt4_3\tt4_4\tt4_5\tt4_6\n')
#writes new  file with headlines of gene, symbol,average FC, and each bee in that gr

while True:
    line = infile.readline()    #reads one entire line from the file
    if not line:
        break
    line = line.strip() #removes white spaces
    gene_symbol = line.split('\t')[0]   #changes line to a list with a tab inbetween
    entrezid = line.split('\t')[1]  #changes line to a list with a tab
    c0bee1 = float(line.split('\t')[3])
    c0bee2 = float(line.split('\t')[4])
    c0bee3 = float(line.split('\t')[5])
    c0bee4 = float(line.split('\t')[6])
    c0bee5 = float(line.split('\t')[7])
    c0bee6 = float(line.split('\t')[8])
    c0bee_list = [c0bee1, c0bee2, c0bee3, c0bee4, c0bee5, c0bee6]
    # [#] identifies position in file
#the above occurs for control 4 hour samples, treatment 0 hour samples, and treatment

    runallthings(c0bee_list, out1, out2, out3)
#runs the data from the new files that were opened

    c4bee1 = float(line.split('\t')[9])
    c4bee2 = float(line.split('\t')[10])
    c4bee3 = float(line.split('\t')[11])
    c4bee4 = float(line.split('\t')[12])
    c4bee5 = float(line.split('\t')[13])
    c4bee6 = float(line.split('\t')[14])
    c4bee_list = [c4bee1, c4bee2, c4bee3, c4bee4, c4bee5, c4bee6]

    runallthings(c4bee_list, out4, out5, out6)

    t0bee1 = float(line.split('\t')[15])
    t0bee2 = float(line.split('\t')[16])
    t0bee3 = float(line.split('\t')[17])
    t0bee4 = float(line.split('\t')[18])
    t0bee5 = float(line.split('\t')[19])
    t0bee6 = float(line.split('\t')[20])
    t0bee_list = [t0bee1, t0bee2, t0bee3, t0bee4, t0bee5, t0bee6]

    runallthings(t0bee_list, out7, out8, out9)

    t4bee1 = float(line.split('\t')[21])
    t4bee2 = float(line.split('\t')[22])
    t4bee3 = float(line.split('\t')[23])
    t4bee4 = float(line.split('\t')[24])
    t4bee5 = float(line.split('\t')[25])
    t4bee6 = float(line.split('\t')[26])
    t4bee_list = [t4bee1, t4bee2, t4bee3, t4bee4, t4bee5, t4bee6]

    runallthings(t4bee_list, out10, out11, out12)

infile.close()
out1.close()
out2.close()
out3.close()
out4.close()
out5.close()
out6.close()
out7.close()
out8.close()
out9.close()
out10.close()
out11.close()
out12.close()
#close all files
```

Appendix N: Average Motor Scores of Honey Bees Collected and Treated with Imidacloprid

Treatment Groups	Concentration of Imidacloprid (ng/10 µL)	Average Abdomen Score	Average leg score	Average Antennae Score	Average P.E.R. score	Average Motor Score	Number of Bees Treated
Negative	0	1.75	1.95	2.00	2.00	7.70	20
1/5	3.6	1.26	1.74	1.53	1.58	6.11	19
1/10	1.8	1.67	1.78	1.78	1.61	6.83	18
1/20	0.9	1.82	1.88	1.82	1.88	7.41	17
1/50	0.36	1.70	1.90	1.95	1.90	7.45	20
1/100	0.18	1.65	1.95	2.00	1.95	7.55	20
1/500	0.036	1.82	1.71	2.00	1.94	7.47	17
Positive	0	1.85	1.69	1.69	1.77	7.00	13

Appendix O: List of 100 most significant changes in Treatment-4h versus Control-0h.

kelch domain-containing protein 10 homolog
vesicle-fusing ATPase 1
serine/threonine-protein kinase 3, transcript variant X1
phosphatidylinositol 5-phosphate 4-kinase type-2 alpha, transcript variant X2
DCN1-like protein 3
fizzy-related protein homolog
WD repeat and FYVE domain-containing protein 2
dnaJ homolog subfamily C member 16
homer protein homolog 2, transcript variant X1
ubiquitin carboxyl-terminal hydrolase 14
sorting nexin lst-4
CTD small phosphatase-like protein 2, transcript variant X3
uncharacterized LOC412397, transcript variant X2
rho GTPase-activating protein 1, transcript variant X1
serine/threonine-protein phosphatase 2A catalytic subunit alpha isoform
tubulin beta chain
lysophospholipase D GDPD1-like, transcript variant X4
dual specificity mitogen-activated protein kinase kinase dSOR1
syntaxin-12, transcript variant X3
transmembrane protein 62, transcript variant X1
actin-related protein 2, transcript variant X1
peroxisomal N(1)-acetyl-spermine/spermidine oxidase
death-associated inhibitor of apoptosis 2, transcript variant X2
leucine-rich repeat protein soc-2 homolog
uncharacterized LOC410622
guanine nucleotide exchange factor for Rab-3A, transcript variant X1
ethanolamine-phosphate cytidylyltransferase, transcript variant X1
staphylococcal nuclease domain-containing protein 1
ribonuclease Z, mitochondrial, transcript variant X1
E3 ubiquitin-protein ligase ZNRF2
sulfhydryl oxidase 1
potential E3 ubiquitin-protein ligase ariadne-1, transcript variant X3
dnaJ homolog subfamily C member 3
uncharacterized LOC413653, transcript variant X2
uncharacterized LOC100576438, transcript variant X2
myb-like protein D
methyltransferase-like protein 23
calmodulin
arfaptin-2, transcript variant X2
cyclin-Y
RING finger and CHY zinc finger domain-containing protein 1, transcript variant X3
galactoside 2-alpha-L-fucosyltransferase 2
beta-1,3-galactosyltransferase 1-like, transcript variant X2
transmembrane protein 64
acidic leucine-rich nuclear phosphoprotein 32 family member A, transcript variant X2
pantothenate kinase 3, transcript variant X1
WD repeat-containing protein 82, transcript variant X1
protein HID1, transcript variant X2
WD repeat-containing protein 48
DNA fragmentation factor subunit alpha

MAPK regulated corepressor interacting protein 2
BTB/POZ domain-containing adapter for CUL3-mediated RhoA degradation protein 3, transcript variant X2
N-alpha-acetyltransferase 30
transmembrane 9 superfamily member 3
UV excision repair protein RAD23 homolog B, transcript variant X2
ras association domain-containing protein 2
GTP-binding protein Rit2, transcript variant X3
alpha-1,3/1,6-mannosyltransferase ALG2
zwei Ig domain protein zig-8, transcript variant X2
choline-phosphate cytidylyltransferase A, transcript variant X3
dnaJ homolog subfamily C member 7, transcript variant X2
protein zyg-11 homolog B, transcript variant X4
V-type proton ATPase subunit C, transcript variant X4
uncharacterized LOC724843, transcript variant X2
uncharacterized LOC551031, transcript variant X1
ceramide synthase 6, transcript variant X1
ER degradation-enhancing alpha-mannosidase-like protein 2
protein spinster, transcript variant X2
actin-binding protein IPP
serine/threonine-protein kinase PINK1, mitochondrial, transcript variant X2
DCN1-like protein 5, transcript variant X1
palmitoyltransferase app, transcript variant X2
dual specificity protein phosphatase CDC14AB, transcript variant X3
mitoferrin-1, transcript variant X1
TOM1-like protein 2, transcript variant X1
hyccin, transcript variant X3
C-terminal-binding protein 2
blastoderm-specific protein 25D
zinc finger BED domain-containing protein 1
ras-related protein Rab-30
NECAP-like protein CG9132, transcript variant X1
WD repeat domain phosphoinositide-interacting protein 3
uncharacterized LOC552002, transcript variant X3
RILP-like protein homolog, transcript variant X2
probable galactose-1-phosphate uridylyltransferase
probable E3 ubiquitin-protein ligase makorin-1, transcript variant X1
ethanolaminephosphotransferase 1
cleft lip and palate transmembrane protein 1 homolog
NADPH--cytochrome P450 reductase, transcript variant X2
uncharacterized LOC408732
condensin complex subunit 2
adipocyte plasma membrane-associated protein
calreticulin
AFG3-like protein 2
E3 ubiquitin-protein ligase NRDP1, transcript variant X2
protein disulfide-isomerase
SH3 domain-binding glutamic acid-rich protein homolog, transcript variant X2
O-phosphoseryl-tRNA(Sec) selenium transferase, transcript variant X3
zinc finger protein 25
WD repeat domain phosphoinositide-interacting protein 2, transcript variant X2

Appendix P: Control Time 4 Hour-Treatment Time 0 Hour KEGG pathways. Genes that are colored red are considered down-regulated (not significant), genes that are colored purple are significantly down-regulated, genes that are colored pink are significantly up-regulated, and genes that are colored orange are considered up-regulated (not significant) (significance $p<0.1$). Enzymes are indicated by the green color.

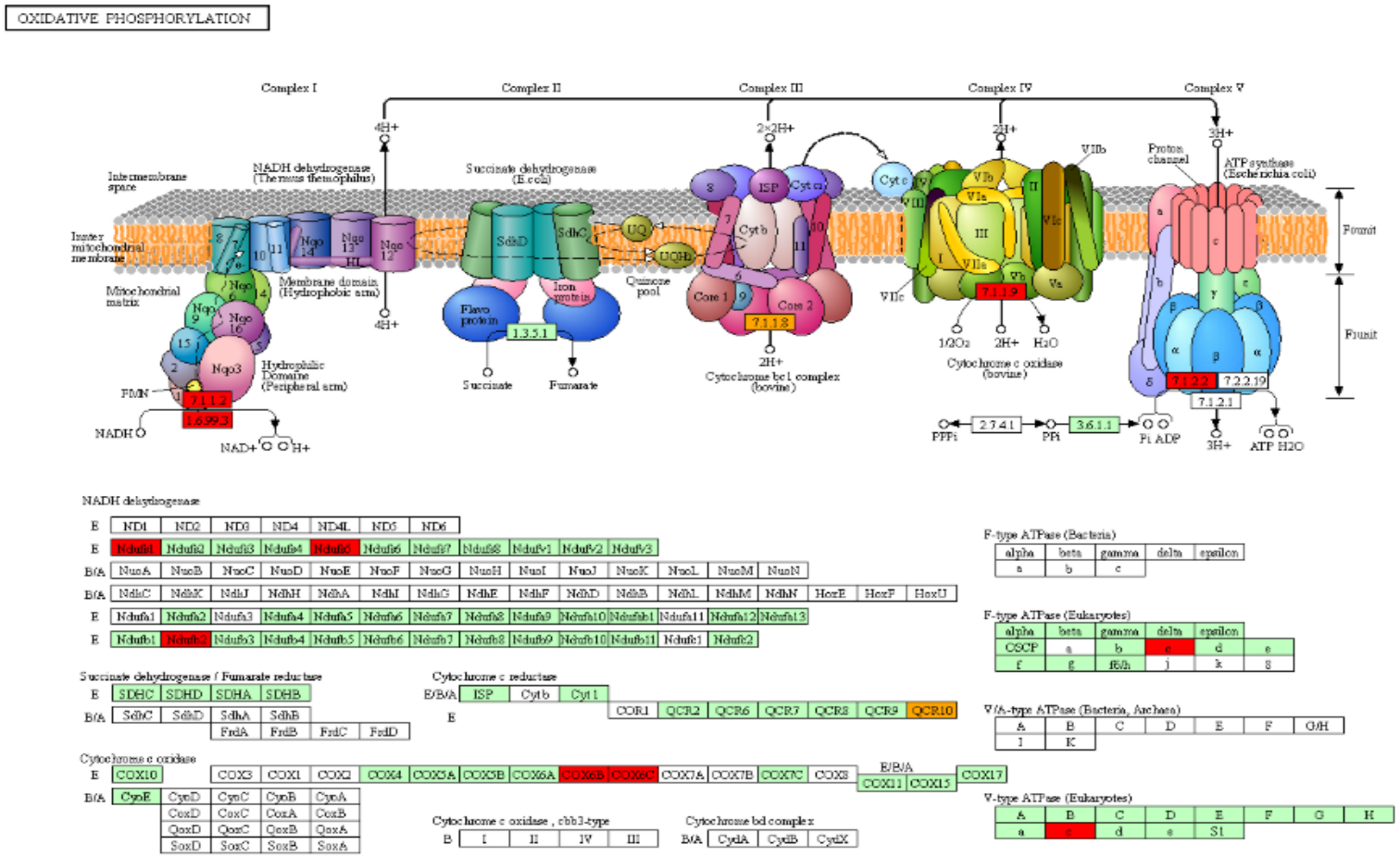

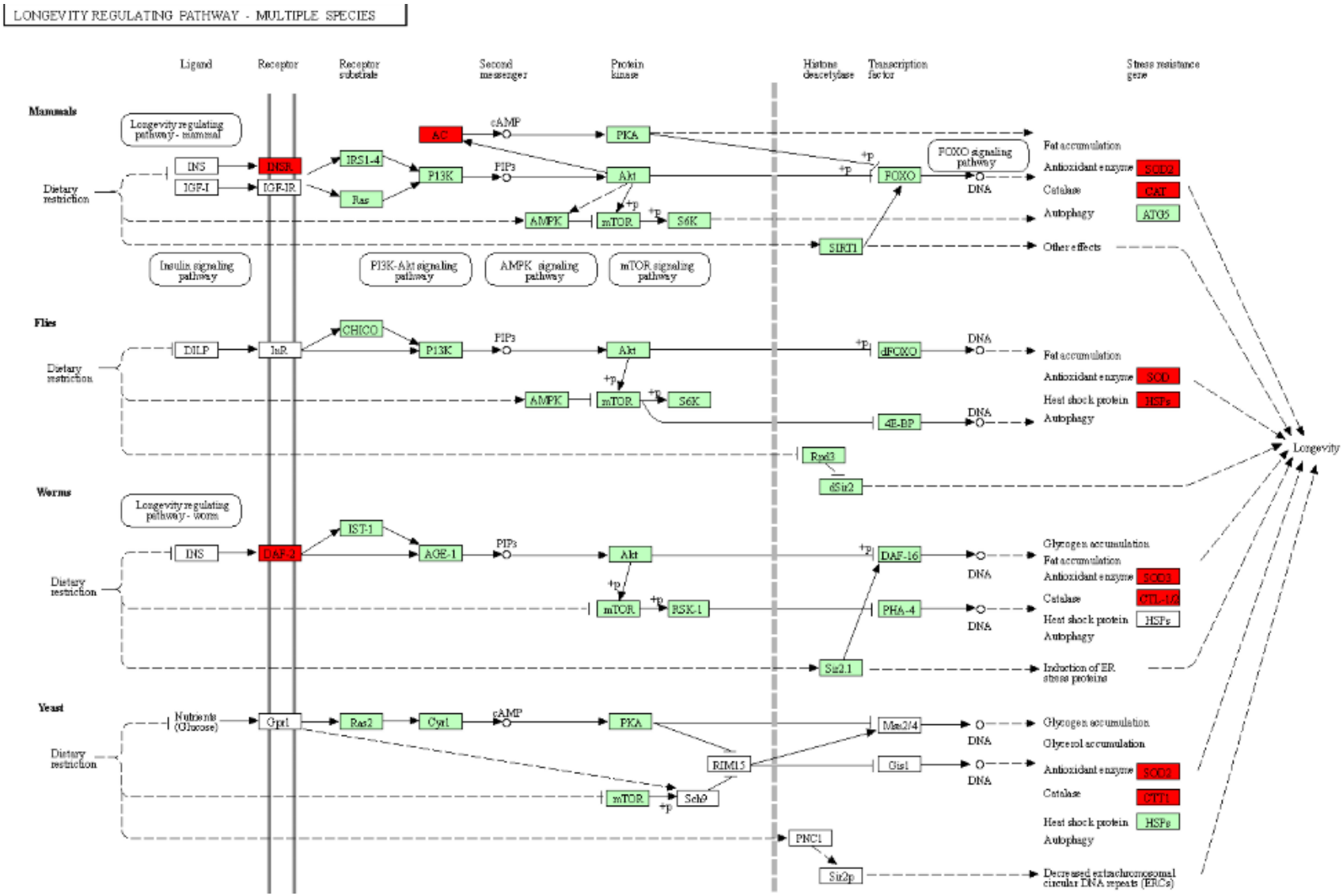
LONGEVITY REGULATING PATHWAY - MULTIPLE SPECIES
Ligand
Receptor
Receptor substrate
Second messenger
Protein kinase
Histone deacetylase
Transcription factor
Stress resistance gene
Mammals
Longevity regulating pathway - mammal
INS
IGF-I
INSR
IGF-IR
IRS1-4
Ras
PI3K
PIP3
AC
cAMP
PKA
Akt
AMPK
mTOR
S6K
FOXO
FOXO signaling pathway
DNA
SIRT1
Dietary restriction
Fat accumulation
Antioxidant enzyme
SOD2
Catalase
CAT
Autophagy
ATG5
Other effects
Insulin signaling pathway
PI3K-Akt signaling pathway
AMPK signaling pathway
mTOR signaling pathway
Flies
DILP
InR
CHICO
dFOXO
4E-BP
Rpd3
dSir2
Fat accumulation
Antioxidant enzyme
SOD
Heat shock protein
HSPs
Autophagy
Worms
Longevity regulating pathway - worm
INS
DAF-2
IST-1
AGE-1
DAF-16
PHA-4
RSK-1
Sir2.1
Glycogen accumulation
Fat accumulation
Antioxidant enzyme
SOD3
Catalase
CTL-1/2
Heat shock protein
HSPs
Autophagy
Induction of ER stress proteins
Yeast
Nutrients (Glucose)
Gpr1
Ras2
Cyr1
PKA
Msn2/4
Gis1
RIM15
mTOR
Sch9
PNC1
Sir2p
Glycogen accumulation
Glycerol accumulation
Antioxidant enzyme
SOD2
Catalase
CTT1
Heat shock protein
HSPs
Autophagy
Decreased extrachromosomal circular DNA repeats (ERCs)
Longevity

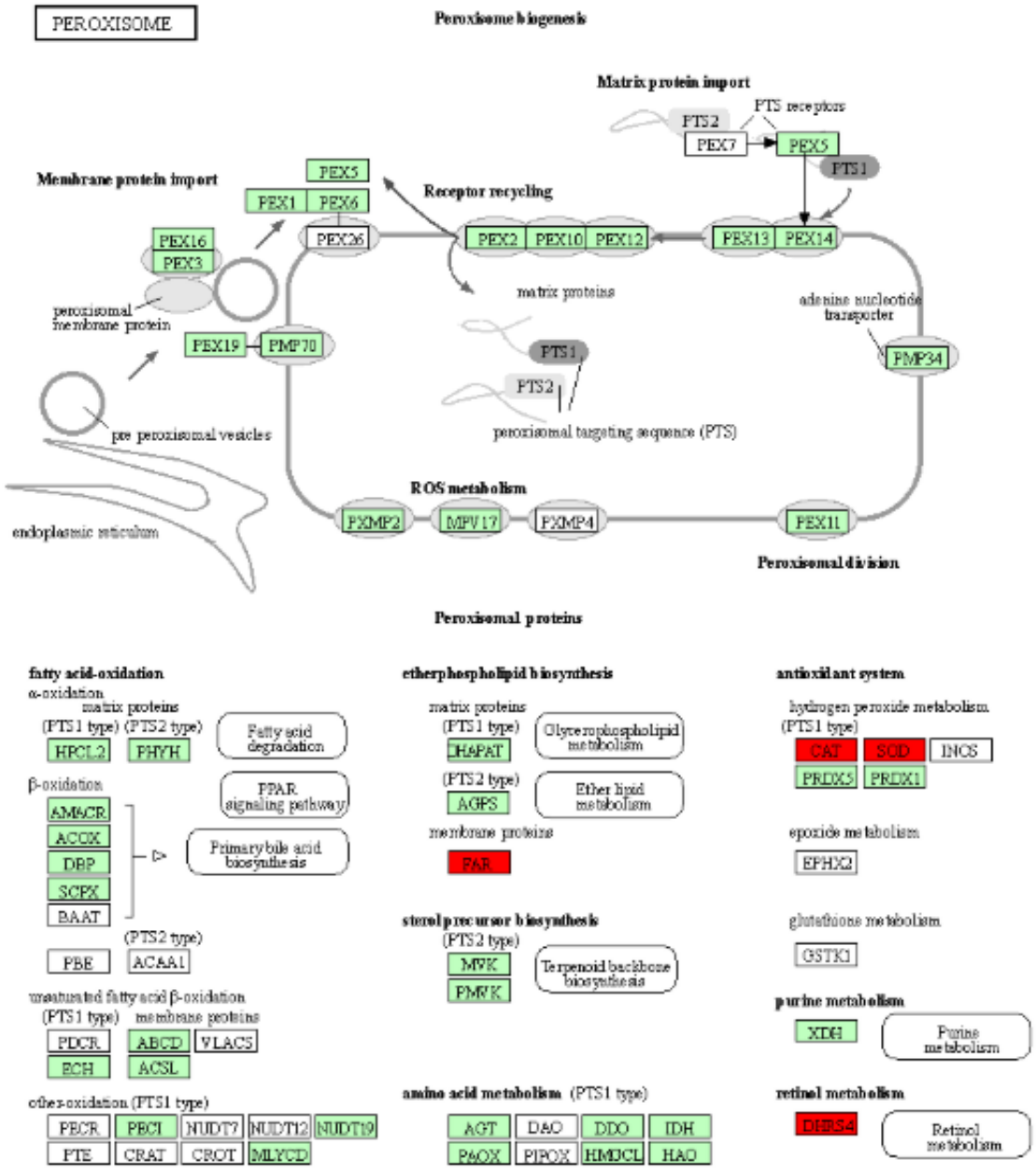
PEROXISOME
Peroxisome biogenesis
Matrix protein import
PTS receptors
PTS2
PEX7
PEX5
PTS1
Membrane protein import
PEX5
PEX1
PEX6
Receptor recycling
PEX16
PEX3
PEX26
PEX2
PEX10
PEX12
PEX13
PEX14
matrix proteins
peroxisomal membrane protein
adenine nucleotide transporter
PEX19
PMP70
PMP34
PTS1
PTS2
peroxisomal targeting sequence (PTS)
pre peroxisomal vesicles
ROS metabolism
endoplasmic reticulum
PXMP2
MPV17
PXMP4
PEX11
Peroxisomal division
Peroxisomal proteins
fatty acid oxidation
α-oxidation
matrix proteins
(PTS1 type)
(PTS2 type)
HPCL2
PHYH
Fatty acid degradation
β-oxidation
AMACR
ACOX
DBP
SCPX
BAAT
PPAR signaling pathway
Primary bile acid biosynthesis
(PTS2 type)
PBE
ACAA1
unsaturated fatty acid β-oxidation
(PTS1 type)
membrane proteins
PDCR
ABCD
VLACS
ECH
ACSL
other oxidation (PTS1 type)
PECR
PECI
NUDT7
NUDT12
NUDT19
PTE
CRAT
CROT
MLYCD
etherphospholipid biosynthesis
matrix proteins
(PTS1 type)
DHAPAT
Glycerophospholipid metabolism
(PTS2 type)
AGPS
Ether lipid metabolism
membrane proteins
PAH
sterol precursor biosynthesis
(PTS2 type)
MVK
PMVK
Terpenoid backbone biosynthesis
amino acid metabolism (PTS1 type)
AGT
DAO
DDO
IDH
PAOX
PIPOX
HMGCL
HAO
antioxidant system
hydrogen peroxide metabolism
(PTS1 type)
CAT
SOD
INOS
PRDX5
PRDX1
epoxide metabolism
EPHX2
glutathione metabolism
GSTK1
purine metabolism
XDH
Purine metabolism
retinol metabolism
DHRS4
Retinol metabolism

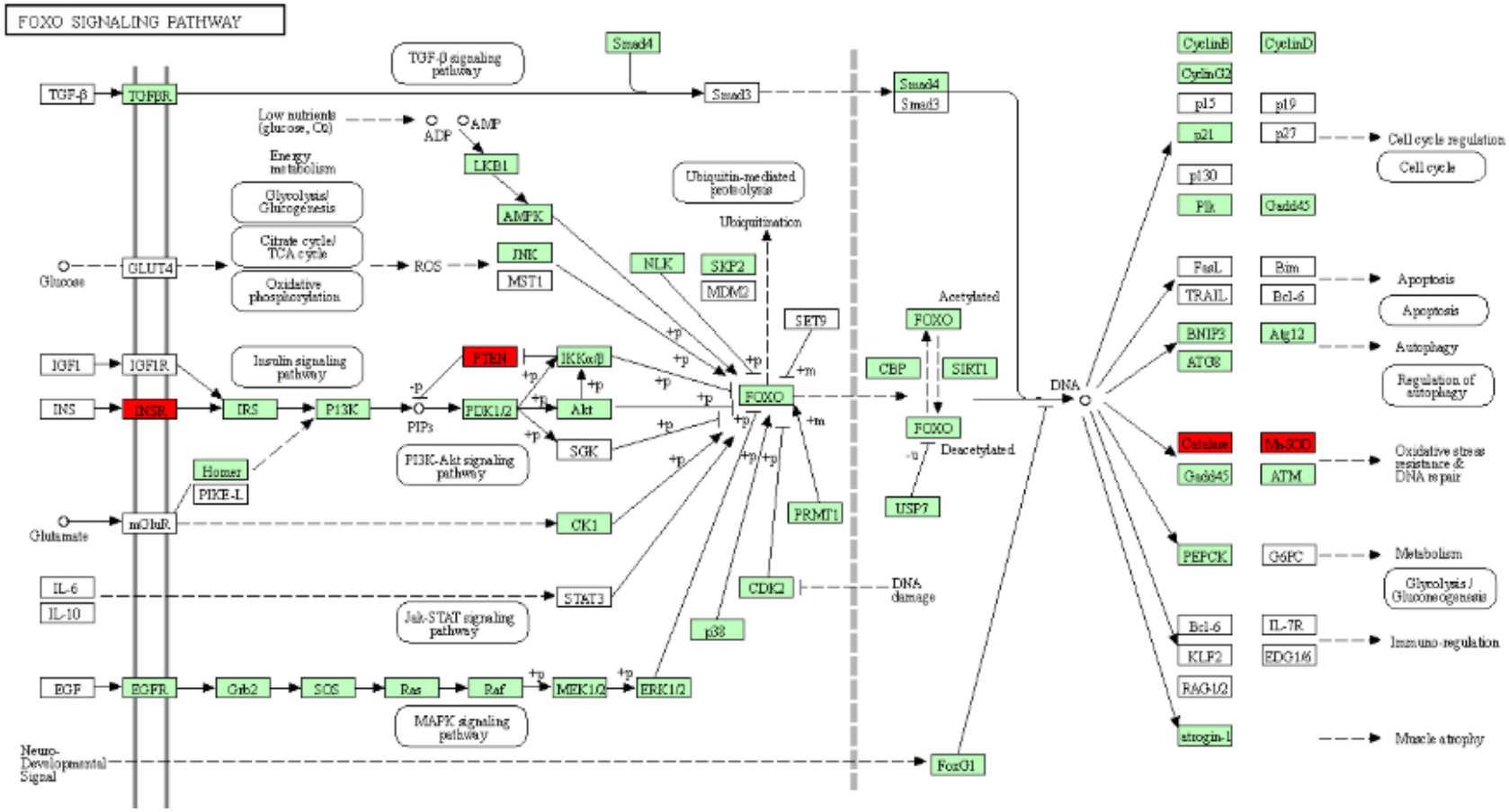
FOXO SIGNALING PATHWAY
TGF-β
TGFβR
TGF-β signaling pathway
Smad4
Smad3
Smad4
Smad3
Low nutrients (glucose, O2)
ADP
AMP
LKB1
Energy metabolism
Glycolysis/ Gluconeogenesis
Citrate cycle/ TCA cycle
Oxidative phosphorylation
ROS
AMPK
JNK
MST1
Ubiquitin-mediated proteolysis
Ubiquitination
NLK
SKP2
MDM2
SET9
Glucose
GLUT4
IGF1
IGF1R
Insulin signaling pathway
INS
INSR
IRS
PI3K
PIP3
PTEN
IKKα/β
PDK1/2
Akt
SGK
PI3K-Akt signaling pathway
FOXO
CBP
SIRT1
Acetylated
FOXO
Deacetylated
USP7
PRMT1
DNA
Homer
PIKE-L
Glutamate
mGluR
CK1
IL-6
IL-10
STAT3
Jak-STAT signaling pathway
CDK2
DNA damage
p38
EGF
EGFR
Grb2
SOS
Ras
Raf
MEK1/2
ERK1/2
MAPK signaling pathway
Neuro-Developmental Signal
FoxO1
CyclinB
CyclinD
CyclinG2
p15
p19
p21
p27
Cell cycle regulation
Cell cycle
p130
Plk
Gadd45
FasL
Bim
TRAIL
Bcl-6
Apoptosis
Apoptosis
BNIP3
Atg12
Autophagy
ATG8
Regulation of autophagy
Catalase
Mn-SOD
Gadd45
ATM
Oxidative stress resistance & DNA repair
PEPCK
G6PC
Metabolism
Glycolysis / Gluconeogenesis
Bcl-6
IL-7R
KLF2
EDG1/6
Immuno-regulation
RAG1/2
atrogin-1
Muscle atrophy

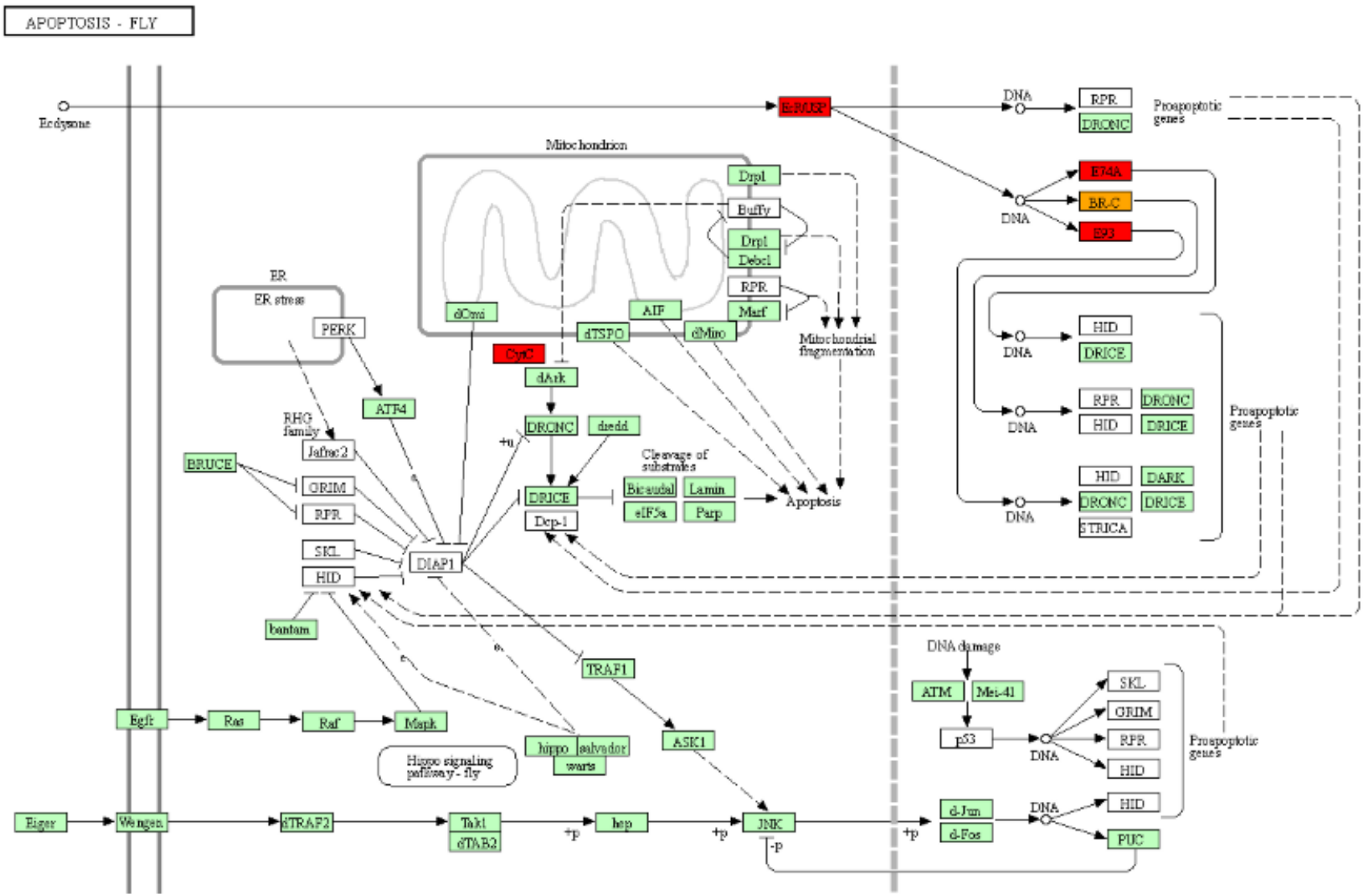
APOPTOSIS - FLY
Ecdysone
EcR/USP
DNA
RPR
DRONC
Proapoptotic genes
E74A
BR-C
E93
Mitochondrion
Drp1
Buffy
Debcl
Marf
ER
ER stress
PERK
dCrm
AIF
dTSPO
dMiro
Mitochondrial fragmentation
CytC
dArk
ATF4
RHG family
Jafrac2
BRUCE
GRIM
RPR
SKL
HID
DIAP1
DRONC
dredd
DRICE
Dcp-1
Cleavage of substrates
Bicaudal
Lamin
eIF5a
Parp
Apoptosis
HID
DRICE
DARK
STRICA
bantam
TRAF1
ASK1
DNA damage
ATM
Mei-41
p53
SKL
GRIM
RPR
HID
Egfr
Ras
Raf
Mapk
hippo
salvador
warts
Hippo signaling pathway - fly
Eiger
Wengen
dTRAF2
Tak1
dTAB2
hep
JNK
d-Jun
d-Fos
PUC

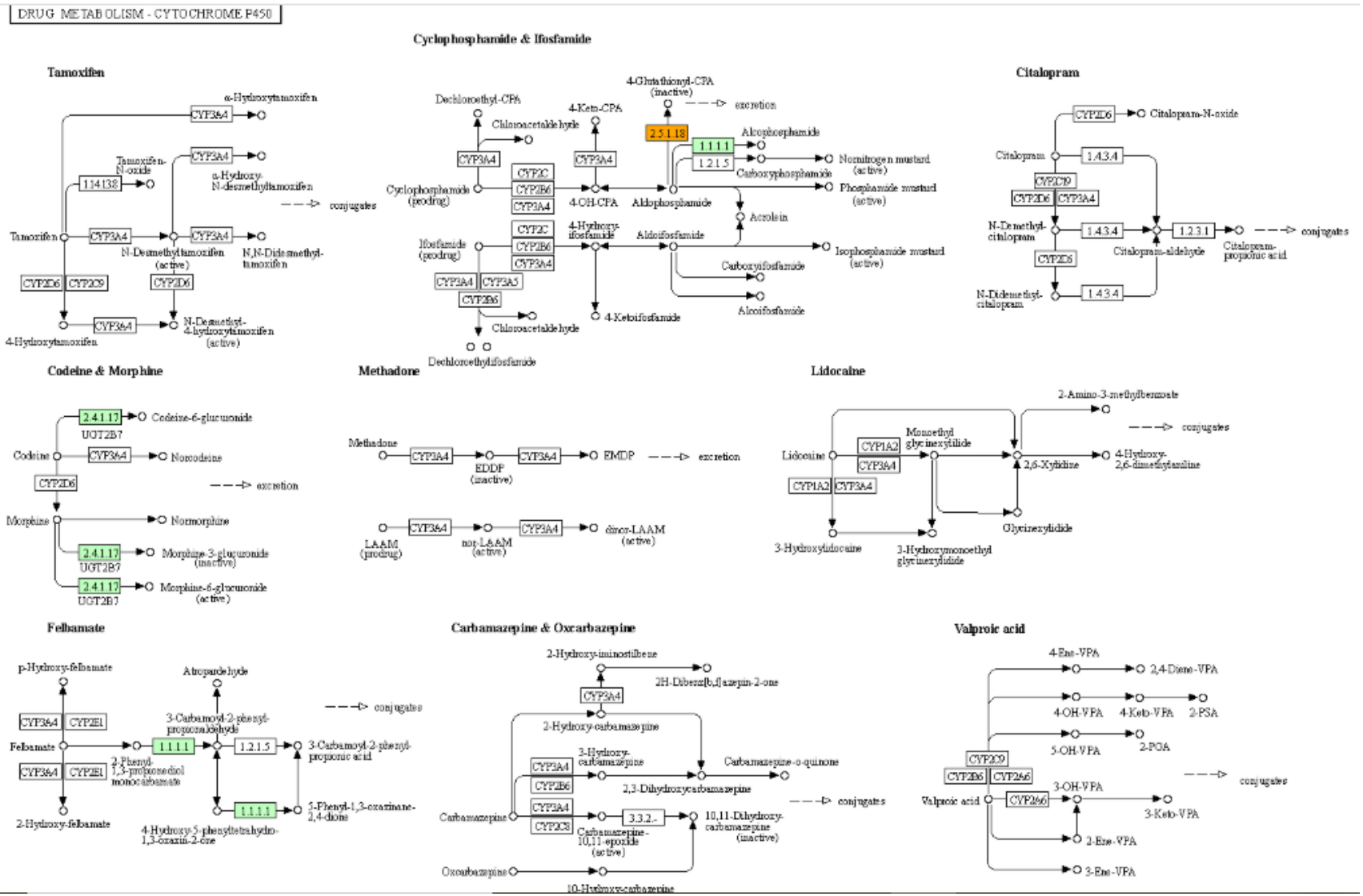
DRUG METABOLISM - CYTOCHROME P450
Cyclophosphamide & Ifosfamide
Tamoxifen
Citalopram
Codeine & Morphine
Methadone
Lidocaine
Felbamate
Carbamazepine & Oxcarbazepine
Valproic acid

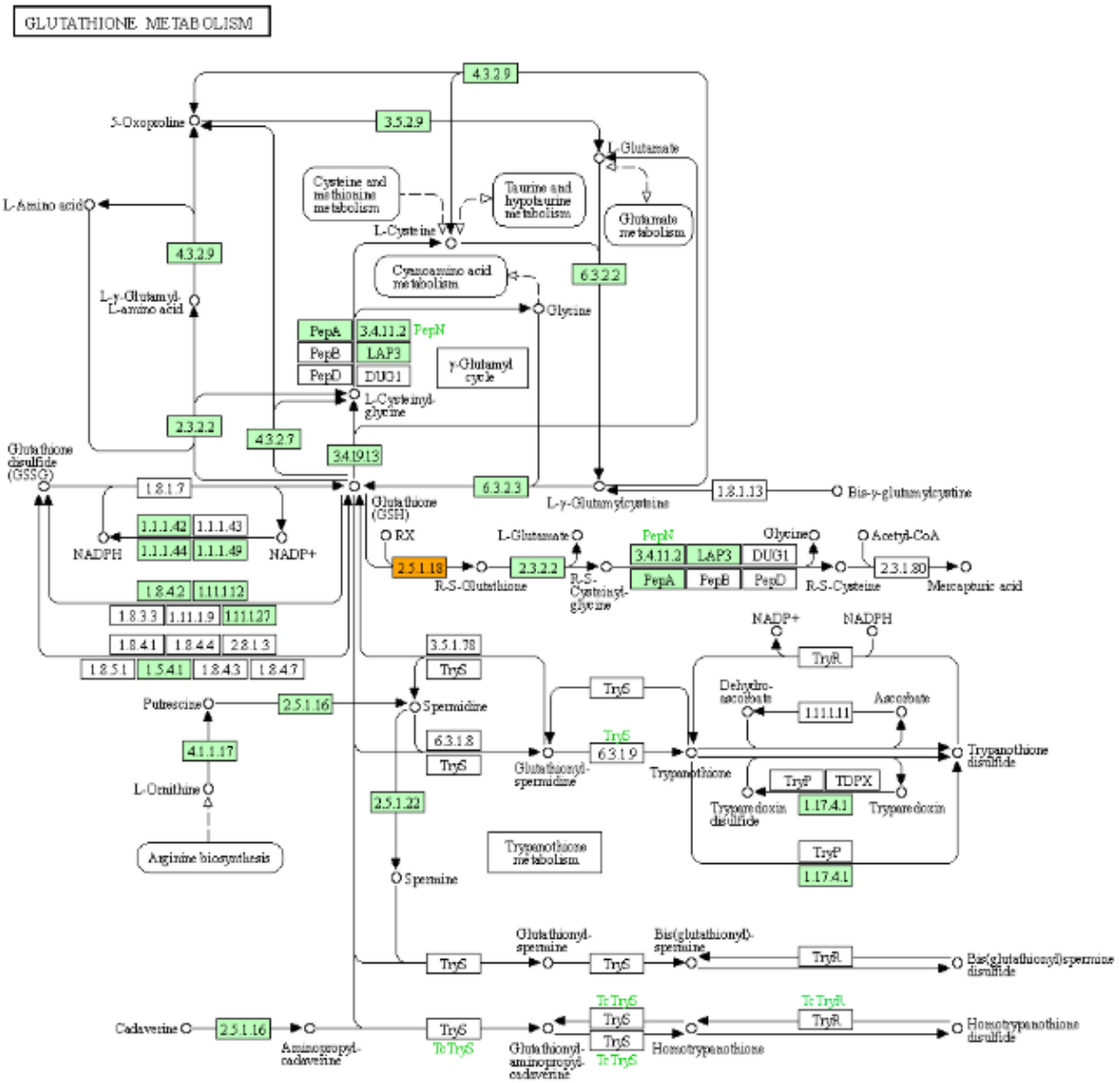
GLUTATHIONE METABOLISM
4.3.2.9
5-Oxoproline
3.5.2.9
L-Glutamate
Cysteine and methionine metabolism
Taurine and hypotaurine metabolism
Glutamate metabolism
L-Amino acid
L-Cysteine
4.3.2.9
Cyanoamino acid metabolism
6.3.2.2
L-γ-Glutamyl-L-amino acid
Glycine
PepA
3.4.11.2
PepN
PepB
LAP3
PepD
DUG1
γ-Glutamyl cycle
L-Cysteinyl-glycine
2.3.2.2
4.3.2.7
3.4.19.13
Glutathione disulfide (GSSG)
1.8.1.7
6.3.2.3
L-γ-Glutamylcysteine
1.8.1.13
Bis-γ-glutamylcystine
Glutathione (GSH)
1.1.1.42
1.1.1.43
1.1.1.44
1.1.1.49
NADPH
NADP+
RX
L-Glutamate
PepN
Glycine
Acetyl-CoA
2.5.1.18
2.3.2.2
3.4.11.2
LAP3
DUG1
PepA
PepB
PepD
2.3.1.80
R-S-Glutathione
R-S-Cysteinyl-glycine
R-S-Cysteine
Mercapturic acid
1.8.4.2
1.11.1.12
1.8.3.3
1.11.1.9
1.11.1.27
1.8.4.1
1.8.4.4
2.8.1.3
1.8.5.1
1.5.4.1
1.8.4.3
1.8.4.7
NADP+
NADPH
TryR
3.5.1.78
TryS
TryS
Dehydro-ascorbate
1.11.1.11
Ascorbate
Putrescine
2.5.1.16
Spermidine
6.3.1.8
TryS
TryS
6.3.1.9
Glutathionyl-spermidine
Trypanothione
Trypanothione disulfide
TryP
TDPX
Trypanredoxin disulfide
1.17.4.1
Trypanredoxin
4.1.1.17
L-Ornithine
2.5.1.22
Arginine biosynthesis
Trypanothione metabolism
Spermine
TryP
1.17.4.1
Glutathionyl-spermine
Bis(glutathionyl)-spermine
TryS
TryS
TryR
Bis(glutathionyl)spermine disulfide
Tc TryS
Tc TryR
Cadaverine
2.5.1.16
Aminopropyl-cadaverine
TryS
Tc TryS
Glutathionyl-aminopropyl-cadaverine
TryS
TryS
Tc TryS
Homotrypanothione
TryR
Homotrypanothione disulfide

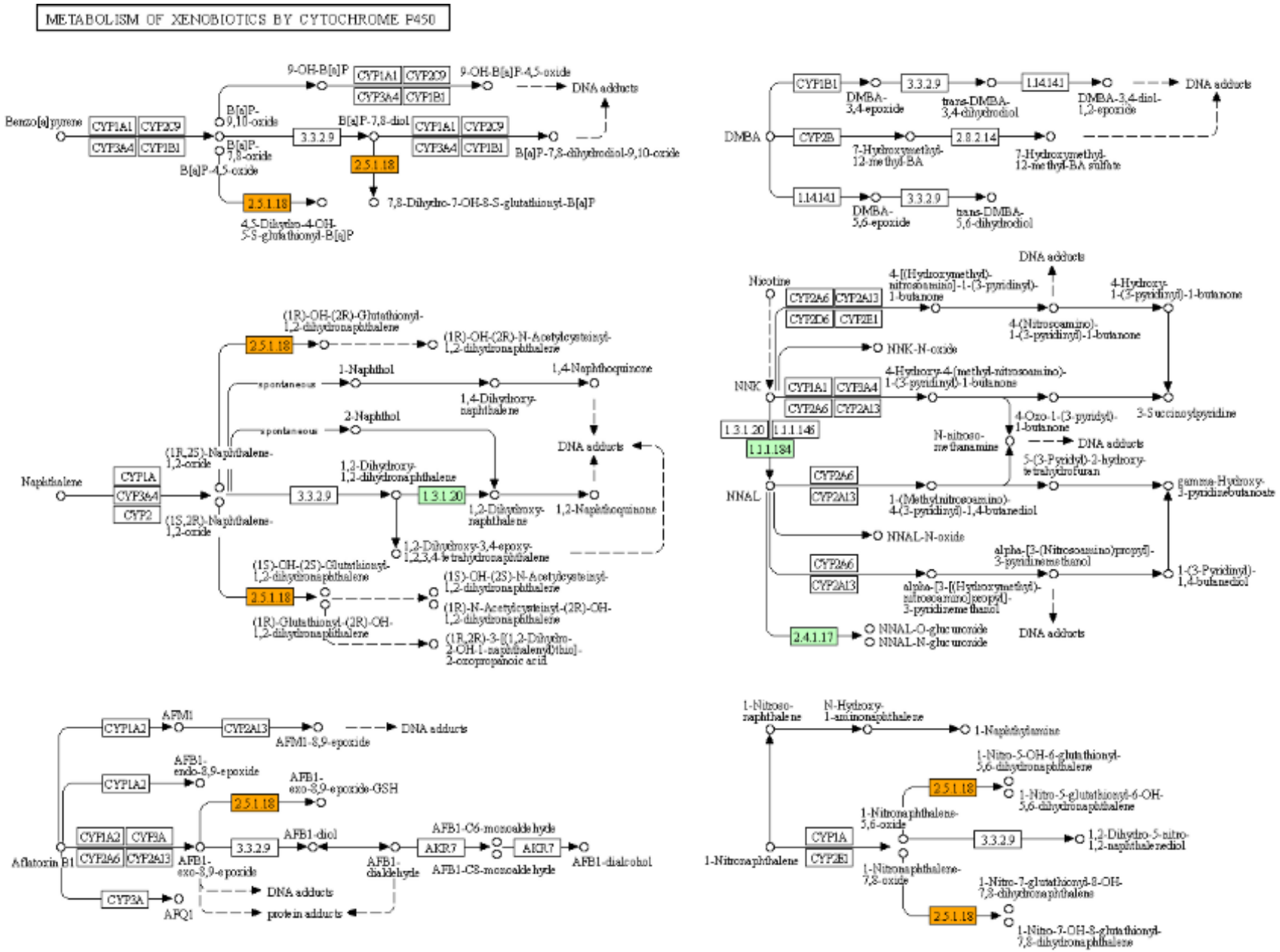
METABOLISM OF XENOBIOTICS BY CYTOCHROME P450
Benzo[a]pyrene
CYP1A1
CYP2C9
CYP3A4
CYP1B1
B[a]P-9,10-oxide
B[a]P-7,8-oxide
B[a]P-4,5-oxide
9-OH-B[a]P
9-OH-B[a]P-4,5-oxide
DNA adducts
3.3.2.9
B[a]P-7,8-diol
B[a]P-7,8-dihydrodiol-9,10-oxide
2.5.1.18
7,8-Dihydro-7-OH-8-S-glutathionyl-B[a]P
4,5-Dihydro-4-OH-5-S-glutathionyl-B[a]P
DMBA
CYP1B1
DMBA-3,4-epoxide
trans-DMBA-3,4-dihydrodiol
1.14.14.1
DMBA-3,4-diol-1,2-epoxide
CYP2B
7-Hydroxymethyl-12-methyl-BA
2.8.2.14
7-Hydroxymethyl-12-methyl-BA sulfate
DMBA-5,6-epoxide
trans-DMBA-5,6-dihydrodiol
Naphthalene
CYP1A
CYP3A4
CYP2
(1R,2S)-Naphthalene-1,2-oxide
(1S,2R)-Naphthalene-1,2-oxide
3.3.2.9
1,2-Dihydroxy-1,2-dihydronaphthalene
1.3.1.20
1,2-Dihydroxy-naphthalene
1,2-Naphthoquinone
1,2-Dihydroxy-3,4-epoxy-1,2,3,4-tetrahydronaphthalene
spontaneous
1-Naphthol
1,4-Naphthoquinone
1,4-Dihydroxy-naphthalene
2-Naphthol
(1R)-OH-(2R)-Glutathionyl-1,2-dihydronaphthalene
(1R)-OH-(2R)-N-Acetylcysteinyl-1,2-dihydronaphthalene
(1S)-OH-(2S)-Glutathionyl-1,2-dihydronaphthalene
(1S)-OH-(2S)-N-Acetylcysteinyl-1,2-dihydronaphthalene
(1R)-N-Acetylcysteinyl-(2R)-OH-1,2-dihydronaphthalene
(1R)-Glutathionyl-(2R)-OH-1,2-dihydronaphthalene
(1R,2R)-3-[(1,2-Dihydro-2-OH-1-naphthalenyl)thio]-2-oxopropanoic acid
Nicotine
CYP2A6
CYP2A13
CYP2D6
CYP2E1
4-[(Hydroxymethyl)-nitrosoamino]-1-(3-pyridinyl)-1-butanone
4-Hydroxy-1-(3-pyridinyl)-1-butanone
4-(Nitrosoamino)-1-(3-pyridinyl)-1-butanone
NNK-N-oxide
NNK
CYP1A1
CYP3A4
CYP2A6
CYP2A13
4-Hydroxy-4-(methyl-nitrosoamino)-1-(3-pyridinyl)-1-butanone
4-Oxo-1-(3-pyridyl)-1-butanone
3-Succinoylpyridine
1.3.1.20
1.1.1.146
1.1.1.184
N-nitroso-methanamine
5-(3-Pyridyl)-2-hydroxy-tetrahydrofuran
NNAL
1-(Methylnitrosoamino)-4-(3-pyridinyl)-1,4-butanediol
gamma-Hydroxy-3-pyridinebutanoate
NNAL-N-oxide
alpha-[3-(Nitrosoamino)propyl]-3-pyridinemethanol
1-(3-Pyridinyl)-1,4-butanediol
alpha-[3-[(Hydroxymethyl)-nitrosoamino]propyl]-3-pyridinemethanol
2.4.1.17
NNAL-O-glucuronide
NNAL-N-glucuronide
Aflatoxin B1
CYP1A2
CYP3A
CYP2A6
CYP2A13
AFM1
AFM1-8,9-epoxide
AFB1-endo-8,9-epoxide
AFB1-exo-8,9-epoxide-GSH
AFB1-exo-8,9-epoxide
AFB1-diol
AFB1-dialdehyde
AFB1-C6-monoaldehyde
AFB1-C8-monoaldehyde
AKR7
AFB1-dialcohol
AFQ1
protein adducts
1-Nitroso-naphthalene
N-Hydroxy-1-aminonaphthalene
1-Naphthylamine
1-Nitro-5-OH-6-glutathionyl-5,6-dihydronaphthalene
1-Nitro-5-glutathionyl-6-OH-5,6-dihydronaphthalene
1-Nitronaphthalene-5,6-oxide
1-Nitronaphthalene
CYP1A
CYP2E1
1,2-Dihydro-5-nitro-1,2-naphthalenediol
1-Nitronaphthalene-7,8-oxide
1-Nitro-7-glutathionyl-8-OH-7,8-dihydronaphthalene
1-Nitro-7-OH-8-glutathionyl-7,8-dihydronaphthalene

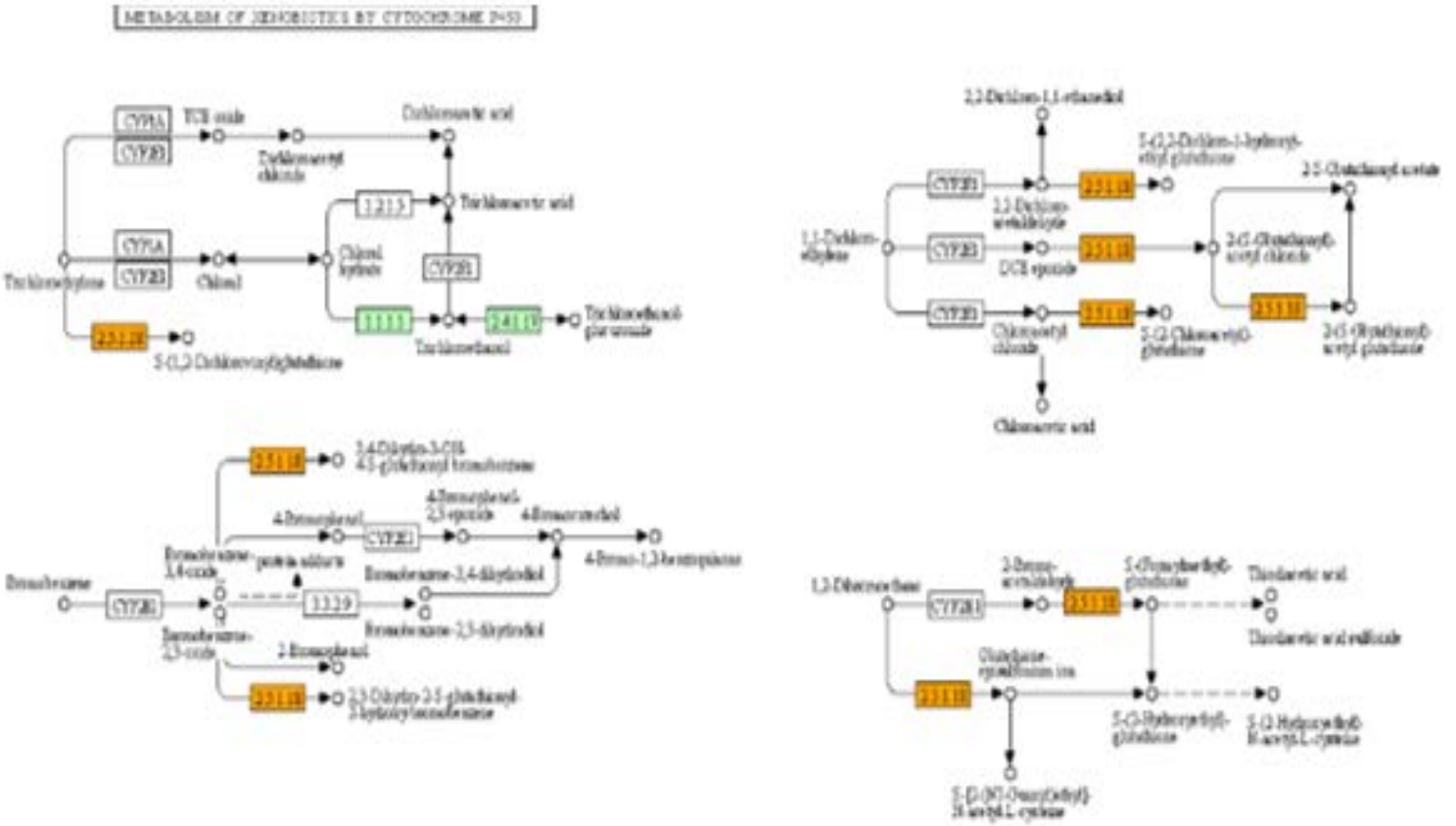
METABOLISM OF XENOBIOTICS BY CYTOCHROME P450
CYP1A
CYP2B
CYP3A
CYP2E1
1.2.1.3
1.1.1.1
2.4.1.1
2.5.1.18
3.3.2.9
Trichloroethylene
Chloral
Chloral hydrate
Trichloroacetic acid
Dichloroacetic acid
Trichloroethanol
Trichloroethanol glucuronide
Bromobenzene
Bromobenzene-3,4-oxide
Bromobenzene-3,4-dihydrodiol
Bromobenzene-2,3-oxide
Bromobenzene-2,3-dihydrodiol
4-Bromophenol
4-Bromophenol 2,3-epoxide
4-Bromocatechol
4-Bromo-1,2-benzoquinone
1,1-Dichloroethylene
2,2-Dichloro-1,1-ethanediol
2,2-Dichloroethenol
DCE epoxide
Chloroacetyl chloride
Chloroacetic acid
S-(2,2-Dichloro-1-hydroxyethyl) glutathione
S-(2-Chloroacetyl) glutathione
2-(S-Glutathionyl) acetyl chloride
2-(S-Glutathionyl) acetic acid
1,2-Dichloroethane
2-Chloroacetaldehyde
S-(2-Chloro-1-hydroxyethyl) glutathione
Thiodiglycolic acid
Thiodiglycolic acid sulfoxide
S-(2-Hydroxyethyl) glutathione
S-(2-Hydroxyethyl)-N-acetyl-L-cysteine

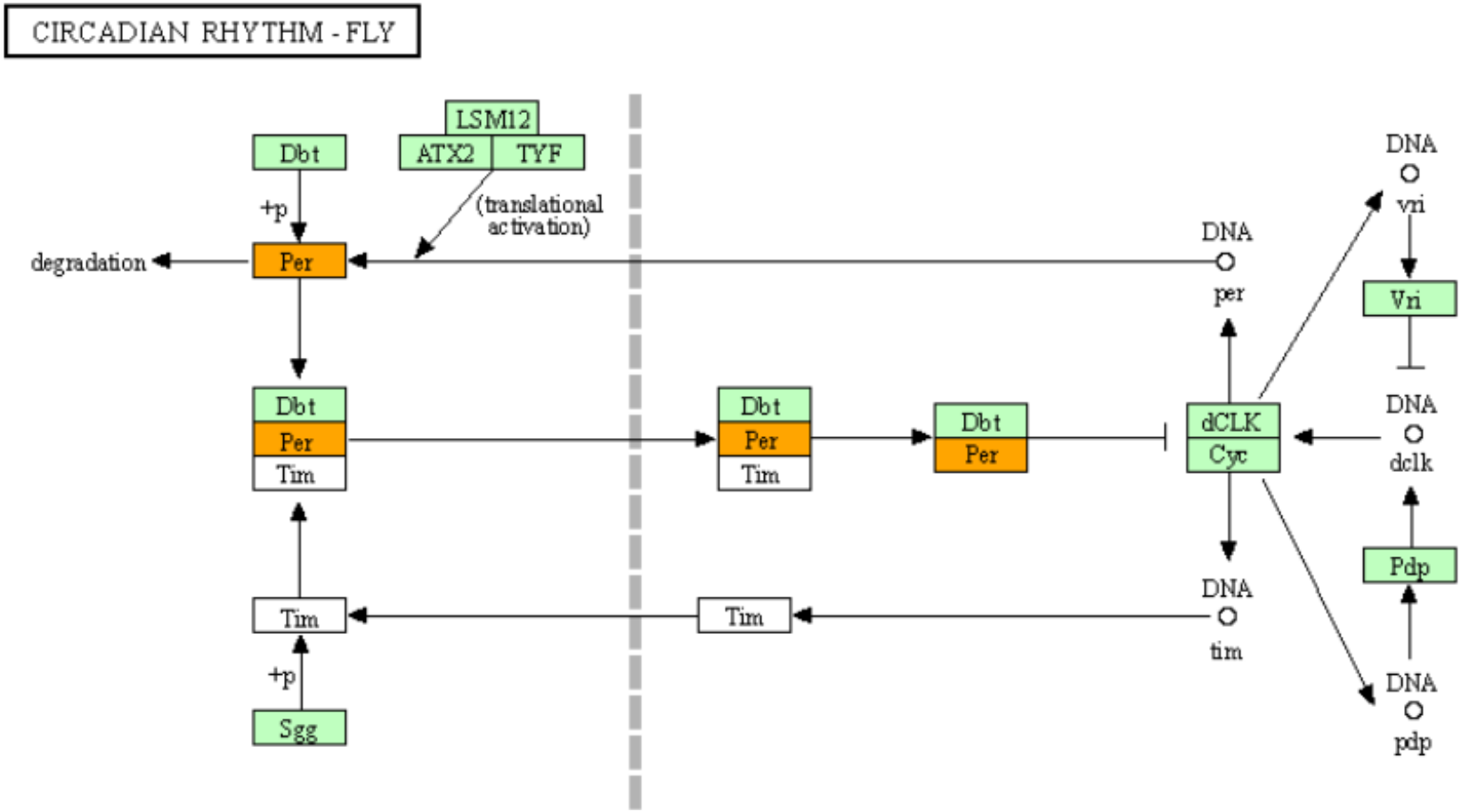
CIRCADIAN RHYTHM - FLY
LSM12
Dbt
ATX2
TYF
+p
(translational activation)
degradation
Per
DNA
per
DNA
vri
Vri
Dbt
Per
Tim
Dbt
Per
Tim
Dbt
Per
dCLK
Cyc
DNA
dclk
Pdp
Tim
Tim
DNA
tim
+p
Sgg
DNA
pdp

Appendix Q: Treatment Time 4 Hour-Control Time 0 Hour KEGG pathways. Genes that are colored red are considered down-regulated (not significant), genes that are colored purple are significantly down-regulated, genes that are colored pink are significantly up-regulated, and genes that are colored orange are considered up-regulated (not significant) (significance p<0.1). Enzymes are indicated by the green color.

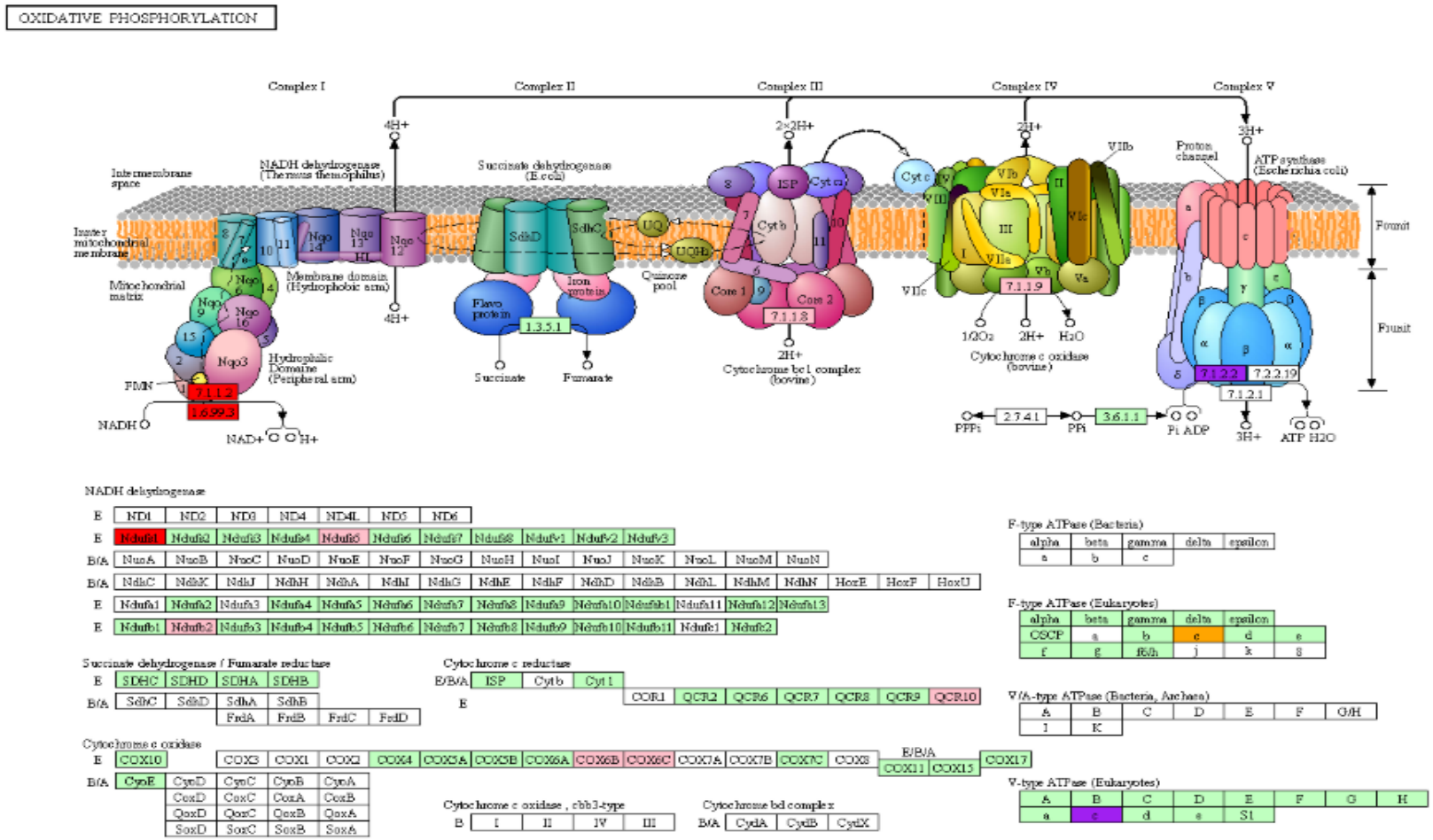

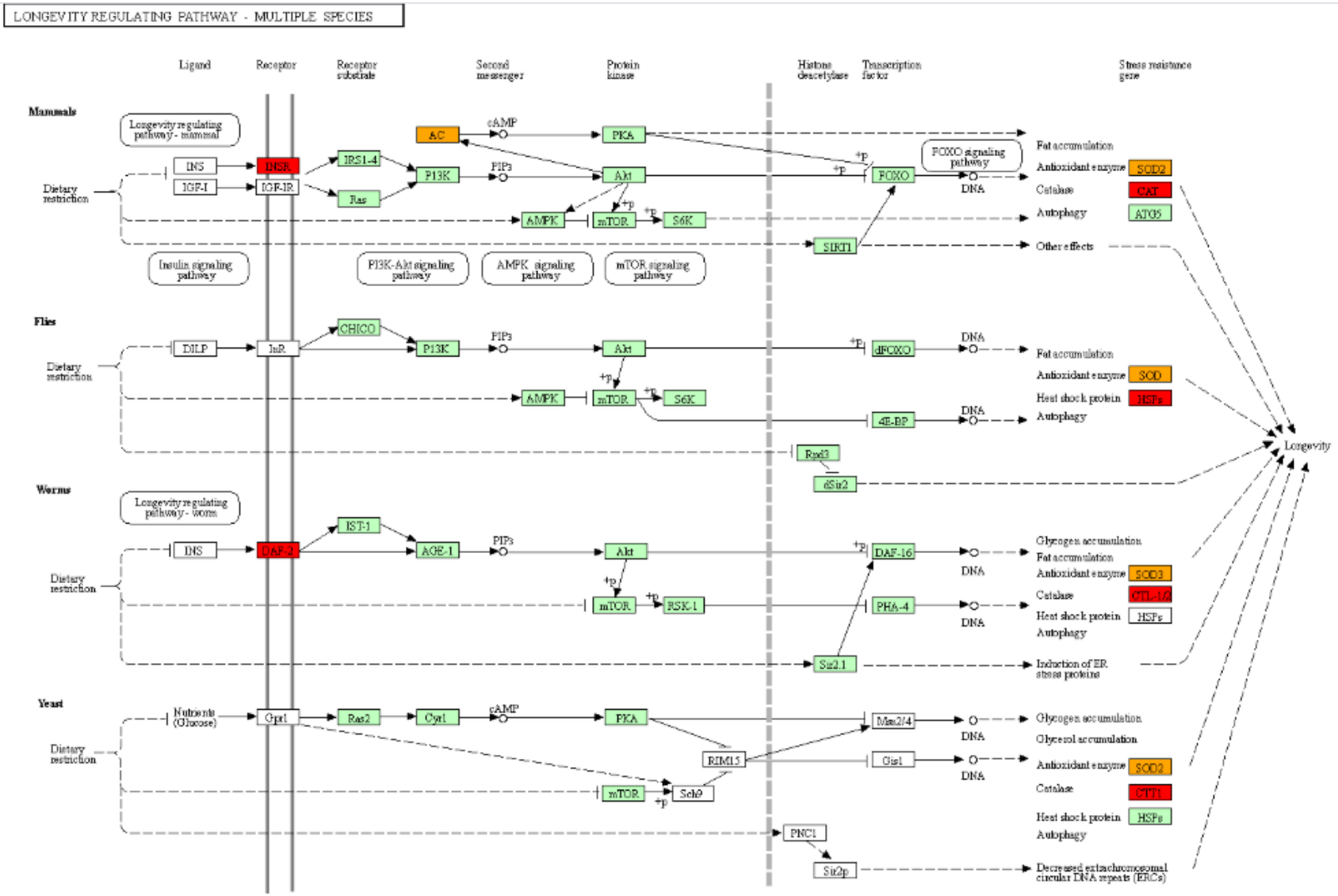
LONGEVITY REGULATING PATHWAY - MULTIPLE SPECIES
Ligand
Receptor
Receptor substrate
Second messenger
Protein kinase
Histone deacetylase
Transcription factor
Stress resistance gene
Mammals
Longevity regulating pathway - mammal
INS
IGF-I
INSR
IGF-1R
IRS1-4
Ras
PI3K
PIPs
AC
cAMP
PKA
Akt
AMPK
mTOR
S6K
SIRT1
FOXO
FOXO signaling pathway
DNA
Fat accumulation
Antioxidant enzyme
SOD2
Catalase
CAT
Autophagy
ATG5
Other effects
Dietary restriction
Insulin signaling pathway
PI3K-Akt signaling pathway
AMPK signaling pathway
mTOR signaling pathway
Flies
DILP
InR
CHICO
dFOXO
4E-BP
Rpd3
dSir2
SOD
Heat shock protein
HSPs
Worms
Longevity regulating pathway - worm
IST-1
AGE-1
DAF-2
DAF-16
PHA-4
SKN-1
Sir2.1
Induction of ER stress proteins
SOD3
CTL-1/2
Yeast
Nutrients (Glucose)
Gpr1
Ras2
Cyr1
RIM15
Msn2/4
Gis1
Sch9
PNC1
Sir2p
Glycogen accumulation
Glycerol accumulation
CTT1
Decreased extrachromosomal circular DNA repeats (ERCs)
Longevity

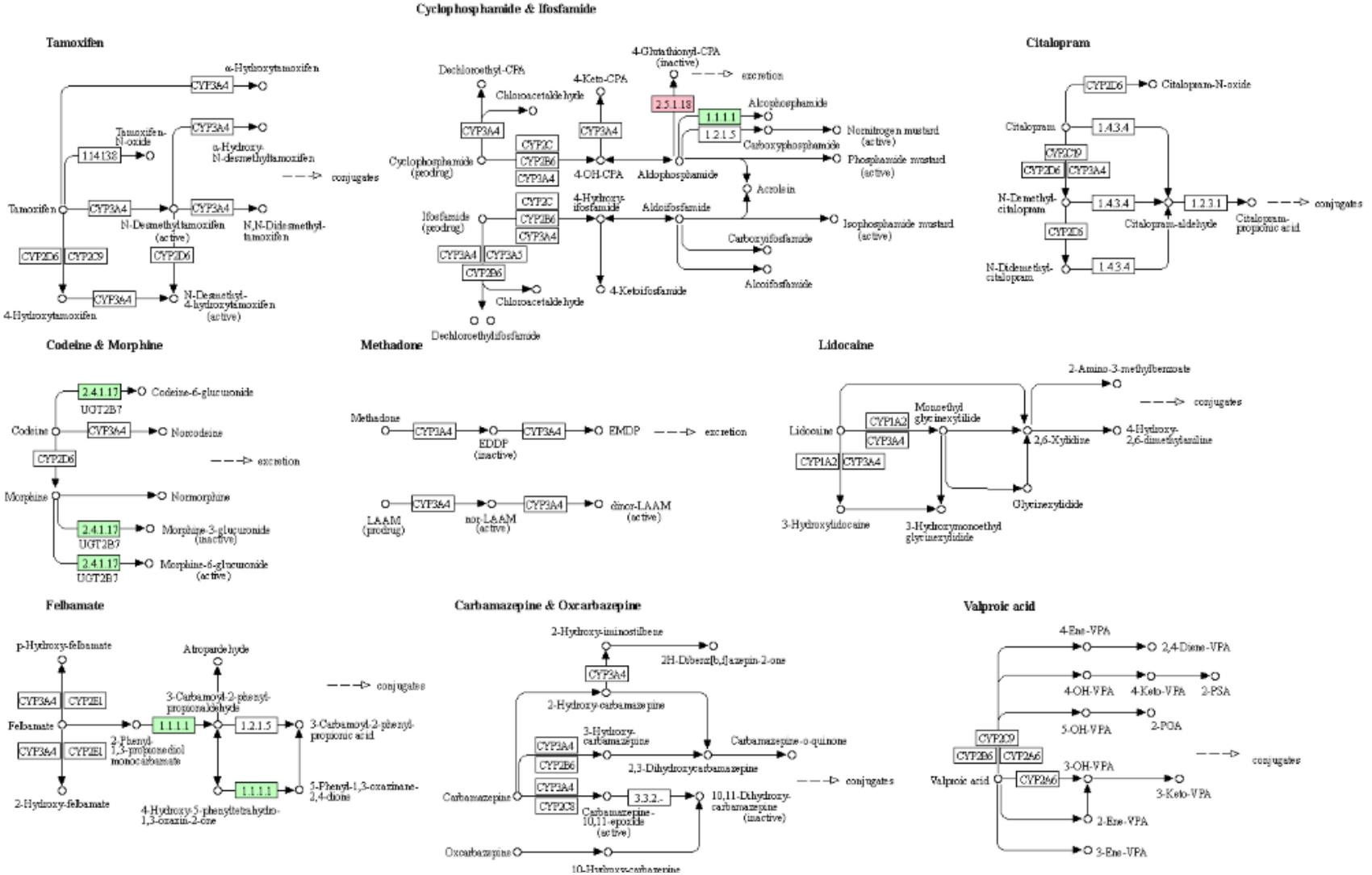
Tamoxifen
α-Hydroxytamoxifen
CYP3A4
Tamoxifen-N-oxide
1.14.13.8
α-Hydroxy-N-desmethyltamoxifen
conjugates
Tamoxifen
CYP3A4
N-Desmethyltamoxifen (active)
N,N-Didesmethyl-tamoxifen
CYP2D6
CYP2C9
CYP2D6
CYP3A4
N-Desmethyl-4-hydroxytamoxifen (active)
4-Hydroxytamoxifen
Cyclophosphamide & Ifosfamide
Dechloroethyl-CPA
4-Keto-CPA
4-Glutathionyl-CPA (inactive)
excretion
Chloroacetaldehyde
2.5.1.18
1.1.1.1
Alcophosphamide
1.2.1.5
Carboxyphosphamide
Nornitrogen mustard (active)
Cyclophosphamide (prodrug)
CYP2C
CYP2B6
CYP3A4
4-OH-CPA
Aldophosphamide
Phosphamide mustard (active)
Acrolein
Ifosfamide (prodrug)
4-Hydroxy-ifosfamide
Aldoifosfamide
Isophosphamide mustard (active)
Carboxyifosfamide
CYP3A4
CYP3A5
CYP2B6
4-Ketoifosfamide
Alcoifosfamide
Chloroacetaldehyde
Dechloroethylifosfamide
Citalopram
CYP2D6
Citalopram-N-oxide
Citalopram
1.4.3.4
CYP2C19
CYP2D6
CYP3A4
N-Demethyl-citalopram
1.4.3.4
1.2.3.1
conjugates
Citalopram-aldehyde
Citalopram-propionic acid
CYP2D6
N-Didemethyl-citalopram
1.4.3.4
Codeine & Morphine
2.4.1.17
Codeine-6-glucuronide
UGT2B7
Codeine
CYP3A4
Norcodeine
CYP2D6
excretion
Morphine
Normorphine
2.4.1.17
Morphine-3-glucuronide (inactive)
UGT2B7
2.4.1.17
Morphine-6-glucuronide (active)
UGT2B7
Methadone
Methadone
CYP1A4
CYP3A4
EMDP
excretion
EDDP (inactive)
LAAM (prodrug)
CYP3A4
nor-LAAM (active)
CYP3A4
dinor-LAAM (active)
Lidocaine
2-Amino-3-methylbenzoate
conjugates
Monoethyl glycinexylidide
Lidocaine
CYP1A2
CYP3A4
2,6-Xylidine
4-Hydroxy-2,6-dimethylaniline
CYP1A2
CYP3A4
Glycinexylidide
3-Hydroxylidocaine
3-Hydroxymonoethyl glycinexylidide
Felbamate
p-Hydroxy-felbamate
Atropaldehyde
conjugates
CYP3A4
CYP2E1
3-Carbamoyl-2-phenyl-propionaldehyde
Felbamate
1.1.1.1
1.2.1.5
3-Carbamoyl-2-phenyl-propionic acid
CYP3A4
CYP2E1
2-Phenyl-1,3-propanediol monocarbamate
1.1.1.1
1-Phenyl-1,3-oxazinane-2,4-dione
2-Hydroxy-felbamate
4-Hydroxy-5-phenyltetrahydro-1,3-oxazin-2-one
Carbamazepine & Oxcarbazepine
2-Hydroxy-iminostilbene
2H-Dibenz[b,f]azepin-2-one
CYP3A4
2-Hydroxy-carbamazepine
3-Hydroxy-carbamazepine
CYP3A4
CYP2B6
Carbamazepine-o-quinone
2,3-Dihydroxycarbamazepine
CYP3A4
CYP2C8
conjugates
Carbamazepine
3.3.2.-
10,11-Dihydroxy-carbamazepine (inactive)
Carbamazepine-10,11-epoxide (active)
Oxcarbazepine
10-Hydroxy-carbazepine
Valproic acid
4-Ene-VPA
2,4-Diene-VPA
4-OH-VPA
4-Keto-VPA
2-PSA
5-OH-VPA
2-POA
CYP2C9
CYP2B6
CYP2A6
conjugates
3-OH-VPA
Valproic acid
CYP2B6
3-Keto-VPA
2-Ene-VPA
3-Ene-VPA

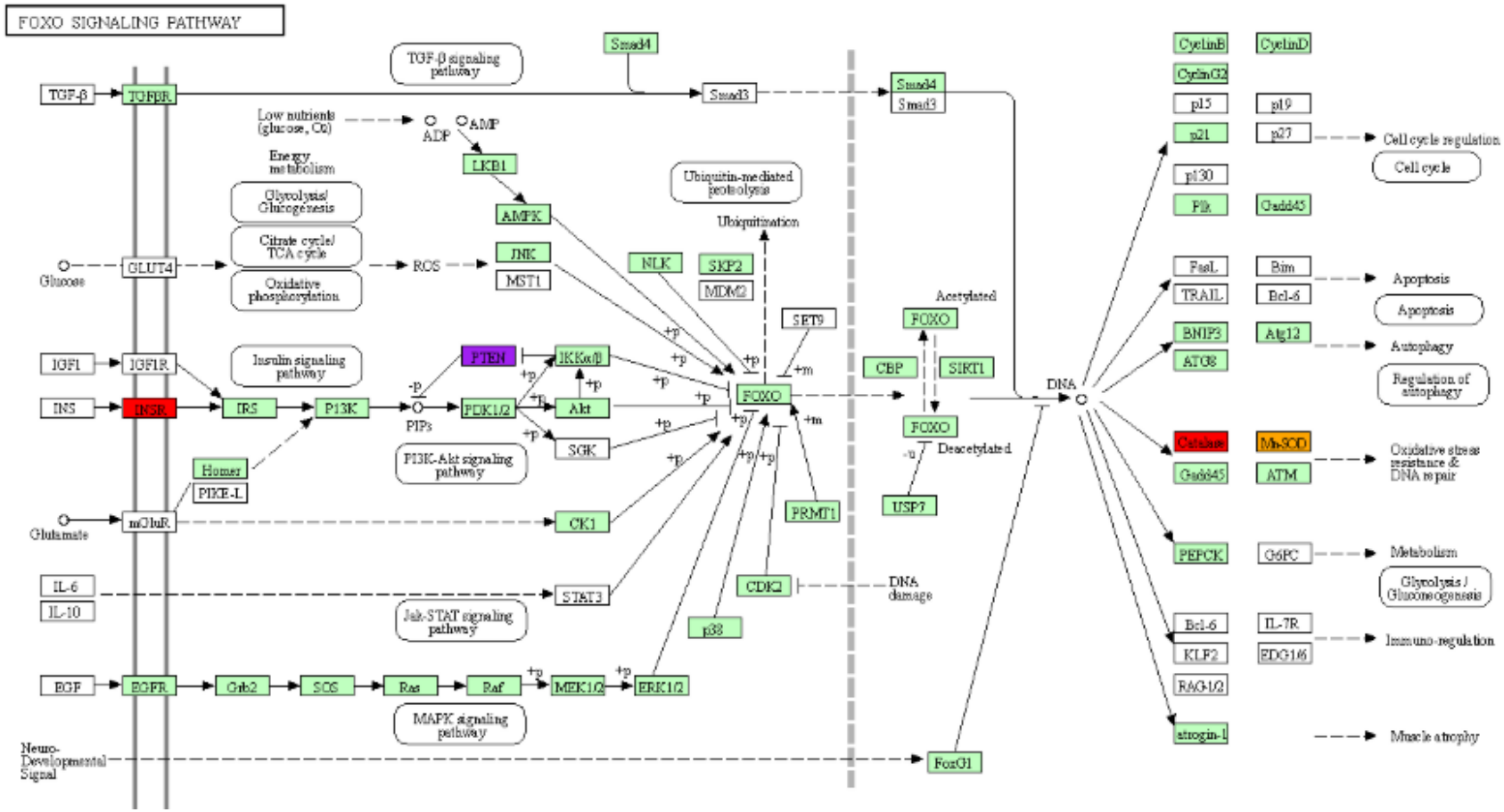
FOXO SIGNALING PATHWAY
TGF-β
TGFBR
TGF-β signaling pathway
Smad4
Smad3
Smad4
Smad3
CyclinB
CyclinD
CyclinG2
p15
p19
p21
p27
Cell cycle regulation
Cell cycle
p130
Fbx
Gadd45
Low nutrients (glucose, O2)
ADP
AMP
LKB1
Energy metabolism
Glycolysis/ Gluconeogenesis
Citrate cycle/ TCA cycle
Oxidative phosphorylation
ROS
AMPK
JNK
MST1
Ubiquitin-mediated proteolysis
Ubiquitination
NLK
SKP2
MDM2
SET9
Acetylated
FOXO
CBP
SIRT1
Glucose
GLUT4
IGF1
IGF1R
Insulin signaling pathway
INS
INSR
IRS
P13K
PIP3
PTEN
PDK1/2
IKKα/β
Akt
SGK
FOXO
PI3K-Akt signaling pathway
PRMT1
USP7
Deacetylated
DNA
FasL
TRAIL
Bim
Bcl-6
Apoptosis
Apoptosis
BNIP3
ATG8
Atg12
Autophagy
Regulation of autophagy
Homer
PIKE-L
Glutamate
mGluR
CK1
Catalase
Gadd45
Mn-SOD
ATM
Oxidative stress resistance & DNA repair
IL-6
IL-10
STAT3
Jak-STAT signaling pathway
CDK2
DNA damage
p38
PEPCK
G6PC
Metabolism
Glycolysis / Gluconeogenesis
Bcl-6
KLF2
RAG1/2
IL-7R
EDG1/6
Immuno-regulation
atrogin-1
Muscle atrophy
EGF
EGFR
Grb2
SOS
Ras
Raf
MEK1/2
ERK1/2
MAPK signaling pathway
Neuro-Developmental Signal
FoxO1

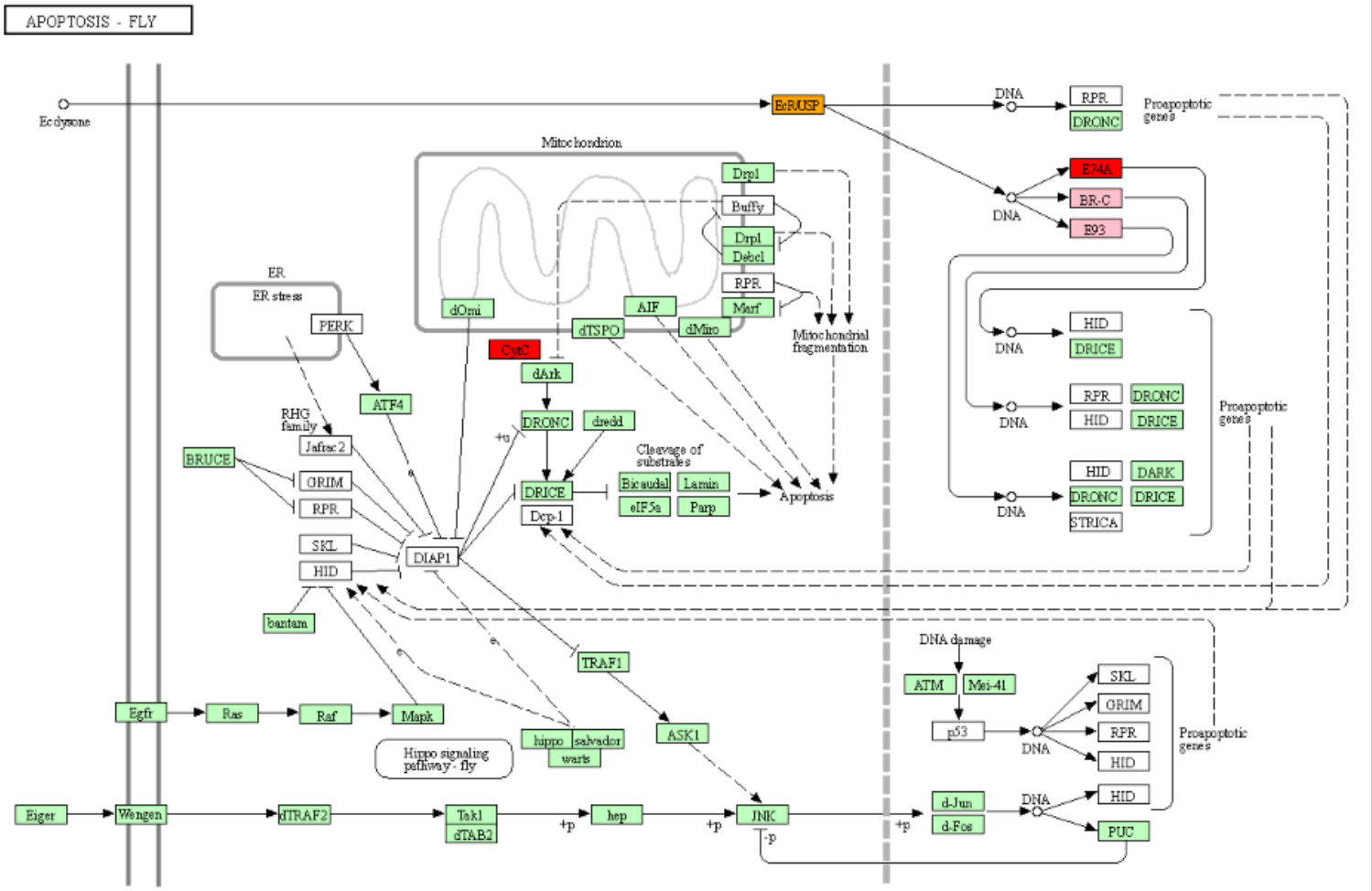
APOPTOSIS - FLY
Ecdysone
EcRUSP
Mitochondrion
Drp1
Buffy
Drp1
Debcl
RPR
Marf
dOmi
AIF
dTSPO
dMiro
Mitochondrial fragmentation
CytC
dArk
ER
ER stress
PERK
ATF4
RHG family
Jafrac2
BRUCE
GRIM
RPR
SKL
HID
DIAP1
bantam
DRONC
dredd
DRICE
Dcp-1
Cleavage of substrates
Bicaudal
Lamin
eIF5a
Parp
Apoptosis
DNA
RPR
DRONC
Proapoptotic genes
E74A
BR-C
E93
HID
DRICE
DARK
STRICA
TRAF1
ASK1
Egfr
Ras
Raf
Mapk
hippo
salvador
warts
Hippo signaling pathway - fly
Eiger
Wengen
dTRAF2
Tak1
dTAB2
hep
JNK
+p
-p
DNA damage
ATM
Mei-41
p53
d-Jun
d-Fos
PUC

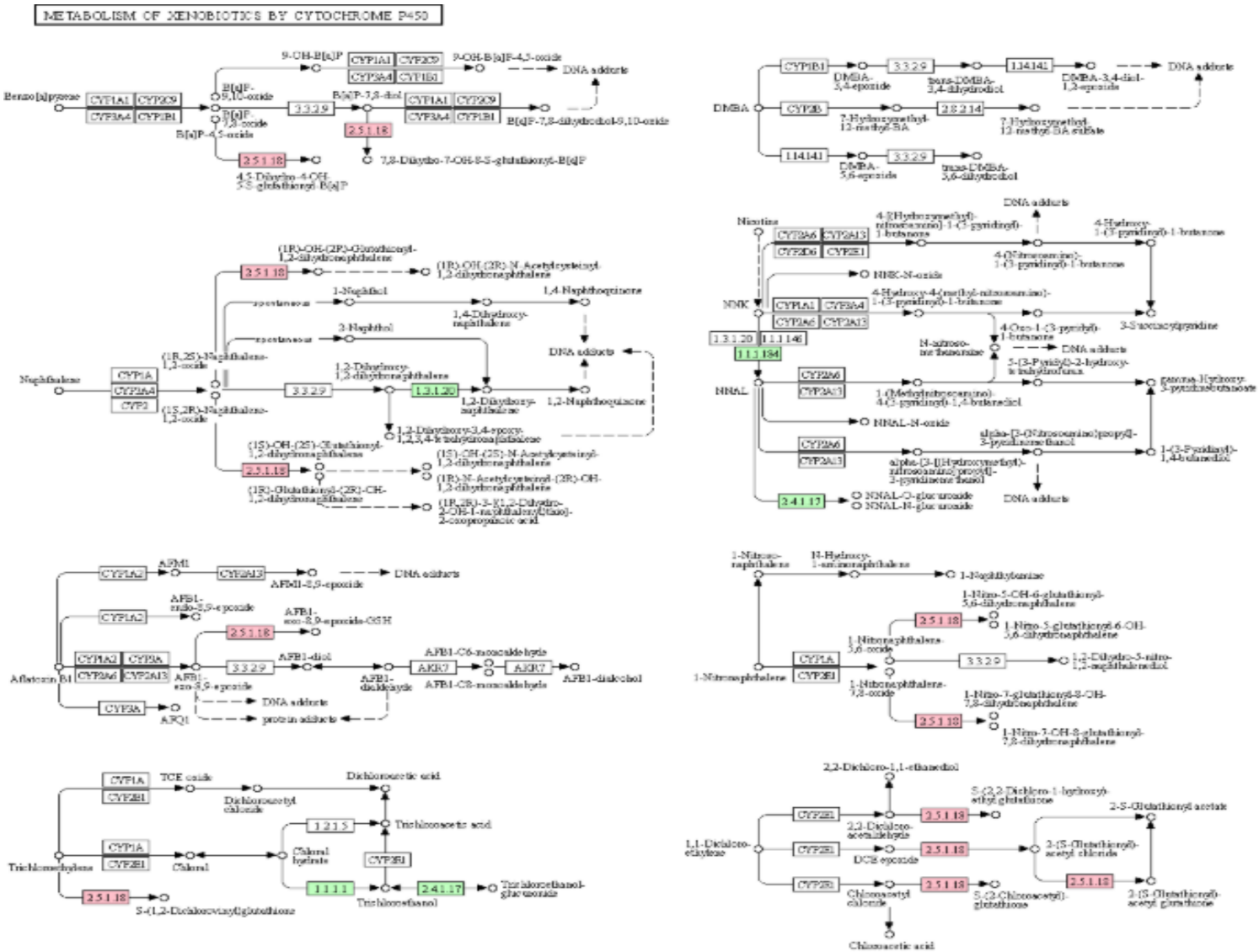
METABOLISM OF XENOBIOTICS BY CYTOCHROME P450
Benzo[a]pyrene
CYP1A1 CYP2C9 CYP3A4 CYP1B1
9-OH-B[a]P
9-OH-B[a]P-4,5-oxide
DNA adducts
B[a]P-9,10-oxide
B[a]P-4,5-oxide
B[a]P-7,8-diol
B[a]P-7,8-dihydrodiol-9,10-oxide
7,8-Dihydro-7-OH-8-S-glutathionyl-B[a]P
4,5-Dihydro-4-OH-5-S-glutathionyl-B[a]P
DMBA
CYP1B1
DMBA-3,4-epoxide
trans-DMBA-3,4-dihydrodiol
DMBA-3,4-diol-1,2-epoxide
CYP2B
7-Hydroxymethyl-12-methyl-BA
7-Hydroxymethyl-12-methyl-BA sulfate
DMBA-5,6-epoxide
trans-DMBA-5,6-dihydrodiol
Nicotine
CYP2A6 CYP2A13 CYP2D6 CYP2E1
4-(Hydroxymethyl)-nitrosamino)-1-(3-pyridinyl)-1-butanone
4-Hydroxy-1-(3-pyridinyl)-1-butanone
4-(Nitrosamino)-1-(3-pyridinyl)-1-butanone
NNK
NNK-N-oxide
CYP1A1 CYP3A4 CYP2A6 CYP2A13
4-Hydroxy-4-(methyl-nitrosamino)-1-(3-pyridinyl)-1-butanone
4-Oxo-1-(3-pyridyl)-1-butanone
3-Succinoylpyridine
1.3.1.20 1.1.1.146 1.1.1.184
N-nitroso-nornicotine
5-(3-Pyridyl)-2-hydroxy-tetrahydrofuran
NNAL
CYP2A6 CYP2A13
1-(Methylnitrosamino)-4-(3-pyridinyl)-1,4-butanediol
gamma-Hydroxy-3-pyridinebutanoate
NNAL-N-oxide
alpha-[3-(Nitrosomino)propyl]-3-pyridinemethanol
1-(3-Pyridinyl)-1,4-butanediol
alpha-[3-[(Hydroxymethyl)-nitrosamino]propyl]-3-pyridinemethanol
2.4.1.17
NNAL-O-glucuronide
NNAL-N-glucuronide
DNA adducts
Naphthalene
CYP1A CYP1A4 CYP2
(1R,2S)-Naphthalene-1,2-oxide
(1S,2R)-Naphthalene-1,2-oxide
3.3.2.9
1,2-Dihydroxy-1,2-dihydronaphthalene
1.3.1.20
1,2-Dihydroxy-naphthalene
1,2-Naphthoquinone
1,2-Dihydroxy-3,4-epoxy-1,2,3,4-tetrahydronaphthalene
(1R)-OH-(2P)-Glutathionyl-1,2-dihydronaphthalene
2.5.1.18
(1R)-OH-(2R)-N-Acetylcysteinyl-1,2-dihydronaphthalene
1-Naphthol
1,4-Naphthoquinone
1,4-Dihydroxy-naphthalene
2-Naphthol
(1S)-OH-(2S)-Glutathionyl-1,2-dihydronaphthalene
2.5.1.18
(1S)-OH-(2S)-N-Acetylcysteinyl-1,2-dihydronaphthalene
(1R)-Glutathionyl-(2R)-OH-1,2-dihydronaphthalene
(1R)-N-Acetylcysteinyl-(2R)-OH-1,2-dihydronaphthalene
(1R,2R)-3-[(1,2-Dihydro-2-OH-1-naphthalenyl)thio]-2-aminopropanoic acid
Aflatoxin B1
CYP1A2
AFM1
AFM1-8,9-epoxide
DNA adducts
CYP1A2
AFB1-endo-8,9-epoxide
AFB1-exo-8,9-epoxide-GSH
2.5.1.18
CYP1A2 CYP3A CYP2A6 CYP2A13
AFB1-exo-8,9-epoxide
3.3.2.9
AFB1-diol
AFB1-dialdehyde
AKR7
AFB1-C6-monoaldehyde
AFB1-C8-monoaldehyde
AFB1-dialcohol
CYP3A
AFQ1
DNA adducts
protein adducts
1-Nitronaphthalene
1-Nitroso-naphthalene
N-Hydroxy-1-aminonaphthalene
1-Naphthylamine
1-Nitro-5-OH-6-glutathionyl-5,6-dihydronaphthalene
2.5.1.18
1-Nitro-5-glutathionyl-6-OH-5,6-dihydronaphthalene
CYP1A CYP2E1
1-Nitronaphthalene-5,6-oxide
3.3.2.9
1,2-Dihydro-5-nitro-1,2-naphthalenediol
1-Nitronaphthalene-7,8-oxide
1-Nitro-7-glutathionyl-8-OH-7,8-dihydronaphthalene
2.5.1.18
1-Nitro-7-OH-8-glutathionyl-7,8-dihydronaphthalene
Trichloroethylene
CYP1A CYP2E1
TCE oxide
Dichloroacetyl chloride
Dichloroacetic acid
1.2.1.5
Trichloroacetic acid
Chloral hydrate
Chloral
CYP2E1
1.1.1.1
2.4.1.17
Trichloroethanol
Trichloroethanol-glucuronide
2.5.1.18
S-(1,2-Dichlorovinyl)glutathione
2,2-Dichloro-1,1-ethanediol
1,1-Dichloro-ethylene
CYP2E1
S-(2,2-Dichloro-1-hydroxyl-ethyl glutathione
2.5.1.18
2-S-Glutathionyl acetate
2,2-Dichloro-acetaldehyde
DCE epoxide
2-(S-Glutathionyl)-acetyl chloride
Chloroacetyl chloride
S-(2-Chloroacetyl)-glutathione
2-(S-Glutathionyl)-acetyl glutathione
Chloroacetic acid

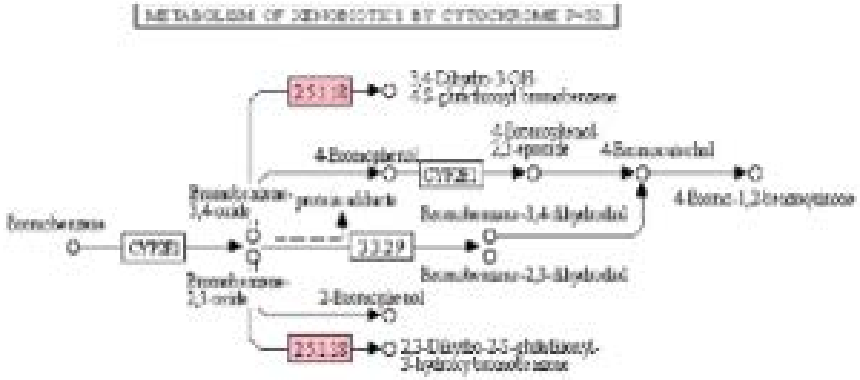
CYP2E1
2.3.1.9
2.5.1.18
4-Bromophenol
4-Bromocatechol
4-Bromo-1,2-benzoquinone
Bromobenzene-3,4-dihydrodiol
Bromobenzene-2,3-dihydrodiol
2-Bromophenol

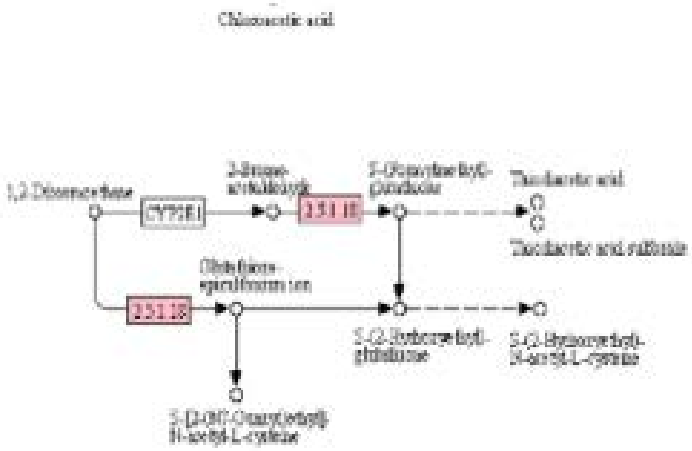
1,2-Dibromobenzene
CYP2E1
2.5.1.18
Thiodiacetic acid
Thiodiacetic acid sulfoxide

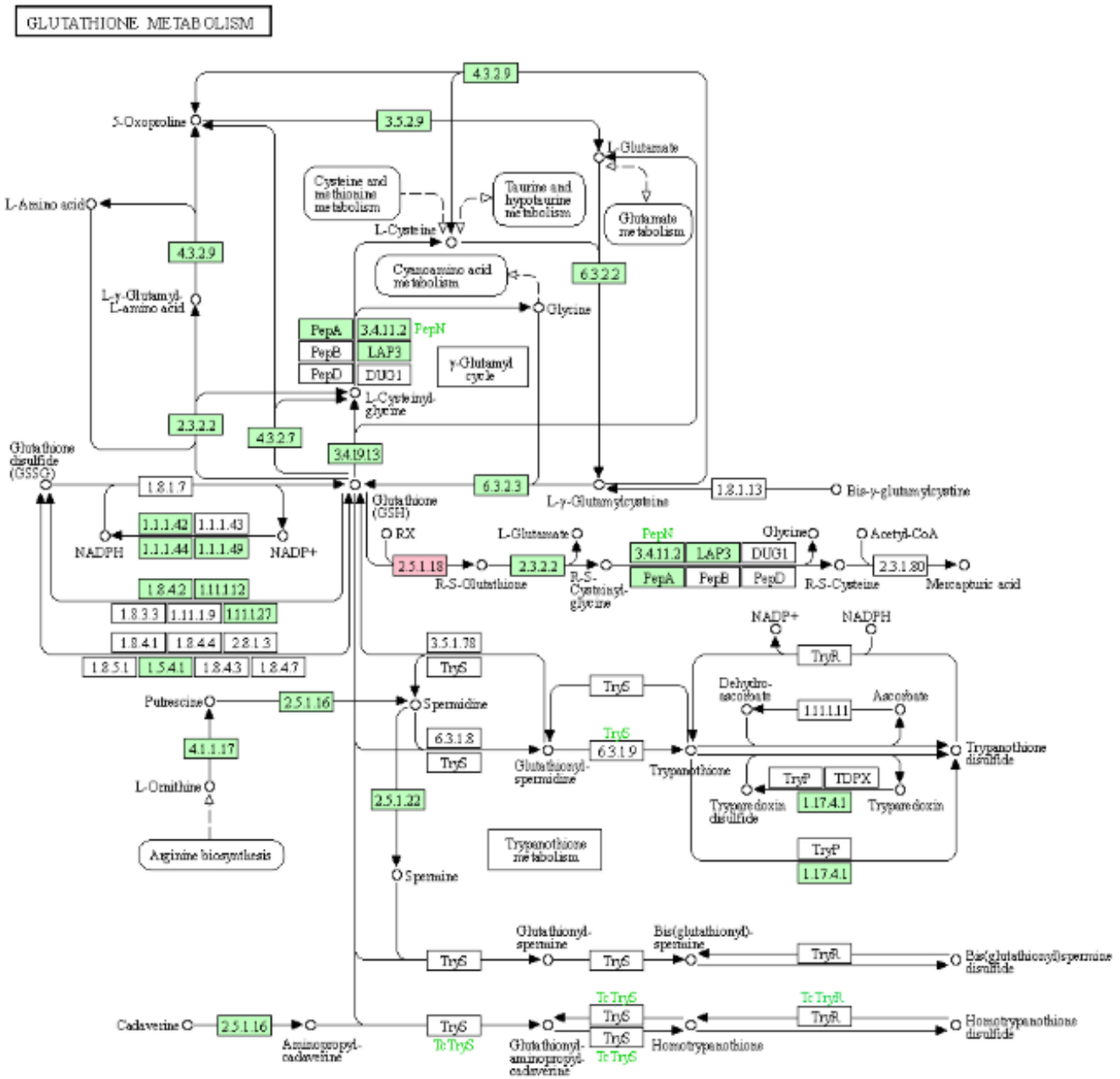
GLUTATHIONE METABOLISM
5-Oxoproline
L-Amino acid
L-Glutamate
Cysteine and methionine metabolism
Taurine and hypotaurine metabolism
Glutamate metabolism
L-Cysteine
Cyanoamino acid metabolism
Glycine
L-γ-Glutamyl L-amino acid
PepA
PepB
PepD
3.4.11.2
PepN
LAP3
DUG1
γ-Glutamyl cycle
L-Cysteinyl-glycine
Glutathione disulfide (GSSG)
Glutathione (GSH)
L-γ-Glutamylcysteine
Bis-γ-glutamylcystine
NADPH
NADP+
RX
R-S-Glutathione
L-Glutamate
R-S-Cysteinyl-glycine
Glycine
Acetyl-CoA
R-S-Cysteine
Mercapturic acid
Putrescine
Spermidine
L-Ornithine
Arginine biosynthesis
Glutathionyl-spermidine
Trypanothione
Trypanothione disulfide
Trypanothione metabolism
TryR
TryS
TryP
TDPX
Dehydro-ascorbate
Ascorbate
Tryparedoxin
Tryparedoxin disulfide
Spermine
Glutathionyl-spermine
Bis(glutathionyl)-spermine
Bis(glutathionyl)spermine disulfide
Cadaverine
Aminopropyl-cadaverine
Glutathionyl-aminopropyl-cadaverine
Homotrypanothione
Homotrypanothione disulfide
TcTryS
TcTryR

Appendix R: DAVID Analysis of significantly ($p<0.1$) enriched genes for Treatment-4h versus Control-0h.

Down-Regulated

Annotation Cluster 1	Enrichment Score: 5.45637131589216
Category	Term
GOTERM_MF_DIRECT	GO:0008270~zinc ion binding
INTERPRO	IPR013083:Zinc finger, RING/FYVE/PHD-type
INTERPRO	IPR001841:Zinc finger, RING-type
SMART	SM00184:RING
Annotation Cluster 2	Enrichment Score: 4.8010075530818375
Category	Term
UP_KEYWORDS	Membrane
UP_KEYWORDS	Transmembrane helix
UP_KEYWORDS	Transmembrane
GOTERM_CC_DIRECT	GO:0016021~integral component of membrane
Annotation Cluster 3	Enrichment Score: 2.942701935144724
Category	Term
GOTERM_BP_DIRECT	GO:0007264~small GTPase mediated signal transduction
INTERPRO	IPR005225:Small GTP-binding protein domain
INTERPRO	IPR001806:Small GTPase superfamily
GOTERM_MF_DIRECT	GO:0005525~GTP binding
UP_KEYWORDS	GTP-binding
INTERPRO	IPR027417:P-loop containing nucleoside triphosphate hydrolase
Annotation Cluster 4	Enrichment Score: 2.800889694997264
Category	Term
GOTERM_MF_DIRECT	GO:0004842~ubiquitin-protein transferase activity
UP_KEYWORDS	Ubl conjugation pathway
GOTERM_MF_DIRECT	GO:0016874~ligase activity
INTERPRO	IPR000569:HECT
SMART	SM00119:HECTc
SMART	SM00456:WW
Annotation Cluster 5	Enrichment Score: 2.7931918200278925
Category	Term
INTERPRO	IPR008271:Serine/threonine-protein kinase, active site
INTERPRO	IPR017441:Protein kinase, ATP binding site
UP_KEYWORDS	Kinase
UP_KEYWORDS	Serine/threonine-protein kinase
GOTERM_MF_DIRECT	GO:0004674~protein serine/threonine kinase activity
INTERPRO	IPR000719:Protein kinase, catalytic domain
SMART	SM00220:S_TKc
INTERPRO	IPR011009:Protein kinase-like domain
UP_KEYWORDS	Nucleotide-binding
UP_KEYWORDS	ATP-binding
GOTERM_MF_DIRECT	GO:0005524~ATP binding

Annotation Cluster 6	Enrichment Score: 2.777276800524685
Category	Term
GOTERM_BP_DIRECT	GO:0035556~intracellular signal transduction
INTERPRO	
SMART	SM00109:C1
Annotation Cluster 7	Enrichment Score: 1.9311441030506946
Category	Term
INTERPRO	IPR011993:Pleckstrin homology-like domain
INTERPRO	IPR001849:Pleckstrin homology domain
SMART	SM00233:PH
Annotation Cluster 8	Enrichment Score: 1.7901506620531265
Category	Term
UP_KEYWORDS	Zinc
UP_KEYWORDS	Metal-binding
UP_KEYWORDS	Zinc-finger
Annotation Cluster 9	Enrichment Score: 1.579437655647095
Category	Term
INTERPRO	IPR011333:BTB/POZ fold
INTERPRO	IPR000210:BTB/POZ-like
SMART	SM00225:BTB
Annotation Cluster 10	Enrichment Score: 1.571201116530967
Category	Term
SMART	SM00253:SOCS
SMART	SM00969:SM00969
INTERPRO	IPR001496:SOCS protein, C-terminal
Annotation Cluster 11	Enrichment Score: 1.4532259278548885
Category	Term
INTERPRO	IPR001452:Src homology-3 domain
SMART	SM00326:SH3
UP_KEYWORDS	SH3 domain
Annotation Cluster 12	Enrichment Score: 1.2000790546574989
Category	Term
INTERPRO	IPR023214:HAD-like domain
INTERPRO	IPR023299:P-type ATPase, cytoplasmic domain N
INTERPRO	IPR001757:Cation-transporting P-type ATPase
INTERPRO	IPR018303:P-type ATPase, phosphorylation site
INTERPRO	IPR008250:P-type ATPase, A domain
GOTERM_MF_DIRECT	GO:0004012~phospholipid-translocating ATPase activity
INTERPRO	IPR006539:Phospholipid-transporting P-type ATPase, subfamily IV
Annotation Cluster 13	Enrichment Score: 1.191896405979736
Category	Term

INTERPRO	IPR011992:EF-hand-like domain
GOTERM_MF_DIRECT	GO:0005509~calcium ion binding
INTERPRO	IPR002048:EF-hand domain
INTERPRO	IPR018247:EF-Hand 1, calcium-binding site
SMART	SM00054:EFh
Annotation Cluster 14	Enrichment Score: 1.1422749230721754
Category	Term
INTERPRO	IPR013763:Cyclin-like
INTERPRO	IPR006671:Cyclin, N-terminal
UP_KEYWORDS	Cyclin
SMART	SM00385:CYCLIN
INTERPRO	IPR004367:Cyclin, C-terminal domain
SMART	SM01332:SM01332
Annotation Cluster 15	Enrichment Score: 1.0468816164360077
Category	Term
INTERPRO	IPR017892:Protein kinase, C-terminal
INTERPRO	IPR000961:AGC-kinase, C-terminal
SMART	SM00133:S_TK_X
Annotation Cluster 16	Enrichment Score: 1.044975678587419
Category	Term
INTERPRO	IPR013761:Sterile alpha motif/pointed domain
SMART	SM00454:SAM
INTERPRO	IPR001660:Sterile alpha motif domain
Annotation Cluster 17	Enrichment Score: 0.9691442961294987
Category	Term
UP_KEYWORDS	Protein phosphatase
INTERPRO	IPR003595:Protein-tyrosine phosphatase, catalytic
SMART	SM00404:PTPc_motif
SMART	SM00194:PTPc
INTERPRO	
INTERPRO	IPR016130:Protein-tyrosine phosphatase, active site
INTERPRO	IPR000387:Protein-tyrosine/Dual specificity phosphatase
GOTERM_MF_DIRECT	GO:0004725~protein tyrosine phosphatase activity
Annotation Cluster 18	Enrichment Score: 0.9629833272596152
Category	Term
INTERPRO	IPR001394:Peptidase C19, ubiquitin carboxyl-terminal hydrolase 2
GOTERM_BP_DIRECT	GO:0016579~protein deubiquitination
INTERPRO	
GOTERM_BP_DIRECT	GO:0006511~ubiquitin-dependent protein catabolic process
GOTERM_MF_DIRECT	GO:0036459~thiol-dependent ubiquitinyl hydrolase activity
INTERPRO	IPR001607:Zinc finger, UBP-type
Annotation Cluster 19	Enrichment Score: 0.9218108166394164
Category	Term

INTERPRO	IPR000300:Inositol polyphosphate-related phosphatase
SMART	SM00128:IPPc
INTERPRO	IPR005135:Endonuclease/exonuclease/phosphatase
GOTERM_BP_DIRECT	GO:0046856~phosphatidylinositol dephosphorylation
Annotation Cluster 20	Enrichment Score: 0.9059256645404106
Category	Term
INTERPRO	IPR018108:Mitochondrial substrate/solute carrier
INTERPRO	IPR023395:Mitochondrial carrier domain
INTERPRO	IPR002067:Mitochondrial carrier protein
Annotation Cluster 21	Enrichment Score: 0.8667189123896825
Category	Term
UP_KEYWORDS	LIM domain
INTERPRO	IPR001781:Zinc finger, LIM-type
SMART	SM00132:LIM
Annotation Cluster 22	Enrichment Score: 0.8600660685290529
Category	Term
KEGG_PATHWAY	ame00072:Synthesis and degradation of ketone bodies
KEGG_PATHWAY	ame00650:Butanoate metabolism
KEGG_PATHWAY	ame00280:Valine, leucine and isoleucine degradation
Annotation Cluster 23	Enrichment Score: 0.8233643535747749
Category	Term
GOTERM_BP_DIRECT	GO:0006888~ER to Golgi vesicle-mediated transport
INTERPRO	IPR006895:Zinc finger, Sec23/Sec24-type
GOTERM_CC_DIRECT	GO:0030127~COPII vesicle coat
Annotation Cluster 24	Enrichment Score: 0.8135565670707758
Category	Term
GOTERM_BP_DIRECT	GO:0015991~ATP hydrolysis coupled proton transport
GOTERM_CC_DIRECT	GO:0033179~proton-transporting V-type ATPase, V0 domain
GOTERM_MF_DIRECT	GO:0015078~hydrogen ion transmembrane transporter activity
Annotation Cluster 25	Enrichment Score: 0.7964987710011121
Category	Term
KEGG_PATHWAY	ame01210:2-Oxocarboxylic acid metabolism
GOTERM_MF_DIRECT	GO:0004449~isocitrate dehydrogenase (NAD+) activity
INTERPRO	IPR024084:Isopropylmalate dehydrogenase-like domain
INTERPRO	IPR001804:Isocitrate and isopropylmalate dehydrogenases family
INTERPRO	IPR004434:Isocitrate dehydrogenase NAD-dependent
SMART	SM01329:SM01329
GOTERM_MF_DIRECT	GO:0051287~NAD binding
GOTERM_BP_DIRECT	GO:0006099~tricarboxylic acid cycle
Annotation Cluster 26	Enrichment Score: 0.7867348565935095
Category	Term
INTERPRO	IPR001623:DnaJ domain

SMART	SM00271:DnaJ
INTERPRO	IPR018253:DnaJ domain, conserved site
Annotation Cluster 27	Enrichment Score: 0.7709951919258211
Category	Term
INTERPRO	IPR004843:Metallophosphoesterase domain
GOTERM_MF_DIRECT	GO:0004721~phosphoprotein phosphatase activity
INTERPRO	
SMART	SM00156:PP2Ac
Annotation Cluster 28	Enrichment Score: 0.7671408489363004
Category	Term
GOTERM_BP_DIRECT	GO:0015991~ATP hydrolysis coupled proton transport
INTERPRO	IPR004100:ATPase, alpha/beta subunit, N-terminal
INTERPRO	
INTERPRO	
Annotation Cluster 29	Enrichment Score: 0.7477835262115027
Category	Term
INTERPRO	IPR017937:Thioredoxin, conserved site
UP_KEYWORDS	Redox-active center
INTERPRO	IPR005788:Disulphide isomerase
INTERPRO	IPR013766:Thioredoxin domain
INTERPRO	IPR012336:Thioredoxin-like fold
GOTERM_BP_DIRECT	GO:0045454~cell redox homeostasis
GOTERM_CC_DIRECT	GO:0005623~cell
Annotation Cluster 30	Enrichment Score: 0.7103214249214863
Category	Term
INTERPRO	IPR001683:Phox homologous domain
GOTERM_MF_DIRECT	GO:0035091~phosphatidylinositol binding
SMART	SM00312:PX
Annotation Cluster 31	Enrichment Score: 0.6979412102539907
Category	Term
GOTERM_MF_DIRECT	GO:0016791~phosphatase activity
INTERPRO	IPR011948:Dullard phosphatase domain, eukaryotic
INTERPRO	IPR004274:NLI interacting factor
SMART	SM00577:CPDc
Annotation Cluster 32	Enrichment Score: 0.6930615590326878
Category	Term
INTERPRO	IPR010504:Arfaptin homology (AH) domain
SMART	SM01015:SM01015
INTERPRO	IPR027267:Arfaptin homology (AH) domain/BAR domain
Annotation Cluster 33	Enrichment Score: 0.6577784257414996
Category	Term
INTERPRO	IPR000301:Tetraspanin

INTERPRO	IPR018499:Tetraspanin/Peripherin
PIR_SUPERFAMILY	PIRSF002419:tetraspanin
INTERPRO	IPR018503:Tetraspanin, conserved site
INTERPRO	IPR008952:Tetraspanin, EC2 domain
Annotation Cluster 34	Enrichment Score: 0.645183527714244
Category	Term
KEGG_PATHWAY	ame01210:2-Oxocarboxylic acid metabolism
KEGG_PATHWAY	ame00220:Arginine biosynthesis
GOTERM_BP_DIRECT	GO:0006520~cellular amino acid metabolic process
Annotation Cluster 35	Enrichment Score: 0.6186519111303531
Category	Term
GOTERM_MF_DIRECT	GO:0016746~transferase activity, transferring acyl groups
SMART	SM00563:PlsC
INTERPRO	IPR002123:Phospholipid/glycerol acyltransferase
KEGG_PATHWAY	ame00561:Glycerolipid metabolism
Annotation Cluster 36	Enrichment Score: 0.5641078769792714
Category	Term
INTERPRO	IPR004827:Basic-leucine zipper domain
SMART	SM00338:BRLZ
GOTERM_MF_DIRECT	
GOTERM_MF_DIRECT	GO:0043565~sequence-specific DNA binding
Annotation Cluster 37	Enrichment Score: 0.5448123900070027
Category	Term
GOTERM_BP_DIRECT	GO:0006486~protein glycosylation
UP_KEYWORDS	Golgi apparatus
UP_KEYWORDS	Glycosyltransferase
GOTERM_MF_DIRECT	GO:0008378~galactosyltransferase activity
INTERPRO	IPR002659:Glycosyl transferase, family 31
GOTERM_CC_DIRECT	GO:0000139~Golgi membrane
Annotation Cluster 38	Enrichment Score: 0.5379325126117979
Category	Term
INTERPRO	IPR017984:Chromo domain subgroup
INTERPRO	IPR023779:Chromo domain, conserved site
INTERPRO	IPR000953:Chromo domain/shadow
INTERPRO	IPR016197:Chromo domain-like
SMART	SM00298:CHROMO
INTERPRO	IPR023780:Chromo domain
Annotation Cluster 39	Enrichment Score: 0.5227346997205058
Category	Term
GOTERM_MF_DIRECT	GO:0004871~signal transducer activity
INTERPRO	IPR011025:G protein alpha subunit, helical insertion
INTERPRO	
GOTERM_MF_DIRECT	GO:0003924~GTPase activity

Annotation Cluster 40	Enrichment Score: 0.5110314775368822
Category	Term
SMART	SM00397:t_SNARE
INTERPRO	IPR000727:Target SNARE coiled-coil domain
INTERPRO	IPR010989:t-SNARE
KEGG_PATHWAY	ame04130:SNARE interactions in vesicular transport
GOTERM_BP_DIRECT	GO:0061025~membrane fusion
Annotation Cluster 41	Enrichment Score: 0.4881309535421234
Category	Term
INTERPRO	IPR011011:Zinc finger, FYVE/PHD-type
INTERPRO	IPR001965:Zinc finger, PHD-type
INTERPRO	IPR019787:Zinc finger, PHD-finger
SMART	SM00249:PHD
INTERPRO	IPR019786:Zinc finger, PHD-type, conserved site
Annotation Cluster 42	Enrichment Score: 0.4842903939578597
Category	Term
INTERPRO	IPR001375:Peptidase S9, prolyl oligopeptidase, catalytic domain
INTERPRO	IPR002469:Peptidase S9B, dipeptidylpeptidase IV N-terminal
GOTERM_MF_DIRECT	GO:0008236~serine-type peptidase activity
Annotation Cluster 43	Enrichment Score: 0.4798650796978842
Category	Term
SMART	SM00558:JmjC
INTERPRO	IPR003347:JmjC domain
INTERPRO	IPR019786:Zinc finger, PHD-type, conserved site
Annotation Cluster 44	Enrichment Score: 0.46779828181778016
Category	Term
GOTERM_MF_DIRECT	GO:0000049~tRNA binding
UP_KEYWORDS	Protein biosynthesis
UP_KEYWORDS	tRNA-binding
UP_KEYWORDS	Aminoacyl-tRNA synthetase
UP_KEYWORDS	Ligase
KEGG_PATHWAY	ame00970:Aminoacyl-tRNA biosynthesis
Annotation Cluster 45	Enrichment Score: 0.44565558536911126
Category	Term
INTERPRO	IPR017983:GPCR, family 2, secretin-like, conserved site
INTERPRO	IPR000832:GPCR, family 2, secretin-like
GOTERM_BP_DIRECT	GO:0007166~cell surface receptor signaling pathway
INTERPRO	IPR017981:GPCR, family 2-like
Annotation Cluster 46	Enrichment Score: 0.42963092505039946
Category	Term
UP_KEYWORDS	Autophagy
GOTERM_BP_DIRECT	GO:0006914~autophagy

KEGG_PATHWAY	ame04140:Regulation of autophagy
Annotation Cluster 47	Enrichment Score: 0.42745931692292394
Category	Term
INTERPRO	IPR001611:Leucine-rich repeat
INTERPRO	IPR003591:Leucine-rich repeat, typical subtype
SMART	SM00369:LRR_TYP
Annotation Cluster 48	Enrichment Score: 0.411021043275444
Category	Term
INTERPRO	IPR011043:Galactose oxidase/kelch, beta-propeller
INTERPRO	IPR006652:Kelch repeat type 1
INTERPRO	IPR011705:BTB/Kelch-associated
INTERPRO	IPR017096:Kelch-like protein, gigaxonin
PIR_SUPERFAMILY	PIRSF037037:kelch-like protein, gigaxonin type
SMART	SM00875:SM00875
INTERPRO	IPR015916:Galactose oxidase, beta-propeller
UP_KEYWORDS	Kelch repeat
SMART	SM00612:Kelch
Annotation Cluster 49	Enrichment Score: 0.3926687745465885
Category	Term
INTERPRO	IPR020084:NUDIX hydrolase, conserved site
INTERPRO	IPR000086:NUDIX hydrolase domain
INTERPRO	IPR015797:NUDIX hydrolase domain-like
Annotation Cluster 50	Enrichment Score: 0.39040159347772047
Category	Term
INTERPRO	IPR017455:Zinc finger, FYVE-related
INTERPRO	IPR000306:Zinc finger, FYVE-type
SMART	SM00064:FYVE
Annotation Cluster 51	Enrichment Score: 0.3892603002223318
Category	Term
INTERPRO	IPR013017:NHL repeat, subgroup
INTERPRO	IPR001258:NHL repeat
INTERPRO	IPR011042:Six-bladed beta-propeller, TolB-like
Annotation Cluster 52	Enrichment Score: 0.3805730839438125
Category	Term
UP_KEYWORDS	Acyltransferase
GOTERM_MF_DIRECT	GO:0019706~protein-cysteine S-palmitoyltransferase activity
INTERPRO	IPR001594:Zinc finger, DHHC-type, palmitoyltransferase
Annotation Cluster 53	Enrichment Score: 0.37907219453909835
Category	Term
INTERPRO	
UP_KEYWORDS	Pyridoxal phosphate
INTERPRO	IPR015424:Pyridoxal phosphate-dependent transferase

INTERPRO	IPR004839:Aminotransferase, class I/classII
GOTERM_MF_DIRECT	GO:0030170~pyridoxal phosphate binding
INTERPRO	
Annotation Cluster 54	Enrichment Score: 0.3747676070971319
Category	Term
UP_KEYWORDS	Lipid biosynthesis
UP_KEYWORDS	Fatty acid metabolism
UP_KEYWORDS	Fatty acid biosynthesis
GOTERM_MF_DIRECT	GO:0102338~3-oxo-lignoceronyl-CoA synthase activity
GOTERM_MF_DIRECT	GO:0102337~3-oxo-cerotoyl-CoA synthase activity
GOTERM_MF_DIRECT	GO:0102336~3-oxo-arachidoyl-CoA synthase activity
INTERPRO	IPR002076:GNS1/SUR4 membrane protein
UP_KEYWORDS	Lipid metabolism
GOTERM_BP_DIRECT	GO:0006633~fatty acid biosynthetic process
Annotation Cluster 55	Enrichment Score: 0.3710498061223294
Category	Term
KEGG_PATHWAY	ame00220:Arginine biosynthesis
INTERPRO	IPR004839:Aminotransferase, class I/classII
GOTERM_BP_DIRECT	GO:0009058~biosynthetic process
GOTERM_MF_DIRECT	GO:0030170~pyridoxal phosphate binding
KEGG_PATHWAY	ame00250:Alanine, aspartate and glutamate metabolism
Annotation Cluster 56	Enrichment Score: 0.3592894436076364
Category	Term
GOTERM_MF_DIRECT	GO:0016805~dipeptidase activity
UP_KEYWORDS	Dipeptidase
INTERPRO	IPR008257:Peptidase M19, renal dipeptidase
UP_KEYWORDS	GPI-anchor
GOTERM_CC_DIRECT	GO:0031225~anchored component of membrane
UP_KEYWORDS	Lipoprotein
UP_KEYWORDS	Metalloprotease
UP_KEYWORDS	Glycoprotein
Annotation Cluster 57	Enrichment Score: 0.3556870936584284
Category	Term
SMART	SM00060:FN3
INTERPRO	IPR003961:Fibronectin, type III
INTERPRO	IPR013783:Immunoglobulin-like fold
Annotation Cluster 58	Enrichment Score: 0.34945909361066296
Category	Term
INTERPRO	IPR004046:Glutathione S-transferase, C-terminal
INTERPRO	IPR010987:Glutathione S-transferase, C-terminal-like
INTERPRO	IPR004045:Glutathione S-transferase, N-terminal
Annotation Cluster 59	Enrichment Score: 0.34163801579538106
Category	Term

UP_KEYWORDS	Gap junction
INTERPRO	IPR000990:Innexin
GOTERM_CC_DIRECT	GO:0005921~gap junction
GOTERM_BP_DIRECT	GO:0006811~ion transport
UP_KEYWORDS	Cell junction
Annotation Cluster 60	Enrichment Score: 0.3254434616120558
Category	Term
INTERPRO	IPR016181:Acyl-CoA N-acyltransferase
GOTERM_MF_DIRECT	GO:0008080~N-acetyltransferase activity
INTERPRO	IPR000182:GNAT domain
Annotation Cluster 61	Enrichment Score: 0.31544957197360024
Category	Term
COG_ONTOLOGY	Lipid metabolism / General function prediction only
INTERPRO	IPR001206:Diacylglycerol kinase, catalytic domain
SMART	SM00046:DAGKc
INTERPRO	IPR016064:ATP-NAD kinase-like domain
Annotation Cluster 62	Enrichment Score: 0.31068677374002557
Category	Term
COG_ONTOLOGY	Cell division and chromosome partitioning / Cytoskeleton
INTERPRO	IPR000408:Regulator of chromosome condensation, RCC1
INTERPRO	
Annotation Cluster 63	Enrichment Score: 0.30633464264590016
Category	Term
GOTERM_MF_DIRECT	GO:0005096~GTPase activator activity
INTERPRO	IPR001164:Arf GTPase activating protein
SMART	SM00105:ArfGap
Annotation Cluster 64	Enrichment Score: 0.2891848053661439
Category	Term
GOTERM_MF_DIRECT	GO:0004930~G-protein coupled receptor activity
INTERPRO	IPR017452:GPCR, rhodopsin-like, 7TM
INTERPRO	IPR000276:G protein-coupled receptor, rhodopsin-like
UP_KEYWORDS	G-protein coupled receptor
SMART	SM01381:SM01381
UP_KEYWORDS	Receptor
UP_KEYWORDS	Transducer
Annotation Cluster 65	Enrichment Score: 0.2786047593988897
Category	Term
INTERPRO	IPR013767:PAS fold
SMART	SM00091:PAS
INTERPRO	IPR000014:PAS domain
Annotation Cluster 66	Enrichment Score: 0.27226162298442
Category	Term

INTERPRO	IPR001433:Oxidoreductase FAD/NAD(P)-binding
INTERPRO	IPR017927:Ferredoxin reductase-type FAD-binding domain
INTERPRO	IPR017938:Riboflavin synthase-like beta-barrel
Annotation Cluster 67	Enrichment Score: 0.27208541441613365
Category	Term
UP_KEYWORDS	Symport
GOTERM_MF_DIRECT	GO:0005328~neurotransmitter:sodium symporter activity
INTERPRO	IPR000175:Sodium:neurotransmitter symporter
Annotation Cluster 68	Enrichment Score: 0.2702830647661103
Category	Term
GOTERM_BP_DIRECT	GO:0008299~isoprenoid biosynthetic process
INTERPRO	IPR000092:Polyprenyl synthetase
INTERPRO	IPR008949:Terpenoid synthase
Annotation Cluster 69	Enrichment Score: 0.2699629563427815
Category	Term
INTERPRO	IPR013098:Immunoglobulin I-set
INTERPRO	IPR003598:Immunoglobulin subtype 2
SMART	SM00408:IGc2
INTERPRO	IPR003599:Immunoglobulin subtype
INTERPRO	IPR007110:Immunoglobulin-like domain
INTERPRO	IPR013783:Immunoglobulin-like fold
SMART	SM00409:IG
Annotation Cluster 70	Enrichment Score: 0.26550020870267177
Category	Term
INTERPRO	IPR020843:Polyketide synthase, enoylreductase
SMART	SM00829:SM00829
INTERPRO	IPR002085:Alcohol dehydrogenase superfamily, zinc-type
INTERPRO	IPR013154:Alcohol dehydrogenase GroES-like
INTERPRO	IPR011032:GroES-like
Annotation Cluster 71	Enrichment Score: 0.2619741382632584
Category	Term
INTERPRO	
GOTERM_MF_DIRECT	GO:0004722~protein serine/threonine phosphatase activity
INTERPRO	IPR015655:Protein phosphatase 2C
SMART	SM00332:PP2Cc
INTERPRO	IPR001932:Protein phosphatase 2C (PP2C)-like
Annotation Cluster 72	Enrichment Score: 0.251991370028117
Category	Term
INTERPRO	
INTERPRO	IPR002172:Low-density lipoprotein (LDL) receptor class A repeat
SMART	SM00192:LDLa
Annotation Cluster 73	Enrichment Score: 0.23337729281327935

Category	Term
INTERPRO	IPR000873:AMP-dependent synthetase/ligase
INTERPRO	IPR020845:AMP-binding, conserved site
INTERPRO	IPR025110:Domain of unknown function DUF4009
Annotation Cluster 74	Enrichment Score: 0.23026181319429512
Category	Term
UP_KEYWORDS	Transit peptide
UP_KEYWORDS	Mitochondrion
UP_KEYWORDS	Mitochondrion inner membrane
Annotation Cluster 75	Enrichment Score: 0.2271800792941584
Category	Term
GOTERM_MF_DIRECT	
UP_KEYWORDS	Tyrosine-protein kinase
INTERPRO	
INTERPRO	IPR020635:Tyrosine-protein kinase, catalytic domain
INTERPRO	IPR008266:Tyrosine-protein kinase, active site
SMART	SM00219:TyrKc
GOTERM_MF_DIRECT	GO:0004713~protein tyrosine kinase activity
Annotation Cluster 76	Enrichment Score: 0.22544319749190608
Category	Term
INTERPRO	IPR011765:Peptidase M16, N-terminal
INTERPRO	IPR011237:Peptidase M16 domain
INTERPRO	IPR007863:Peptidase M16, C-terminal domain
INTERPRO	IPR011249:Metalloenzyme, LuxS/M16 peptidase-like
Annotation Cluster 77	Enrichment Score: 0.21006627649126675
Category	Term
INTERPRO	IPR008984:SMAD/FHA domain
INTERPRO	IPR000253:Forkhead-associated (FHA) domain
SMART	SM00240:FHA
Annotation Cluster 78	Enrichment Score: 0.20856794298872536
Category	Term
INTERPRO	IPR014710:RmlC-like jelly roll fold
INTERPRO	IPR018490:Cyclic nucleotide-binding-like
INTERPRO	IPR000595:Cyclic nucleotide-binding domain
SMART	SM00100:cNMP
Annotation Cluster 79	Enrichment Score: 0.19850784761592796
Category	Term
INTERPRO	IPR000033:LDLR class B repeat
SMART	SM00135:LY
UP_KEYWORDS	EGF-like domain
INTERPRO	IPR011042:Six-bladed beta-propeller, TolB-like
INTERPRO	IPR000742:Epidermal growth factor-like domain
SMART	SM00181:EGF

INTERPRO	IPR013032:EGF-like, conserved site
INTERPRO	IPR000152:EGF-type aspartate/asparagine hydroxylation site
INTERPRO	IPR018097:EGF-like calcium-binding, conserved site
INTERPRO	IPR001881:EGF-like calcium-binding
SMART	SM00179:EGF_CA
Annotation Cluster 80	Enrichment Score: 0.1802901776532616
Category	Term
INTERPRO	IPR004087:K Homology domain
SMART	SM00322:KH
INTERPRO	IPR004088:K Homology domain, type 1
Annotation Cluster 81	Enrichment Score: 0.1801460591858231
Category	Term
INTERPRO	IPR000504:RNA recognition motif domain
INTERPRO	IPR012677:Nucleotide-binding, alpha-beta plait
GOTERM_MF_DIRECT	GO:0000166~nucleotide binding
SMART	SM00360:RRM
Annotation Cluster 82	Enrichment Score: 0.17775599841826317
Category	Term
INTERPRO	IPR020472:G-protein beta WD-40 repeat
INTERPRO	IPR001680:WD40 repeat
INTERPRO	IPR019775:WD40 repeat, conserved site
INTERPRO	IPR015943:WD40/YVTN repeat-like-containing domain
SMART	SM00320:WD40
INTERPRO	IPR017986:WD40-repeat-containing domain
Annotation Cluster 83	Enrichment Score: 0.16148128454678556
Category	Term
INTERPRO	IPR020902:Actin/actin-like conserved site
INTERPRO	IPR004001:Actin, conserved site
INTERPRO	IPR004000:Actin-related protein
SMART	SM00268:ACTIN
Annotation Cluster 84	Enrichment Score: 0.16081630065951844
Category	Term
INTERPRO	IPR015415:Vps4 oligomerisation, C-terminal
INTERPRO	IPR003960:ATPase, AAA-type, conserved site
INTERPRO	IPR003959:ATPase, AAA-type, core
INTERPRO	IPR003439:ABC transporter-like
INTERPRO	IPR003593:AAA+ ATPase domain
SMART	SM00382:AAA
Annotation Cluster 85	Enrichment Score: 0.15164473051291671
Category	Term
INTERPRO	IPR018980:FERM, C-terminal PH-like domain
SMART	SM01196:SM01196
INTERPRO	IPR014352:FERM/acyl-CoA-binding protein, 3-helical bundle

INTERPRO	IPR019748:FERM central domain
INTERPRO	IPR000299:FERM domain
INTERPRO	IPR019749:Band 4.1 domain
SMART	SM00295:B41
GOTERM_CC_DIRECT	GO:0005856~cytoskeleton
Annotation Cluster 86	Enrichment Score: 0.15163681821618055
Category	Term
INTERPRO	IPR013087:Zinc finger C2H2-type/integrase DNA-binding domain
INTERPRO	IPR007087:Zinc finger, C2H2
INTERPRO	IPR015880:Zinc finger, C2H2-like
SMART	SM00355:ZnF_C2H2
GOTERM_MF_DIRECT	GO:0003676~nucleic acid binding
Annotation Cluster 87	Enrichment Score: 0.1447026494466192
Category	Term
UP_KEYWORDS	Initiation factor
GOTERM_MF_DIRECT	GO:0003743~translation initiation factor activity
GOTERM_BP_DIRECT	GO:0001731~formation of translation preinitiation complex
GOTERM_BP_DIRECT	GO:0006446~regulation of translational initiation
GOTERM_CC_DIRECT	GO:0033290~eukaryotic 48S preinitiation complex
GOTERM_CC_DIRECT	GO:0005852~eukaryotic translation initiation factor 3 complex
GOTERM_CC_DIRECT	GO:0016282~eukaryotic 43S preinitiation complex
Annotation Cluster 88	Enrichment Score: 0.13266945000734792
Category	Term
INTERPRO	IPR001005:SANT/Myb domain
SMART	SM00717:SANT
INTERPRO	IPR017884:SANT domain
Annotation Cluster 89	Enrichment Score: 0.12602538486178053
Category	Term
UP_KEYWORDS	Cell junction
UP_KEYWORDS	Ion transport
INTERPRO	IPR018000:Neurotransmitter-gated ion-channel, conserved site
GOTERM_MF_DIRECT	
INTERPRO	IPR002394:Nicotinic acetylcholine receptor
INTERPRO	
INTERPRO	IPR006201:Neurotransmitter-gated ion-channel
INTERPRO	IPR006202:Neurotransmitter-gated ion-channel ligand-binding
INTERPRO	
UP_KEYWORDS	Ion channel
UP_KEYWORDS	Cell membrane
UP_KEYWORDS	Synapse
UP_KEYWORDS	Ligand-gated ion channel
GOTERM_CC_DIRECT	GO:0030054~cell junction
UP_KEYWORDS	Postsynaptic cell membrane
GOTERM_CC_DIRECT	GO:0045211~postsynaptic membrane

Annotation Cluster 90	Enrichment Score: 0.11824316826224841
Category	Term
SMART	SM00324:RhoGAP
INTERPRO	IPR000198:Rho GTPase-activating protein domain
INTERPRO	IPR008936:Rho GTPase activation protein
Annotation Cluster 91	Enrichment Score: 0.1122557843932693
Category	Term
UP_KEYWORDS	ANK repeat
INTERPRO	IPR002110:Ankyrin repeat
INTERPRO	IPR020683:Ankyrin repeat-containing domain
SMART	SM00248:ANK
Annotation Cluster 92	Enrichment Score: 0.0989335301525666
Category	Term
GOTERM_MF_DIRECT	GO:0016831~carboxy-lyase activity
INTERPRO	IPR002129:Pyridoxal phosphate-dependent decarboxylase
GOTERM_BP_DIRECT	GO:0019752~carboxylic acid metabolic process
Annotation Cluster 93	Enrichment Score: 0.09851299268707042
Category	Term
INTERPRO	IPR005829:Sugar transporter, conserved site
INTERPRO	IPR005828:General substrate transporter
GOTERM_MF_DIRECT	GO:0022891~substrate-specific transmembrane transporter activity
INTERPRO	IPR003663:Sugar/inositol transporter
Annotation Cluster 94	Enrichment Score: 0.09768413675411028
Category	Term
UP_KEYWORDS	Transcription regulation
UP_KEYWORDS	Transcription
GOTERM_BP_DIRECT	GO:0006351~transcription, DNA-templated
UP_KEYWORDS	DNA-binding
Annotation Cluster 95	Enrichment Score: 0.0837907843821477
Category	Term
UP_KEYWORDS	Flavoprotein
UP_KEYWORDS	FAD
INTERPRO	
GOTERM_MF_DIRECT	GO:0050660~flavin adenine dinucleotide binding
Annotation Cluster 96	Enrichment Score: 0.07081323934904664
Category	Term
GOTERM_MF_DIRECT	GO:0005089~Rho guanyl-nucleotide exchange factor activity
INTERPRO	IPR000219:Dbl homology (DH) domain
SMART	SM00325:RhoGEF
GOTERM_BP_DIRECT	GO:0035023~regulation of Rho protein signal transduction
Annotation Cluster 97	Enrichment Score: 0.05047884032128006
Category	Term

GOTERM_MF_DIRECT	GO:0004386~helicase activity
INTERPRO	
UP_KEYWORDS	Helicase
INTERPRO	IPR014014:RNA helicase, DEAD-box type, Q motif
INTERPRO	IPR011545:DNA/RNA helicase, DEAD/DEAH box type, N-terminal
INTERPRO	IPR001650:Helicase, C-terminal
INTERPRO	IPR014001:Helicase, superfamily 1/2, ATP-binding domain
SMART	SM00490:HELICc
SMART	SM00487:DEXDc
Annotation Cluster 98	Enrichment Score: 0.04918923169182432
Category	Term
UP_KEYWORDS	Isomerase
UP_KEYWORDS	Rotamase
GOTERM_MF_DIRECT	GO:0003755~peptidyl-prolyl cis-trans isomerase activity
Annotation Cluster 99	Enrichment Score: 0.03762514320883115
Category	Term
COG_ONTOLOGY	Lipid metabolism
INTERPRO	IPR002018:Carboxylesterase, type B
INTERPRO	IPR019819:Carboxylesterase type B, conserved site
Annotation Cluster 100	Enrichment Score: 0.03326704008907252
Category	Term
INTERPRO	IPR019734:Tetratricopeptide repeat
INTERPRO	IPR011990:Tetratricopeptide-like helical
SMART	SM00028:TPR
INTERPRO	IPR013026:Tetratricopeptide repeat-containing domain
Annotation Cluster 101	Enrichment Score: 0.01841829322131753
Category	Term
KEGG_PATHWAY	ame03420:Nucleotide excision repair
KEGG_PATHWAY	ame03440:Homologous recombination
KEGG_PATHWAY	ame03410:Base excision repair
KEGG_PATHWAY	ame03030:DNA replication
KEGG_PATHWAY	ame03430:Mismatch repair
Annotation Cluster 102	Enrichment Score: 0.003912689477190467
Category	Term
UP_KEYWORDS	Homeobox
GOTERM_MF_DIRECT	GO:0043565~sequence-specific DNA binding
INTERPRO	IPR001356:Homeodomain
INTERPRO	IPR009057:Homeodomain-like
INTERPRO	IPR017970:Homeobox, conserved site
UP_KEYWORDS	DNA-binding
SMART	SM00389:HOX
Annotation Cluster 103	Enrichment Score: 0.00310129416944087
Category	Term

UP_KEYWORDS	Cytoskeleton
UP_KEYWORDS	Microtubule
GOTERM_CC_DIRECT	GO:0005874~microtubule
Annotation Cluster 104	Enrichment Score: 1.6099659718154894E-9
Category	Term
GOTERM_BP_DIRECT	GO:0006412~translation
GOTERM_CC_DIRECT	GO:0005840~ribosome
GOTERM_MF_DIRECT	GO:0003735~structural constituent of ribosome

Up-Regulated

Annotation Cluster 1	Enrichment Score: 22.67329895357984
Category	Term
KEGG_PATHWAY	ame03010:Ribosome
GOTERM_MF_DIRECT	GO:0003735~structural constituent of ribosome
GOTERM_BP_DIRECT	GO:0006412~translation
GOTERM_CC_DIRECT	GO:0005840~ribosome
UP_KEYWORDS	Ribonucleoprotein
UP_KEYWORDS	Ribosomal protein
Annotation Cluster 2	Enrichment Score: 2.5402277919420313
Category	Term
SMART	SM00651:Sm
INTERPRO	IPR001163:Ribonucleoprotein LSM domain
INTERPRO	IPR010920:Like-Sm (LSM) domain
GOTERM_CC_DIRECT	GO:0005732~small nucleolar ribonucleoprotein complex
GOTERM_BP_DIRECT	GO:0000398~mRNA splicing, via spliceosome
Annotation Cluster 3	Enrichment Score: 1.9332490052024476
Category	Term
GOTERM_CC_DIRECT	GO:0015934~large ribosomal subunit
INTERPRO	IPR008991:Translation protein SH3-like domain
INTERPRO	IPR014722:Ribosomal protein L2 domain 2
Annotation Cluster 4	Enrichment Score: 1.815880938858488
Category	Term
INTERPRO	IPR000504:RNA recognition motif domain
INTERPRO	IPR012677:Nucleotide-binding, alpha-beta plait
GOTERM_MF_DIRECT	GO:0000166~nucleotide binding
SMART	SM00360:RRM
Annotation Cluster 5	Enrichment Score: 1.625730862268895
Category	Term
GOTERM_CC_DIRECT	GO:0005576~extracellular region
GOTERM_BP_DIRECT	GO:0006030~chitin metabolic process
INTERPRO	IPR002557:Chitin binding domain
GOTERM_MF_DIRECT	GO:0008061~chitin binding
SMART	SM00494:ChtBD2

Annotation Cluster 6	Enrichment Score: 1.3835193027092916
Category	Term
SMART	SM00409:IG
INTERPRO	IPR003599:Immunoglobulin subtype
UP_KEYWORDS	Immunoglobulin domain
INTERPRO	IPR007110:Immunoglobulin-like domain
SMART	SM00408:IGc2
INTERPRO	IPR003598:Immunoglobulin subtype 2
INTERPRO	IPR013783:Immunoglobulin-like fold
INTERPRO	IPR013106:Immunoglobulin V-set
INTERPRO	IPR013098:Immunoglobulin I-set
Annotation Cluster 7	Enrichment Score: 1.265004431125057
Category	Term
KEGG_PATHWAY	ame03020:RNA polymerase
GOTERM_MF_DIRECT	GO:0003899~DNA-directed RNA polymerase activity
KEGG_PATHWAY	ame00230:Purine metabolism
KEGG_PATHWAY	ame00240:Pyrimidine metabolism
Annotation Cluster 8	Enrichment Score: 1.131040798336076
Category	Term
INTERPRO	IPR024079:Metallopeptidase, catalytic domain
INTERPRO	IPR018497:Peptidase M13, C-terminal domain
INTERPRO	IPR008753:Peptidase M13, N-terminal domain
INTERPRO	IPR000718:Peptidase M13
GOTERM_MF_DIRECT	GO:0004222~metalloendopeptidase activity
INTERPRO	IPR001590:Peptidase M12B, ADAM/reprolysin
COG_ONTOLOGY	Posttranslational modification, protein turnover, chaperones
Annotation Cluster 9	Enrichment Score: 1.130658683742131
Category	Term
SMART	SM00401:ZnF_GATA
INTERPRO	IPR000679:Zinc finger, GATA-type
INTERPRO	IPR013088:Zinc finger, NHR/GATA-type
Annotation Cluster 10	Enrichment Score: 1.0098475187450022
Category	Term
UP_KEYWORDS	Nucleus
GOTERM_CC_DIRECT	GO:0005634~nucleus
UP_KEYWORDS	DNA-binding
Annotation Cluster 11	Enrichment Score: 0.9577376672440894
Category	Term
GOTERM_BP_DIRECT	GO:0006351~transcription, DNA-templated
UP_KEYWORDS	Transcription
UP_KEYWORDS	Transcription regulation
Annotation Cluster 12	Enrichment Score: 0.9469867847459708
Category	Term

INTERPRO	IPR006170:Pheromone/general odorant binding protein
SMART	SM00708:PhBP
GOTERM_MF_DIRECT	GO:0005549~odorant binding
Annotation Cluster 13	Enrichment Score: 0.9007408634727754
Category	Term
INTERPRO	IPR001353:Proteasome, subunit alpha/beta
GOTERM_MF_DIRECT	GO:0004298~threonine-type endopeptidase activity
KEGG_PATHWAY	ame03050:Proteasome
UP_KEYWORDS	Threonine protease
UP_KEYWORDS	Proteasome
INTERPRO	IPR016050:Proteasome, beta-type subunit, conserved site
INTERPRO	IPR023333:Proteasome B-type subunit
GOTERM_BP_DIRECT	GO:0051603~proteolysis involved in cellular protein catabolic process
GOTERM_CC_DIRECT	GO:0005839~proteasome core complex
Annotation Cluster 14	Enrichment Score: 0.7858097993262126
Category	Term
INTERPRO	IPR013524:Runt domain
INTERPRO	IPR000040:Acute myeloid leukemia 1 protein (AML1)/Runt
INTERPRO	IPR012346:p53/RUNT-type transcription factor, DNA-binding domain
INTERPRO	IPR008967:p53-like transcription factor, DNA-binding
Annotation Cluster 15	Enrichment Score: 0.6925895493040148
Category	Term
INTERPRO	IPR018525:Mini-chromosome maintenance, conserved site
SMART	SM00350:MCM
INTERPRO	IPR001208:Mini-chromosome maintenance, DNA-dependent ATPase
Annotation Cluster 16	Enrichment Score: 0.6797839875585538
Category	Term
UP_KEYWORDS	Extracellular matrix
GOTERM_CC_DIRECT	GO:0005578~proteinaceous extracellular matrix
UP_KEYWORDS	Wnt signaling pathway
SMART	SM00097:WNT1
INTERPRO	IPR018161:Wnt protein, conserved site
INTERPRO	IPR005817:Wnt
GOTERM_BP_DIRECT	GO:0016055~Wnt signaling pathway
UP_KEYWORDS	Developmental protein
GOTERM_BP_DIRECT	GO:0007275~multicellular organism development
KEGG_PATHWAY	ame04310:Wnt signaling pathway
Annotation Cluster 17	Enrichment Score: 0.6410156227205825
Category	Term

UP_KEYWORDS	Respiratory chain
GOTERM_CC_DIRECT	GO:0070469~respiratory chain
UP_KEYWORDS	Mitochondrion inner membrane
UP_KEYWORDS	Mitochondrion
UP_KEYWORDS	Electron transport
Annotation Cluster 18	Enrichment Score: 0.6324483589697669
Category	Term
UP_KEYWORDS	Cell membrane
INTERPRO	IPR006029:Neurotransmitter-gated ion-channel transmembrane domain
INTERPRO	IPR006202:Neurotransmitter-gated ion-channel ligand-binding
INTERPRO	IPR006201:Neurotransmitter-gated ion-channel
GOTERM_MF_DIRECT	GO:0005230~extracellular ligand-gated ion channel activity
INTERPRO	IPR018000:Neurotransmitter-gated ion-channel, conserved site
INTERPRO	IPR006028:Gamma-aminobutyric acid A receptor
UP_KEYWORDS	Synapse
GOTERM_CC_DIRECT	GO:0045202~synapse
GOTERM_CC_DIRECT	GO:0030054~cell junction
UP_KEYWORDS	Cell junction
UP_KEYWORDS	Postsynaptic cell membrane
INTERPRO	IPR002394:Nicotinic acetylcholine receptor
GOTERM_MF_DIRECT	GO:0004889~acetylcholine-activated cation-selective channel activity
GOTERM_CC_DIRECT	GO:0045211~postsynaptic membrane
INTERPRO	IPR027361:Nicotinic acetylcholine-gated receptor, transmembrane domain
UP_KEYWORDS	Ion channel
UP_KEYWORDS	Ligand-gated ion channel
UP_KEYWORDS	Ion transport
UP_KEYWORDS	Transport
Annotation Cluster 19	Enrichment Score: 0.6132021357488939
Category	Term
UP_KEYWORDS	Cleavage on pair of basic residues
UP_KEYWORDS	Amidation
UP_SEQ_FEATURE	signal peptide
Annotation Cluster 20	Enrichment Score: 0.608900338508913
Category	Term
INTERPRO	IPR009053:Prefoldin
GOTERM_CC_DIRECT	GO:0016272~prefoldin complex
GOTERM_BP_DIRECT	GO:0006457~protein folding
Annotation Cluster 21	Enrichment Score: 0.5999526779710416
Category	Term
SMART	SM01057:SM01057

INTERPRO	IPR001148:Alpha carbonic anhydrase
INTERPRO	IPR023561:Carbonic anhydrase, alpha-class
KEGG_PATHWAY	ame00910:Nitrogen metabolism
Annotation Cluster 22	Enrichment Score: 0.591646731049165
Category	Term
UP_KEYWORDS	Antibiotic
UP_KEYWORDS	Antimicrobial
GOTERM_BP_DIRECT	GO:0042742~defense response to bacterium
UP_KEYWORDS	Immunity
UP_KEYWORDS	Innate immunity
Annotation Cluster 23	Enrichment Score: 0.5860972080757149
Category	Term
INTERPRO	IPR019956:Ubiquitin subgroup
INTERPRO	IPR000626:Ubiquitin
SMART	SM00213:UBQ
Annotation Cluster 24	Enrichment Score: 0.5579361534291644
Category	Term
INTERPRO	IPR017975:Tubulin, conserved site
GOTERM_MF_DIRECT	GO:0005200~structural constituent of cytoskeleton
SMART	SM00864:SM00864
INTERPRO	IPR023123:Tubulin, C-terminal
INTERPRO	IPR000217:Tubulin
INTERPRO	IPR008280:Tubulin/FtsZ, C-terminal
INTERPRO	IPR003008:Tubulin/FtsZ, GTPase domain
GOTERM_BP_DIRECT	GO:0007017~microtubule-based process
UP_KEYWORDS	Cytoskeleton
SMART	SM00865:SM00865
INTERPRO	IPR018316:Tubulin/FtsZ, 2-layer sandwich domain
GOTERM_MF_DIRECT	GO:0003924~GTPase activity
GOTERM_CC_DIRECT	GO:0005874~microtubule
UP_KEYWORDS	Microtubule
UP_KEYWORDS	GTP-binding
Annotation Cluster 25	Enrichment Score: 0.5191879138867295
Category	Term
UP_KEYWORDS	Translocation
INTERPRO	IPR004217:Tim10/DDP family zinc finger
GOTERM_BP_DIRECT	GO:0015031~protein transport
UP_KEYWORDS	Protein transport
Annotation Cluster 26	Enrichment Score: 0.5124139398620224
Category	Term
UP_KEYWORDS	DNA recombination
GOTERM_BP_DIRECT	GO:0006310~DNA recombination
UP_KEYWORDS	DNA repair
UP_KEYWORDS	DNA damage

Annotation Cluster 27	Enrichment Score: 0.4338065435913677
Category	Term
GOTERM_MF_DIRECT	GO:0005319~lipid transporter activity
INTERPRO	IPR015816:Vitellinogen, beta-sheet N-terminal
INTERPRO	IPR015819:Lipid transport protein, beta-sheet shell
INTERPRO	IPR001747:Lipid transport protein, N-terminal
Annotation Cluster 28	Enrichment Score: 0.42386467373610426
Category	Term
INTERPRO	IPR002018:Carboxylesterase, type B
INTERPRO	IPR019826:Carboxylesterase type B, active site
COG_ONTOLOGY	Lipid metabolism
INTERPRO	IPR019819:Carboxylesterase type B, conserved site
GOTERM_MF_DIRECT	GO:0016787~hydrolase activity
Annotation Cluster 29	Enrichment Score: 0.400740212682717
Category	Term
INTERPRO	IPR002464:DNA/RNA helicase, ATP-dependent, DEAH-box type, conserved site
INTERPRO	IPR011709:Domain of unknown function DUF1605
SMART	SM00847:SM00847
INTERPRO	IPR007502:Helicase-associated domain
GOTERM_MF_DIRECT	GO:0008026~ATP-dependent helicase activity
SMART	SM00490:HELICc
SMART	SM00487:DEXDc
INTERPRO	IPR014001:Helicase, superfamily 1/2, ATP-binding domain
INTERPRO	IPR001650:Helicase, C-terminal
INTERPRO	IPR014014:RNA helicase, DEAD-box type, Q motif
INTERPRO	IPR011545:DNA/RNA helicase, DEAD/DEAH box type, N-terminal
INTERPRO	IPR000629:RNA helicase, ATP-dependent, DEAD-box, conserved site
Annotation Cluster 30	Enrichment Score: 0.39178387696985084
Category	Term
GOTERM_CC_DIRECT	GO:0000276~mitochondrial proton-transporting ATP synthase complex, coupling factor F(o)
GOTERM_BP_DIRECT	GO:0015986~ATP synthesis coupled proton transport
GOTERM_MF_DIRECT	GO:0015078~hydrogen ion transmembrane transporter activity
Annotation Cluster 31	Enrichment Score: 0.38898139582192814
Category	Term
SMART	SM00082:LRRCT
INTERPRO	IPR000483:Cysteine-rich flanking region, C-terminal
UP_KEYWORDS	Leucine-rich repeat
SMART	SM00369:LRR_TYP
INTERPRO	IPR003591:Leucine-rich repeat, typical subtype
INTERPRO	IPR001611:Leucine-rich repeat

Annotation Cluster 32	Enrichment Score: 0.3648985169547037
Category	Term
INTERPRO	IPR009000:Translation elongation/initiation factor/Ribosomal, beta-barrel
INTERPRO	IPR004161:Translation elongation factor EFTu/EF1A, domain 2
GOTERM_MF_DIRECT	GO:0003924~GTPase activity
INTERPRO	IPR000795:Elongation factor, GTP-binding domain
Annotation Cluster 33	Enrichment Score: 0.34621265468482626
Category	Term
INTERPRO	IPR011645:Haem NO binding associated
INTERPRO	IPR001054:Adenylyl cyclase class-3/4/guanylyl cyclase
GOTERM_MF_DIRECT	GO:0004383~guanylate cyclase activity
INTERPRO	IPR018297:Adenylyl cyclase class-3/4/guanylyl cyclase, conserved site
SMART	SM00044:CYCc
UP_KEYWORDS	Lyase
GOTERM_BP_DIRECT	GO:0035556~intracellular signal transduction
Annotation Cluster 34	Enrichment Score: 0.3440696455289717
Category	Term
SMART	SM00072:GuKc
INTERPRO	IPR008145:Guanylate kinase/L-type calcium channel
UP_KEYWORDS	SH3 domain
SMART	SM00326:SH3
INTERPRO	IPR001452:Src homology-3 domain
Annotation Cluster 35	Enrichment Score: 0.3400209199980145
Category	Term
INTERPRO	IPR002172:Low-density lipoprotein (LDL) receptor class A repeat
SMART	SM00192:LDLa
INTERPRO	IPR023415:Low-density lipoprotein (LDL) receptor class A, conserved site
Annotation Cluster 36	Enrichment Score: 0.329492518239019
Category	Term
UP_KEYWORDS	Metalloprotease
GOTERM_MF_DIRECT	GO:0008237~metallopeptidase activity
UP_KEYWORDS	Glycoprotein
Annotation Cluster 37	Enrichment Score: 0.32693725189266776
Category	Term
UP_KEYWORDS	G-protein coupled receptor
INTERPRO	IPR017452:GPCR, rhodopsin-like, 7TM
INTERPRO	IPR000276:G protein-coupled receptor, rhodopsin-like
SMART	SM01381:SM01381
UP_KEYWORDS	Receptor

UP_KEYWORDS	Transducer
GOTERM_MF_DIRECT	GO:0004930~G-protein coupled receptor activity
Annotation Cluster 38	Enrichment Score: 0.31768016228988083
Category	Term
INTERPRO	IPR020479:Homeodomain, metazoa
INTERPRO	IPR009057:Homeodomain-like
UP_KEYWORDS	DNA-binding
SMART	SM00389:HOX
INTERPRO	IPR001356:Homeodomain
GOTERM_MF_DIRECT	GO:0043565~sequence-specific DNA binding
UP_KEYWORDS	Homeobox
INTERPRO	IPR017970:Homeobox, conserved site
GOTERM_BP_DIRECT	GO:0006355~regulation of transcription, DNA-templated
Annotation Cluster 39	Enrichment Score: 0.3172230438459506
Category	Term
INTERPRO	IPR001304:C-type lectin
INTERPRO	IPR016186:C-type lectin-like
INTERPRO	IPR016187:C-type lectin fold
Annotation Cluster 40	Enrichment Score: 0.30358499885476903
Category	Term
SMART	SM00339:FH
INTERPRO	IPR001766:Transcription factor, fork head
INTERPRO	IPR011991:Winged helix-turn-helix DNA-binding domain
Annotation Cluster 41	Enrichment Score: 0.30133995954774584
Category	Term
SMART	SM00449:SPRY
INTERPRO	IPR003877:SPla/RYanodine receptor SPRY
INTERPRO	IPR001870:B30.2/SPRY domain
INTERPRO	IPR013320:Concanavalin A-like lectin/glucanase, subgroup
Annotation Cluster 42	Enrichment Score: 0.28921563699416075
Category	Term
INTERPRO	IPR001314:Peptidase S1A, chymotrypsin-type
SMART	SM00020:Tryp_SPc
INTERPRO	IPR001254:Peptidase S1
INTERPRO	IPR009003:Trypsin-like cysteine/serine peptidase domain
GOTERM_MF_DIRECT	GO:0004252~serine-type endopeptidase activity
INTERPRO	IPR018114:Peptidase S1, trypsin family, active site
UP_KEYWORDS	Serine protease
Annotation Cluster 43	Enrichment Score: 0.2527851472350029
Category	Term

SMART	SM00298:CHROMO
INTERPRO	IPR016197:Chromo domain-like
INTERPRO	IPR000953:Chromo domain/shadow
Annotation Cluster 44	Enrichment Score: 0.24026228886816542
Category	Term
INTERPRO	IPR009072:Histone-fold
GOTERM_CC_DIRECT	GO:0000786~nucleosome
UP_KEYWORDS	Chromosome
UP_KEYWORDS	Nucleosome core
INTERPRO	IPR007125:Histone core
Annotation Cluster 45	Enrichment Score: 0.23476796871215266
Category	Term
INTERPRO	IPR001557:L-lactate/malate dehydrogenase
INTERPRO	IPR022383:Lactate/malate dehydrogenase, C-terminal
INTERPRO	IPR015955:Lactate dehydrogenase/glycoside hydrolase, family 4, C-terminal
GOTERM_MF_DIRECT	GO:0016616~oxidoreductase activity, acting on the CH-OH group of donors, NAD or NADP as acceptor
KEGG_PATHWAY	ame00270:Cysteine and methionine metabolism
GOTERM_BP_DIRECT	GO:0019752~carboxylic acid metabolic process
KEGG_PATHWAY	ame00620:Pyruvate metabolism
GOTERM_BP_DIRECT	GO:0005975~carbohydrate metabolic process
Annotation Cluster 46	Enrichment Score: 0.22385608725379771
Category	Term
GOTERM_MF_DIRECT	GO:0046872~metal ion binding
INTERPRO	IPR007087:Zinc finger, C2H2
INTERPRO	IPR013087:Zinc finger C2H2-type/integrase DNA-binding domain
SMART	SM00355:ZnF_C2H2
INTERPRO	IPR015880:Zinc finger, C2H2-like
Annotation Cluster 47	Enrichment Score: 0.21992443018159333
Category	Term
INTERPRO	IPR000488:Death domain
INTERPRO	IPR011029:Death-like domain
GOTERM_BP_DIRECT	GO:0007165~signal transduction
Annotation Cluster 48	Enrichment Score: 0.21316119066385328
Category	Term
SMART	SM00320:WD40
INTERPRO	IPR001680:WD40 repeat
INTERPRO	IPR019775:WD40 repeat, conserved site
INTERPRO	IPR017986:WD40-repeat-containing domain
INTERPRO	IPR015943:WD40/YVTN repeat-like-containing domain
Annotation Cluster 49	Enrichment Score: 0.20816885012417152
Category	Term

INTERPRO	IPR012132:Glucose-methanol-choline oxidoreductase
PIR_SUPERFAMILY	PIRSF000137:glucose-methanol-choline oxidoreductase
INTERPRO	IPR007867:Glucose-methanol-choline oxidoreductase, C-terminal
INTERPRO	IPR000172:Glucose-methanol-choline oxidoreductase, N-terminal
GOTERM_MF_DIRECT	GO:0016614~oxidoreductase activity, acting on CH-OH group of donors
GOTERM_MF_DIRECT	GO:0050660~flavin adenine dinucleotide binding
INTERPRO	IPR023753:Pyridine nucleotide-disulphide oxidoreductase, FAD/NAD(P)-binding domain
Annotation Cluster 50	Enrichment Score: 0.1791919509442036
Category	Term
INTERPRO	IPR005814:Aminotransferase class-III
GOTERM_MF_DIRECT	GO:0008483~transaminase activity
UP_KEYWORDS	Pyridoxal phosphate
INTERPRO	IPR015421:Pyridoxal phosphate-dependent transferase, major region, subdomain 1
GOTERM_MF_DIRECT	GO:0030170~pyridoxal phosphate binding
INTERPRO	IPR015424:Pyridoxal phosphate-dependent transferase
INTERPRO	IPR015422:Pyridoxal phosphate-dependent transferase, major region, subdomain 2
Annotation Cluster 51	Enrichment Score: 0.17779540327888022
Category	Term
SMART	SM01100:SM01100
INTERPRO	IPR001071:Cellular retinaldehyde binding/alpha-tocopherol transport
INTERPRO	IPR011074:CRAL/TRIO, N-terminal domain
SMART	SM00516:SEC14
INTERPRO	IPR001251:CRAL-TRIO domain
GOTERM_MF_DIRECT	GO:0005215~transporter activity
Annotation Cluster 52	Enrichment Score: 0.16468810755496266
Category	Term
UP_KEYWORDS	Zinc
UP_KEYWORDS	Metal-binding
UP_KEYWORDS	Zinc-finger
Annotation Cluster 53	Enrichment Score: 0.15292023006330072
Category	Term
GOTERM_MF_DIRECT	GO:0004672~protein kinase activity
UP_KEYWORDS	Serine/threonine-protein kinase
SMART	SM00220:S_TKc
INTERPRO	IPR000719:Protein kinase, catalytic domain
INTERPRO	IPR008271:Serine/threonine-protein kinase, active site
INTERPRO	IPR017441:Protein kinase, ATP binding site
UP_KEYWORDS	Kinase
GOTERM_MF_DIRECT	GO:0004674~protein serine/threonine kinase activity
INTERPRO	IPR011009:Protein kinase-like domain

UP_KEYWORDS	Transferase
Annotation Cluster 54	Enrichment Score: 0.14849403552329868
Category	Term
INTERPRO	IPR019594:Glutamate receptor, L-glutamate/glycine-binding
GOTERM_MF_DIRECT	GO:0005234~extracellular-glutamate-gated ion channel activity
INTERPRO	IPR001320:Ionotropic glutamate receptor
GOTERM_MF_DIRECT	GO:0004970~ionotropic glutamate receptor activity
Annotation Cluster 55	Enrichment Score: 0.1465758655346196
Category	Term
GOTERM_MF_DIRECT	GO:0015035~protein disulfide oxidoreductase activity
INTERPRO	IPR012336:Thioredoxin-like fold
GOTERM_BP_DIRECT	GO:0045454~cell redox homeostasis
GOTERM_CC_DIRECT	GO:0005623~cell
INTERPRO	IPR013766:Thioredoxin domain
Annotation Cluster 56	Enrichment Score: 0.14457633756131663
Category	Term
INTERPRO	IPR000742:Epidermal growth factor-like domain
SMART	SM00179:EGF_CA
INTERPRO	IPR001881:EGF-like calcium-binding
SMART	SM00181:EGF
INTERPRO	IPR000152:EGF-type aspartate/asparagine hydroxylation site
INTERPRO	IPR018097:EGF-like calcium-binding, conserved site
INTERPRO	IPR013032:EGF-like, conserved site
UP_KEYWORDS	EGF-like domain
INTERPRO	IPR009030:Insulin-like growth factor binding protein, N-terminal
GOTERM_MF_DIRECT	GO:0005509~calcium ion binding
Annotation Cluster 57	Enrichment Score: 0.1331274369109913
Category	Term
GOTERM_MF_DIRECT	GO:0005216~ion channel activity
SMART	SM00248:ANK
INTERPRO	IPR002110:Ankyrin repeat
INTERPRO	IPR020683:Ankyrin repeat-containing domain
UP_KEYWORDS	ANK repeat
Annotation Cluster 58	Enrichment Score: 0.13063392323374434
Category	Term
UP_KEYWORDS	Isomerase
INTERPRO	IPR002130:Cyclophilin-like peptidyl-prolyl cis-trans isomerase domain
INTERPRO	IPR024936:Cyclophilin-type peptidyl-prolyl cis-trans isomerase
UP_KEYWORDS	Rotamase

GOTERM_BP_DIRECT	GO:0006457~protein folding
GOTERM_MF_DIRECT	GO:0003755~peptidyl-prolyl cis-trans isomerase activity
Annotation Cluster 59	Enrichment Score: 0.12260609909013652
Category	Term
GOTERM_MF_DIRECT	GO:0008080~N-acetyltransferase activity
INTERPRO	IPR000182:GNAT domain
INTERPRO	IPR016181:Acyl-CoA N-acyltransferase
Annotation Cluster 60	Enrichment Score: 0.11097685475483653
Category	Term
SMART	SM00322:KH
INTERPRO	IPR004087:K Homology domain
INTERPRO	IPR004088:K Homology domain, type 1
Annotation Cluster 61	Enrichment Score: 0.09367797840987173
Category	Term
INTERPRO	IPR001781:Zinc finger, LIM-type
SMART	SM00132:LIM
UP_KEYWORDS	LIM domain
Annotation Cluster 62	Enrichment Score: 0.08458418914700383
Category	Term
UP_KEYWORDS	Monooxygenase
GOTERM_MF_DIRECT	GO:0020037~heme binding
COG_ONTOLOGY	Secondary metabolites biosynthesis, transport, and catabolism
INTERPRO	IPR002401:Cytochrome P450, E-class, group I
UP_KEYWORDS	Heme
INTERPRO	IPR001128:Cytochrome P450
GOTERM_MF_DIRECT	GO:0016705~oxidoreductase activity, acting on paired donors, with incorporation or reduction of molecular oxygen
INTERPRO	IPR017972:Cytochrome P450, conserved site
GOTERM_MF_DIRECT	GO:0004497~monooxygenase activity
UP_KEYWORDS	Iron
GOTERM_MF_DIRECT	GO:0005506~iron ion binding
UP_KEYWORDS	Oxidoreductase
Annotation Cluster 63	Enrichment Score: 0.08261573613344135
Category	Term
SMART	SM00454:SAM
INTERPRO	IPR001660:Sterile alpha motif domain
INTERPRO	IPR013761:Sterile alpha motif/pointed domain
Annotation Cluster 64	Enrichment Score: 0.08249855974494377
Category	Term
INTERPRO	IPR005828:General substrate transporter
INTERPRO	IPR003663:Sugar/inositol transporter

GOTERM_MF_DIRECT	GO:0022891~substrate-specific transmembrane transporter activity
INTERPRO	IPR005829:Sugar transporter, conserved site
Annotation Cluster 65	Enrichment Score: 0.05823738247560854
Category	Term
UP_KEYWORDS	GTP-binding
INTERPRO	IPR020849:Small GTPase superfamily, Ras type
GOTERM_CC_DIRECT	GO:0016020~membrane
GOTERM_MF_DIRECT	GO:0005525~GTP binding
INTERPRO	IPR005225:Small GTP-binding protein domain
GOTERM_BP_DIRECT	GO:0007264~small GTPase mediated signal transduction
INTERPRO	IPR001806:Small GTPase superfamily
Annotation Cluster 66	Enrichment Score: 0.04909501010032386
Category	Term
INTERPRO	IPR011701:Major facilitator superfamily
INTERPRO	IPR020846:Major facilitator superfamily domain
GOTERM_BP_DIRECT	GO:0055085~transmembrane transport
Annotation Cluster 67	Enrichment Score: 0.03187953124700801
Category	Term
INTERPRO	IPR000210:BTB/POZ-like
INTERPRO	IPR011333:BTB/POZ fold
SMART	SM00225:BTB
Annotation Cluster 68	Enrichment Score: 0.026813697036988098
Category	Term
INTERPRO	IPR003960:ATPase, AAA-type, conserved site
INTERPRO	IPR003959:ATPase, AAA-type, core
INTERPRO	IPR003593:AAA+ ATPase domain
SMART	SM00382:AAA
Annotation Cluster 69	Enrichment Score: 0.01851786526800038
Category	Term
UP_KEYWORDS	Nucleotide-binding
UP_KEYWORDS	ATP-binding
GOTERM_MF_DIRECT	GO:0005524~ATP binding
Annotation Cluster 70	Enrichment Score: 0.016374083153132487
Category	Term
GOTERM_CC_DIRECT	GO:0005886~plasma membrane
GOTERM_MF_DIRECT	GO:0005549~odorant binding
UP_KEYWORDS	Olfaction
UP_KEYWORDS	Sensory transduction
INTERPRO	IPR004117:Olfactory receptor, Drosophila
GOTERM_MF_DIRECT	GO:0004984~olfactory receptor activity
Annotation Cluster 71	Enrichment Score: 0.009703276678371543
Category	Term

INTERPRO	IPR018247:EF-Hand 1, calcium-binding site
INTERPRO	IPR011992:EF-hand-like domain
GOTERM_MF_DIRECT	GO:0005509~calcium ion binding
INTERPRO	IPR002048:EF-hand domain
Annotation Cluster 72	Enrichment Score: 0.004441392633435781
Category	Term
INTERPRO	IPR013026:Tetratricopeptide repeat-containing domain
INTERPRO	IPR011990:Tetratricopeptide-like helical
SMART	SM00028:TPR
INTERPRO	IPR019734:Tetratricopeptide repeat
Annotation Cluster 73	Enrichment Score: 8.697889380509524E-5
Category	Term
UP_KEYWORDS	Membrane
UP_KEYWORDS	Transmembrane helix
UP_KEYWORDS	Transmembrane
GOTERM_CC_DIRECT	GO:0016021~integral component of membrane

Appendix S: Enriched Genes at Control-4h and Treatment-0h. DAVID was used for enrichment analysis. Genes that had an FDR<0.05 were considered significantly enriched. Down-regulated genes had an FDR <0.09. Included in this table for comparison.

Annotation Number	Function of Cluster	Enrichment Score	Up-regulated	Down-Regulated	Unique Genes in Cluster
1	Transmembrane	0.7		√	uncharacterized protein PF11_0207-like (LOC100578519) uncharacterized LOC725682 sex peptide receptor-like (LOC724225) dual oxidase (LOC551970)
1	Transmembrane	4.59	√		beta-1,4-glucuronyltransferase 1-like(LOC727358) CAAX prenyl protease 1 homolog(LOC551466) cadherin-23(LOC410368) dopamine receptor, D1(Dop1) facilitated trehalose transporter Tret1-like(LOC100577385) glutamate receptor 3-like(LOC100577496) GPI mannosyltransferase 4(LOC551642) innexin inx7(LOC552285) leukocyte tyrosine kinase receptor(LOC408718) nanchung(LOC552792) neprilysin-2(LOC724616) neuropeptide Y receptor-like(LOC411614) odorant receptor 27(Or27) odorant receptor 30(Or30) organic cation transporter protein-like(LOC102653922) probable phospholipid-transporting ATPase VD(LOC409192) proton-coupled amino acid transporter 4(LOC410741) sodium/bile acid cotransporter 7-like(LOC724999) sushi, von Willebrand factor type A, EGF and pentraxin domain-containing protein 1-like(LOC100578434) transmembrane protein 114(LOC725318) uncharacterized LOC100576461(LOC100576461) uncharacterized LOC100576683(LOC100576683)

					uncharacterized LOC551778(LOC551778) uncharacterized LOC725724(LOC725724) uncharacterized LOC727444(LOC727444) zinc transporter 1(LOC727479)
2	Immunoglobulin	1.15	√		uncharacterized LOC100576471 uncharacterized LOC725354 cell adhesion molecule 2-like (LOC409000)